

**Benefit and Application of Antibodies
Against the H1 Carbohydrate Recognition
Domain of the Human Hepatic
Asialoglycoprotein Receptor**

**High Yield Recombinant Production of the H1 Carbohydrate
Recognition Domain**

And

**Production and Characterization of Murine Monoclonal and
Chicken Polyclonal Antibodies against the H1 Carbohydrate
Recognition Domain**

Inauguraldissertation

zur Erlangung der Würde eines Doktors der Philosophie, vorgelegt der
Philosophisch-Naturwissenschaftlichen Fakultät der Universität Basel

von

Rita Born

aus Niederbipp BE, Schweiz

Referent: Prof. Dr. Beat Ernst

Korreferent: Prof. Dr. Med. et Phil. Nat. Gennaro De Libero

Basel, September 2005

**Benefit and Application of Antibodies
Against the H1 Carbohydrate Recognition
Domain of the Human Hepatic
Asialoglycoprotein Receptor**

**High Yield Recombinant Production of the H1 Carbohydrate
Recognition Domain**

And

**Production and Characterization of Murine Monoclonal and
Chicken Polyclonal Antibodies against the H1 Carbohydrate
Recognition Domain**

Inauguraldissertation

zur Erlangung der Würde eines Doktors der Philosophie,

vorgelegt der

Philosophisch-Naturwissenschaftlichen Fakultät

der Universität Basel

von

Rita Born

aus Niederbipp BE, Schweiz

Basel, September 2005

Die Inauguraldissertation wurde im Departement der Pharmazeutischen Wissenschaften
im Institut für Molekulare Pharmazie an der Universität Basel erstellt.

Genehmigt von der Philosophisch-Naturwissenschaftlichen Fakultät auf Antrag von

Prof. Dr. Beat Ernst, Institut für Molekulare Pharmazie, Universität Basel.

Prof. Dr. Med. et Phil. Nat. Gennaro De Libero, Experimentelle Immunologie,
Universitätsspital Basel.

Basel, den 20. September 2005

Prof. Dr. Hans-Jakob Wirz

Dekan

Meinen Eltern

Va und Mue

Acknowledgements

Supervisor of my Ph.D. Thesis

Prof. Dr. Beat Ernst,

For helpful discussions and support

Prof. Dr. Med. et Phil. Nat. Gennaro De Libero and his Group

For productive discussions and practical support in the monoclonal antibody production

Rene W. Fischer

For practical support in the monoclonal antibody production

Dr. Frank Bootz

For chicken immunization

Prof. Dr. Rer. Nat. Michael Przybylski and his Group

For epitope mapping collaboration

Dr. Luigi Terracciano

For immunohistochemical investigations

Prof. Martin Spiess

For supply of the H1-CRD encoding plasmid

The Group of Prof. Dr. Beat Ernst, especially Dr. Daniel Ricklin and Karin Johansson

For the good cooperation in the ASGPR project and the good atmosphere

My Diploma students Daniela Weiss, Nicole Kuster and Daniela Stokmaier

For their precious work in parts of my thesis

The Roche Research Foundation

For financial support

My parents, my brother and my running partners

For being at my side all the way and helping me when I struggled.

Contents

Contents	I
Abbreviations	XI
Legends of appendices, equations, figures, formulations and tables.....	XVII
Summary	1
1 Introduction	2
1.1 The hepatic asialoglycoprotein receptor (ASGPR)	3
1.1.1 Location of the ASGPR.....	3
1.1.2 Structure of the ASGPR.....	3
1.1.3 ASGPR-ligand interaction – determinants of high avidity binding	5
1.1.4 ASGPR-mediated endocytosis pathways	6
1.1.5 Physiological functions of the ASGPR	9
1.1.6 Recombinant expression of protein in <i>E.coli</i>	9
1.1.6.1 Construction of <i>E.coli</i> expression systems – the “protein factories”.....	10
1.1.6.2 Expression.....	12
1.1.6.3 Protein purification and protein renaturation from inclusion bodies	12
1.2 The antibodies – structure, feature and production	14
1.2.1 Antibody structure	14
1.2.2 Immune response – the avian and mammalian humoral immune system	18
1.2.2.1 Antibody diversity	18
1.2.2.2 Clonal selection.....	20
1.2.3 Antigen-antibody interface	20
1.2.3.1 Antigenic site and antigen combining site	20
1.2.3.2 Antigenicity and immunogenicity	22
1.2.4 Production of monoclonal and polyclonal antibodies	24
1.2.4.1 Monoclonal antibody production	24
1.2.4.1.1 <i>In vivo</i> stage - the immunization	24
1.2.4.1.2 <i>In vitro</i> stage – the somatic hybridization and clonal selection	25
1.2.4.1.3 Propagation of hybridoma clones – the “antibody factories”.....	28
1.2.4.2 Polyclonal antibody production.....	29
1.2.4.2.1 <i>In vivo</i> stage – from immunization to antibodies in the egg yolk.....	29
1.2.4.2.2 <i>In vitro</i> stage – the isolation of IgY antibodies from eggs	30
1.3 Application of antibodies in immunochemical techniques.....	32

1.3.1	Immunoblotting	33
1.3.2	Immunoassay	34
1.3.3	Immunocytochemistry	36
1.3.4	Immunohistochemistry	37
1.3.5	Immunoaffinity / Mass spectrometry (epitope mapping)	38
1.3.6	Surface Plasmon Resonance - Biacore	40
1.3.7	Monoclonal versus polyclonal antibodies.....	41
1.4	Thesis	42
2	Materials and Methods	44
2.1	Database research.....	44
2.1.1	Sequence alignments.....	44
2.1.2	Epitope prediction plots.....	44
2.2	Cloning, expression and purification of the H1 Carbohydrate Recognition Domain.....	45
	(H1-CRD)	45
2.2.1	Buffers and Media	45
2.2.1.1	Buffers	45
2.2.1.2	Media.....	45
2.2.2	General DNA methods.....	46
2.2.2.1	OD ₆₀₀ measurement.....	46
2.2.2.2	Bacteria cultivation and storage.....	46
2.2.2.2.1	Overnight and starter cultures	47
2.2.2.2.2	Cultures on LB / agar plate for short time storage	47
2.2.2.2.3	Glycerol stocks (15%) for long time storage.....	47
2.2.2.2.4	MgCl ₂ / CaCl ₂ competent cells.....	47
2.2.2.3	Plasmid extraction.....	48
2.2.2.4	Agarose-gel electrophoresis	48
2.2.2.5	NaOAc / ethanol precipitation	49
2.2.2.6	Quantification of DNA.....	49
2.2.2.6.1	Quantification of plasmid dsDNA by A ₂₆₀ :A ₂₈₀ measurement	49
2.2.2.6.2	Quantification of plasmid dsDNA by agarose-gel electrophoresis.....	50
2.2.3	Cloning.....	50
2.2.3.1	Amplification of H1-CRD cDNA by Polymerase chain reaction.....	50
2.2.3.1.1	Calculation of melting temperature and annealing temperature	50
2.2.3.1.2	Polymerase chain reaction using <i>Taq</i> and <i>Pfu</i> DNA polymerase.....	51
2.2.3.2	Digest of H1-CRD cDNA and plasmid vectors pEZZ18 for ligation.....	52
2.2.3.2.1	Restriction digest of H1-CRD cDNA.....	52
2.2.3.2.2	Restriction digest and dephosphorylation of plasmid vector pEZZ18.....	52
2.2.3.3	Ligation	54

2.2.3.3.1	Molar ratio of H1-CRD cDNA to plasmid vector pEZZ18	54
2.2.3.3.2	Ligation of H1-CRD cDNA into pEZZ18 vector	54
2.2.3.4	Transformation	55
2.2.3.5	Analysis of <i>E. coli</i> transformants	56
2.2.3.5.1	PCR analysis	56
2.2.3.5.2	Restriction digest analysis	56
2.2.3.5.3	Plasmid DNA sequence verification of <i>E. coli</i> expression clone	57
2.2.4	General protein methods	58
2.2.4.1	TCA / acetone precipitation	58
2.2.4.2	Polyacrylamide-gel Electrophoresis (PAGE) and staining	58
2.2.4.2.1	Reducing SDS-PAGE	58
2.2.4.2.2	Non-reducing SDS-PAGE	60
2.2.4.2.3	Native SDS-PAGE	60
2.2.4.2.4	Silver-staining	60
2.2.4.3	Electroblotting and immunostaining (immunoblotting)	60
2.2.4.3.1	PAGE	61
2.2.4.3.2	Electroblotting	61
2.2.4.3.3	Staining	61
2.2.4.4	Protein quantification	62
2.2.4.4.1	Protein quantification by A_{280} measurement	62
2.2.4.4.2	Protein quantification by Bradford assay	62
2.2.4.4.3	Protein quantification by SDS-PAGE	63
2.2.5	H1-CRD expression and purification	64
2.2.5.1	H1-CRD expression	64
2.2.5.2	Optimization of the H1-CRD expression	64
2.2.5.2.1	Selection of the <i>E. coli</i> expression strain and clone	64
2.2.5.2.2	Selection of expression conditions	65
2.2.5.3	Optimization of the H1-CRD purification	65
2.2.5.3.1	Fraction analysis of the selected <i>E. coli</i> expression clone	65
2.2.5.3.2	Inclusion bodies denaturation and reduction	67
2.2.5.3.3	H1-CRD refolding	68
2.2.5.3.4	H1-CRD affinity purification on Gal-Sepharose by FPLC	70
2.2.5.4	Size exclusion chromatography of the H1-CRD by FPLC	71
2.2.5.5	Preparative scale production of the H1-CRD	71
2.3	Production and purification of polyclonal antibodies	73
2.3.1	Hen immunization and egg handling	73
2.3.2	IgY purification	73
2.3.2.1	Purification optimization	73
2.3.2.1.1	Egg white and yolk separation	73
2.3.2.1.2	Protein / Lipid separation methods	73
2.3.2.1.3	Protein / total IgY separation methods	74
2.3.2.1.4	Dialysis of IgY solutions	75
2.3.2.1.5	Extraction of specific anti-H1 IgY	75

2.3.2.2	Preparative scale extraction of total IgY by PEG precipitation	76
2.3.2.3	Analysis	76
2.4	Production and purification of monoclonal antibodies	77
2.4.1	Buffers and media	77
2.4.1.1	Buffers	77
2.4.1.2	Media	77
2.4.2	General methods	79
2.4.2.1	Viability check and cell counting by trypan blue	79
2.4.2.2	Cell thawing	79
2.4.2.3	Cell cultivation	80
2.4.2.3.1	Collagen coating of culture plates and flasks	80
2.4.2.3.2	Cell splitting and propagation	80
2.4.2.4	Cell freezing	81
2.4.2.5	Screening ELISA	81
2.4.2.5.1	Alkaline phosphatase ELISA	81
2.4.2.5.2	Horse radish peroxidase ELISA	82
2.4.3	Production of hybridomas	82
2.4.3.1	Immunization	82
2.4.3.1.1	Immunization of NMRI outbred mice	83
2.4.3.1.2	Immunization of Balb/c inbred mice	83
2.4.3.1.3	Serum titer determination	84
2.4.3.2	Polyethylene glycol fusion	84
2.4.3.2.1	PEG1500 fusion of NMRI splenocytes and P3X63-Ag8.563 myeloma cells	84
2.4.3.2.2	PEG4000 fusion of Balb/c splenocytes and P3X63-Ag8.563 myeloma cells	86
2.4.3.3	Hybridoma cultivation and screening	87
2.4.3.3.1	NMRI hybridoma cultivation and screening	87
2.4.3.3.2	Balb/c hybridoma cultivation and screening	88
2.4.3.4	Terasaki cloning	88
2.4.4	Production of monoclonal antibodies	89
2.4.4.1	Propagation of clones	89
2.4.4.2	Affinity purification	89
2.4.4.2.1	Ig κ purification on Protein L-Sepharose spinning columns	89
2.4.4.2.2	IgG1 purification on a Protein A-agarose column (FPLC)	90
2.4.4.2.3	IgG1 and IgG2a purification on a Protein G-Sepharose column (FPLC)	90
2.4.4.2.4	IgM purification on a H1-CRD-Sepharose column (FPLC)	91
2.4.4.2.5	Analysis	91
2.5	Antibody characterization	92
2.5.1	Protein assays	92
2.5.1.1	Polyacrylamide-gel Electrophoresis	92
2.5.1.2	Immunoblotting	92
2.5.1.2.1	Immunoblotting of antibodies	92
2.5.1.2.2	Immunoblotting of the H1-CRD	92

2.5.1.3	Colorimetric assay.....	93
2.5.1.3.1	Isotyping ELISA.....	93
2.5.1.3.2	Titration ELISA.....	93
2.5.1.3.3	Competitive GalNAc-polymer assay.....	93
2.5.1.4	Epitope mapping.....	94
2.5.1.4.1	Reduction and alkylation of the H1-CRD.....	94
2.5.1.4.2	Preparation of the anti-H1 mAb-Sepharose column.....	95
2.5.1.4.3	Epitope extraction of digested H1-CRD.....	95
2.5.1.4.4	Epitope excision of mAb-bound H1-CRD.....	96
2.5.1.4.5	MS measurement.....	97
2.5.1.4.6	Solid phase synthesis of acylated epitope fragments and biotin labeling.....	97
2.5.1.4.7	Extraction of acetylated epitope fragments.....	97
2.5.1.4.8	Epitope ELISA with acetylated biotin-labeled epitope fragments.....	98
2.5.1.5	Surface plasmon resonance.....	98
2.5.2	Cell assays.....	99
2.5.2.1	Fluorescence flow cytometry.....	99
2.5.2.1.1	Intracellular flow cytometry of fixed cells.....	99
2.5.2.1.2	Extracellular flow cytometry of not fixed or fixed cells.....	100
2.5.2.2	Immunofluorescence microscopy with HepG2 and SK-Hep1 cells.....	101
2.5.2.2.1	Labeling of antibodies and asialofetuin with Texas Red fluorochrome.....	101
2.5.2.2.2	Preparation of cell cultures on coverslips.....	102
2.5.2.2.3	Immunodetection of anti-H1 antibody binding to fixed cells.....	103
2.5.2.2.4	Immunodetection of anti-H1 antibody internalization into cells prior to fixation.....	104
2.5.3	Tissue assays.....	105
2.5.3.1	Immunostaining of liver tissue.....	105
3	Result.....	106
3.1	ASGPR database research.....	106
3.1.1	ASGPR and H1-CRD alignments.....	106
3.1.2	H1-CRD epitope prediction.....	108
3.2	Cloning, expression and purification of the H1-CRD.....	110
3.2.1	Preparative scale expression in <i>E. coli</i> JM109pET3H1.....	110
3.2.2	Optimization of the <i>E. coli</i> expression system.....	110
3.2.2.1	Plasmid pET3H1 expression system.....	110
3.2.2.2	Plasmid pEZZ18H1 expression system.....	111
3.2.2.3	Selection of a high expressing <i>E. coli</i> production clone.....	112
3.2.2.4	Sequence verification of the H1-CRD.....	113
3.2.3	Optimization of expression conditions.....	117
3.2.3.1	IPTG concentration and expression period in <i>E. coli</i> ADpET3H1.4.....	117
3.2.3.2	ADpET3H1.4 cell density at induction time.....	118
3.2.3.3	Growth medium of ADpET3H1.4.....	119

3.2.4	Optimization of purification procedures.....	119
3.2.4.1	Identification of the H1-CRD localization in <i>E.coli</i> ADpET3H1.4.....	119
3.2.4.2	Renaturation and affinity chromatography of the H1-CRD.....	120
3.2.4.2.1	Denaturation and reduction by the FD, NFD and IB method.....	120
3.2.4.2.2	Refolding in buffer systems A to D.....	120
3.2.4.2.3	Affinity chromatography.....	121
3.2.4.2.4	Effect of reductants.....	124
3.2.4.2.5	Control of Gal-Sepharose binding specificity.....	124
3.2.5	Preparative scale expression in <i>E.coli</i> ADpET3H1.4.....	125
3.2.6	Size exclusion chromatography.....	126
3.3	Production and purification of polyclonal antibodies.....	129
3.3.1	Production of IgY.....	129
3.3.2	Purification of IgY.....	129
3.3.2.1	Optimization of the total IgY extraction.....	129
3.3.2.2	Extraction of specific anti-H1 IgY.....	133
3.3.2.3	Optimized IgY extraction.....	135
3.3.2.4	Preparative scale purification of total IgY.....	135
3.3.3	IgY characterization.....	136
3.3.3.1	<i>In vitro</i> characterization.....	136
3.3.3.2	<i>On cell</i> characterization.....	137
3.4	Production and purification of monoclonal antibodies.....	138
3.4.1	Production of hybridomas.....	138
3.4.1.1	Immunization of mice.....	138
3.4.1.1.1	Immunization of NMRI outbred mice.....	138
3.4.1.1.2	Immunization of Balb/c inbred mice.....	138
3.4.1.2	Fusion and hybridoma screening.....	139
3.4.1.2.1	PEG fusion of NMRI splenocytes with myeloma cells.....	139
3.4.1.2.2	PEG fusion of Balb/c splenocytes with myeloma cells.....	140
3.4.1.3	Fingerprint characterization of hybridomas.....	141
3.4.1.3.1	Isotyping.....	141
3.4.1.3.2	Immunoblotting.....	141
3.4.1.3.3	ELISA.....	142
3.4.1.3.4	Fluorescence flow cytometry.....	143
3.4.2	Production and propagation of clones.....	146
3.4.2.1	Terasaki single-cell cloning of hybridomas.....	146
3.4.2.2	Propagation of clones.....	149
3.5	Antibody characterization.....	150
3.5.1	Monoclonal A47.3 IgM.....	150
3.5.1.1	Purification of A47.3 IgM.....	150
3.5.1.2	<i>In vitro</i> characterization.....	151

3.5.1.2.1	Immunoblotting.....	151
3.5.1.2.2	ELISA	152
3.5.1.2.3	GalNAc-polymer assay	153
3.5.1.3	<i>On cell</i> characterization.....	154
3.5.1.3.1	Immunofluorescence flow cytometry	154
3.5.1.3.2	Immunofluorescence microscopy	155
3.5.2	Monoclonal B01.4 IgG1	156
3.5.2.1	Purification of B01.4 IgG1	156
3.5.2.2	<i>In vitro</i> characterization	157
3.5.2.2.1	Immunoblotting.....	157
3.5.2.2.2	ELISA	158
3.5.2.2.3	GalNAc-polymer assay	159
3.5.2.2.4	Biacore	160
3.5.2.2.5	Epitope excision and extraction	161
3.5.2.3	<i>On cell</i> characterization.....	164
3.5.2.3.1	Immunofluorescence flow cytometry	164
3.5.2.3.2	Immunofluorescence microscopy	165
3.5.2.4	<i>On tissue</i> characterization	166
3.5.2.4.1	Immunohepatochemistry.....	166
3.5.3	Monoclonal C09.1 IgG1	167
3.5.3.1	Purification of C09.1 IgG1	167
3.5.3.2	<i>In vitro</i> characterization	168
3.5.3.2.1	Immunoblotting.....	168
3.5.3.2.2	ELISA	169
3.5.3.2.3	GalNAc-polymer assay	170
3.5.3.2.4	Biacore	171
3.5.3.3	<i>On cell</i> characterization.....	171
3.5.3.3.1	Immunofluorescence flow cytometry	171
3.5.3.3.2	Immunofluorescence microscopy	172
3.5.3.4	<i>On tissue</i> characterization	173
3.5.3.4.1	Immunohepatochemistry.....	173
3.5.4	Monoclonal C11.1 IgG1	174
3.5.4.1	Purification of C11.1 IgG1	174
3.5.4.2	<i>In vitro</i> characterization	175
3.5.4.2.1	Immunoblotting.....	175
3.5.4.2.2	ELISA	176
3.5.4.2.3	GalNAc-polymer assay	177
3.5.4.2.4	Biacore	178
3.5.4.2.5	Epitope excision and extraction	179
3.5.4.3	<i>On cell</i> characterization.....	181
3.5.4.3.1	Immunofluorescence flow cytometry	181
3.5.4.3.2	Immunofluorescence microscopy	182
3.5.4.4	<i>On tissue</i> characterization	182
3.5.4.4.1	Immunohepatochemistry	182

3.5.5	Monoclonal C14.6 IgG2a	184
3.5.5.1	Purification of C14.6 IgG2a	184
3.5.5.2	<i>In vitro</i> characterization	185
3.5.5.2.1	Immunoblotting	185
3.5.5.2.2	ELISA	186
3.5.5.2.3	GalNAc-polymer assay	187
3.5.5.3	<i>On cell</i> characterization	188
3.5.5.3.1	Immunofluorescence flow cytometry	188
3.5.5.3.2	Immunofluorescence microscopy	188
3.5.5.4	<i>On tissue</i> characterization	189
3.5.5.4.1	Immunohepatochemistry	189
3.5.6	Monoclonal C18.1 IgG1	190
3.5.6.1	Purification of C18.1 IgG1	190
3.5.6.2	<i>In vitro</i> characterization	191
3.5.6.2.1	Immunoblotting	191
3.5.6.2.2	ELISA	192
3.5.6.2.3	GalNAc-polymer assay	193
3.5.6.2.4	Biacore	194
3.5.6.2.5	Epitope excision and extraction	195
3.5.6.3	<i>On cell</i> characterization	195
3.5.6.3.1	Immunofluorescence flow cytometry	195
3.5.6.3.2	Immunofluorescence microscopy	196
3.5.6.4	<i>On tissue</i> characterization	196
3.5.6.4.1	Immunohepatochemistry	196
3.5.7	Monoclonal C23.8 IgG1	198
3.5.7.1	Purification of C23.8 IgG1	198
3.5.7.2	<i>In vitro</i> characterization	199
3.5.7.2.1	Immunoblotting	199
3.5.7.2.2	ELISA	200
3.5.7.2.3	GalNAc-polymer assay	202
3.5.7.2.4	Biacore	202
3.5.7.3	<i>On cell</i> characterization	203
3.5.7.3.1	Immunofluorescence flow cytometry	203
3.5.7.3.2	Immunofluorescence microscopy	204
3.5.8	Monoclonal C48.9 IgG1	205
3.5.8.1	Purification of C48.9 IgG1	205
3.5.8.2	<i>In vitro</i> characterization	207
3.5.8.2.1	Immunoblotting	207
3.5.8.2.2	ELISA	208
3.5.8.2.3	GalNAc-polymer assay	209
3.5.8.2.4	Biacore	209
3.5.8.3	<i>On cell</i> characterization	210
3.5.8.3.1	Immunofluorescence flow cytometry	210
3.5.8.3.2	Immunofluorescence microscopy	211

4	Discussion	212
4.1	H1-CRD immunogenicity and antigenicity – a problem?	212
4.2	H1-CRD production – from minute to gigantic yields	213
4.2.1	Optimization of <i>E. coli</i> intrinsic features – the vector- <i>E. coli</i> strain relationship	215
4.2.2	Optimization of <i>E. coli</i> extrinsic features – the expression conditions	217
4.2.3	Optimization of the purification procedure	219
4.2.4	Conclusion – the optimized H1-CRD “protein-factory”	224
4.3	From active H1-CRD to highly pure monomeric and dimeric H1-CRD species	225
	– a one step strategy	225
4.4	Monoclonal and polyclonal anti-H1 antibodies – overview of the production,	226
	purification and characterization	226
4.5	Polyclonal antibodies – the way from hen to pure anti-H1 IgY	228
4.6	Monoclonal antibodies – the way from mice to anti-H1 Ig	232
4.6.1	Mice, fusion and hybridomas – from mortal to immortal anti-H1	232
	“antibody-factories”	232
4.6.2	Hybridomas screening, expansion and fingerprint characterization – sift the	234
	chaff from the wheat.....	234
4.7	Monoclonal anti-H1 Ig – features <i>in vitro</i>, <i>on cell</i> and <i>on tissue</i>	236
4.7.1	Antibody B01.4 – take a look at the monoclonal anti-H1 IgG1	236
4.7.1.1	Purification.....	236
4.7.1.2	Epitope mapping by immunoaffinity / MS.....	236
4.7.1.3	Immunoblotting.....	238
4.7.1.4	Immunoassay	240
4.7.1.5	Affinity and kinetics of the B01.4 IgG1 by Biacore	241
4.7.1.6	Immunostaining of cells and tissue.....	242
4.7.2	Comparison of the monoclonal anti-H1 Ig – which one is “the best”	243
4.7.2.1	Extraction of different isotypes of antibodies from culture supernatant	243
4.7.2.2	Epitope mapping by immunoaffinity / MS.....	244
4.7.2.3	Immunoblotting.....	246
4.7.2.4	Immunoassay	247
4.7.2.5	Affinity and kinetics of anti-H1 IgG1 by Biacore	250
4.7.2.6	Immunofluorescence staining of cells and tissue.....	252
4.8	Conclusion	255
5	References	259

Appendices 269
Curriculum vitae

Abbreviations

A_{260} ; A_{280}	Absorbance at 260nm ; absorbance at 280nm
Ab	Antibody
ABTS	2,2'-azino-di-[3-ethylbenzthiazoline-6-sulfonic acid]
amp	Ampicilline
Anti-H1	Specific against the H1-CRD
AP	Alkaline phosphatase
APS	Ammonium persulfate
AS	Ammonium sulfate
ASF	Asialofetuin
ASGPR	Asialoglycoprotein receptor
ASGPR-1	Human asialoglycoprotein receptor subunit 1 amino acid sequence
ASGPR-2	Human asialoglycoprotein receptor subunit 2 amino acid sequence
ASOR	Asialoorosomuroid
ATP	Adenosine triphosphate
Blast	Basic local alignment search tool
BSA	Bovine serum albumine
C	Constant region
cam	Chloramphenicole
carb	Carbenicilline
CDR	Complementarity determining region
CFA	Complete Freund's adjuvant
C_H ; C_L	Constant region of heavy chain ; constant region of light chain
CIAP	Calf intestinal alkaline phosphatase
CRD	Carbohydrate recognition domain
CURL	Compartment for uncoupling of receptors and ligands
D	Diversity gene segment

DMEM	Dulbecco's modified Eagle's medium
DMSO	Dimethylsulfoxide
DNA	Desoxyribonucleic acid
dNTP	Deoxynucleotidetriphosphate
DPBS	Dulbecco's PBS
dsDNA	Double strand DNA
DTT	Dithiothreitol
EC ₅₀	Concentration for half maximal effect
<i>E.coli</i>	<i>Escherichia coli</i>
ELISA	Enzyme linked sorbent assay
EDTA	Ethylendiaminetetraacetate
ESI-FT-ICR	Electro-spray ionization Fourier-transformation cyclotron resonance
F/T	"Freeze / Thaw" lipid precipitation method
Fab	Fragment having the antigen binding-site
Fc	Fragment that crystallize
FCS	Fetal calf serum
FD	"Fast dilution" solubilization method
FITC	Fluorescein isothiocyanate
FPLC	Fast performance liquid chromatography
Gal	Galactose
GalNAc	<i>N</i> -Acetyl-galactosamine
GAM	Goat anti-mouse
GlcNAc	<i>N</i> -Acetyl-glucosamine
GSH ; GSSG	Reduced glutathione ; oxidized glutathione
H	Heavy chain
H1	Asialoglycoprotein receptor subunit 1
H1fw ; H1bw	H1 forward primer ; H1 backward primer
H2a-c	Asialoglycoprotein receptor subunit 2 isoforms a-c
HAT	Hypoxanthine, aminopterin, thymidine

HEPES	4-(2-hydroxyethyl)piperazine-1-ethanesulfonic acid
hGMCSF	Human granulocyte-macrophage colony-stimulating factor
HL	Human lectin
HPLC	High performance liquid chromatography
HPRT	Hypoxanthine-guanine phosphoribosyltransferase
HRP	Horseradish peroxidase
HT	Hypoxanthine, thymidine
IB	“Inclusion body” solubilization method
IB	Inclusion body
IC ₅₀	Concentration for half maximal inhibition
IFA	Incomplete Freund’s adjuvant
Ig	Immunoglobulin
IL ; hIL	Interleukin ; human interleukin
IMDM	Iscove’s modified Dulbecco’s medium
IPTG	Isopropyl-β-D-thiogalactopyranoside
J	Joining gene segment
kan	Kanamycine
K _D	Dissociation constant
k _{on} ; k _{off}	Association rate, dissociation rate
KOAc	Potassium acetate
KPBS	Kreis’ PBS
L	Light chain
LB	Luriani Bertani
m ; mAb	Monoclonal : monoclonal antibody
MALDI-FT-ICR	Matrix-assisted laser desorption ionization Fourier-transformation cyclotron resonance
Man	Mannose
MHCII	Major histocompatibility complex II
NaOAc	Sodium acetate

NBT/BCIP	Nitroblue tetrazoliumchloride 5-bromo-4-chloro-3-indolyphosphate
NEAA	Non essential amino acids
NFD	“Non fast dilution” solubilization method
NK	Neutral killer
OD ₆₀₀	Optical density at 600nm
OPD	o-phenylenediamine dihydrochloride
p ; pAb	Polyclonal ; polyclonal antibody
PAGE	Polyacrylamide gel-electrophoresis
PBS	Phosphate buffered saline
PCR	Polymerase chain reaction
PEG	Polyethyleneglycol
pET3H1	pET3b vector encoding cDNA of H1-CRD
pEZZ18H1	pEZZ18 vector encoding cDNA of H1-CRD
PMSF	Phenylmethane sulfonylfluoride
R ²	Correlation coefficient
RACH	Rabbit anti-chicken
rcf	Relative centrifugal force
RPE	R-phycoerythrine
rpm	Rounds per minute
RT	Room temperature
SDS	Sodiumdodecylsulfate
SEC	Size exclusion chromatography
TB	Terrific broth
TCA	Trichloric acid
TEMED	tetramethylethylenediamine
tet	Tetracycline
TFA	Trifluoric acid
T _m	Melting temperature
TNF	Tumor necrosis factor

TR	Texas Red
V	Variable region
V	Variable gene segment
V _H ; V _L	Variable region of heavy chain ; variable region of light chain
WD	“Water dilution” lipid precipitation method

Appendices

Appendix 1 Substances	269
Appendix 2 Equipments	276
Appendix 3 Expression vectors	280
Appendix 4 <i>E.coli</i> cloning and expression strains	281
Appendix 5 Cell lines	282

Equations

Equation 1 Calculation of the <i>E.coli</i> cell density by measuring OD ₆₀₀	46
Equation 2 Calculation of the plasmid dsDNA concentration by measuring of A ₂₆₀	49
Equation 3 Estimation of the melting temperature according to Wetmur.....	50
Equation 4 Estimation of the melting temperature according to Suggs	50
Equation 5 Calculation of the amount of cDNA for ligation into a vector	54
Equation 6 Calculation of the protein concentration by measuring A ₂₈₀	62
Equation 7 Determination of the cell density	79
Equation 8 Determination of the cell viability.....	79
Equation 9 Texas Red labeling of anti-H1 Ig.....	101

Figures

Figure 1	Human hepatic ASGPR, model by Hardy <i>et al.</i>	4
Figure 2	ASGPR-mediated endocytosis pathway.....	7
Figure 3	Recombinant expression of protein in <i>E.coli</i>	10
Figure 4	Basic antibody structure	15
Figure 5	Murine IgM, IgG and chicken IgY structure.	16
Figure 6	Gene rearrangement and class switching of murine antibodies.	19
Figure 7	Gene rearrangement of chicken antibodies.....	19
Figure 8	Encoding of the heavy and light chain amino acid sequence.....	21
Figure 9	PEG fusion and HAT selection of hybridomas.....	27
Figure 10	Single-cell cloning by limited dilution.....	28
Figure 11	Extraction of specific IgY from egg yolk.....	31
Figure 12	Indirect immunoblotting	33
Figure 13	Indirect antibody-capture immunoassay.....	34
Figure 14	Direct competitive antibody-capture immunoassay.....	35
Figure 15	Indirect extracellular immunofluorescence-staining of surface antigen.....	36
Figure 16	Indirect intracellular immunostaining of internalized antigen	37
Figure 17	Indirect immunostaining of surface antigen in tissue.	38
Figure 18	Epitope excision.....	39
Figure 19	Epitope extraction	39
Figure 20	Surface Plasmon Resonance (Biacore)	40
Figure 21	T-COFFEE alignment of Lech_human, Lech_mouse and Lech_chicken	106
Figure 22	T-COFFEE alignment of Lech_human with homologous receptors	108
Figure 23	ProScale antigenicity, hydrophobicity and accessibility plots	109
Figure 24	Transformation control ADpET3H1 (standard PCR, restriction digest).....	111
Figure 25	SDS-PAGE gel of expression in JMpET3H1, ADpET3H1, RGpET3H1.....	112
Figure 26	Blastn alignment pET3H1 with ASGPR-1 ID [HUMASGPR1].....	113
Figure 27	Blastp alignment of translated pET3H1 with ASGPR-1 sp [P07306]	114
Figure 28	ESI-FT-ICR of the H1-CRD, produced in ADpET3H1.4	115
Figure 29	MALDI-FT-ICR of the trypsin-digested H1-CRD, from ADpET3H1.4	116
Figure 30	Expression in ADpET3H1.4, effect of the IPTG concentration	117
Figure 31	SDS-PAGE gel of 0 to 9h expression in ADpET3H1.4.....	118

Figure 32	Expression in ADpET3H1.4, effect of the cell density	118
Figure 33	Expression in ADpET3H1.4, effect of the medium.....	119
Figure 34	SDS-PAGE gel of expression in ADpET3H1.4, fraction analysis	120
Figure 35	Gal-Sepharose FPLC chromatograms of FD, NFD and IB methods	122
Figure 36	SDS-PAGE gel of H1-CRD purified by the FD, NFD and IB method	122
Figure 37	Yields of H1-CRD purified by the FD, NFD and IB methods	123
Figure 38	SDS-PAGE gel of H1-CRD purified by the FD, NFD and IB methods	123
Figure 39	Gal-Sepharose FPLC chromatograms and SDS-PAGE gel of NFD _{β-ME} and NFD _{DTT} methods.....	124
Figure 40	Gal and blank Sepharose HPLC chromatograms of H1-CRD binding	125
Figure 41	SDS-PAGE gel of active concentrated H1-CRD.....	125
Figure 42	SEC FPLC chromatograms in SEC _{Ca} , SEC ₀ and SEC _{EDTA}	127
Figure 43	SDS-PAGE gels of SEC-purified active H1-CRD	128
Figure 44	SDS PAGE gel of total IgY purified by the 9 different procedures	129
Figure 45	Comparison of lipid extraction and total IgY precipitation methods	130
Figure 46	Yield of total IgY purified by the 9 different procedures.....	131
Figure 47	Activity of IgY after lipid extraction and IgY precipitation.....	131
Figure 48	Activity of total IgY purified by the 9 different procedures	132
Figure 49	Comparison of the 9 different purification procedures M1-M9.....	132
Figure 50	Chromatogram of the anti-H1 IgY extraction on H1-CRD Sepharose.....	133
Figure 51	Yields of specific anti-H1 IgY antibodies	133
Figure 52	Fraction of specific anti-H1 IgY in % of the total IgY	134
Figure 53	SDS-PAGE gel of specific anti-H1 IgY of the 9 different procedures.....	134
Figure 54	SDS-PAGE gel of preparative total IgY extraction by procedure M8	135
Figure 55	Immunoblot of the H1-CRD staining with total IgY	136
Figure 56	Fluorescence microscopy of stained HepG2 and SK-Hep1 cells	137
Figure 57	Isotyping of the hybridomas.....	141
Figure 58	Immunoblot of the H1-CRD staining in supernatant of hybridomas	142
Figure 59	Binding of antibodies to the H1-CRD and H2-CRD in HRP-ELISA.....	142
Figure 60	Calcium dependence of hybridoma antibody binding in HRP-ELISA.....	143
Figure 61	Extracellular flow cytometry with hybridoma antibodies to HepG2	144
Figure 62	Intracellular flow cytometry of hybridomas of fusion A	144
Figure 63	Terasaki-cloning of hybridoma A47.....	146
Figure 64	Terasaki-cloning of hybridoma B01.....	147

Figure 65	Terasaki-cloning of hybridoma C48	147
Figure 66	Terasaki-cloning of hybridomas C09, C11, C14, C18 and C23.....	149
Figure 67	A47.3 IgM H1-Sepharose FPLC chromatogram and SDS-PAGE gel.....	150
Figure 68	A47.3 IgM Yield of the H1 and L-Sepharose chromatography.	151
Figure 69	A47.3 IgM Denaturing and native immunoblot of the H1-CRD	151
Figure 70	A47.3 IgM Titration in an HRP-ELISA	152
Figure 71	A47.3 IgM Ca sensitivity in an HRP-ELISA	153
Figure 72	A47.3 IgM Competition in the GalNAc-polymer assay.	153
Figure 73	A47.3 IgM Flow cytometry of HepG2, SK-Hep1, THP-1, macrophages and dendritic cells	154
Figure 74	A47.3 IgM Fluorescence microscopy of HepG2 and SK-Hep1 cells.....	155
Figure 75	B01.4 IgG1 G-Sepharose FPLC chromatogram and SDS-PAGE gel.....	156
Figure 76	B01.4 IgG1 Yield of the G and A-Sepharose chromatography.....	157
Figure 77	B01.4 IgG1 Denaturing and native immunoblot of the H1-CRD	158
Figure 78	B01.4 IgG1 Titration in an HRP-ELISA	158
Figure 79	B01.4 IgG1 Calcium sensitivity in an HRP-ELISA.....	159
Figure 80	B01.4 IgG1 Competition in the GalNAc-polymer assay	160
Figure 81	B01.4 IgG1 Biacore assay on H1-CRD monomer and dimer surfaces..	160
Figure 82	B01.4 IgG1 Binding kinetics in a Biacore assay	161
Figure 83	B01.4 IgG1 Epitope extraction and excision of the H1-CRD	162
Figure 84	B01.4 IgG1 Epitope extraction of the synthetic acetylated peptide	163
Figure 85	B01.4 IgG1 Epitope excision of the proteinase K-digested H1-CRD.	163
Figure 86	B01.4 IgG1 Flow cytometry of HepG2, SK-Hep1, THP-1, macrophages and dendritic cells	165
Figure 87	B01.4 IgG1 Fluorescence microscopy of HepG2 and SK-Hep1 cells.....	165
Figure 88	B01.4 IgG1 Immunostaining of non-pathological liver tissue.....	166
Figure 89	C09.1 IgG1 G-Sepharose FPLC chromatogram and SDS-PAGE gel.....	167
Figure 90	C09.1 IgG1 Yield of the G and L-Sepharose chromatography.....	168
Figure 91	C09.1 IgG1 Denaturing and native immunoblot of the H1-CRD	168
Figure 92	C09.1 IgG1 Titration in an HRP-ELISA	169
Figure 93	C09.1 IgG1 Calcium sensitivity in an HRP-ELISA	170
Figure 94	C09.1 IgG1 Competition in the GalNAc-polymer assay	170
Figure 95	C09.1 IgG1 Biacore assay on H1-CRD monomer and dimer surfaces.....	171
Figure 96	C09.1 IgG1 Flow cytometry of HepG2, SK-Hep1, THP-1, macrophages	

and dendritic cells	172
Figure 97 C09.1 IgG1 Fluorescence microscopy of HepG2 and SK-Hep1 cells.....	172
Figure 98 C09.1 IgG1 Immunostaining of non-pathological liver tissue.....	173
Figure 99 C11.1 IgG1 G-Sepharose FPLC chromatogram and SDS-PAGE gel.....	174
Figure 100 C11.1 IgG1 Yield of the G and L-Sepharose chromatography.....	175
Figure 101 C11.1 IgG1 Denaturing and native immunoblot of the H1-CRD	175
Figure 102 C11.1 IgG1 Titration in an HRP-ELISA	176
Figure 103 C11.1 IgG1 Calcium sensitivity in an HRP-ELISA	177
Figure 104 C11.1 IgG1 Competition in the GalNAc-polymer assay	178
Figure 105 C11.1 IgG1 Biacore assay on H1-CRD monomer and dimer surfaces.....	178
Figure 106 C11.1 IgG1 Binding kinetics in a Biacore assay	179
Figure 107 C11.1 IgG1 Epitope extraction of the trypsin-digested H1-CRD.....	180
Figure 108 C11.1 IgG1 Epitope extraction of the trypsin-digested, pronase K- excised H1-CRD	181
Figure 109 C11.1 IgG1 Flow cytometry of HepG2, SK-Hep1, THP-1, macrophages and dendritic cells	181
Figure 110 C11.1 IgG1 Fluorescence microscopy of HepG2 and SK-Hep1 cells.....	182
Figure 111 C11.1 IgG1 Immunostaining of non-pathological liver tissue.....	184
Figure 112 C14.6 IgG2a G-Sepharose FPLC chromatogram and SDS-PAGE gel.....	185
Figure 113 C14.6 IgG2a Yield of the G and L-Sepharose chromatography.....	185
Figure 114 C14.6 IgG2a Denaturing and native immunoblot of the H1-CRD	185
Figure 115 C14.6 IgG2a Titration in an HRP-ELISA	186
Figure 116 C14.6 IgG2a Calcium sensitivity in an HRP-ELISA	187
Figure 117 C14.6 IgG2a Competition in the GalNAc-polymer assay	187
Figure 118 C14.6 IgG2a Flow cytometry of HepG2, SK-Hep1, THP-1, macrophages and dendritic cells	188
Figure 119 C14.6 IgG2a Fluorescence microscopy of HepG2 and SK-Hep1 cells.....	189
Figure 120 C14.6 IgG1 Immunostaining of non-pathological liver tissue.....	189
Figure 121 C18.1 IgG1 H1-Sepharose FPLC chromatogram and SDS-PAGE gel.....	190
Figure 122 C18.1 IgG1 Yield of the H1, G and L-Sepharose chromatography.....	191
Figure 123 C18.1 IgG1 Denaturing and native immunoblot of the H1-CRD	191
Figure 124 C18.1 IgG1 Titration in an HRP-ELISA	192
Figure 125 C18.1 IgG1 Calcium sensitivity in an HRP-ELISA	193
Figure 126 C18.1 IgG1 Competition in the GalNAc-polymer assay	193

Figure 127 C18.1 IgG1 Biacore assay on H1-CRD monomer and dimer surfaces.....	194
Figure 128 C18.1 IgG1 Binding kinetics in a Biacore assay	194
Figure 129 C18.1 IgG1 Flow cytometry of HepG2, SK-Hep1, THP-1, macrophages and dendritic cells	195
Figure 130 C18.1 IgG1 Fluorescence microscopy of HepG2 and SK-Hep1 cells.....	196
Figure 131 C18.1 IgG1 Immunostaining of non-pathological liver tissue.....	197
Figure 132 C23.8 IgG1 H1-Sepharose FPLC chromatogram and SDS-PAGE gel.....	198
Figure 133 C23.8 IgG1 Yield of the H1, G and L-Sepharose chromatography.....	199
Figure 134 C23.8 IgG1 Denaturing and native immunoblot of the H1-CRD	200
Figure 135 C23.8 IgG1 Titration in an HRP-ELISA	201
Figure 136 C23.8 IgG1 Calcium sensitivity in an HRP-ELISA	201
Figure 137 C23.8 IgG1 Competition in the GalNAc-polymer assay	202
Figure 138 C23.8 IgG1 Biacore assay on H1-CRD monomer and dimer surfaces.....	202
Figure 139 C23.8 IgG1 Flow cytometry of HepG2, SK-Hep1, THP-1, macrophages and dendritic cells	203
Figure 140 C23.8 IgG1 Fluorescence microscopy of HepG2 and SK-Hep1 cells.....	204
Figure 141 C48.9 IgG1 H1-Sepharose FPLC chromatogram and SDS-PAGE gel.....	206
Figure 142 C48.9 IgG1 Yield of the H1, G and L-Sepharose chromatography.....	206
Figure 143 C48.9 IgG1 Denaturing and native immunoblot of the H1-CRD	207
Figure 144 C48.9 IgG1 Titration in an HRP-ELISA	208
Figure 145 C48.9 IgG1 Calcium sensitivity in an HRP-ELISA	208
Figure 146 C48.9 IgG1 Competition in the GalNAc-polymer assay	209
Figure 147 C48.9 IgG1 Biacore assay on H1-CRD monomer and dimer surfaces.....	210
Figure 148 C48.9 IgG1 Flow cytometry of HepG2, SK-Hep1, THP-1, macrophages and dendritic cells.	210
Figure 149 C48.9 IgG1 Fluorescence microscopy of HepG2 and SK-Hep1 cells.....	211
Figure 150 Overview of the H1-CRD production	214
Figure 151 H1-CRD disulfide linkage according to the MS.....	217
Figure 152 Overview of the expression optimization	217
Figure 153 Overview of the purification optimization	220
Figure 154 Overview of the refolding buffer composition.....	221
Figure 155 Effect of β -mercaptoethanol and DTT onto the refolding	222
Figure 156 Comparison of the 6 different purification procedures.....	223
Figure 157 Contribution of the optimization steps to the H1-CRD production	224

Figure 158 Overview of the anti-H1 antibody production and characterization.....	227
Figure 159 Immunization scheme of hens to produce polyclonal anti-H1 IgY	228
Figure 160 Extraction of the specific IgY from egg yolk.....	229
Figure 161 IgY yield/egg arranged by the total IgY extraction methods.	230
Figure 162 Immunization scheme of mice to produce monoclonal anti-H1 Ig	233
Figure 163 Hybridomas from fusions A, B and C.	234
Figure 164 Features of the selected hybridomas.	235
Figure 165 Minimal epitope of the monoclonal B01.4 IgG1.	237
Figure 166 Disulfide linkage in the H1-CRD. A: proposed. B: by Spiess <i>et al.</i> ...	239
Figure 167 Yields of monoclonal anti-H1 antibodies	244
Figure 168 B01.4 and C11.1 epitopes on the surface of the H1-CRD.....	245
Figure 169 Types of the calcium sensitivity	248
Figure 170 Ranking of the anti-H1 Ig according to the EC_{50} , the IC_{50} and the I%.....	249
Figure 171 Plot of the monoclonal anti-H1 IgG1 ranking in the Biacore assay.....	251
Figure 172 Binding kinetics of the anti-H1 IgG1 B01.4, C11.1 and C18.1.....	252
Figure 173 Overall ranking of the monoclonal anti-H1 antibodies.....	255

Formulations

Formulation 1	Composition of the PCR mastermix with <i>Taq</i> and <i>Pfu</i> polymerase.....	51
Formulation 2	Composition of the restriction digest of H1-CRD cDNA with <i>BamH</i> I.....	52
Formulation 3	Composition of the restriction digest of pEZZ18 with <i>Sma</i> I or <i>BamH</i> I ..	53
Formulation 4	Composition of the dephosphorylation of linearized pEZZ18	53
Formulation 5	Composition of the ligation of H1-CRD cDNA into pEZZ18.....	54
Formulation 6	Setup of the restriction digest with <i>Nde</i> I or with <i>Nde</i> I and <i>BamH</i> I	57
Formulation 7	Composition of the PAGE separating and stacking gel.....	59
Formulation 8	Composition of the supplemented cell culture media.....	77

Tables

Table 1	Differences of the state 1 and 2 endocytosis pathways of the ASGPR.....	8
Table 2	Characteristics of the antibody classes of mice and chicken.....	17
Table 3	Choice of antibodies in immunochemical methods	41
Table 4	Antibiotics for the cultivation of <i>E.coli</i> strains and transformants	46
Table 5	Primary and secondary antibodies of the immunostaining	62
Table 6	Refolding buffer systems A to D.....	69
Table 7	Sequence homologies of the ASGPR-1, H1-CRD and its binding site..	107
Table 8	Concentration of additives to the basic refolding buffer after refolding .	121
Table 9	Yields of the preparative expressions	126
Table 10	Yields of IgY/egg purified by the different method procedures	135
Table 11	Schedule of the NMRI mice immunization and PEG fusions.....	138
Table 12	Schedule of the Balb/c mice immunization and PEG fusions	139
Table 13	Loss of positive hybridomas from fusions A and B	140
Table 14	Loss of positive hybridomas from fusion C	140
Table 15	Summary of the hybridoma fingerprint characterization	145
Table 16	Blastp of the B01.4 epitope against the non-redundant GenBank.....	164

Summary

The asialoglycoprotein receptor (ASGPR), composed of the subunits H1 and H2, is predominantly expressed on the sinusoidal surface of mammalian hepatocytes and involved in the endocytosis of desialylated multiantennary glycans with terminal Gal or GalNAc residues via the clathrin-coated pit pathway. Although investigated for many years, the physiological function and ligands are still unknown. Until nowadays, only polyclonal antibodies and two monoclonal against the ASGPR are reported. However, no monoclonal antibodies, which are specifically directed against the carbohydrate recognition domain (CRD), responsible for Gal binding and internalization, are available. Such antibodies would be precious tools for ASGPR examination. In addition, since the human ASGPR is a promising liver-specific therapeutic target, an antibody-based high affine and specific drug or gene delivery system would be valuable.

The H1-CRD was recombinantly expressed in *E.coli* and purified active H1-CRD was used for immunization to produce antibodies. Because the published expression and purification method of Meier *et al.*²⁶ yielded only an H1-CRD amount of 130µg/L culture, various *E.coli* strains, vectors, expression conditions and renaturation procedures were tested. With the optimized expression in *E.coli* AD494(DE3), which was transformed with the H1-CRD cDNA-encoding pET3b vector, and with the following modified purification procedure, 55mg (20mg/L) active H1-CRD were successfully produced.

For analytical purpose, polyclonal antibodies directed against the H1-CRD (anti-H1) were obtained by chicken immunization and IgY purified from egg yolk by PEG precipitation. The 12g (45mg/egg) purified total IgY contained approximately 7% anti-H1 specific IgY. Total IgY and isolated anti-H1 specific IgY antibodies showed to be suitable in various immunochemical *in vitro* methods but not in immunocytochemistry.

Although the amino acid sequences of the mouse and human ASGPR H1-CRD are 79% identical, monoclonal antibodies were successfully produced by the hybridoma technology. Eight of twenty hybridomas were selected and cloned for further characterization of their monoclonal antibodies: *in vitro* in immunoblotting, immunoassays, Biacore assays and in epitope mapping, *on cell* in flow cytometry and fluorescence microscopy and *in tissue* in immunohistochemical tests. Two of them, C14.6 and particularly C11.1 showed a very interesting profile, not only for application in immunochemical techniques but probably also for diagnostic and therapeutic use.

1 Introduction

The liver is the main metabolic organ, is involved in production of inflammatory mediators and serum plasma proteins. Hence, hepatocytes are an attractive target for selective gene therapy to correct genetic defects, such as analbuminaemia, hemophilia and lipoprotein receptor deficiency, or for specific delivery of drugs to cure hepatitis B and C and hepatocellular carcinoma.¹

One potential liver specific receptor is the asialoglycoprotein receptor (ASGPR), a carbohydrate binding protein (lectin), which specifically recognizes desialylated glycans with terminal galactose (Gal) or galactosamine (GalNAc) residues, for the internalization via the clathrin-mediated endocytosis pathway.

Until nowadays, many attempts were undertaken to specifically deliver galactosylated carriers to the liver.² However, as carbohydrate-protein interactions are exceptionally weak, higher affine glycomimetics or antibodies would be of great advantage for targeted therapies.

Although such a promising therapeutic receptor, there exists no antibody-based delivery system to the ASGPR and even, there is only reported of some polyclonal and of two partially characterized monoclonal antibodies directed against the whole ASGPR. However, no monoclonal antibodies exist, which specifically interact with the carbohydrate binding site of the human ASGPR^{3,4,5,6,7}.

This branding task was the topic of this thesis, namely the production and characterization of monoclonal and polyclonal antibodies directed against the carbohydrate recognition domain of the human hepatic ASGPR.

In the following, the first part will introduce the ASGPR to get familiar with its structure and function. Furthermore, some methodological information to the recombinant production of the carbohydrate binding-domain, which served as antigen, is enclosed. The second part will deal with the counterpart of the antigen, the antibody. On the one hand, the production of antibodies *in vivo*, which results in different types of antibodies, the antibody structures and the antibody characteristics, will briefly be mentioned. On the other hand, the production of antibodies *in vitro* will be outlined to understand where monoclonal and polyclonal antibodies are originated. The third part finally will give some theoretical background to the various immunochemical methods, which were applied for the characterization of the different antibodies.

1.1 The hepatic asialoglycoprotein receptor

The hepatic ASGPR was first reported by Ashwell G. *et al.*⁸ and is also designated Ashwell lectin, hepatic lectin (HL) or hepatic binding protein.

1.1.1 Location of the ASGPR

The hepatic ASGPR is predominantly expressed on the sinusoidal, basolateral surface of hepatocytes.

In human, homologous ASGPR are only found on primary cells like peritoneal macrophages, immature dendritic cells and granulocytes (but were absent on T-cells, B-cells, neutral killer cells, monocytes and mature dendritic cells)^{9,10}, on renal proximal tubular epithelial cells¹¹, on sperm¹² and on thymocytes¹³. In great contrary to rat, human Kupffer cells do not express the ASGPR.¹⁴

The ASGPR was also identified on continuous human hepatic cell lines like HepG2,¹⁵ HUH-7,¹⁶ and PRF/5 hepatoma cells but not on Chang or SK-Hep1 hepatoma cells. Also extrahepatic human cell lines like HT-29¹⁷ and Caco-2¹⁸ intestinal epithelial cells, Tera-1 embryonal carcinoma cells and surprisingly Jurkat lymphoblastic cells were ASGPR-positive. Other extrahepatic cell lines like HeLa fibroblastic cells, HL-60R promyelocytic cells, WISH amnion cells, A498 kidney cells and U87-MG neuronal cells did not express the ASGPR.⁵

The Gal / GalNAc specific hepatic lectins of mammalian, like mouse, rat, rabbit and human, exhibit high amino acid sequence homologies, but also the phylogenetically more distant birds, like chicken possess an analogous but glucosamine (GlcNAc) specific hepatic lectin.¹⁹

1.1.2 Structure of the ASGPR

To deduce the primary structure of the ASGPR (see Figure 1), the cDNA was isolated from HepG2 cells.

Structure of the human ASGPR

The ASGPR is a heterooligomeric glycoprotein, formed by two homologous subunits, the major H1 and the minor H2. The subunit composition in and the size of the functional receptor are still not established and are controversially reported. The estimated minimal size of the active ASGPR is 140kDa.²⁰ In agreement with that, Hardy *et al.*²¹ proposed a trimeric core, composed of two H1 and one H2. But Bider *et al.*²² demonstrated, that H1

and H2 preferentially form heterotetramers in a ratio of 2:2 and Henis *et al.*²³ concluded, that the ASGPR consists of a trimeric H1 core which can associate with one to three H2, resulting in H1:H2 heterooligomers of 3:1 to 1:1.

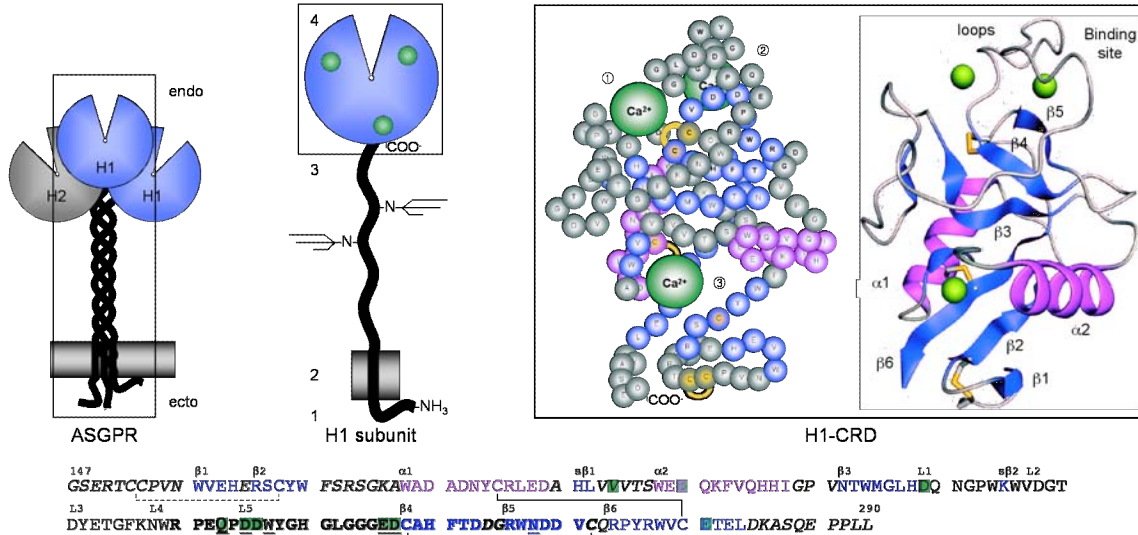


Figure 1: Human hepatic ASGPR, a heterooligomeric complex composed of homologous H1 and H2 subunits, model by Hardy *et al.* The H1 subunit is a type-II integral glycoprotein with the cytoplasmic N-terminal domain (1), the transmembrane domain (2) and two extracellular domains: the twice N-glycosylated stalk region and the C-terminal CRD, containing three calcium ions. The H1-CRD forms three conserved intramolecular disulfide bridges and binds calcium-dependent to Gal or GalNAc. The essential calcium ion for binding is located in site 2 (②) whereas the other two calcium ions in sites 1 (①) and 3 (③) are necessary for the structure. They are coordinated by 11 amino acid residues (■). The primary structure is folded into 6 long β -strands (β 1- β 6) and 2 short β -strands ($s\beta$ 1, $s\beta$ 2), which form 3 β -sheets, 2 α -helices (α 1, α 2) and 5 loops (L1-L5). The active binding site (**bold**) lies in the region of L4, L5, β 4 and β 5 and contains the calcium 2. This calcium ion is coordinated to Q²³⁹, D²⁴¹, E²⁵², N²⁶⁴, D²⁶⁵ and O atoms of two water, which are replaced by O atoms of 3' and 4' OH of GalNAc upon binding. GalNAc in addition undergoes interactions with 6 amino acid residues (Q²³⁹, D²⁴¹, W²⁴³, E²⁵², D²⁵³, N²⁶⁴).

Glycosylated H1 and H2 are about 46kDa (deglycosylated about 34kDa)⁶ and 50kDa in size. They are mainly distinct in an 18 amino acid insert, which is only present in H2,²⁴ and in the number of N-linked glycosylations, that are two for H1 and three for H2. Both are similar organized integral proteins and exhibit 58% amino acid sequence identity.^{3,24,25}

Structure of the H1 subunit

The H1 subunit is a type-II membrane glycoprotein, which spans 290 amino acid residues and is composed of the N-terminal cytoplasmic domain, the single-spanning transmembrane domain and the extracellular domain, formed by a stalk region and the C-terminal carbohydrate recognition domain (CRD).²⁵

The cytoplasmic domain encloses 40 residues and encodes the tyrosine-based sorting signal YXXØ (Tyr⁵Gln⁶Asp⁷Leu⁸) for endocytosis, is transiently phosphorylated at Tyr⁵, Ser¹⁶ and Ser³⁷, and is palmitoylated at Cys³⁶.

The transmembrane domain includes about 20 residues.

The stalk region is formed by about 80 residues and carries two N-linked glycosylations (Asp⁷⁹PheThr, Asp¹⁴⁷GlySer) with terminal sialyl acids, which are probably essential to retain the receptor in its active state. The heptad repeats stalk region may oligomerize with the stalk regions of other subunits to constitute a α -helical coiled coil stalk.²²

The H1-CRD of 145 residues finally is a globular domain, which contains three calcium ions and three intramolecular S-S bonds. Therefore, the H1-CRD belongs to the long-form C-type lectins.

The structure of the H1-CRD domain

The X-ray structure of the 16'860Da H1-CRD was elucidated by Meier *et al.*²⁶

The H1-CRD is a globular domain with the C-terminus close to the N-terminus. The primary structure is folded to six long and two short β -strands, which are arranged in three β -sheets, two α -helices and five loops. Three calcium ions are an integral part of the H1-CRD. The two calcium ions in sites 1 and 3 contribute to the structural maintenance, whereas the calcium in site 2 is essential for Gal and GalNAc binding. This calcium, together with loop 4, the glycine rich loop 5, β -strand 4 and β -strand 5 form the sugar binding site (Arg²³⁶-Cys²⁶⁸). The binding site is enclosed by an intramolecular disulfide bridge (Cys¹⁸¹-Cys²⁷⁶) and contains an internal S-S bond (Cys²⁵⁴-Cys²⁶⁸). The third disulfide linkage could not be positioned in X-ray, but was proposed to pair Cys¹⁶⁴ and Cys¹⁵² or Cys¹⁵³.

1.1.3 ASGPR-ligand interaction – determinants of high avidity binding

Binding mode

The binding mode of GalNAc to the H1-CRD was proposed according to Drickamer *et al.*²⁷ In this model, Gal NAc interacts with carboxy and amino groups of six amino acid residues (Q²³⁹, D²⁴¹, W²⁴³, E²⁵², D²⁵³, N²⁶⁴) in the binding site. In addition, the 3' and 4' hydroxy groups of GalNAc replace the O atoms of two water molecules, which are coordinated to the calcium in site 2.

Structure of the ligands

The ligands are complex-type N-linked desialylated glycans with terminal β -Gal or β -D-GalNAc residues, e.g. asialoorosomuroid (ASOR) and asialofetuin (ASF). The affinities are low, but about 20-fold higher for GalNAc compared to Gal.²⁸ Surprisingly, Park *et al.*²⁹ reported, that H1 also bound to sialylated glycans with terminal Sia α -2,6-GalNAc.

High avidity binding of ligands to the ASGPR

The ligand specificity of the ASGPR mainly depends on the terminal sugar, the ligand valency and the carbohydrate spacing. The affinity of GalNAc and especially of Gal to the CRD is low. Simultaneous binding of multiantennary glycosides to multiple subunits of the ASGPR increases the avidity significantly. Whereas the affinity of a monoantennary galactoside is only in the mM range, the avidity of a triantennary or tetraantennary galactoside is in the nM range. Hardy *et al.*²¹ as well as Henis *et al.*²³ concluded, that the interaction of the triantennary or tetraantennary ligand involves one H2 and two H1 binding sites of the ASGPR. This simultaneous binding is only possible when the terminal sugars are at least 1.5nm spaced.^{30,31}

Furthermore, the ASGPR must be functional and active. H2 homooligomers alone cannot, but H1 homooligomers are able to bind to asialoorosomuroid.^{11,32} Additionally, mouse H1 alone can bind to ASOR, but for high affinity binding and for endocytosis, the ASGPR must be a heterooligomeric complex composed of both subunits, the H1 and the H2.^{33,34}

Finally, the N-linked glycosides on the stalk of the ASGPR must be sialylated. The hyposialylated ASGPR is inactive. This was presumed to be the result of self-binding to the exposed penultimate Gal among subunits of the ASGPR.³⁵

1.1.4 ASGPR-mediated endocytosis pathways

Glycans with terminal Gal or GalNAc are selectively internalized into hepatocytes by clathrin-mediated endocytosis via the ASGPR, an endocytic recycling receptor.³⁶ In contrast, glycans with terminal Man are targeted to Kupffer cells (see Figure 2).

Tolchinsky *et al.*³⁷ and Yik *et al.*³⁸ reported, that there exist ASGPR subpopulations, which mediate distinguishable, parallel endocytosis pathways, the state 1 and the state 2. Both follow the common clathrin-coated pit pathway, but state 2 exhibit some peculiarities and is more stringent regulated. The internalization and recycling pathways were mainly investigated in HepG2 cells.

ASGPR subpopulations

H2 exists in three isoforms, designated H2a, H2b and H2c, which result from distinct DNA splicing. They differ in a 19 amino acid cytoplasmic insert and a 5 amino acid juxtamembrane insert, which serves as a cleavage signal. H2a express both inserts and get cleaved proteolytically. Hence, the entire ectodomain is secreted into the blood and H2a does not oligomerize with H1 to ASGPR complexes. H2b contains the 19 residues insert but lacks the pentapeptid signal, and H2c lacks both inserts and therefore undergo no proteolysis. Both form membrane-anchored complexes with H1 but were never present in the same ASGPR complex. As a consequence, there exist two distinct ASGPR subpopulations, the H1/H2b and the H1/H2c heterooligomers. The H2b but not H2c can be phosphorylated at Ser of the 19 residues insert, which enables receptor modulation. Hence, H1/H2b complexes were proposed to mediate the faster state 2 endocytosis and H1/H2c complexes to traffic to the slower state 1 pathway.³⁸

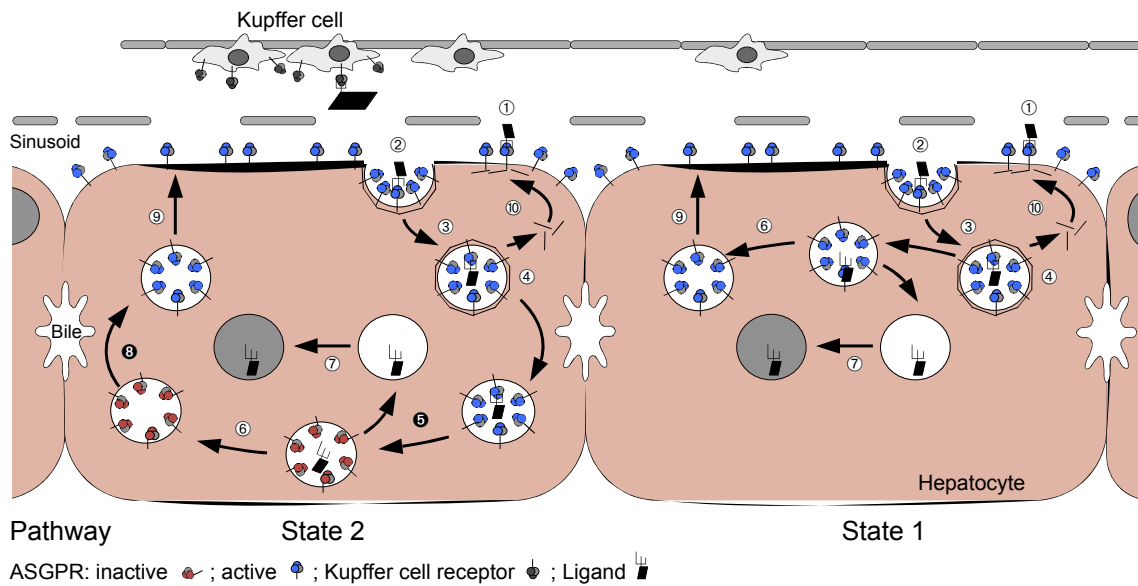


Figure 2: Selective uptake of glycoconjugates with terminal Gal or GalNAc into hepatocytes via the ASGPR-mediated endocytosis pathways. In contrast glycoconjugates with terminal Man are targeted to Kupffer cells. ① Ligand binding; ② ASGPR-ligand clustering; ③ ASGPR-ligand internalization in clathrin-coated vesicles; ④ ASGPR-ligand dissociation and fusion with CURL; ⑤ ASGPR inactivation; ⑥ Segregation of ASGPR and ligand by fission of CURL into ligand-containing and ASGPR-containing vesicles; ⑦ ligand delivery to lysosomes and degradation; ⑧ ASGPR reactivation in the trans-golgi-network; ⑨ ASGPR recycling; ⑩ clathrin recycling.

ASGPR endocytosis pathway

The ASGPR is highly abundant in HepG2 cells, with about $2.25 \cdot 10^5$ /cells. 50-80% of them are found at the surface and the remaining ones intracellular. It is internalized constitutively and also in the absence of ligand, but upon ligand binding, the endocytosis rate increases and the number of surface receptors decreases.^{3,39}

The ASGPR-ligand complexes cluster in clathrin-coated pits and recruit clathrin-associated adaptor complexes, which recognize the Tyr-containing endocytosis signal of H1. After invagination into the clathrin-coated vesicles, the clathrin cages unseat and the early endosomes fuse with the CURL (compartment for uncoupling of receptors and ligands). In the acidic environment of pH 5.4 in these prelysosomal endocytic vesicles, the ASGPR and the ligand dissociate and segregate by fission of CURL into receptor-containing and ligand-containing vesicles. The ligand is delivered to lysosomes for degradation, whereas the ASGPR recycles to the sinusoidal plasma membrane.⁴⁰

State 1 versus state 2 pathway

Only about 20% of ligands are endocytosed by the slower state 1 pathway, whereas the faster state 2 pathway mediates about 80% of ligand internalization and degradation and therefore is at least 7 times more efficient.

Table 1: Differences between state 1 and state 2 endocytosis pathways of the H1/H2c and H1/H2b ASGPR.

Endocytosis pathway	State 1	State 2
ASGPR complex	H1/H2c	H1/H2b
Dissociation, K_D (ASOR)	Fast, 1.6nM	Slow, 3.9nM
ASGPR I/R cycle	Yes I: (ATP depletion, drugs, low temperature) R: (Cys palmitoylation)	No
Constitutive recycling	No	Yes

In the state 1 endocytosis pathway, dissociation of ASGPR-ligand complexes is mediated by acidification in the CURL, that causes the lost of calcium affinity in the ASGPR. The efficiency of dissociation is dependent on the ligand concentration in the vesicle. In contrast, in the state 2 pathway, the ASGPR-ligand complex dissociation is caused by ASGPR inactivation due to ATP depletion. Hence, the efficiency of ligand release is independent of its concentration in the CURL, is rapid and complete. Prior to recycling to the surface, the ASGPR is reactivated by Cys palmitoylation, probably at H1 or H2b. Beside this inactivation / reactivation cycle, another peculiarity is, that the state 2

ASGPR internalizes and recycles constitutively and also in the absence of ligands, whereas the state 1 ASGPR does not (see also Table 1).

Modulation of the ASGPR endocytosis

As already mentioned, hyposialylation of the N-linked carbohydrate chains on the stalk keeps the ASGPR in an inactive state due to self-binding to the exposed terminal Gal. This allows fast receptor up-regulation, i.e. the increase of the glucose concentration enhances the number of active ASGPR and their binding affinity, whereas the total number of ASGPR at the surface remains constant.⁴¹ However, IL-1 β , IL-6 and TNF- α rise and ethanol lowers the total number of ASGPR in the plasma membrane.⁴²

1.1.5 Physiological functions of the ASGPR

The ASGPR is investigated for about thirty years, but nevertheless, neither the endogenous ligand(s) nor the physiological function(s) are established.

Although homozygous H1 or H2-deficient knockout mice are unable to clear ASOR, they display no phenotypic abnormalities and do not accumulate desialylated glycoproteins or glycolipids. The ASGPR is postulated to clear defective desialylated plasma glycoproteins.⁴³ Beside ASOR and ASF, chylomicron remnants and low density lipoproteins bind and hence, the ASGPR may be involved in lipid uptake *in vivo*.⁴⁴ The ASGPR may also play a potential role in the phagocytosis of dying cells, since the isolated ASGPR mediates mitogen-stimulated cellular cytotoxicity.⁴⁵

Furthermore, the ASGPR is reported to be involved in several hepatic disorders. Autoimmune hepatitis is connected with the appearance of autoantibodies against the H1 in human.⁴⁶ The ASGPR is inhibited by IgA and may be involved in pathogenesis of IgA nephropathy and cirrhosis.⁴⁷ In addition, the ASGPR also recognizes exogenous glycans on pathogens like Hepatitis B and Marburg virus, which are reported to enter hepatocytes via the ASGPR.^{48,49}

1.1.6 Recombinant expression of protein in *E.coli*

In vitro, protein can be produced in bacterial, yeast, insect or mammalian expression systems. In contrast to eukaryotic expression, in procaryotic expression, proteins are not posttranslationally modified.

The recombinant production of a mammalian protein in *E.coli* consists of three stages. The first stage is the construction of the *E.coli* expression system and is composed of

the cDNA cloning into the expression vector followed by the transformation of the recombinant plasmid into *E.coli* expression strains. In the second stage, the protein is expressed in the culture of recombinant *E.coli* in soluble form or in insoluble inclusion bodies. The protein accumulates in the reductive cytoplasm, is directed to the oxidative periplasm or is secreted into the medium. In the third stage, the expressed protein is purified from the expression culture and renatured to the native and active protein (see Figure 3).⁵⁰

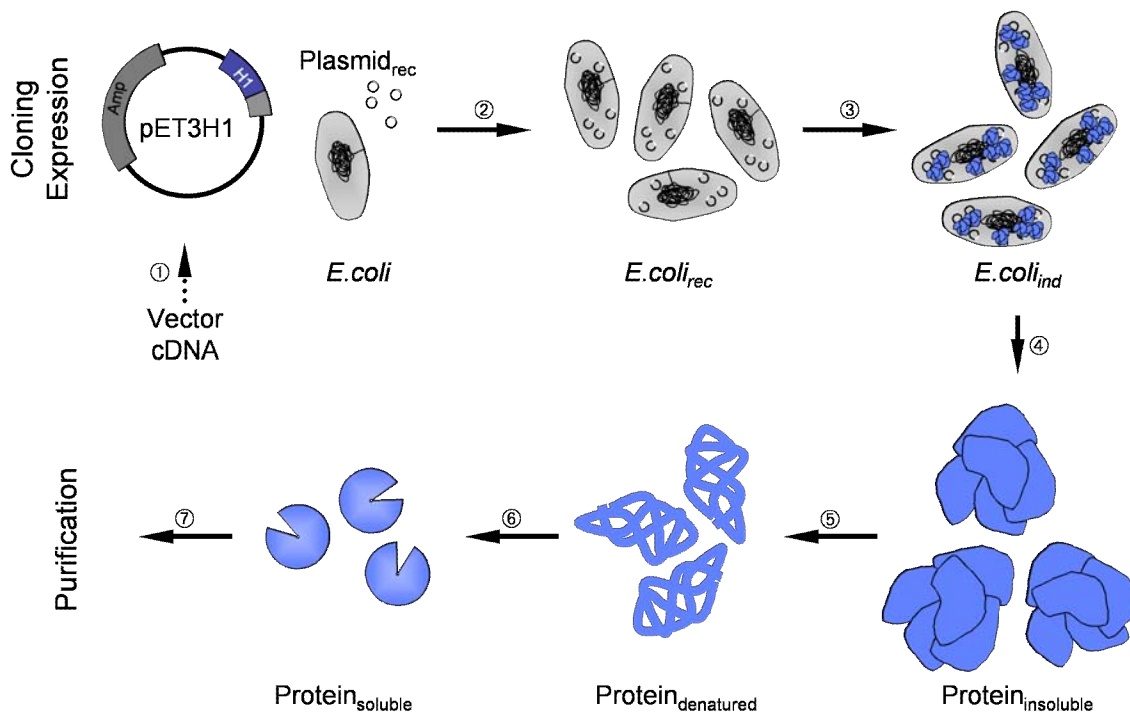


Figure 3: Overexpression of recombinant mammalian protein in *E.coli*. ① Cloning of cDNA into the expression vector to get the recombinant plasmid; ② Transformation of *E.coli* with recombinant plasmid; ③ Expression of protein in a culture of transformed *E.coli*; ④ Cell lysis and isolation of insoluble inclusion bodies ⑤ Reductive solubilization of inclusion bodies; ⑥ Oxidative refolding of soluble denatured protein; ⑦ Refolding of soluble protein.

1.1.6.1 Construction of *E.coli* expression systems – the “protein factories”

In a first step, the *E.coli* system is constructed. The protein-encoding cDNA is amplified with a high-fidelity DNA polymerase to prevent mutations in the coding region, then is introduced into expression vectors and transformed into *E.coli* strains. The optimal vector-*E.coli* strain combination mainly depends on the features of the recombinant protein, i.e. the content of Cys, solubility, stability and the content of rare *E.coli* codons. The best expression system must be determined empirically.

Expression vectors – keep in the cell or turn out of the cell

The expression vector guides the protein expression, directs the expression rate and the location. An efficient *E.coli* expression vector contains a strong and regulated promoter for efficient transcription, a Shine-Dalgarno site for rRNA binding, the translation initiation codon ATG for translation start and a transcription terminator. In addition, the vector requires an origin of DNA replication and a selection marker. The regulatory gene to control the promoter activity and expression level can be integrated in the vector or in the *E.coli* chromosome. The pET3b vector⁵¹ for example is under the control of the strong T7 promoter that enables transcription by the T7 RNA polymerase. The gene for T7 RNA polymerase (λ DE3) is encoded by the *E.coli* genome, under the control of the IPTG-inducible lacUV5 promoter. The inducer IPTG permits to initiate the protein expression and to regulate the expression rate.

The vectors, which guide the protein to the periplasmic space or into the medium includes additionally a signal sequence for secretion. Optionally, the expression vector may encode a fusion tag or protein to enhance the efficient translation initiation, to improve native folding, stability and solubility of the expressed protein and to facilitate the protein purification. The pEZZ18 vector for example encodes the protein A signal sequence for secretion and the ZZ domain, a synthetic IgG binding domain, which is fused to the recombinant protein. This enables to direct the fusion protein into the medium and to purify it simply by affinity to IgG.

Commonly, cytoplasmic production is simpler, but the protein tends to accumulate in inclusion bodies and the reductive environment hinders the formation of disulfide bridges. In contrast, periplasmic production or secretion is often difficult, because the protein has to cross the membrane. However, the oxidizing environment of the periplasmic space enables the pairing of disulfide bridges and facilitates proper folding. Nevertheless, also in the periplasm, the protein can aggregate in inclusion bodies especially, when the protein contains multiple S-S bonds.⁵²

E.coli strain – selection of the most generous host by try and error

There exist many *E.coli* expression strains. They differ in their features to support folding, solubility and stability of the expressed protein. The vector and the encoded protein define the strains that are suitable, but they must be established empirically.

In *E.coli*, the cytoplasmic thioredoxin-glutaredoxin system catalyzes reductive processes and hinders disulfide pairing.⁵³ The *E.coli* strains, which are deficient in this system, e.g.

AD494(DE3) and Rosetta-gami(DE3)TM offer a more oxidizing cytoplasmic environment and that enables the formation of S-S bonds. The protease-deficient *E.coli* strains minimize protein degradation during expression, but also during purification. The *E.coli* strains, which coexpress the tRNA for rare *E.coli* codons, e.g. Rosetta-gami(DE3)TM facilitate the expression of proteins with a high number of rare amino acids.

1.1.6.2 Expression

The production level of a recombinant *E.coli* expression system is not only influenced by *E.coli* intrinsic factors, i.e. the expression vector and the *E.coli* strain, but also by *E.coli* extrinsic expression conditions: i.e. the medium, the cell density, the temperature, the pH, the aeration, the inducer concentration and the expression period.

There exist no general rules and the optimal expression conditions must be determined for each individual recombinant expression system empirically.

1.1.6.3 Protein purification and protein renaturation from inclusion bodies

Cytoplasmic overexpressed protein often accumulates in high dense, insoluble and inactive inclusion bodies. The protein in inclusion bodies is shielded from proteolytic attack. The aggregate contains relatively pure denatured protein in oxidized and reduced, monomeric and multimeric states. The inclusion body formation is mostly advantageous for purification. The main difficulty is to recover active protein.

The renaturation of isolated inclusion bodies is a two-step procedure: i.e. the reductive solubilization and the oxidative refolding.⁵⁴ There exist no general rules for efficient renaturation. Solubilization and refolding must be optimized empirically for each individual protein.

*Reductive solubilization*⁵⁵

The solubilization consists of three steps: the cell lysis, the isolation of inclusion bodies and the solubilization of inclusion bodies proteins. The cells are completely disrupted by sonication, by French press or by enzymatic cleavage with lysozyme and the inclusion bodies are isolated by centrifugation. To remove contaminations of membrane proteins, the isolated inclusion bodies are stringently washed. The inclusion bodies are solubilized with denaturants (urea, guanidine HCl), which form hydrophobic interactions with the protein, and the misspaired disulfide bridges are reversible broken with reductants, i.e. β -mercaptoethanol or dithiothreitol.

*Oxidative refolding*⁵⁶

The major problem of oxidative refolding is the competition between intramolecular folding and intermolecular aggregation. This competition mainly depends on refolding conditions, i.e. the ionic buffer strength, the protein concentration and purity, the temperature, the pH, the time and the presence of folding enhancers. The tendency to aggregate is correlated with the protein itself and the number of S-S bonds.

- Protein concentration. Only denatured protein but not native protein is susceptible to aggregation. A low concentration of denatured protein minimizes intermolecular interaction and favors folding. Mostly, the protein is fast diluted to avoid a high local concentration of denatured protein and the formation of instable folding intermediates.
- Temperature. The temperature significantly influences the refolding rate.
- pH. The pH defines the protein charge. At its isoelectric point, the protein is minimal soluble and preferentially aggregates. A neutral to alkaline pH enables rapid disulfide bridge formation while an acidic pH inhibits disulfide pairing.⁵⁷
- Time. The time for refolding varies from seconds to days. The oxidative refolding often requires longer periods of up to weeks.
- Folding enhancers: Folding enhancers are low molecular weight additives, which interfere with protein refolding mainly by slight destabilization: i.e. denaturants in subdenaturing concentrations, glycerol, metal ions if proteins contain cofactors in the native state and ligands to destabilize folding intermediates and stabilize native folded protein. In oxidative refolding of Cys-containing proteins, a thiol-active redox-system, mostly reduced and oxidized glutathione enable reshuffling of misspaired Cys and facilitate the formation of correct disulfide bridges. In the S-S reshuffling, glutathione interacts in a first stage with one Cys thiol group of the protein to form a mixed disulfide and in a second stage, the mixed disulfide reacts with a second Cys thiol group of the protein to form a disulfide bond.⁵⁸ In proteins with multiple disulfide bonds, the number of possible combinations for S-S bonds pairing increases rapidly: e.g. with 7 Cys, 48 folding intermediates may be formed.

Refolding of solubilized inclusion bodies is mostly performed by dilution and dialysis or gel filtration. During dialysis, solubilizing agents are slowly removed and simultaneously, stable conformational intermediates are formed, which are finally converted into the native and active protein.

1.2 The antibodies – structure, feature and production

The antibodies, also called immunoglobulins are glycoproteins, which have all the same basic structure but exhibit highly diverse binding specificities.

1.2.1 Antibody structure

The antibody structure (see Figure 4) can be described from a molecular or functional point of view.

Molecular antibody structure

The basic Y-shaped antibody molecule is composed of two identical heavy (H) and two identical light (L) chains, those are held together by inter-chain disulfide bonds and non-covalent interactions. The chains can be divided into two main regions, based on the variability of their amino acid sequence: the constant (C) and the variable (V) region. The regions are formed by one to four globular domains of about 110 amino acid residues, which all include an intra-chain disulfide bond.

The light chain (23kDa) contains one N-terminal V domain (V_L) and one C-terminal C domain (C_L). The heavy chain (50-70kDa) is composed of one N-terminal V domain (V_H) but of three or four C-terminal C domains (C_{H1-4}).

The primary structure of the V domain is fold to four β -strands of framework regions (FR1-4), which enclose three loops of hypervariable complementarity-determining regions (CDR1-3).

Each CDR consists of 5 to 10 highly variable amino acid residues. However, all except CDR3 of the H chains exhibit one out of few main chain conformations, which are designated canonical structures. The framework regions contain conserved amino acid residues and form the backbone of the CDR1-3.

Functional antibody structure

The basic antibody can be divided into two major functional regions, the fragments having the antigen binding site (Fab) and the fragment that crystallize (Fc). A hinge region connects the two identical Fab regions to one Fc region.

The variable monovalent Fab region is composed of the aligned N-terminal domains of one H and one L chain. Within the Fab region, the V_L and V_H form together the variable fragment Fv and a disulfide bond pairs the C_L and C_{H1} . The Fab provides the antigen binding and the specificity.

The flexible hinge region allows lateral and rotational movement of the Fab, which is important for binding to the antigen. The hinge region links the two heavy chains with disulfide bridges. The number of S-S bonds and the length of the hinge region define the degree of flexibility.

The constant Fc region is formed by the associated C-terminal domains of the two H chains, i.e. C_{H2}, C_{H3} (and C_{H4}), and exhibits various effector functions.

Depending on the class, antibodies differ in their effector functions: i.e. the fixation and activation of complement, the binding to Fc receptors on macrophages, which promote phagocytosis, or the interaction with Fc receptors on lymphocytes and natural killer cells, which induce cytotoxicity (see following section).

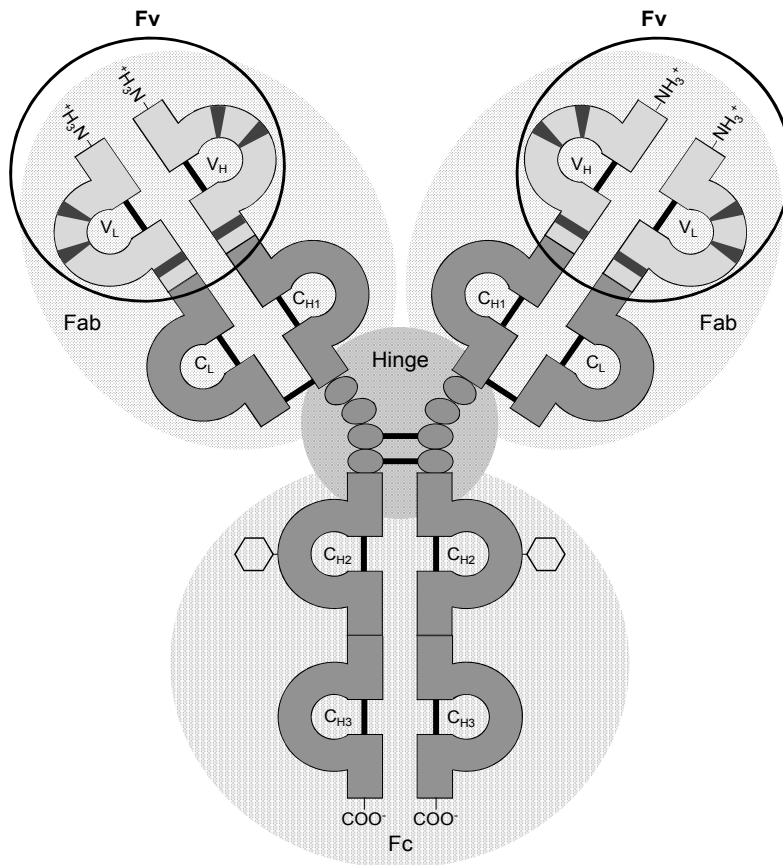


Figure 4: Basic antibody structure. The functional structure is divided into the fragments, which the antigen (Fab), the fragment, that crystallizes (Fc) and the hinge region. S-S bonds (—) and sugar (hexagon).

Antibody classes and subclasses

Based on the primary structure (gene sequence) of the C_H , antibodies can be grouped into various classes and subclasses (isotypes). Different species express a distinct set of isotypes. Mammalian murine antibodies are classified into IgM, IgG, IgA, IgD and IgE immunoglobulins, which differ in their H chain isotypes of μ , γ , α , δ and ϵ , respectively. The IgG are further subdivided into IgG1, IgG2a, IgG2b and IgG3 subclasses. In contrast, avian chicken antibodies are grouped into IgM, IgY and IgB, having a μ , ν or β H chain isotype. IgY and IgB are also called chicken IgG and IgA.

The classes vary mainly in the number of C_H and in the number and position of disulfide bridges and glycosylations (see Figure 5 and Table 2). IgM, IgG and IgY are N-glycosylated at C_{H2} in the Fc. Some are also reported to carry N-linked glycosylations in the Fv, which may interfere with the antigen binding.⁵⁹ In contrast to the glycosylations of the Fc, the Fv carbohydrate chains are at the surface of the antibody and are accessible to lectin binding.⁶⁰

The L chain is of the types λ or κ for mammals and only of the type L for avian.

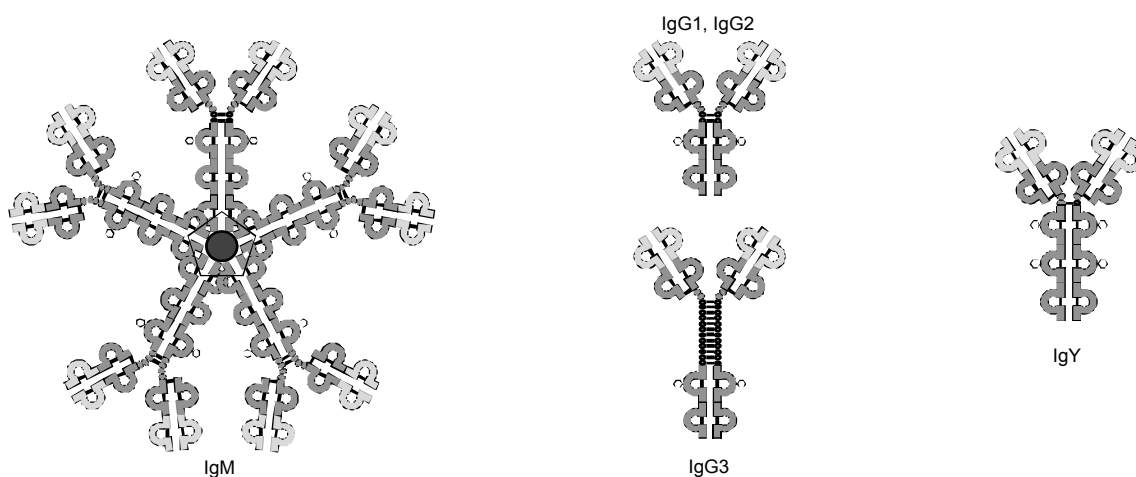


Figure 5: Murine IgM, murine IgG and chicken IgY structure.

IgM

The secreted pentameric IgM molecule (900kDa) is decavalent. It contains an additional J chain (15kDa), which is responsible for oligomerization of the extra C_{H4} domains and is N-glycosylated at C_{H2} . Generally, the IgM is the typical antibody of the primary response, which does not undergo affinity maturation and therefore binds with low affinity but high avidity.

The secreted IgM antibody in the serum can fix complement and agglutinate antigen but cannot cross the placenta.

IgG

The monomeric IgG molecule (150kDa) is divalent and N-glycosylated at Asn²⁹⁷ in the C_H2. The IgG subclasses mainly vary in the number of S-S bonds and the length of the hinge region. Generally, the IgG antibody binds the antigen with high affinity as it is the typical antibody of the secondary immune response and therefore is matured.

The IgG comprises the major antibody in the serum. It can cross the placenta, can fix the complement and bind to the Fc receptors on macrophages, monocytes and some lymphocytes.

IgY

The monomeric IgY molecule (180kDa) is divalent, includes additional C_H4 domains but lacks the hinge region and therefore is less flexible than IgG. In addition to the C_H2 domain, also C_H3 is N-glycosylated.⁶¹

The IgY is the main serum antibody and the only yolk antibody. In contrast to IgG and IgM, it can neither activate complement nor bind to mammalian Fc receptors.^{62,63}

The avian IgY is suggested to be the phylogenetically progenitor of mammalian IgG and IgE.⁶⁴

Table 2: Characteristics and features of the different antibody classes of mice and chicken.^{65,66,67,68}

	IgM	IgG	IgY
MW	900kDa	150kDa	180kDa
Heavy chain	80kDa	55kDa	65 – 67kDa
	μ	γ	ν
Light chain	25kDa	25kDa	23 – 25kDa
	κ or λ	κ or λ	L
	$(\mu_2\kappa_2)_5$ or $(\mu_2\lambda_2)_5$	$\gamma_2\kappa_2$ or $\gamma_2\lambda_2$	ν_2L_2
Valency	10	2	2
Carbohydrate	12%	3%	
Hexose	5%	1%	2.2%
Cell	Immature B	Mature B	
Function	Primary response	Secondary response	Secondary response
Complement activation	Strong	Medium	No
Fc receptor binding	Yes	Yes	No
Protein A and G binding	No	Yes	No
Protein L binding	Yes	Yes	Yes [†]
Papain digest		2 Fab + Fc	2 Fab + Fc
Pepsin digest		F(ab) ₂ + Fc	2 Fab + Fc
Isoelectric point		7.8	6.8
Acidic stability		Low	High
Heat stability		Low	High

†: Depending on literature

1.2.2 Immune response – the avian and mammalian humoral immune system

Birds and mammals divided more than 300 million years ago. Although, their cellular and humoral immune systems and immunoglobulins are not identical, they exhibit many analogies. The avian immunoglobulin classes IgM, IgY and IgB exhibit similar functions to the mammalian IgM, IgG/E and IgA, but differ in the structure. However, the important mechanism, which is responsible for antibody diversity differs significantly. In mammals, diversity is introduced by gene recombinations and somatic mutations, whereas in avian, diversity originates from gene conversions.

B-lymphocytes arise from progenitor stem cells in the mammalian bone marrow or in the avian bursa of fabricius. In these primary lymphoid organs, the antigen-independent gene rearrangement takes place, followed by the antigen-dependent clonal selection in the mammalian secondary lymphoid organs, the spleen and lymph nodes, or in the bursa of fabricius again, as birds have no lymph nodes.

1.2.2.1 Antibody diversity

Antigen-independent gene recombination of mammals

Mammalian progenitor germline DNA encodes different variable (V), joining (J) gene segments for L chains and in addition different diversity (D) gene segments for H chains. During differentiation of B-cells, one V and one J gene segment recombine and arrange with the C region to form the functional VJC gene of the L chain. In addition one D, one J and one V gene segment recombine and arrange with the C region to form the functional VDJC of the H chain. The variability is further increased, due to imprecise DNA recombination, which introduces random nucleotides at the recombination sites of V, D and J gene segments, and due to point mutation in the recombined gene. The random association of these different H and L chains allows the production of about 10^{12} distinct antigen binding sites (see Figure 6).⁶⁹

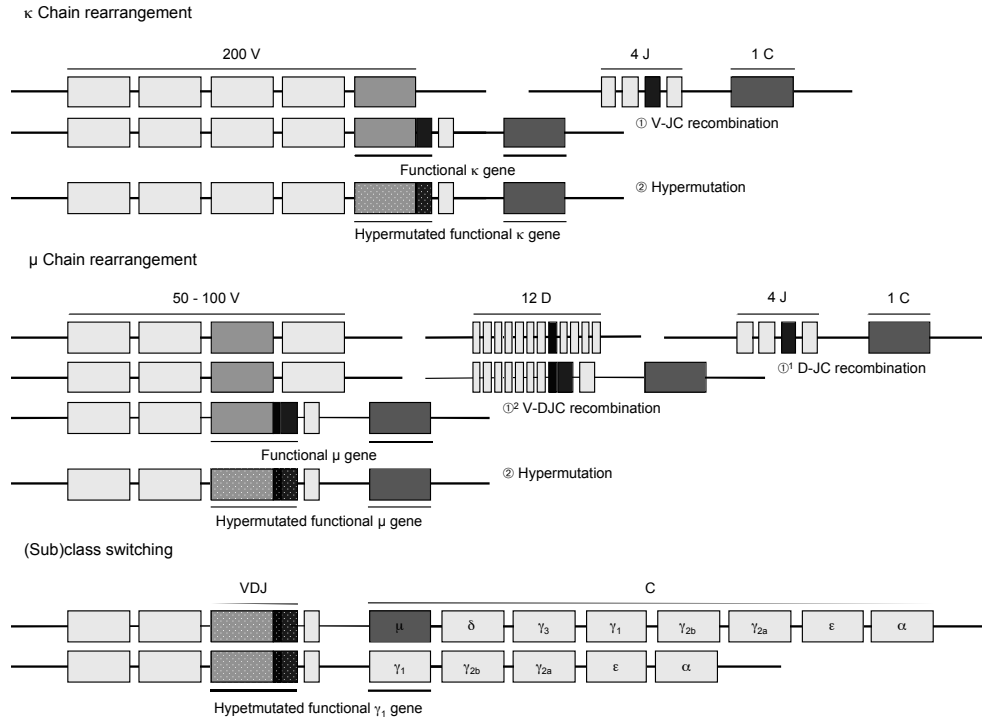


Figure 6: Gene rearrangement of the murine light and heavy chain and class switching of the heavy chain. ① Gene segment recombination (first ①¹ and second ①²), ② Point mutation and random nucleotide insertion.

Antigen-independent gene conversion of birds

In avian progenitor stem cells, the antibody repertoire is developed by a distinct strategy.⁷⁰ Avian DNA only encodes one single V and J gene segment, but additionally several pseudo V gene segments. The V and J gene segment recombines to the functional VJC gene and creates only limited diversity by imprecise DNA recombination at the recombination site of the V and J gene segments. In the following gene conversion, the variability is further increased by exchange of various V gene segments with pseudo V gene segments and by point mutations (see Figure 7).

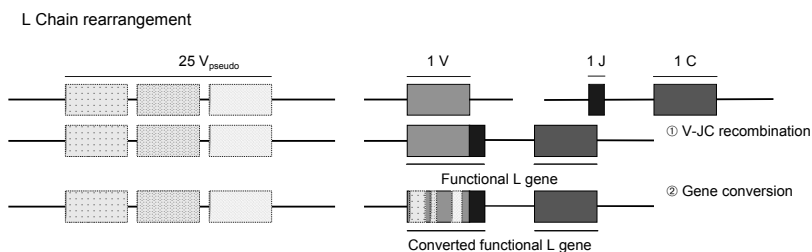


Figure 7: Gene rearrangement of the chicken light chain.

The different mechanisms of the antibody repertoire formation in birds compared to mammals, result in antibodies of distinct characteristics.

1.2.2.2 Clonal selection

The first exposure to an antigen induces a relatively weak primary immune response. The exposed antigen binds to specific surface immunoglobulins on B-cells. After internalization and processing, antigen fragments are bound to the major histocompatibility complex II (MHCII) and are presented to helper T-cells. The interaction of the T-cell receptor on helper T-cells, and the antigen-MHCII complex on B-cells is essential. It stimulates the differentiation and proliferation of B-cells to plasma and memory cells. The plasma cells only live 3 to 4 days. They are responsible for antibody secretion and are essential for the first immune response. The long-living memory cells on the other hand, do not secrete antibodies but are inevitable for promotion of a strong and fast secondary immune response after reexposure to the antigen.

Because surface B-cell receptors and secreted antibodies express the same antigen binding site, only antigen-specific B-cell clones are selected. Their proliferation is accompanied by hypermutation of V regions, which allows affinity maturation, and by the class switching.

The hypermutation of V regions leads to B-cells with different antigen affinities. The cells, which exhibit higher affinity compared to the original B-cell, were preferentially selected for proliferation.

The class shifting does not contribute to diversity, but allows adapting the antibodies to different effector functions during immune response. Another type of C_H gene is recombined with the same V_H gene.

Hence, in the primary immune response, IgM are most abundant. In the secondary response, affinity-matured mammalian IgG or avian IgY predominate.⁷¹

1.2.3 Antigen-antibody interface

The antibody recognizes not the entire antigen. Only the antigen combining site is in close contact with the antigenic site of the antigen.

1.2.3.1 Antigenic site and antigen combining site

The antigenic site of the antigen and the antigen combining site of the antibody are designated epitope and paratope, respectively.

Epitope

The antigenic sites are areas at the antigen surface and are called (structural) epitopes. Depending on the epitope architecture, the epitopes are grouped to continuous or discontinuous epitopes. Continuous epitopes are also designated linear or sequential epitopes and consist of a coherent part of the primary sequence. Discontinuous epitopes are also called assembled and conformational epitopes and contain amino acid residues, which are separated in the primary sequence, but brought to close proximity in the folded antigen.

The borderline between discontinuous and continuous epitopes however is fluent. Discontinuous epitopes usually contain several continuous stretches of a few contiguous residues and conversely, continuous epitopes tend to include a number of indifferent residues, that are not involved in the binding interaction.⁷² 90% of the structural epitopes on the surface of a native antigen are suggested to be mainly discontinuous.⁷²

Paratope

The six CDR of the V_L and V_H those are aligned in the Fv form the antigen combining site. The CDR1-3 of L chain and the CDR1-2 of the H chain, which are encoded by the V and J gene segments, accept a small number of main chain conformations, i.e. the canonical structures. In contrast, the CDR3 of the H chain is mainly encoded by the D gene segment and folded to various different conformations (see Figure 8).

The specificity and affinity of the antigen binding site to the antigen mostly depend on the canonical structure, the size and polarity of the amino acid residues at the surface and on the relative position of the six CRD.^{73,74} Especially the CDR3 of the H chain contributes to binding.⁷⁵

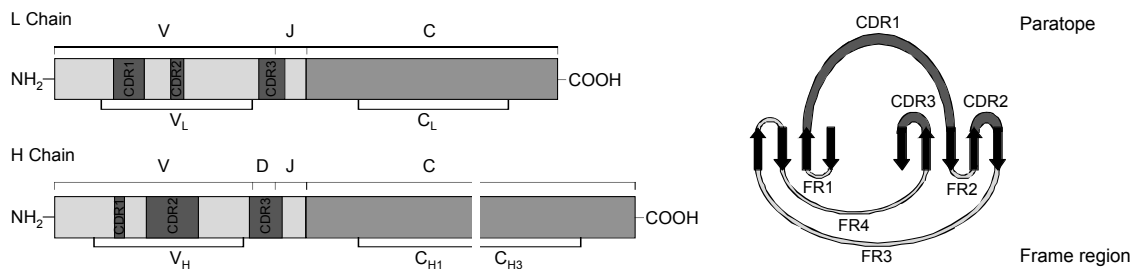


Figure 8: Encoding of the heavy and light chain amino acid sequences. V and J gene segments of the light chain encode CDR 1-3. The V gene segment of the heavy chain encodes CDR1-2 and mainly gene segment D, but also J encodes CDR3. Inter-chain S-S bonds enclose CDR1 and CDR2 of the heavy and the light chain, respectively.

Epitope-paratope interaction

The interaction of the epitope and the paratope induces conformational changes to optimize the complementarity in shape and charge. Their contacting surface is about 600-900Å² and is formed by 15 to 20 amino acid residues of the structural epitope and the paratope.⁷⁵ Thereof, only 3 to 5 residues significantly contribute to binding. These are designated functional epitope and paratope.

The binding is mainly mediated by Van der Waals interactions and hydrogen bonds, but less by salt bridges or hydrophobic interactions.⁷⁵ Hence, epitopes contain amino acids His, Lys, Ala, Leu, Asp and Arg with high frequency.⁷⁶

The antibody affinities range from K_D 10⁻⁵-10⁻¹²M. The higher affine antibodies of the second immune response often comprise affinities of $K_D \leq 10^{-7}$ M. The antibody avidity is the overall stability of the antibody-antigen complex and depends on the antibody affinity as well as on the antibody and antigen valency.⁶⁵

1.2.3.2 Antigenicity and immunogenicity

The immunogenicity refers to the ability to elicit an immune response, whereas the antigenicity refers to the ability to be recognized by the product of an immune response, i.e. T-cell receptor, B-cell receptor and antibody.

Factors, intrinsic to the antigen, define the antigenicity of the epitopes. But, which of these antigenic sites are immunogenic depends on factors extrinsic to the antigen, the host species-defined factors.⁷⁶

Intrinsic factors

The properties, intrinsic to the antigen are the accessibility, the hydrophilicity and the mobility.

The accessibility of surface amino acid residues may be hindered by posttranslational modifications, i.e. glycosylations. The hydrophilicity and polarity of amino acid residues in the epitope has to be complementary to the paratope to allow hydrogen bonding and Van der Waals contacts. The flexibility and segmental mobility, e.g. high in loops, may be essential to achieve optimal epitope-paratope complementarity.

In the prediction of epitopes, most algorithms only consider intrinsic factors. Hence, they are based on the physicochemical properties of amino acids in the primary sequence and therefore only permit to predict continuous epitopes.⁷⁶

Putative epitopes must span a part of the surface to be accessible. Therefore, they mainly include hydrophilic amino acid residues. Hopp and Woods⁷⁷ suggested, that antigenic sites could be predicted from the primary sequence by determination of the most hydrophilic part of the sequence. Since a functional epitope often spans 3 to 5 amino acid residues, the antigenicity algorithm of Hopp and Woods averages the hydrophilicity parameters for overlapping segments of six amino acid residues. Parker *et al.*⁷⁸ used a modified hydrophilic scale. Fraga⁷⁹ extended this approach by considering recognition factors. They reflect the probability, that hydrophilic amino acids may interact with one another and therefore may be buried in the protein, despite to be hydrophilic. The antigenicity algorithm of Welling *et al.*⁸⁰ is based on the property of amino acid residues to be recognized by antibodies. An antigenicity scale was derived statistically from known epitopes. The antigenic potential is highest for Leu, followed by His, Asp, Thr and Ala, but low for Cys, Asn, Gly, Met and Phe and lowest for Ile.

Most often, the algorithms of Hopp and Woods, and of Kyte and Doolittle are used.⁸¹

Extrinsic factors

As mentioned before, only some of all antigenic sites will be immunogenic due to properties, extrinsic to the antigen, i.e. the self-tolerance, the set of MHCII and T-B reciprocity.

Antigens, that are highly homologous to a protein of the host species initiate self-tolerance. However in another species, the same antigen may be immunogenic.

Each individual has another set of MHCII. Rarely, an individual may lack an MHCII for the antigen. This is more frequent in inbred strains, which all have the same MHCII set, than in outbred strains.

To initiate an immune response, an antigen must provide three different binding sites: the B-cell epitope, the MHCII binding site and the T-cell epitope. As a consequence, the antigen must have a minimal size of 3 – 5kDa to be immunogenic.

First, a B-cell epitope must be accessible for binding to the B-cell receptor. After antigen phagocytosis, processing and migration to the B-cell surface, the antigen fragment(s) must furthermore have a binding site for MHCII to allow antigen presentation to helper T-cells. Finally, the MHCII-bound antigen fragment must provide a T-cell epitope, which can simultaneously be recognized by the T-cell receptor to promote cell-to-cell communication between B-cells and helper T-cells.

The intrinsic factors have to be considered for the antigen selection, to use entire antigen protein, protein fragment or modified antigen. The extrinsic factors influence the antibody production, i.e. the selection of the host animal and the dose for immunization (see Section 1.2.4.1.1).

1.2.4 Production of monoclonal and polyclonal antibodies

The production of monoclonal antibodies consists of three stages: the immunization, to stimulate antigen specific B-cells *in vivo*, the selection of immortalized antigen-specific B-cell clones *in vitro* and the propagation of selected B-cell clone *in vitro*, followed by isolation of antibodies from supernatant.

In contrast, the production of polyclonal antibodies is only composed of one stage: the immunization *in vivo*, directly followed by isolation of antibodies from collected sera or egg yolks. As a consequence, polyclonal and monoclonal antibodies have distinct characteristics:

Polyclonal antibodies are produced from various distinct plasma cell clones. Each provides an antibody, specific to one single epitope. Therefore, polyclonal antibodies are a mixture of various antibodies and antibody classes, directed against distinct epitopes.

Since the monoclonal antibody production includes an *in vitro* clone selection step, identical monoclonal antibodies are secreted from one single clone. They are homogenous, specific to one single epitope and exhibit defined affinity and specificity.

Another important feature is, that monoclonal antibody-secreting clones provide an infinite antibody source, whereas polyclonal antibodies are limited.

1.2.4.1 Monoclonal antibody production

Monoclonal antibodies are produced by the phage and ribosome technology or classically by the hybridomas technology from Köhler and Milstein.⁸²

Hybridoma expression systems are advantageous for the production of antibodies, because myeloma cells are professional immunoglobulin-secreting cells and are able to make posttranslational modifications. Proper glycosylations are important for the antibody function⁸³.

1.2.4.1.1 *In vivo* stage - the immunization

The immunization is only successful, if the antigen is immunogenic. The immunogenicity depends on factors intrinsic and extrinsic to the antigen (see Section 1.2.3.2). These

factors can be modulated by selection of species, antigen dose and form, injection site and adjuvant.⁶⁵

- Host species. For monoclonal antibodies, mice are still the standard species. Mainly inbred strains like Balb/c are chosen, but in case of low response, other strains, particularly outbred strains, like NMRI mice, may be of advantage.
- Antigen dose. The dose must lie within the immunogenic window. Lower, but also higher doses, may induce tolerance. The dose is commonly 5 – 50µg/injection and should not exceed 500µg/injection for mice.
- Antigen form. Particular antigens are much stronger immunogens than soluble molecules. The aggregation of proteins or the coupling to carrier proteins may therefore enhance the immune response.
- Injection route. Subcutaneous (sc) and intraperitoneal (ip) injections are commonly used for immunization and boost of mice with soluble or particulate immunogen with adjuvant. Final boost however should be applied intravenous (iv) without adjuvant to induce a short-lived strong response.
- Adjuvant. They are unspecific stimulators of the immune response that ensure a strong, memory-enhanced immune response. Most adjuvants are composed of two components, one for sustained antigen release and the other to recruit antigen-presenting cells to the injection site. The Incomplete Freund's adjuvant includes unmetabolizable mineral oil i.e. croton oil, that forms a stable water-in-oil emulsion with the aqueous antigen solution, and prolongs the immune response. The Complete Freund's adjuvant additionally contains heat-inactivated *Mycobacteria tuberculosis* or *butyricum*, which induce local inflammation.

Mice are primed but also boosted to promote affinity maturation and class switch to IgG. A final boost about three days prior to fusion synchronizes maturation and increases portion of antigen-specific B-cells in the spleen.

1.2.4.1.2 *In vitro* stage – the somatic hybridization and clonal selection

The hybridoma technology of Köhler G. and Milstein C.⁸² allows the infinite growth of antibody-secreting cells. The main steps to achieve the desired, stable hybridomas are: the PEG fusion of myeloma cells and splenocytes, the drug selection of hybrid cells (hybridomas), the screening for desired hybridomas and their cloning (see Figure 9).

The B lymphoblastic myeloma cells provide the correct genes for continuous cell division in culture and are gene defective, for selection; e.g. the P3-X63Ag8.653 myeloma cell line, which is derived from Balb/c mice, lacks the ability to produce immunoglobulins and is 8-azaguanine resistant. The antibody-secreting B-cells contribute the functional rearranged immunoglobulin genes for production of an antibody with defined specificity.

PEG fusion “myeloma cells + splenocytes = fusion cells”

Splenocytes and myeloma cells are fused with the help of polyethylene glycol (PEG, $\text{OH}(\text{CH}_2\text{CH}_2\text{O})_n\text{H}$). The PEG destabilizes the plasma membranes and allows adjacent cells to combine to a single cell with two or more nuclei. However generally, only about 1% of all cells are fused and only 0.001% form viable hybrids. The hybridomas are instable due to the abnormal number of chromosomes. During cell division, the chromosomes are not equally segregated and up to 40% may be lost, including the gene that encodes the functional rearranged immunoglobulin.

The propagation of the delicate hybridoma cells can either be stimulated with feeder-cells or with conditioned medium, containing proliferation-stimulating factors, e.g. growth factors and IL-6. The feeder-cells, commonly splenocytes, macrophages or T-lymphocytes, provide growth factors and increase the cell density.

Drug selection “fusion cells – (splenocytes + myeloma cells) = hybridomas”

After fusion, (un)fused mortal splenocytes, (un)fused immortal myeloma cells or fused immortal hybridomas cells are mixed. Splenocytes die after three to four days, but myeloma cells have to be killed to select the hybridomas.

The 8-azaguanine resistant myeloma cells are hypoxanthine-guanine phosphoribosyl-transferase (HPRT) mutants. The HPRT enzyme catalyzes the condensation of phosphoribosyl-pyrophosphate and a purine base to form a purine monophosphate nucleotide, in the nucleotide *salvage* pathway. As a consequence, myeloma cells can only provide nucleotides by the *de novo* pathway.

The myelomas die in HAT (hypoxanthine, aminopterin and thymidine) containing medium. The aminopterin hampers the *de novo* synthesis of pyrimidines directly and of purines indirectly. Hybridomas have the mutated HPRT gene of myeloma cells, but also the functional HPRT gene of the splenocytes. Hence, they can provide nucleotides by the *salvage* pathway in the presence of thymidine and hypoxanthine precursors.

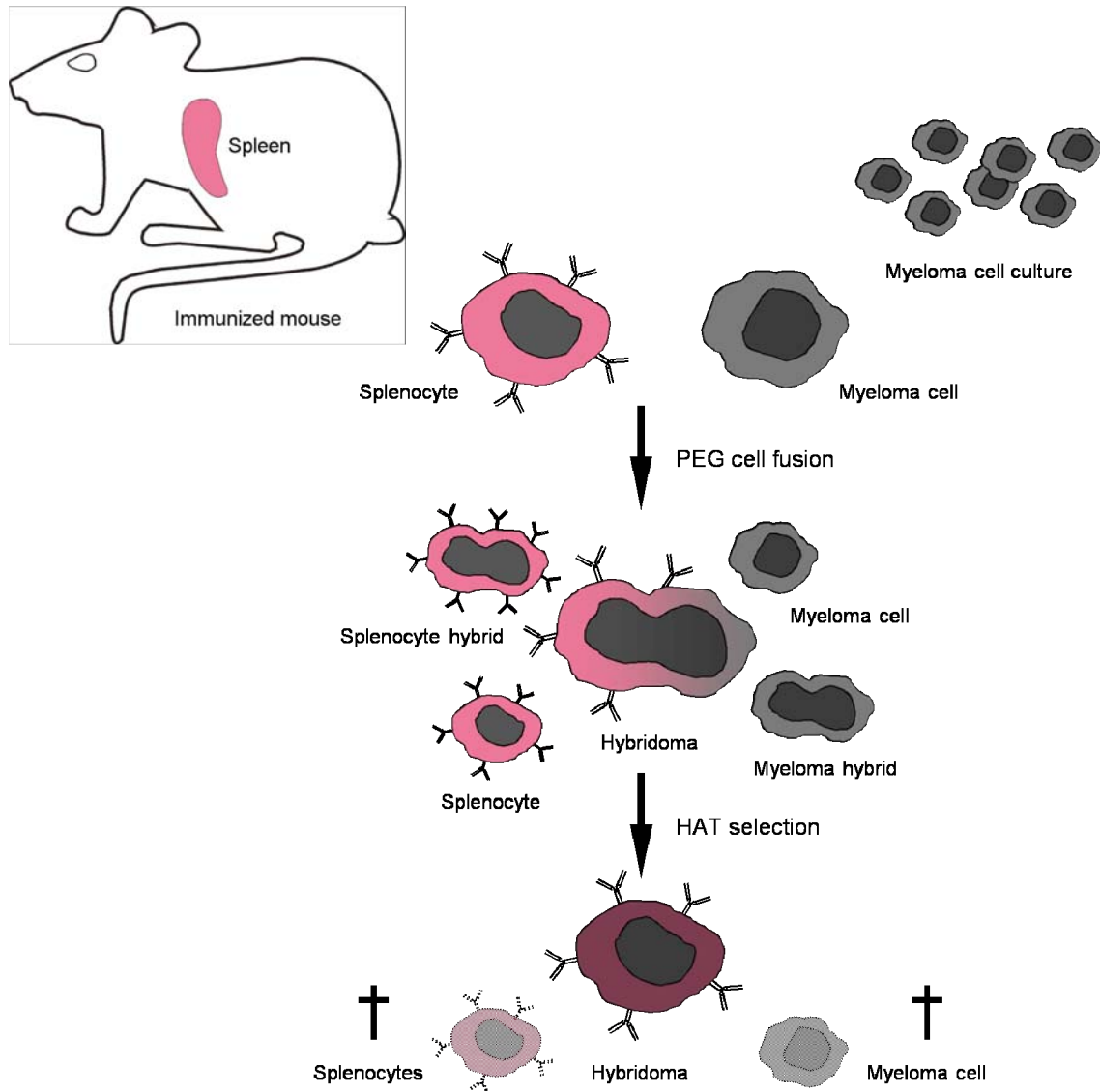


Figure 9: PEG fusion of antibody-producing splenocytes and HPRT-defective myeloma cells, followed by HAT selection of hybridomas.

Hybridoma screening

Normally 500 to 1'000 hybridomas are obtained from one fusion and thereof, about 90% are positive in screen.

The hybridoma screening is of main importance, because it determines the hybridomas, which are further expanded and cloned. Hence, the screening assay must be fast to allow testing of all hybridomas in a short time, but most crucial, must be selective for the desired antibody feature. Common assay types are the antigen-capturing ELISA and the antibody-capturing ELISA, but also functional assays are applied.

Single-cell cloning by limited dilution

A specific antibody-secreting hybridoma can either be a single clone or a mixture of different hybridoma clones, which produce distinct antigen-specific or irrelevant antibodies or even no antibodies. Such hybridomas are separated in single-cell cloning by limited dilution (see Figure 10). In limited dilution, cells are diluted to concentrations of 1 cell/well culture or less. To keep such diluted and isolated cells viable, small culture volumes and feeder layers or conditioned medium with proliferation-stimulating factors are essential.

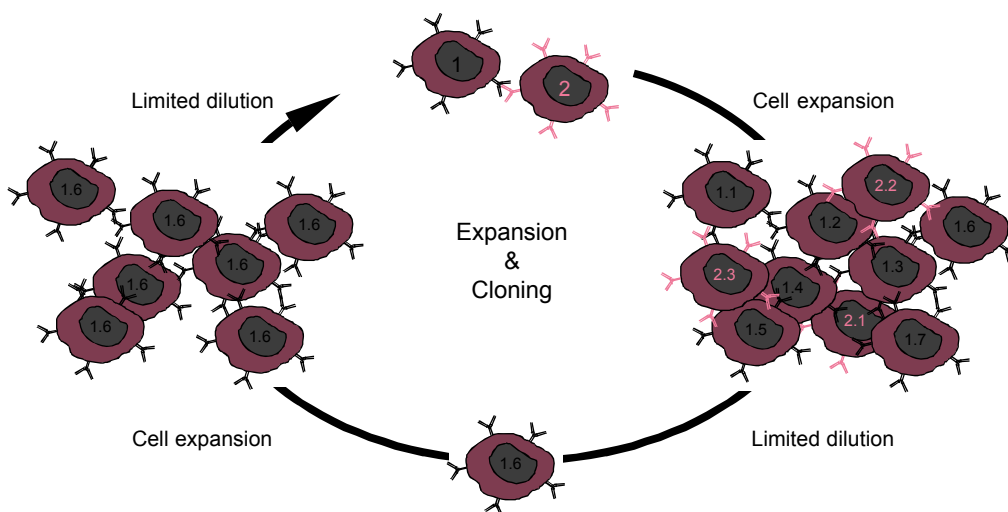


Figure 10: Single-cell cloning by limited dilution.

Single-cell cloning also allows the selection of more stable clones or of clones, which secrete a switched isotype of the antibody.

1.2.4.1.3 Propagation of hybridoma clones – the “antibody factories”

In the past, monoclonal antibodies were produced *in vivo* by injection of hybridoma clones into the peritoneal cavity of mice, but nowadays, they are obtained from *in vitro* hybridoma clone cultures. The secreted monoclonal antibodies are then simply harvested from culture supernatant.

1.2.4.2 Polyclonal antibody production

Polyclonal antibodies are commonly produced in mammals like rabbits, goats, sheep and mice, but seldom in chicken. In 1980, IgY antibodies from egg yolk were for the first time used as a source of polyclonal antibodies, by Polson *et al.*⁸⁴

As chicken is phylogenetically more distant to mammals, the production and the features of polyclonal IgY differ in some aspects from polyclonal IgG:

- Immunogenicity. Highly conserved mammalian antigens may be immunogenic in chicken but not in mammals.
- Epitope recognition. Chicken antibodies may recognize other epitope structures than mammalian, resulting in antibodies with distinct specificities.⁸⁵
- Antibody collection. Chicken egg collection is non-invasive, whereas mammalian bleeding is invasive.⁸⁵
- Rheumatoid factors and complement. Chicken antibodies do neither interact with mammalian rheumatoid factors nor activate mammalian complement system. This is advantageous in some immunoassays.^{62,86}
- Protein A and G. Chicken antibodies do neither interact with Protein A nor G^{87,88}. The binding to Protein L is controversial discussed.
- Yield. The monthly amount of polyclonal IgY produced from one hen is about ten times the yield obtained from the bleeding of one rabbit in the same period.

The majority of these differences are a plus for IgY.

IgY are successfully applied in various immunochemical techniques, e.g. in immunoblotting, immunoprecipitation,⁸⁹ immunoassay, immunohistochemistry⁹⁰ and Biacore assay.⁹¹

1.2.4.2.1 *In vivo* stage – from immunization to antibodies in the egg yolk

The successful immunization of chicken, which initiates a long-lasting immune response, depends on the same factors as valid for mammals (see Section 1.2.4.1.1). The antigen needs a minimal molecular weight of at least 5 – 10kDa to be immunogenic. Generally, 100 – 250µg antigen with adjuvant are injected intramuscularly or subcutaneously.⁹²

About 16 days after immunization, antigen-specific IgY antibodies appear in the serum and 3 to 4 days later in the yolk. Within following 10 days, they reach peak concentration and remain high for at least 70 days, without further boosting.⁸⁵

In the ovary, IgY antibodies are selectively and actively transported from hen circulation to the yolk.⁹³ The yolk is surrounded by the vitellin membrane, passes down the oviduct, where the egg white, that contains ovalbumin-bound IgM and IgB, is secreted, and is finally wrapped by the shell membrane and the shell. Hence, the egg yolk only contains IgY but no IgM or IgB. This is an important advantage for the isolation of IgY antibodies.

1.2.4.2.2 *In vitro* stage – the isolation of IgY antibodies from eggs

The standard purification method for mammalian IgG antibodies is by affinity to Protein A or G, but chicken IgY antibodies bind to none.⁹⁴ Until now, no standard method is established for avian IgY extraction. But most of reported methods follow a common multi-step strategy, which is the consequence of the egg composition (see Figure 11).

Egg composition

The yolk is an oil-in-water emulsion, which is formed by 33% oily yolk granules and 66% watery phase. Latter is composed of 48% water, 17% proteins and 1% carbohydrates. The yolk proteins belong mainly to four groups: 47% vitellin-lipovitellin (400kDa), 39% vitellelin, 10% livetin and 4% phosvitin (36kDa). The livetins comprise the γ -globulin like IgY (180kDa), the albumin-like α -livetin (54kDa) and the α 2-glycoprotein-like β -livetin. The concentration of total and specific IgY in the yolk and the serum are similar. One yolk contains about 6mg total IgY, and 2 to 10% of total IgY antibodies are antigen-specific IgY.⁹²

IgY extraction methods

The majority of reported IgY purification procedures follow a multi-step strategy, composed of precipitation steps and of chromatographic steps. They vary substantially in yield, purity and biological affinity of IgY, but can hardly be compared in literature.

In a typical IgY extraction, egg white and egg yolk are separated first, to avoid the contamination of yolk with IgB and IgM from egg white. After removal of yolk lipids, the total IgY, which contain the antigen-specific and irrelevant IgY, are extracted. Depending on the application, the antigen-specific IgY must be isolated (see Figure 12).

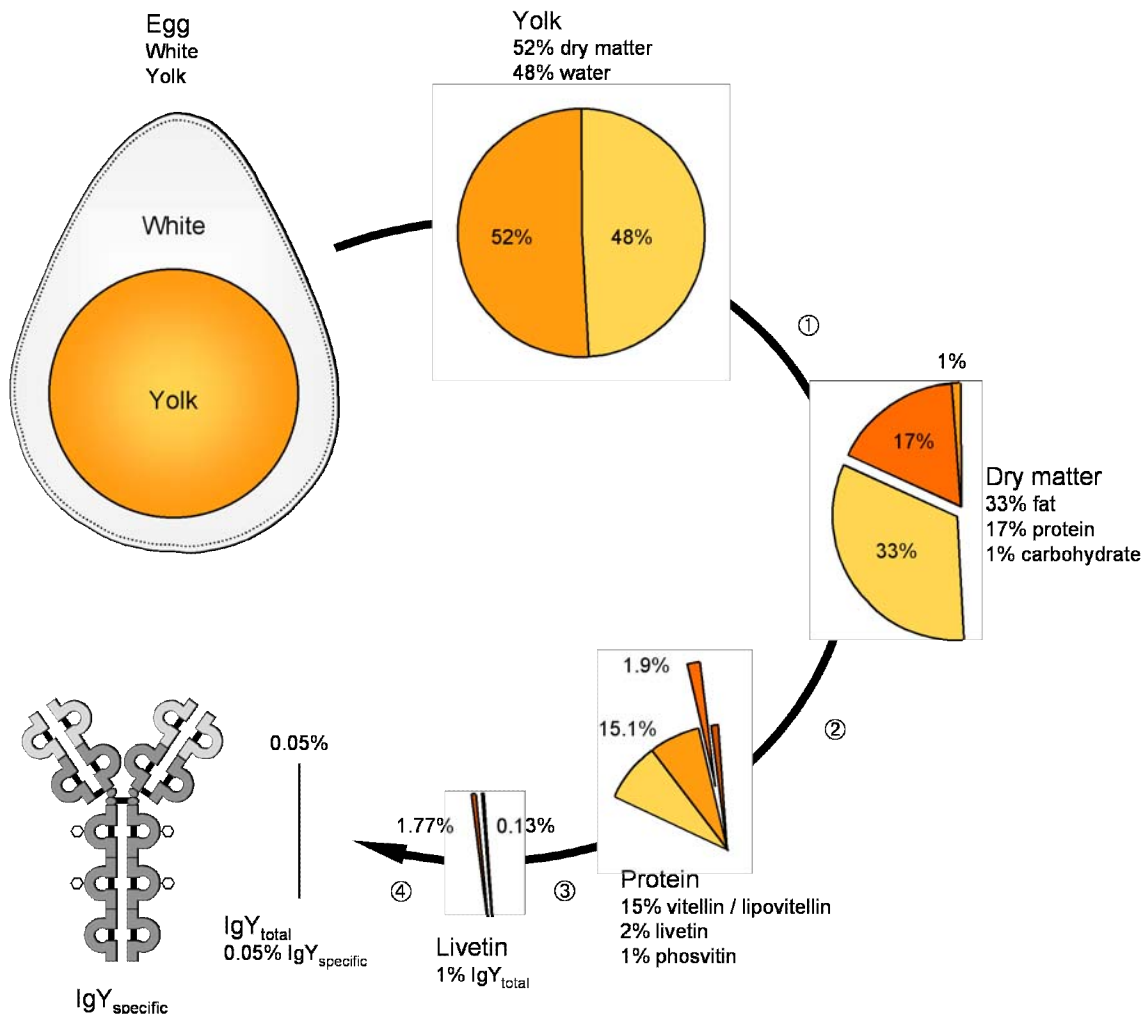


Figure 11: Extraction of specific IgY from egg yolk. ① Separation of the egg white and yolk; ② Removal of lipids to get the total proteins; ③ Extraction of the total IgY from the total proteins; ④ Isolation of the specific IgY from the total IgY.

Lipids are mainly precipitated with salts (ammonium sulfate,⁹⁵ dextran sulfate,⁹⁶ PEG⁹⁷) or extracted with organic solvent^{97,98}. Two other simple but effective methods are reported by Jensenius *et al.*⁹⁶ and by Atika *et al.*⁹⁹, the repeated freeze / thaw and the water dilution method.

After removal of disturbing lipids, the total IgY can efficiently be salt,⁹⁶ or PEG^{84,100} precipitated or are chromatographically purified by gel filtration, by ion exchange on MonoQ and DEAE,⁸⁵ or by thiophilic interaction chromatography on T-gel.¹⁰¹

1.3 Application of antibodies in immunochemical techniques

The application of an antibody in different immunochemical methods allows the characterization of the antigen and antibody as well as the comparison of distinct antibodies, directed against the same antigen.

Monoclonal antibodies may exhibit technique restrictions and must be validated for each method. Five major factors determine the success of an antibody in an immunochemical technique: the avidity and the specificity for the antigen, the alteration of the epitope, the antigen accessibility and in indirect methods the quality of secondary reagents.

- **Avidity.** The avidity is mainly defined by the antibody affinity and valency but also influenced by the local epitope concentration. Avidity effects arise, when several distinct antibodies can simultaneously bind to an antigen, when one antibody can simultaneously bind multiple identical epitopes on a homooligomeric antigen and when one antibody can bridge two adjacent fixed monomeric antigens.
- **Specificity.** The specificity of antibodies, directed against denaturation-sensitive epitopes is often higher. Antibodies, which recognize denaturation-resistant epitopes, are more susceptible to cross-react with related epitopes of irrelevant proteins.
- **Epitope alteration.** The immunochemical preparation procedure may alter the epitope structure, mainly due to denaturation of the native structure and due to chemical modification of amino acid residues in cell and tissue fixation.
- **Epitope accessibility.** The presence of competing molecules, the posttranslational antigen modification and the antigen orientation on the cell or in the tissue influence the access of antibodies to their epitope.

The detection can either be direct or indirect. In direct methods, the purified antigen-specific antibody is labeled and directly binds to the antigen. In indirect methods, the binding of unlabeled pure or crude antigen-specific primary antibody is detected with a labeled secondary anti-Ig antibody.

Although the indirect detection includes an additional step, it is commonly favored, because the signal amplification increases sensitivity and because the purification and labeling of the antigen-specific antibody can be circumvented.

In the following sections, the different immunochemical techniques, which were applied for the characterization of the monoclonal and polyclonal antibodies, are described.

1.3.1 Immunoblotting

The immunoblotting allows to investigate antigen features and to characterize antibodies. The antigen is not only identified due to interaction with the specific antibody but also due to its molecular weight. The method is quite sensitive, especially in combination with immunoprecipitation.⁶⁵

In immunoblotting, the antigen-containing (crude) proteins are separated by denaturing SDS-PAGE or native PAGE, and protein bands are blotted to a membrane. Following blocking of unoccupied binding sites on the membrane, antigen is captured with an antigen-specific enzyme-labeled or unlabeled antibody. Unlabeled antibody is in an additional step detected with the enzyme-labeled anti-Ig-specific antibody. The antigen-antibody complex is finally localized by the enzyme-catalyzed conversion of a colorless substrate to the colored chromogen precipitate (see Figure 12).

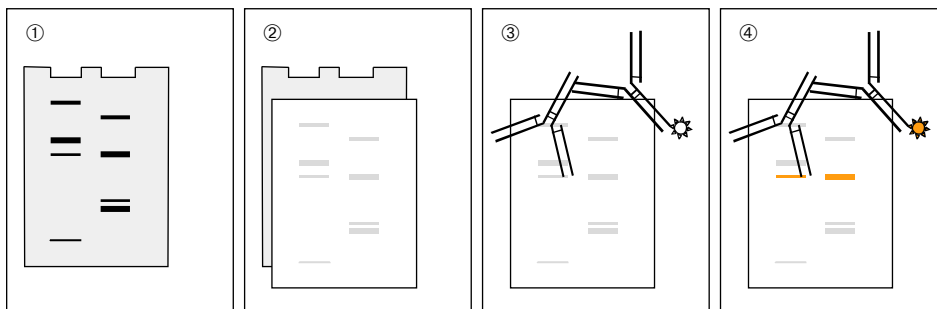


Figure 12: Indirect immunoblotting. ① Separation of the antigen-containing proteins by denaturing SDS PAGE or native PAGE ② Blotting of proteins onto the membrane ③ Antigen capturing with the antigen-specific primary antibody ④ Detection of the primary antibody with the enzyme-labeled secondary antibody ⑤ Signal development by the enzyme-catalyzed conversion of the soluble colorless chromogen to an insoluble colored chromogen.

For most application, the indirect detection with an enzyme-labeled anti-Ig-specific antibody is best.

In immunoblotting, the native antigen is denatured or may change conformation and therefore, the binding of antibodies to denaturation-sensitive epitopes is hindered. A high local antigen concentration on the blot enables avidity effects and permits even low-affine antibodies to bind.

The sensitivity of immunoblotting, using polyclonal antibodies is high, but background may be strong too. Monoclonal antibodies may fail due to epitope denaturation, but may also cross-react due to strong avidity. Therefore, mostly pooled distinct monoclonal antibodies or affinity-purified polyclonal antibodies work best.

1.3.2 Immunoassay

The immunoassay permits to explore antigens and antibodies qualitatively and quantitatively.¹⁰²

The three main classes of immunoassays are the antibody-capture, the antigen-capture and the antibody-sandwich assay, which are applied in innumerable variations.

The antibody-capture assay is often used to determine the antibody and antigen presence and level (hybridomas screening, antibody, serum titer determination), to determine antibody isotypes and to compare epitopes. Furthermore, the indirect antibody-capture assay permits to estimate the affinity or avidity, which is defined as the concentration of antibody required for half maximal binding.

In an antibody-capture immunoassay, the antigen is attached to the solid support. After blocking of remaining free binding sites on the solid support, the antigen-specific enzyme-labeled or unlabeled antibody is captured by the antigen. In an additional step, unlabeled antibody is detected with the enzyme-labeled anti-Ig antibody. The presence of the antigen-antibody complex is finally visualized and quantified, after enzymatic conversion of the colorless substrate to the soluble colored chromogen (see Figure 13).

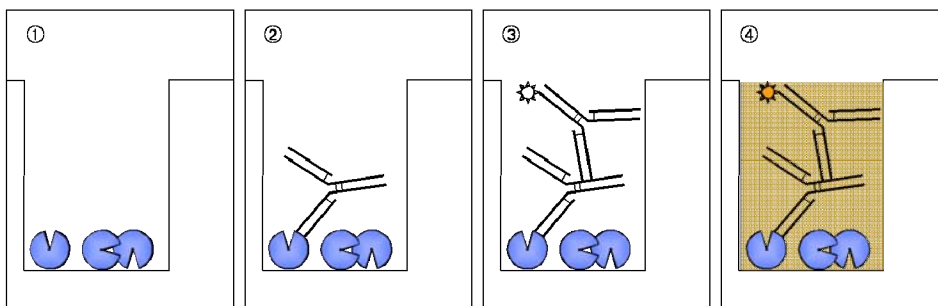


Figure 13: Indirect antibody-capture immunoassay ① Immobilization of antigen on the solid support and blocking of remaining binding sites ② Capturing of the antigen-specific antibody ③ Detection of the primary antibody with enzyme-labeled anti-Ig-specific antibody ④ Signal development by the enzyme-catalyzed conversion of the soluble colorless substrate to the soluble colored chromogen.

The sensitivity is mainly affected by the amount of the antigen, bound to the solid support, the avidity and specificity of the antibody and the type of labeling. The increase of local antigen concentration and consequently of avidity effects, allows low-affine antibodies to bind. The immobilization may change the conformation of native antigen. For most application, the indirect detection with enzyme-labeled anti-Ig antibody is sufficient.

In a competition antibody-capture immunoassay, the capacity of an antibody to inhibit binding of another antibody or a ligand can be determined. If they recognize identical, overlapping or adjacent but sterically interfering epitopes, they compete for binding.

In the direct competitive GalNAc-polymer immunoassay by Stokmaier¹⁰³ the antigen is immobilized on the solid support and unoccupied binding sites are blocked. The antigen-specific antibody competes with the enzyme-labeled GalNAc-polymer for binding to the antigen. Finally, antigen-bound GalNAc-polymer is quantified by enzymatic conversion of the soluble colorless substrate to the soluble colored product (see Figure 14).

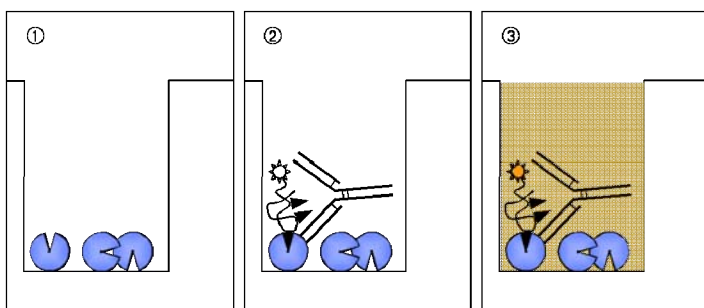


Figure 14: Direct competitive antibody-capture immunoassay. ① Immobilization of antigen on the solid support ② Competition of the enzyme-labeled GalNAc-polymer with the antigen-specific antibody for binding to the antigen ③ Detection of the enzyme-catalyzed conversion of the soluble colorless substrate to the soluble colored chromogen.

In these immunoassays, avidity-dependent constants but no absolute affinity-defined constants of the antibodies are determined. But they are suitable for the ranking of antibodies of the same isotype.

In the antigen-capture assay, the antigen-specific antibody is bound to the solid support and the antigen caught. In the sandwich assay, the antigen, bound to the immobilized antigen-specific antibody is additionally detected with a distinct labeled antigen-specific antibody.

The sensitivity of the immunoassay, using polyclonal antibodies, is often low and the background high. Monoclonal antibodies work excellent, but rarely fail due to epitope denaturation and a too low avidity. The applicability of affinity-purified polyclonal antibodies or of pooled distinct monoclonal antibodies is excellent.

1.3.3 Immunocytochemistry

Immunostaining of cells can be used to pinpoint the subcellular localization of an antigen and to follow its change in response to stimuli.⁶⁵

The two main classes of staining are the intracellular staining of cellular or internalized antigens and the extracellular staining of surface antigens. There exist a panel of variants, which mainly differ in the need of cell fixation and permeabilization to preserve cell architecture.

In the extracellular immunostaining of surface antigen, EGTA-detached adherent cells and suspension cells are prepared and optionally fixed. The surface antigen is captured with antigen-specific fluorochrome-labeled or unlabeled antibody. Unlabeled antibody is detected with fluorochrome-labeled anti-Ig-specific antibody. The antigen-antibody complex is finally visualized by fluorescence microscopy or quantified by flow cytometry (see Figure 15).

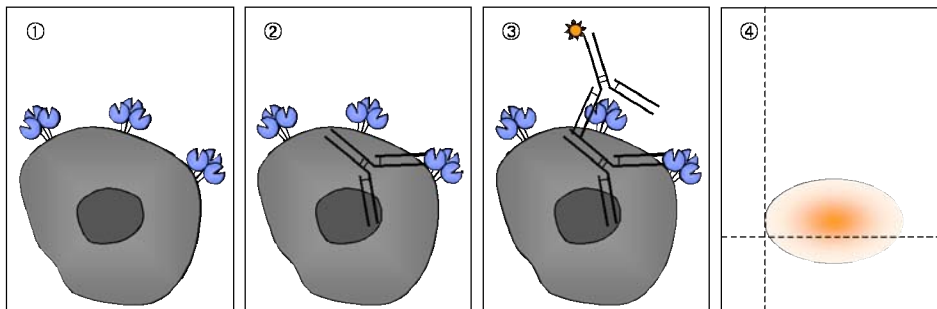


Figure 15: Indirect extracellular immunofluorescence staining of surface antigen. ① Detachment of adherent cells and optionally fixation of suspension and adherent cells ② Capturing of surface antigen with the antigen-specific antibody ③ Detection of the antigen-specific antibody with the fluorochrome-labeled anti-Ig antibody ④ Quantification of the fluorescent antigen-antibody complexes by flow cytofluorimetry.

Flow cytofluorimetry provides a statistical profile of the cell population and allows distinguishing cell subpopulations.

In the intracellular immunofluorescence staining of endocytosed antibody-antigen complex, the EGTA-detached adherent cells and suspension cells are prepared first. The surface antigen is captured with the fluorochrome-labeled or unlabeled antigen-specific antibody. Following internalization of the antigen-antibody complex, cells are fixed. Unlabeled antigen-specific antibody is detected with fluorochrome-labeled anti-Ig-specific antibody after cell permeabilization. The fluorescent label is finally visualized by fluorescence microscopy (see Figure 16).

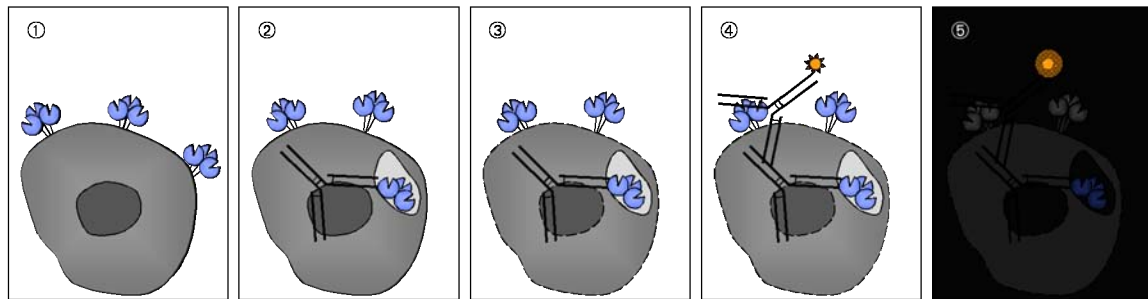


Figure 16: Indirect intracellular immunofluorescence staining of the internalized antigen-antibody complex ① Preparation of suspension and EGTA-detached adherent cells ② Antigen capturing with the antigen-specific antibody and internalization of the antigen-antibody complex ③ Cell fixation and permeabilization ④ Detection of the antigen-specific antibody with fluorochrome-labeled anti-Ig antibody ⑤ Visualization of fluorescent label by fluorescence microscopy.

The major determinants of the cell immunostaining are the local antigen concentration, the epitope accessibility and, if cells are fixed, the epitope alteration and masking.

The cell fixation prevents antigen leakage and maintains the cell structure, but can alter the epitope and therefore hinders antibody binding, although the antigen is present. The cells are either fixed by protein precipitation with hydrophilic organic solvent, i.e. acetone or ethanol, or by protein cross-linking. Formalin or (para)formaldehyde link primary amino groups of Lys and form lattices, which maintain the molecules at their original location. These fixed cells have to be permeabilized with detergent, like saponine to provide antibody access to intracellular antigens.

Normally, indirect staining is recommended, but direct staining can be advantageous in double staining.

In immunostaining, polyclonal antibodies exhibit high sensitivity, but also background may be high. Monoclonal antibodies are less sensitive but more specific. However, monoclonal antibodies may fail due to antigen modification during fixation, or due to surface antigen alteration during cell detachment. Affinity-purified polyclonal and pooled monoclonal antibodies generally stain excellent.

1.3.4 Immunohistochemistry

The immunostaining of tissues is used to examine the localization and distribution of the antigen in physiological and pathological tissue. Cells and tissues, which express an antigen or a homologous protein, can be identified and the antibody specificity can be verified. Furthermore, it permits to investigate misexpression, exclusive expression or misslocalization of an antigen under pathological conditions.⁶⁵

This technique preserves the tissue architecture and allows the recognition of cell types.

In immunostaining, the tissue is fixed and mostly embedded in paraffin. Tissue sections are devaxed and the antigen retrieved. After optional blocking, the antigen-specific antibody is captured by the surface antigen and detected with the enzyme-labeled anti-Ig antibody. The presence of the antigen-antibody complex is finally visualized after the enzymatic conversion of the colorless soluble substrate to the insoluble colored chromogen and the counterstaining of the tissue section (see Figure 17).

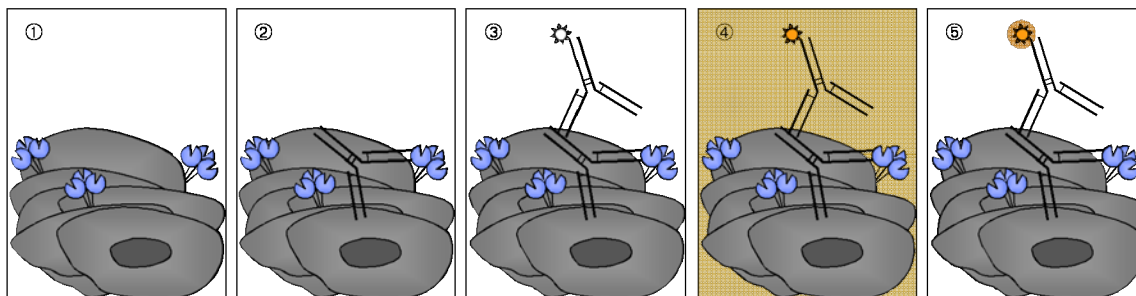


Figure 17: Indirect immunostaining of the surface antigen in tissue. ① Fixation, embedding of tissue and antigen retrieval in the devaxed tissue section ② Capturing of the surface antigen with the antigen-specific antibody ③ Detection of the bound antigen-specific antibody with the enzyme-labeled anti-Ig antibody ④ Detection of the enzyme-catalyzed conversion of soluble colorless substrate to insoluble colored chromogen ⑤ Counterstaining and visualization by microscopy.

The immunostaining of tissue has many constraints: the local antigen concentration is low, the epitopes may be altered, masked or inaccessible by fixation or incomplete antigen retrieval, and the antibody may cross-react. Hence, also antibodies, which work excellent in all other described immunochemical methods, may easily fail.

All kinds of antibodies, polyclonal, affinity-purified polyclonal, pooled monoclonal and individual monoclonal antibodies can be applied and may work excellent. Generally, sensitivity with polyclonal antibodies is higher due to avidity effects and due to the recognition of denaturation-resistant epitopes, which is important in paraformaldehyde-fixed, paraffin-embedded tissue.

1.3.5 Immunoaffinity / Mass spectrometry (epitope mapping)

Epitope mapping allows the identification of monoclonal antibodies, which recognize distinct epitopes on the same antigen or the determination of antigen modification sites.

There exist many techniques for epitope mapping, but each of these has its limitations. One constraint is, that almost all methods fail in the determination of conformation-dependent epitopes, which enclose about 80% of all epitopes.¹⁰⁴ In addition, they are

time-consuming, as they are based on libraries of overlapping antigen fragments, which have to be prepared first, by synthetic peptide synthesis, by gene fragment expression or by phage display.

The sensitive and rapid method by Suckau *et al.*¹⁰⁵ and Macht *et al.*¹⁰⁶ enables the determination of conformation-dependent epitopes by mass spectrometry and includes a set of two complementary experiments, the epitope excision and the epitope extraction.

In epitope excision, the antigen-specific antibody is covalently coupled to the Sepharose matrix. The native or acetylated antigen is bound to the immobilized antibody and enzymatically digested. After removal of unbound fragments, the epitope-containing antigen fragment is eluted and identified by matrix-assisted laser desorption ionization Fourier-transformation cyclotron resonance (MALDI-FT-ICR, see Figure 18).

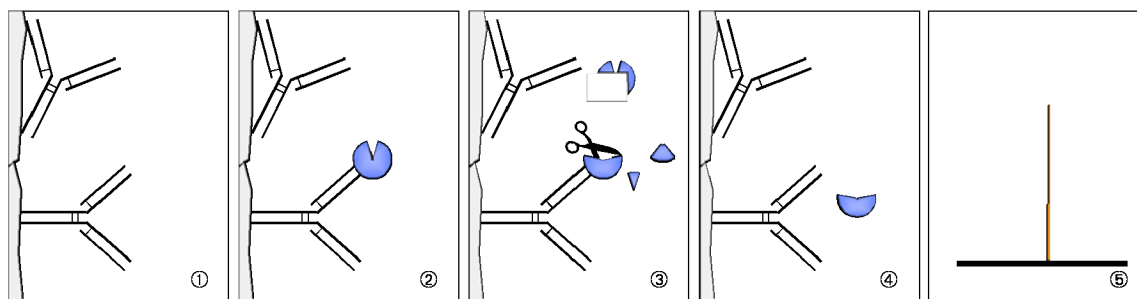


Figure 18: Epitope excision. ① Covalent coupling of the antigen-specific antibody to the Sepharose matrix ② Capturing of antigen by the immobilized antibody ③ Enzymatic proteolysis of bound antigen ④ Elution of the epitope-containing antigen fragment ⑤ Identification of the epitope fragment by MALDI-FT-ICR.

In epitope extraction, the native or acetylated antigen is enzymatically digested in solution. The epitope-containing antigen fragment is captured by the immobilized, antigen-specific antibody, and after removal of unbound fragments, it is eluted and identified by MALDI-FT-ICR (see Figure 19).

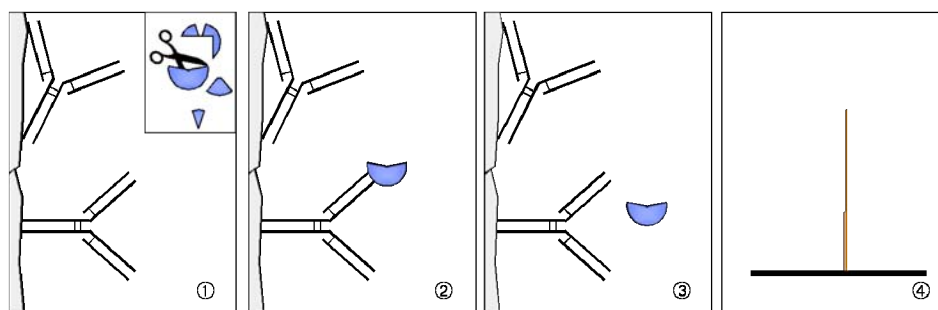


Figure 19: Epitope extraction. ① Covalent coupling of the antigen-specific antibody to the Sepharose matrix and enzymatic digest of antigen in solution ② Capturing of the epitope-containing antigen fragment ③ Elution of the epitope-containing antigen fragment ④ Identification of the epitope fragment by MALDI-FT-ICR.

The method bases on the high resistance of antibodies against proteolytic digest compared to the resistance of other proteins, and on the shielding effect,¹⁰⁷ that protects the epitope in the antigen-antibody complex from enzymatic degradation.

Digest with trypsin or α -chymotrypsin is suitable for most antigens, resulting in fragments of adequate size of 500 – 3'000kDa.

1.3.6 Surface Plasmon Resonance - Biacore

Biacore (Biomolecular Interaction Analysis) is used for the qualitative and quantitative analysis of bispecific interactions in real time. Affinities and binding kinetics can be determined and epitopes be mapped.

In Biacore antibody-capturing, the antigen is coupled to the dextran matrix of the sensor chip. In the injection phase, the antigen-specific antibody flows over the antigen surface and can associate. In the postinjection phase, the antibody dissociates. Finally, the antigen surface is regenerated to remove the remaining bound antibody (see Figure 20).

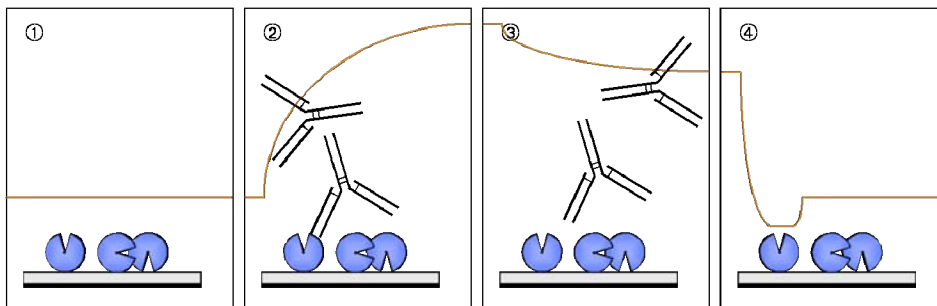


Figure 20: Surface Plasmon Resonance (Biacore) antibody-capturing in real time. ① Immobilization of the antigen on the dextran matrix of the sensorchip ② Association of the antigen-specific antibody to the antigen surface ③ Dissociation of the antibody from the antigen surface ④ Regeneration of the antigen surface.

The merits of Biacore are that no antibody labeling or purification is needed, and that the dissociation constant (K_D), the association rate (k_{on}), dissociation rate (k_{off}) and the binding mode can rapidly be determined. Affinities of antibodies can range from K_D $10^{-5}M$ to $10^{-12}M$.

Exact affinities can be calculated for monoclonal antibodies, but for polyclonal antibodies, only overall avidity can be measured.

1.3.7 Monoclonal versus polyclonal antibodies

In most immunochemical techniques, polyclonal and monoclonal antibodies are applicable.

Polyclonal antibodies allow the staining of fixed cells, since they bind to distinct denaturation-sensitive and resistant epitopes. For the same reason, multiple binding to one antigen molecule can occur, that result in stronger stain. However, as polyclonal include not antigen-specific antibodies, background problems are common, due to unspecific or specific binding to irrelevant proteins. This drawback can be avoided by immunoaffinity purification of polyclonal antibodies to get polyclonal antigen-specific antibodies, which are excellent in immunochemical techniques

Monoclonal antibodies commonly work good or excellent in all immunochemical methods, but since they bind only to one single epitope, they may fail in some techniques due to low avidity, epitope alteration or modification or due to hindered epitope access. The background is seldom high, but cross-reactions may cause troubles. Pooling of distinct non-competitive monoclonal antibodies bypass this problem (see Table 3).

Table 3: Choice of antibodies in immunochemical methods.

Immunochemical method		Blotting	Assay	Staining	Epitope affinity
Polyclonal Ab	Total	Good	Fair	Good	Not recommended
	Affinity pure	Excellent	Excellent	Better	Not recommended
Monoclonal Ab	Individual	Good	Good	Better	Best
	Pooled	Excellent	Excellent	Not recommended	Not recommended
Specificity / cross-reaction		Common	Occasional	Common	Occasional
Epitope		Denatured	Most native	Native / denatured	Native / denatured
Access	Multimeric binding	No	Common	Possible	Common
	Antigen modification	Possible	Possible	Possible	Possible
Factors for success	Antigen orientation	No	No	Common	No
		Denatured epitope	High-affinity Ab	Specificity	High-affinity Ab
Kinetic	Local Ag concentration	Mixed	Mixed	Mixed	Low
	Ag	Fixed	Free / fixed	Fixed	Free
	Ab	Free	Fixed / free	Free	Fixed
Binding kinetic		Slow	Fast	Slow	
	Antibody affinity	10^{-6} - 10^{-8} M		10^{-6} - 10^{-8} M	

High-affinity antibodies perform better in all immunochemical techniques, due to the higher stability and due to the increased number of antibody-antigen complexes.

1.4 Thesis

In the last few years various polyclonal antibodies against the entire human ASGPR or against specific regions of the ASGPR were raised in rabbit or goat but not in chicken. Bischoff *et al.*^{3,37} produced various polyclonal antibodies, directed against peptides at the C-terminus of H1 or H2, i.e. in the CRD domains or against the juxtamembrane sequence with the pentapeptide signal insert only present in H2a. Bider *et al.*⁴ also generated polyclonal antibodies, recognizing a C-terminal peptide in the CRD domain, specific to the epitope E²⁷⁷ – E²⁸⁶ of H1 and to H2. Finally, Yik *et al.*³⁸ got antibodies, specific to the same area of the H1-CRD, the epitope C²⁷⁶ – L²⁹¹, to the H2-CRD, and to the 19-residue insert, only present in H2a and H2b.

Interestingly, Park *et al.*⁵ raised polyclonal but not monoclonal antibodies in mice. The antibodies are directed against residues C¹⁶⁴ – Y¹⁸⁰ of the H1-CRD, the part of helix α 1, which exhibits the lowest homology to the murine H1-CRD.

In contrast to the many polyclonal antibodies, there are only reports of two monoclonal antibodies against the entire human ASGPR. First, the monoclonal antibody of Schwartz *et al.*⁶ was raised against the entire ASGPR isolated from human liver. Its epitope may be present on the H1 and / or the H2 domain, as nothing is told. Second, Kohgo *et al.*⁷ selected the monoclonal antibody 302011, which is also directed against the full-length human ASGPR. In addition, one reported monoclonal antibody is directed against the rat H1 subunit. This monoclonal antibody 8D7 however cross-reacts with the human H1 subunit. Finally, one monoclonal antibody against the entire rat and human ASGPR, with unknown epitope, is commercially available at Calbiochem.¹⁰⁸

For investigating the ASGPR function and for analytical, diagnostic and therapeutic application, monoclonal antibodies directed against the H1-CRD would be especially precious.

The final goal of this Ph.D. thesis was to produce and characterize monoclonal antibodies, particularly blocking antibodies against the H1-CRD, which can be used as an analytical tool for ASGPR isolation and purification, for testing of potential ASGPR agonists and antagonists, for drug targeting to hepatocytes, metabolic studies and the specific blocking of physiological processes.

First, mg quantities of H1-CRD had to be produced for immunization and antibody characterization. The recombinant *E.coli* expression system for the H1-CRD production

was available from Prof. Spiess,¹⁵⁸ and Meier M. *et al.*²⁶ had already published an H1-CRD purification method.

The monoclonal antibodies, produced by the hybridoma technology, should be characterized, and especially their ability to block the binding of ligands be investigated. Therefore, the design of a competitive ELISA was planned. The epitope and probably the paratope of the most promising antibodies should further be mapped.

To complete the set of investigational tools, also polyclonal antibodies against the H1-CRD should be raised and characterized.

2 Materials and Methods

Substances and equipments are listed in Appendix 1 (page 269).

2.1 Database research

2.1.1 Sequence alignments

The H1 subunit (ASGPR-1), the H1-CRD and its binding site sequence were aligned with homologous protein sequences of *homo sapiens* but also of *mus musculus* and *gallus gallus*, using the programs of Basic Local Alignment Search Tool (BLAST)¹⁰⁹ of the National Center for Biotechnology Information (NCBI) server.

Local similarities were searched with protein-protein BLAST (blastp) in non-redundant GenBank CDS (translations, RefSeq proteins, Brookhaven Protein Data Bank PDB, Swiss Protein Database SwissProt, PIR and PRF) with expect 10, word size 3 and matrix BLOSUM62 or with expect 20'000, word size 2 and matrix PAM30.

Nucleotide or protein sequences were aligned with bl2seq¹¹⁰ with both strands options, expect 10.0 and word size 11.

Multi-sequence alignments were performed with the T-COFFEE program¹¹¹ of Expert Protein Analysis System (ExPASy), available on the proteomics server of the Swiss Institute of Bioinformatics.

2.1.2 Epitope prediction plots

Plots for B-cell epitope prediction in the H1-CRD and its binding site were performed with the help of the ProScale program of ExPASy, using the algorithms of Hopp and Woods¹¹², Parker⁷⁸ and Welling⁸⁰ for antigenicity prediction, of Kyte and Doolittle¹¹³, Sweet and Eisenberg¹¹⁴, Janin¹¹⁵, Fauchere¹¹⁶ and Manavalan¹¹⁷ for hydrophobicity plots and the buried and accessible residues algorithms and Fraga recognition factor⁷⁹ algorithm for accessibility plots.

Window size was 9 with a linear weight variation model. Scales were normalized from 0 to 1 to allow overlay of the different plots using the Prism4 software.

2.2 Cloning, expression and purification of H1 Carbohydrate Recognition Domain

2.2.1 Buffers and Media

2.2.1.1 Buffers

TAE (40mM TrisOAc, 1mM EDTA)

TBE 0.5x (45mM TrisBorate, 1mM EDTA)

TE (10mM TrisHCl, 1mM EDTA, pH 8.0)

TBS (20mM TrisHCl, 500mM NaCl, pH 7.5)

TTBS (20mM TrisHCl, 500mM NaCl, 0.05% Tween20, pH 7.5)

TTBS-Ca20 (20mM TrisHCl, 500mM NaCl, 20mM CaCl₂, 0.05% Tween20, pH 7.5)

2.2.1.2 Media

Media were prepared as described in Sambrook J. *et al.*¹¹⁸

LB medium

10.0g Bacto tryptone, 5.0g Bacto yeast and 10.0g NaCl were dissolved in 950ml water. Upon setting the pH to 7.5 with NaOH (1M), the volume was adjusted to 1'000ml with water. The medium was autoclaved for 20min at 121°C and was stored at 4°C until use.

LB/agar plate

10.0g Bacto tryptone, 5.0g Bacto yeast and 10.0g NaCl were dissolved in 950ml water. Upon setting the pH to 7.5 with NaOH (1M), 15.0g Bacto agar was added and the volume was adjusted to 1'000ml with water. The medium was autoclaved for 20min at 121°C and cooled to 50°C while stirring magnetically. 1ml of antibiotic stock 1'000x (see Table 4) were diluted in the medium, before 40ml/plate were poured into Petri dishes. The solid LB/agar plates were enveloped with parafilm and stored at 4°C until use.

TB medium

12.0g Bacto tryptone, 24.0g Bacto yeast and 4.0ml glycerol were dissolved to 900ml in water and separately, 2.31g KH₂PO₄ and 12.54g K₂HPO₄ were solved to 100ml in water. Both, TB and phosphate buffer were autoclaved for 20min at 121°C and stored at 4°C. Just prior to use, they were combined (9:1) to get the TB medium.

SOC medium

2.0g Bacto tryptone, 0.5g Bacto yeast, 1ml NaCl (1M), 0.5ml KCl (1M) and 1ml MgCl₂ (2M) were dissolved to 95ml in water. Upon setting the pH to 7.0 with NaOH (1M), the volume was adjusted to 99ml with water. The medium was autoclaved for 20min at 121°C and was cooled to room temperature (RT) before 1ml sterile filtered glucose (2M) was added.

2.2.2 General DNA methods

2.2.2.1 OD₆₀₀ measurement

The cell density of *E.coli* cultures was controlled spectrometrically by measuring the optical density at 600nm (OD₆₀₀) according to Sambrook J. *et al.*¹¹⁸

Cell densities were calculated with Equation 1 using a conversion factor at OD₆₀₀ of 5.0·10⁸ cells/ml.

$$c = f \cdot OD_{600} \quad (\text{Eq. 1})$$

Equation 1: Calculation of the *E.coli* cell density (c) in cultures by measuring OD₆₀₀ using the conversion factor (f) of *E.coli* (5.0·10⁸ cells/ml).

E.coli culture aliquots were diluted to suitable concentrations in medium. 300µl diluted culture or blank (medium) were transferred into plastic semi-micro cuvettes and the turbidity was measured at OD₆₀₀ in a SmartSpec3000 cuvette spectrophotometer.

2.2.2.2 Bacteria cultivation and storage

E.coli strains were cultured as described by Sambrook J. *et al.*¹¹⁸ and by the pET System manual.¹¹⁹

In cultures of *E.coli* transformants, ampicilline, which is sensitive to low pH and β-lactamase was replaced by carbenicilline. 1% glucose was included in the medium to suppress the basal protein expression.

Table 4: Antibiotics and selective markers for cultivation of different *E.coli* strains and its transformants.

<i>E.coli</i> strain	Antibiotic resistance	Plasmid	Selective marker
JM109	No	+ pET3b + pEZZ18	+ carb (100µg/ml)
JM109(DE3)	No	+ pET3b	+ carb (100µg/ml)
AD494(DE3)	kan (15µg/ml)	+ pET3b	+ carb (100µg/ml)
Rosetta-gami(DE3)	kan (15µg/ml), tet (12.5µg/ml), cam (34µg/ml)	+ pET3b	+ carb (100µg/ml)
Top10	kan (15µg/ml), amp (50µg/ml), tet (12.5µg/ml)	+ pEZZ18	+ X-gal

Table 4 shows the antibiotics and selection markers, which were included in the media of used *E.coli* strains and their transformants.

2.2.2.2.1 Overnight and starter cultures

A few μl *E.coli* were scratched from the frozen glycerol stock using a pipet tip and were inoculated into 3ml medium containing 3 μl of each suitable antibiotic stock 1'000x and 150 μl glucose (20%) in a loosely closed culture tube (14ml). The culture was incubated overnight at 37°C, while shaking with 300rpm in a slightly oblique position.

2.2.2.2.2 Cultures on LB / agar plate for short time storage

A few μl *E.coli* overnight cultures were streaked on LB / agar plates containing suitable antibiotics, using a loop. The culture dishes were incubated cover-side up overnight at 37°C. afterwards, they were enveloped with parafilm and stored up to 1month at 4°C.

2.2.2.2.3 Glycerol stocks (15%) for long time storage

3ml LB medium in a culture tube were supplemented with 3 μl of each suitable antibiotic stock 1'000x prior to the inoculation with 200 μl *E.coli* overnight culture. The culture was incubated at 37°C, while shaking with 300rpm in a slightly oblique position until an OD₆₀₀ of 0.6-0.8 was reached. 850 μl aliquots were transferred to cryotubes and mixed with 150 μl sterile glycerol by vortexing, followed by immediate shock-freezing in liquid nitrogen (N₂). The frozen glycerol stocks were stored for indefinite time at -80°C.

2.2.2.2.4 MgCl₂ / CaCl₂ competent cells

Chemocompetent *E.coli* were prepared according to Morrison D.A.¹²⁰.

3ml LB medium in a culture tube containing no antibiotics or 3 μl of each suitable antibiotic stock 1'000x of were inoculated with 30 μl *E.coli* overnight culture and incubated at 37°C, while shaking with 300rpm in a slightly oblique position until an OD₆₀₀ of approximately 0.8 was reached. Cells were collected by centrifugation at 3'000rcf for 20min at 4°C and the pellet was washed once with 1ml ice-cold MgCl₂ (100mM), followed by centrifugation as before. The pellet was resuspended in 1ml ice-cold MgCl₂ by vortexing, and the cells were made competent by incubation on ice for 20min. After centrifugation as before, the pellet was resuspended in 255 μl ice-cold CaCl₂ (100mM) and was thoroughly mixed with 45 μl glycerol without vortexing, immediately followed by shock-freezing of 20 μl and 50 μl aliquots in liquid N₂. Competent *E.coli* cells were stored at -80°C.

2.2.2.3 Plasmid extraction

Plasmid DNA of *E.coli* transformants was prepared by alkali lysis according to Sambrook J. *et al.*¹¹⁸

One clone of transformed *E.coli* was cultured in 2ml LB medium containing appropriate antibiotics (see Section 2.2.2.2) overnight at 37°C. Cells were harvested at 16'000rcf for 1min and after complete removal of the supernatant by tapping onto a paper towel, the bacterial pellet was resuspended in 100µl ice-cold solution 1 (25mM TrisHCl, 50mM glucose, 10mM EDTA, pH 8.0) by vortexing and was gently mixed with 200µl solution 2 (200mM NaOH, 1% SDS) by inverting the tube five times. Following incubation on ice for 5min, 150µl ice-cold solution 3 (3M KOAc, 2M acetic acid) was added and dispersed by gently vortexing until precipitated proteins were resuspended completely. The lysate was incubated on ice for 5min and cleared by centrifugation at 11'000rcf for 5min at 4°C.

1 volume supernatant was extracted with 1 volume chloroform-phenol (1:1) by vortexing followed by spinning at 11'000rcf for 3min at 4°C. The upper phase was combined with 2 volumes ethanol by vortexing and the DNA was precipitated during incubation for 2min. After centrifugation at 11'000rcf for 3min at 4°C, the DNA pellet was rinsed once with 2 volumes ice-cold ethanol (70%) and air-dried for 10min. The purified plasmid DNA was dissolved in 25-50µl TE buffer (pH8.0) containing RNase A (20µg/ml) and was stored at -20°C.

2.2.2.4 Agarose-gel electrophoresis

Agarose-gel electrophoresis was performed according to Sambrook J. *et al.*¹¹⁸ The resolution is optimal for DNA in the range of 0.5-7kbp on a 1% gel, of 0.4-6kbp on a 1.2% gel, of 0.2-3kbp on a 1.5% gel and of 0.1-2kbp on a 2% gel.

DNA sample preparation

DNA samples and the molecular DNA ladder were diluted to 10µl with TE buffer (pH8.0), mixed with 2µl gel loading buffer 6x and spun down.

Agarose-gel preparation

0.8g to 1.6 g agarose was dissolved in 80ml TBE buffer 0.5x by heating in a microwave until boiling. The agarose solution was cooled to about 50°C. The gel was supplemented with 0.8µl ethidium bromide solution (10mg/ml) and poured into a horizontal electrophoresis chamber (100·100mm, 16 pockets).

Electrophoresis

The solid 1-2% agarose-gel containing ethidium bromide (0.1µg/ml) was overlaid with TBE buffer 0.5x just prior to use. After loading samples into the gel-pockets, the gel electrophoresis was run at 80-100mV (0.8 to 1mV/mm).

Ethidium-stained DNA fragments were visualized under UV light and documented using GelDoc2000 and the software Quantity One 4.1.

2.2.2.5 NaOAc / ethanol precipitation

The DNA was purified and concentrated by NaOAc / ethanol precipitation according to a method modified from Sambrook J. *et al.*¹¹⁸

0.9 volume DNA sample was placed on ice for 5min and mixed with 0.1 volume NaOAc (3M, pH6.5), and then 2.5 volumes ethanol absolute were added. After incubation for 1h at -80°C and centrifugation at 11'000rpm for 20min at 4°C, the DNA pellet was twice washed with 2 volumes ice-cold ethanol 70%. The purified DNA pellet was air-dried for 5min at 37°C and dissolved in 0.45volume TE buffer (pH8.0) containing RNase A (20µg/ml).

2.2.2.6 Quantification of DNA

The DNA was quantified by different methods, depending on the amount, the concentration and the purity of the DNA.

2.2.2.6.1 Quantification of plasmid dsDNA by $A_{260}:A_{280}$ measurement

The plasmid dsDNA concentration was determined spectrophotometrically by measuring the absorbance at 260nm (A_{260}) according to Sambrook J. *et al.*¹¹⁸

The concentration was calculated with Equation 2 using the conversion factor at A_{260} for dsDNA (50µg/ml). The DNA purity was controlled, by comparing the absorbance at 260nm to 280nm (A_{280}). The ratio of $A_{260}:A_{280}$ for pure DNA lies in the range of 1.6-1.8.

$$c = f \cdot A_{260} \quad (\text{Eq. 2})$$

Equation 2: Calculation of the plasmid dsDNA concentration (c) by measuring of the absorbance at (A_{260}) using the conversion factor (f) of dsDNA (50µg/ml).

The plasmid dsDNA samples were diluted in TE buffer (pH8.0) to a concentration up to 50µg/ml. 300µl samples or blank (TE buffer, pH8.0) were transferred into a quartz semi-micro cuvette (path length 1cm) and the absorbance was measured at 260nm and

280nm in a SmartSpec3000 cuvette spectrophotometer. Using the SmartSpec software, concentrations of plasmid dsDNA and ratios of $A_{260}:A_{280}$ were calculated.

2.2.2.6.2 Quantification of plasmid dsDNA by agarose-gel electrophoresis

The quantification of plasmid DNA by ethidium bromide staining on an agarose-gel was modified from Sambrook J. *et al.*¹¹⁸

The λ dsDNA standard was diluted in TE buffer (pH8.0) to 0.25, 0.5, 1.0, 2.0, 3.0, 4.5, 6.0, 8.0 and 10.0 μ g/ml and the sample to concentrations in the range of the standard.

10 μ l standards and samples were mixed with 2 μ l gel loading buffer 6x and run on an agarose-gel containing ethidium bromide (0.1 μ g/ml) following the method described in Section 2.2.2.4.

Using the GelDoc2000 and Quantity One 4.1 software, the gel was photographed (UV mode) and the standard calibration curve were drawn to estimate the content of plasmid dsDNA in the samples.

2.2.3 Cloning

2.2.3.1 Amplification of H1-CRD cDNA by Polymerase chain reaction

21bp forward primer (H1fw) including a *Nde* I restriction site and backward primer (H1bw) coding for two stop codons adjacent to a *Bam*H I restriction site were used for the amplification of the H1-CRD-encoding cDNA of the pET3H1 plasmid (H1-CRD cDNA).

2.2.3.1.1 Calculation of melting temperature and annealing temperature

The melting temperature (T_m) of the selected primers was calculated according to the two empirical equations of Wetmur J.G. *et al.*¹²¹ (Equation 3) and of Suggs S.V. *et al.*¹²² (Equation 4).

$$T_m(^{\circ}\text{C}) = 81.5 + 0.41(\text{g}\% + \text{c}\%) + 16.61\text{g}[\text{Na}^+] - 500/\text{length} \quad (\text{Eq. 3})$$

Equation 3: Melting temperature (T_m) estimation according to Wetmur: T_m calculation of a primer of defined length containing g% guanosine and c% cytosine, dissolved in a 0.05M Na^+ .

$$T_m(^{\circ}\text{C}) = 2^{\circ}\text{C}(\text{a} + \text{t}) + 4^{\circ}\text{C}(\text{c} + \text{g}) \quad (\text{Eq. 4})$$

Equation 4: Melting temperature (T_m) estimation according to Suggs: T_m determination of a primer containing a adenine, t thymidine, c cytosine and g guanosine nucleotides.

The forward primer H1fw 5'-catatgggctcagaaaggacc-3' (calculated T_m 57.6°C and 64°C) was used in combination with the backward primer H1bw 5'-ggatccttattaaaggagagg-3' (calculated T_m 53.7°C and 60°C) or with the M13 standard primer 5'-tgtaaacgacggccag-3' (calculated T_m 35.8°C and 54°C).

For both primer pairs the annealing temperature was set 5°C below the T_m of the primer with the lower T_m . The annealing temperatures were therefore 48°C for primer pair H1fw / H1bw and 45°C for primer pair H1fw / M13.

2.2.3.1.2 Polymerase chain reaction using *Taq* and *Pfu* DNA polymerase

The polymerase chain reaction (PCR) method was adapted from the *Taq* PCR handbook¹²³, originally based on the method by Mullis K. *et al.*¹²⁴.

For n samples, n -40µl mastermix 1 or 2 were assembled on ice according to Formulation 1 and distributed into n PCR tubes. 25-250ng of template DNA (purified pET3H1 plasmid DNA, see Section 2.2.2.3) diluted to 10µl in water or 10µl water (negative control) were added to the mastermix and amplified using the oil-free iCycler thermal cycler.

	Mastermix 1	Mastermix 2
<i>Taq</i> PCR buffer 10x	5µl	
<i>Pfu</i> PCR buffer 10x		5µl
dNTP mix (10mM)	1µl	1µl
Forward primer H1fw (20µM)	1µl	1µl
Backward primer H1bw (20µM)	1µl	1µl
<i>Taq</i> DNA polymerase (5U/µl)	0.5µl	
<i>Pfu</i> DNA polymerase (2.5U/µl)	0.1µl	1µl
Nanopur water	31.4µl	31µl
	40µl	40µl

Formulation 1: Composition of the mastermix 1 and 2 for 50µl PCR reactions to get final concentrations of 200µM dNTP (dATP, dCTP, dGTP, dTTP), 400nM forward primer, 400nM backward primer, 2.5U *Taq* DNA polymerase and / or 2.5U *Pfu* DNA polymerase in PCR buffer 1x.

After 2-3min initial denaturation at 94°C, the amplification of H1-CRD cDNA was run for 32-36 cycles of 30s denaturation at 94°C, 30s annealing at the appropriate temperature and 1min (with *Taq* / *Pfu* DNA polymerases) or 2min (with *Pfu* DNA polymerase) extension at 72°C. The final extension was for 10min at 72°C.

The PCR products were analyzed by agarose-gel electrophoresis as described in Section 2.2.2.4. The H1-CRD cDNA was ligated into plasmid vectors without or after trimming of cDNA ends (see Section 2.2.3.2).

2.2.3.2 Digest of H1-CRD cDNA and plasmid vectors pEZZ18 for ligation

The restriction of H1-CRD cDNA and plasmid vectors pEZZ18 prior to the ligation was planned using the Cloning Manager software.

The plasmid vector pEZZ18 has one restriction site for *Sma* I (2932) and *Bam*H I (2935) but no restriction site for *Nde* I in the multiple-cloning site. *Bam*H I produce 5'-gatcc-protruding termini allowing the specific cohesive, so-called "sticky" ligation. *Sma* I produce blunt termini and was therefore used for the unspecific blunt ligation (see Appendix 3, page 280).

2.2.3.2.1 Restriction digest of H1-CRD cDNA

The PCR-amplified H1-CRD cDNA was digested with *Bam*H I, producing 5'-sticky cDNA fragments for blunt-sticky ligation into pEZZ18.

Pfu DNA polymerase-amplified H1-CRD cDNA (see Section 2.2.3.1) was cut with *Bam*H I at the 5' end according to the instructions of the manufacturer.

*Bam*H I digest

NE <i>Bam</i> H I buffer 10x	3µl
H1-CRD cDNA (<i>Pfu</i> -amplified)	20µl
BSA (1mg/ml)	3µl
Water	2.5µl
<i>Bam</i> H I (10U/µl)	1.5µl
	30µl

Formulation 2: Composition of *Bam*H I restriction digest of H1-CRD cDNA.

30µl *Bam*H I restriction digest (*Pfu*-amplified H1-CRD cDNA, 0.01% BSA, 15U *Bam*H I in NE *Bam*H I buffer) was assembled on ice in a 1.5ml tube according to Formulation 2 and briefly spun down. After incubation at 37°C for 3h, while shaking with 300rpm, the *Bam*H I was inactivated by incubation at 85°C for 15min, while shaking with 300rpm.

The restricted H1-CRD cDNA were analyzed by agarose-gel electrophoresis (see Section 2.2.2.4) and purified by NaOAc / ethanol precipitation or by agarose-gel extraction (see Section 2.2.2.4) prior to ligation.

2.2.3.2.2 Restriction digest and dephosphorylation of plasmid vector pEZZ18

Restriction digest of plasmid vectors pEZZ18 with Sma I and BamH I

The plasmid vector was either cut with the restriction enzyme *Sma* I for blunt-blunt ligation or double digested with *Sma* I and *Bam*H I for blunt-sticky ligation.

The plasmid vector pEZZ18 was first digested according to the manufacturer instructions.

	<i>Sma</i> I digest	<i>Bam</i> H I digest
Y ⁺ / Tango buffer 10x	5µl	-
Plasmid pEZZ18	30µl	-
Plasmid pEZZ18 (<i>Sma</i> I-digested)	-	25µl
Water	10µl	10µl
<i>Sma</i> I (10U/µl)	5µl	-
BSA (10mg/ml)		1.5µl
NE <i>Bam</i> H I buffer 10x		1.5µl
<i>Bam</i> H I (10U/µl)		2µl
	50µl	40µl

Formulation 3: Composition of the restriction digest of pEZZ18 with *Sma* I or *Bam*H I.

50µl *Sma* I restriction digest (pEZZ18 plasmid DNA, 50U *Sma* I in Y⁺ / Tango buffer) was mixed according to Formulation 3 in a 1.5ml tube and was briefly spun down prior to incubation overnight at 30°C, while shaking with 300rpm. Then, 40µl *Bam*H I restriction digest (*Sma* I-digested linear pEZZ18 plasmid DNA, 0.01% BSA, 20U *Bam*H I in NE *Bam*H I buffer) was assembled and was incubated for 3h at 37°C, while shaking again with 300rpm. Finally restriction enzymes were inactivated during incubation at 65°C for 20min, while shaking with 300rpm.

Dephosphorylation of digested plasmid vector pEZZ18

The linear plasmid vector pEZZ18 was dephosphorylated with calf intestinal alkaline phosphatase (CIAP) according to the manufacturer instructions.

	Dephosphorylation reaction 1 (<i>Sma</i> I-digested pEZZ18)	Dephosphorylation reaction 2 (<i>Sma</i> I / <i>Bam</i> H I-digested pEZZ18)
CIAP buffer 10x	4µl	5µl
Plasmid pEZZ18 (digested)	25µl	40µl
Water	8µl	2µl
CIAP (1U/µl)	3µl	3µl
	40µl	50µl

Formulation 4: Composition of the dephosphorylation reaction of the linearized plasmid vector pEZZ18.

40µl dephosphorylation reaction 1 (25µl *Sma* I-digested pEZZ18 DNA, 3U CIAP in CIAP buffer) and 50µl dephosphorylation reaction 2 (40µl *Sma* I and *Bam*H I-digested pEZZ18 DNA, 3U CIAP in CIAP buffer) was assembled according to Formulation 4, was vortexed and briefly spun down. After incubation for 30min at 37°C, the dephosphorylation was stopped by inactivation of the alkaline phosphatase at 85°C for 15min, while shaking with 300rpm.

The digested and dephosphorylated plasmid vector pEZZ18 was analyzed by agarose-gel electrophoresis (see Section 2.2.2.4) and purified by NaOAc / ethanol precipitation or by agarose-gel extraction (see Section 2.2.2.5) prior to ligation.

2.2.3.3 Ligation

2.2.3.3.1 Molar ratio of H1-CRD cDNA to plasmid vector pEZZ18

A molar DNA ratio of insert : plasmid vector in the range of 3:1 to 1:3 is recommended.¹²⁵ The amount of H1-CRD cDNA and plasmid vector pEZZ18 was calculated using Equation 5.

$$\frac{M_i}{M_v} \cdot \frac{bp_i}{bp_v} \cdot x_v = x_i \quad (\text{Eq. 5})$$

Equation 5: Amount of H1-CRD cDNA (x_i) for ligation into a known amount of plasmid vector (x_v) in a molar ratio of insert : plasmid ($M_i:M_v$) of 3:1 to 1:3. The size of the H1 cDNA PCR fragment (bp_i) is 450bp (undigested), 445bp (*BamH* I-digested) or 443bp (*Nde* I and *BamH* I-digested). The plasmid vector pEZZ18 is 4591bp (*Sma* I-digested) or 4588bp (*Sma* I and *BamH* I-digested) in length (bp_v).

2.2.3.3.2 Ligation of H1-CRD cDNA into pEZZ18 vector

The blunt-blunt ligation of the purified undigested H1-CRD cDNA (see Section 2.2.3.1.2) into the purified *Sma* I-digested and dephosphorylated pEZZ18_{blunt} vector (see Section 2.2.3.2.2) or the blunt-sticky ligation of the purified *BamH* I-digested H1-CRD cDNA into the purified *Sma* I and *BamH* I-digested and dephosphorylated pEZZ18_{sticky} vector using T4 DNA ligase was performed according to the manufacturer instructions.

The molar ratio of insert : plasmid was chosen 1:1

	Ligation into pEZZ18 _{blunt}	Ligation into pEZZ18 _{sticky}
T4 DNA ligase buffer 10x	2µl	2µl
Plasmid pEZZ18 vector DNA (x_v/v_v)	x_v	x_v
H1-CRD cDNA (x_i/v_i)	v_i	v_i
Water	8µl-(v_v+v_i)	11µl-(v_v+v_i)
PEG6000 50%	2µl	1µl
T4 DNA ligase (MBI Fermentas)	8µl	6µl
	20µl	20µl

Formulation 5: Composition of the reaction for the ligation of H1-CRD cDNA into the pEZZ18 plasmid vector.

20µl blunt ligation reaction (x_v plasmid pEZZ18_{blunt}, x_i H1-CRD cDNA, 5% PEG6000, 8U T4 DNA ligase in T4 DNA ligase buffer) and 20µl sticky ligation reaction (x_v plasmid pEZZ18_{sticky}, x_i H1-CRD cDNA, 2.5% PEG6000, 6U T4 DNA ligase in T4 DNA ligase buffer) were set up in 1.5ml tubes on ice according to Formulation 5. After briefly

spinning down, the ligation reactions were incubated overnight at 16°C, followed by the ligase inactivation for 10min at 65°C.

Recombinant plasmids (pEZZ18H1_{blunt}, pEZZ18H1_{sticky}) were used without purification to transform the *E.coli* cloning strain JM109 (see Section 2.2.3.4).

2.2.3.4 Transformation

In the plasmid pET3H1, the expression of the H1-CRD cDNA is under the control of a T7 promoter. The plasmid was first amplified by transformation of *recA*⁻ and *endA*⁻ *E.coli* cloning strain JM109. For protein expression, the extracted plasmid pET3H1 was used to transform λ DE3 lysogenic *E.coli* expression strains JM109(DE3), AD494(DE3) and Rosetta-gami(DE3). The plasmid-encoded ampicilline resistance allowed the selection of transformants (see Table 4).

Plasmids pEZZ18, pEZZ18H1_{blunt} and pEZZ18H1_{sticky} use a *lacUV5* promoter. For the plasmid amplification *E.coli* JM109 and for the expression *E.coli* cloning and expression host Top10 were used. JM109 transformants can be selected with ampicilline and Top10 transformants by α -complementation (see Appendix 4, page 281).

Plasmids pET3H1, pEZZ18, pEZZ18H1_{blunt} and pEZZ18_{sticky} were transformed into chemocompetent *E.coli* cells according to the manufacturer instructions and to the Competent Cell Manual¹²⁶.

Two aliquots of 20-50 μ l chemocompetent *E.coli* cells in 1.5ml tubes were thawed in ice-water. 1-2 μ l pEZZ18H1 ligation reaction, 5-10ng purified plasmid pEZZ18H1 or pET3H1 (see Section 2.2.2.3 and 2.2.2.5) or water for negative control were added and mixed by flicking. After incubation on ice for 20min, the plasmid was transformed into *E.coli* cells by heat shock for 45s at 42°C on a heating block without shaking, immediately followed by the incubation in ice-water for 2min. Cells were diluted with 80 μ l SOC medium and incubated for 1h at 37°C, while shaking with 300rpm. 50-100 μ l transformed *E.coli* were plated on a LB / agar plate containing selective marker and incubated cover-side down overnight at 37°C.

A number of transformed clones were analyzed to control the transformation (see Section 2.2.3.5) followed by freezing of selected *E.coli* clones (see Section 2.2.2.3).

2.2.3.5 Analysis of *E.coli* transformants

2.2.3.5.1 PCR analysis

Colony PCR

The colony PCR of *E.coli* transformants were performed according to the pET System Manual.¹¹⁹

Colonies of transformed *E.coli* were picked from the transformation LB / agar plate (see Section 2.2.3.4) using a pipet tip and were suspended in 25µl TritonX100 (0.1%) by pipetting and vortexing. After incubation for 1h at 55°C, while shaking with 300rpm, cell lysates were cleared at 16'000rcf for 5min.

10µl lysate supernatants were taken and hold template DNA was amplified by PCR (see Section 2.2.3.1.2). The presence of H1-CRD cDNA was verified using insert-specific primers H1fw and H1bw and additionally, the orientation of H1-CRD cDNA in pEZZ18H1_{blunt} was checked using the H1-CRD DNA-specific primer H1fw in combination with the plasmid vector-specific primer M13 (annealing temperature 45°C).

PCR products were analyzed by agarose-gel electrophoresis (see Section 2.2.2.4).

Standard PCR

Colonies of transformed *E.coli* were picked from the transformation LB / agar plate (see Section 2.2.3.4) using a pipet tip and were inoculated into 3ml LB medium containing appropriate antibiotics followed by incubation overnight at 37°C, while shaking with 300rpm (see Section 2.2.2.2.1).

The plasmid DNA was extracted (see Section 2.2.2.3). 10µl of ten to hundred times diluted plasmid DNA in water were taken and hold template DNA was amplified by PCR (see Section 2.2.3.1.2) using the H1-CRD DNA-specific primer pair H1fw and H1bw (annealing temperature 48°C).

PCR products were analyzed by agarose-gel electrophoresis (see Section 2.2.2.4).

2.2.3.5.2 Restriction digest analysis

Colonies of transformed *E.coli* were picked from the transformation LB / agar plate (see Section 2.2.3.4) using a pipet tip and were inoculated into 3ml LB medium containing suitable antibiotics, followed by incubation overnight at 37°C, while shaking with 300rpm, according to the procedure described in Section 2.2.2.2.1. The plasmid DNA was

extracted (see Section 2.2.2.3) and either digested with *Nde* I or double digested with *Nde* I and *Bam*H I, according to the manufacturer instructions.

	<i>Nde</i> I digest	<i>Nde</i> I & <i>Bam</i> H I digest	Negative control	Blank control
NE 2 buffer 10x	2µl	2µl	2µl	2µl
Plasmid DNA	14µl	14µl	14µl	-
BSA (1mg/ml)	2µl	2µl	2µl	2µl
Water	1µl	-	2µl	14µl
<i>Nde</i> I (20U/µl)	1µl	1µl	-	1µl
<i>Bam</i> H I (10U/µl)	-	1µl	-	1µl
	20µl	20µl	20µl	20µl

Formulation 6: Setup of the restriction digest with *Nde* I or of the double digest with *Nde* I and *Bam*H I. Both enzymes are 100% active in NE 2 buffer.

20µl restriction digests (extracted plasmid DNA, 0.01% BSA, 10U *Bam*H I and / or 20U *Nde* I in NE 2 buffer) were assembled in 1.5ml tubes according to Formulation 6, spun down briefly and were incubated for 3h at 37°C, while shaking with 300rpm.

Restriction digest controls containing all components except restriction enzymes in negative control or except plasmid DNA in blank control were set up in parallel.

The digested plasmid DNA was analyzed by agarose-gel electrophoresis, according to the procedure described in Section 2.2.2.4.

2.2.3.5.3 Plasmid DNA sequence verification of *E.coli* expression clone

A starter culture of the selected *E.coli* expression clone in 3ml LB medium containing suitable antibiotics was prepared as described in Section 2.2.2.2.1 and was incubated for 9h at 37°C, while shaking with 300rpm.

One loop of starter culture was streaked on a LB / agar plate containing antibiotics according to Section 2.2.2.2.2 and was incubated coverside-down overnight at 37°C.

The cultured LB / agar plate was sent for sequencing at Microsynth GmbH sequencing group (Balgach). The plasmid DNA was sequenced in both directions using the T7 primer for forward sequencing and the T7term primer for backward sequencing of the complementary strand.

Sequences of H1-CRD cDNA were verified by the alignment with H1-CRD DNA sequence (accession 1DV8) using BLAST programs bl2seq, blastn and blastx of the NCBI server.

2.2.4 General protein methods

2.2.4.1 TCA / acetone precipitation

Proteins of *E.coli* culture samples were purified and ten times concentrated by TCA / acetone precipitation according to the pET System manual.¹¹⁹

The pellet of 1-2ml *E.coli* culture sample was suspended in 1 volume PBS (pH7.5). The sample was mixed with 0.1 volume ice-cold TCA (100%) by vortexing and proteins were precipitated during incubation on ice for 30min. After collection at 16'000rcf for 10min at 4°C, the pellet was once washed with 0.1 volume ice-cold acetone and centrifuged at 16'000rcf for 5min at 4°C. The purified protein pellet was air-dried for 1h prior to dissolving in 0.1 volume PBS (pH7.5) by sonication in a water bath for a few minutes.

The concentrated protein sample was mixed with the same volume reducing sample buffer 2x (80mM TrisHCl, 100mM DTT, 15% glycerol, 2% SDS, 0.006% bromophenol blue, pH 6.8) followed by sonication in a water bath for 5min and boiling for 5min at 95°C, while shaking with 1'200rpm. The reduced and denatured sample was centrifuged at 16'000rcf for 5min and stored at -20°C until SDS-PAGE and Western blot analyses (see Sections 2.2.4.2 and 2.2.4.3).

2.2.4.2 Polyacrylamide-gel Electrophoresis and staining

The discontinuous polyacrylamide-gel electrophoresis (PAGE) was performed according to the Protein Methods,¹²⁷ derived originally from Ornstein L.¹²⁸, Davis B.J.¹²⁹ and Laemmli E.K.¹³⁰. Proteins were separated in the native PAGE under native conditions and in the denaturing SDS-PAGE under reducing or non-reducing conditions.

2.2.4.2.1 Reducing SDS-PAGE

Proteins were separated according to their molecular weight on a SDS-PAGE gel by the method of Laemmli.

Protein sample preparation

The low or high molecular weigh marker, the reference sample and protein samples were diluted to an suitable volume in water, combined with 0.25 volume sample buffer 5x (200mM TrisHCl, 37.5% glycerol, 5% SDS, 250mM DTT or 2M β -mercaptoethanol, 0.015% bromophenol blue, pH 6.8) by vortexing and were boiled for 5min at 95°C, while

shaking with 1'200rpm. Denatured samples were spun down briefly and stored on ice until use.

Polyacrylamide-gel preparation

The percentage of polyacrylamide in the gel was adjusted, dependent on the molecular weight of analyzed proteins. The resolution for proteins with a molecular weight in the range of 16-68kDa was best on a 10% gel, of 14-55kDa on a 12% gel and of 16-68kDa on a 15% gel. The thickness of the gel was chosen, in dependence of the protein concentration and the following procedure. Generally, 1.0mm gels were prepared for staining and 1.5mm gels for electroblotting.

Inner and outer glass plates, spacers (0.75-1.5mm) and the comb (0.75-1.5mm, 15teeth) were rinsed with water and ethanol prior to assembly. The separating gel solution (375mM TrisHCl, x% polyacrylamide, 1% SDS, 0.05% TEMED, 0.03-0.1% APS, pH 8.8) was mixed according to Formulation 7, was poured immediately and mounted with some μ l water. After polymerization, the stacking gel (125mM TrisHCl, 5% polyacrylamide, 1% SDS, 0.1% TEMED, 0.03-0.1% APS, pH6.8) was mixed, immediately poured and the comb was introduced prior to polymerization.

	Separating gel x%	Stacking gel
Acrylamide solution 30% (acrylamide:bisacrylamide 37.5:1)	0.5-xml	1.7ml
Water	11.8-(0.5-x)ml	7.2ml
TrisHCl 1.875M (pH8.8)	3.0ml	
TrisHCl 1.25M (pH6.8)		1.0ml
Sodiumdodecylsulfate (SDS) 10%	150 μ l	100 μ l
N,N,N,N'-Tetramethylethylenediamine (TEMED)	7.5 μ l	10 μ l
Ammoniumpersulfate (APS) 10-40%	50 μ l	33 μ l
	15.0ml	10.0ml

Formulation 7: Composition of the separating gel containing x% polyacrylamide and of the stacking gel.

Electrophoresis

After complete polymerization, gels were submersed in running buffer (25mM Tris, 200mM glycine, 0.1% SDS) and samples were loaded into the gel-pockets using a Hamilton syringe. The electrophoresis was run at a constant current of 30mA/gel (stacking gel) and of 40mA/gel (separating gel) in a Mini Protean gel cell.

After PAGE, gel slabs were stained with silver stain for qualitative protein analysis (see Section 2.2.4.2.4) and with Coomassie Brilliant Blue G250 stain for quantitative analysis (see Section 2.2.4.4.3) or were blotted to nitrocellulose (see Section 2.2.4.3)

2.2.4.2.2 Non-reducing SDS-PAGE

The non-reducing SDS-PAGE followed the same procedure as described for reducing SDS-PAGE (see Section 2.2.4.2.1) but differed in the sample buffer composition by excluding reductants β -mercaptoethanol and DTT.

2.2.4.2.3 Native SDS-PAGE

The native PAGE followed the same procedure as described for reducing SDS-PAGE (see Section 2.2.4.2.1) but gels, running and sample buffers contained no SDS and no reductants β -mercaptoethanol and DTT and samples were not denatured by boiling.

2.2.4.2.4 Silver staining

Electrophoretically separated proteins on a PAGE gel slab were silver-stained using the Pharmacia Biotech Silver staining kit according to the instruction manual, originally derived from the method of Heukeshoven J. *et al.*¹³¹ that allows the detection of protein down to 2-10ng/band.

The PAGE gel slab was incubated in 125ml fixation buffer (40% ethanol, 10% acetic acid) in a plastic container for 30min, while shaking with 70rpm and was soaked in 125ml sensitizing solution (30% ethanol, 68mg/ml NaOAc, 2mg/ml NaThiosulphate, 0.125% glutaraldehyde) for 30min, while shaking with 70rpm. After washing three times in about 200ml water for 5min, the gel slab was stained in 125ml silver solution (2.5mg/ml silvernitrate, 0.015% formaldehyde) for 20min, while shaking with 70rpm and destained twice in about 200ml water for 1min. The stain of protein bands was developed in 125ml developing solution (25mg/ml NaCarbonate, 0.0075% formaldehyde) for an appropriate time and stopped in 125ml stopping solution (14.6mg/ml Na₂EDTA·2H₂O) during incubation for 5min, followed by rinsing once in about 200ml water.

Stained gels were documented using the GelDoc2000 and Quantity One 4.1 software.

2.2.4.3 Electroblothing and immunostaining (immunoblotting)

Separated proteins on a PAGE gel were electrophoretically blotted to the nitrocellulose membrane according to a semi-dry transfer method adapted from Kyhse-Andersen J. *et al.*¹³² Three different buffers, originally derived from Towbin H. *et al.*¹³³ were used.

2.2.4.3.1 PAGE

Sample proteins were separated by SDS-PAGE or native PAGE according to the protocol described in Section 2.2.4.2.

2.2.4.3.2 Electroblotting

18 sheets of Whatman 3M absorbent paper and 1 sheet of nitrocellulose membrane (pore size 0.2 μ m) were cut to the size of the PAGE gel (60mm·85mm) and the membrane was wet in water. To assemble the blot sandwich, 6 papers were soaked for a few minutes in anode buffer 1 (300mM Tris, 20% methanol) and piled up on the bottom anode, followed by 3 papers and the membrane soaked in anode buffer 2 (25mM Tris, 20% methanol), the PAGE gel and 9 papers soaked in cathode buffer (40mM 6-aminocaproic acid, 20% methanol) and the cathode at the top. After electroblotting for 90min at 15V using a TransBlot semi-dry transfer cell, the blotted PAGE gel was silver-stained (see Section 2.2.4.2.4) and the nitrocellulose membrane was colored with Ponceau S prior to the immunostaining.

2.2.4.3.3 Staining

Ponceau S staining of blotted total proteins

The blotted nitrocellulose membrane was stained in Sigma Ponceau S solution (0.1%) in a plastic container for a few minutes, while shaking with 70rpm and was destained twice in about 100ml water. Visible protein bands were marked with pencil before immunostaining.

Immunostaining of blotted specific protein

The unspecific binding to the blotted nitrocellulose membrane was blocked during incubation in 50ml blocking buffer (4% non-fat dried milk powder in TBS) in a plastic container for 4h (or overnight at 4°C), while shaking with 70rpm. After washing three times in about 50ml TTBS-Ca20 (20mM CaCl₂ in TTBS) for 5min, the blot was incubated in 10ml primary antibody solution (anti-H1 antibodies according to Table 5, 1% BSA in TTBS-Ca20) overnight at 4°C (or for 2h at room temperature), while shaking with 70rpm. The membrane was washed three times in about 50ml TTBS-Ca20 for 5min prior to the incubation in 10ml secondary antibody (alkaline phosphatase (AP)-labeled antibodies according to Table 5, 1% BSA in TTBS-Ca20) for 2h, while shaking with 70rpm. After washing twice thoroughly in about 50ml TTBS-Ca and once in about 50ml TBS for 5min,

bands of the specific protein were revealed in 10ml substrate solution (0.4% NBT/BCIP, 100mM TrisHCl, 100mM NaCl, 5mM MgCl₂, pH 8.8) for an appropriate time. The stain was stopped, by rinsing the membrane briefly in water or 5mM EDTA (pH8.0).

Table 5: Primary and secondary antibodies, which were used for immunostaining.

Primary antibody	Working dilution	Secondary antibody	Working dilution
Monoclonal anti-H1 IgG	0.5-5µg/ml	GAM-IgG(whole)-AP	1:2'000 to 1:5000
Anti-H1 IgG-containing supernatants	No	GAM-Ig(polyvalent)-AP	1:2000 to 1:5000
Anti-H1 IgY-containing total IgY	100µg/ml	RACH-IgY(whole)-AP	1:5000

The immunostained blot was documented using the GelDoc2000 and Quantity One 4.1 software (white mode).

2.2.4.4 Protein quantification

2.2.4.4.1 Protein quantification by A₂₈₀ measurement

The protein concentration was spectrophotometrically estimated, by measuring the absorbance at 280nm (A₂₈₀) according to Harlow E. *et al.*¹⁰², originally derived from Layne E.¹³⁴ and Peterson G.L.¹³⁵.

Concentrations were calculated with Equation 6 using the protein-specific conversion factors at A₂₈₀ for BSA (0.7mg/ml), IgM (1.2mg/ml), IgG (1.35mg/ml) and for IgY (1.31-1.44mg/ml).⁶⁷ The method is sensitive in the range of 0.2-2mg/ml proteins.¹²⁷

$$c = f \cdot A_{280} \quad (\text{Eq. 6})$$

Equation 6: Calculation of the protein concentration (c) by measuring absorbance at 280nm (A₂₈₀) using protein-specific conversion factors (f).

Samples were diluted to suitable concentrations with sample buffer (blank).

300µl sample or blank were transferred into a quartz semi-micro cuvette (path length 1cm) and the absorbance was measured at 280nm in a SmartSpec3000 cuvette spectrophotometer.

Sample concentrations were calculated using the SmartSpec or Excel software.

2.2.4.4.2 Protein quantification by Bradford assay

The Bradford assay, originally introduced by Bradford M.M.¹³⁶ was performed according to the standard method, the micro method¹³⁷ or the spot method.¹⁰² The assay is sensitive in the range of 25-200µg/ml proteins.¹²⁷

Bradford standard assay

The BSA standard was diluted to 0, 20, 40, 60, 80, 100, 120, 160 and 200µg/ml and samples were diluted in sample buffer (blank) to concentrations in the range of the standard. Standards and samples were measured in duplicates or triplicates.

20µl BSA standard dilutions, protein samples or blank were mixed with 50µl NaOH (1M) by pipetting in semi-micro cuvettes (path length 1cm) prior to addition of 1'000µl dye solution (0.01% Coomassie Brilliant Blue G250, 10% phosphoric acid 85%, 5% ethanol). After mixing by inversion and incubation for at least 5min, the absorbance was measured within 1h at 595nm in a SmartSpec3000 cuvette spectrophotometer.

Using SmartSpec or Excel software, the linear regression graph of standards was drawn and, if the correlation coefficient R^2 was > 0.95 , concentrations of the samples were calculated.

Bradford micro assay

The BSA standard was diluted to 0, 100, 200, 400, 600, 800 and 1'000µg/ml and samples were diluted in sample buffer (blank) to concentrations in the range of the standard. Standards and samples were measured in duplicates or triplicates.

10µl BSA standard dilutions, protein samples or blank were transferred to wells on 96-well culture plates, already containing 200µl dye solution (0.01% Coomassie Brilliant Blue G250, 10% phosphoric acid 85%, 5% ethanol) and were mixed by tapping the plate. After incubation for at least 5min, the absorbance was measured within 1h at 595nm in a Spectramax190 plate reader.

Using the software Spectramax PRO 4.0 or Excel, the linear regression graph of standards was drawn and, if the correlation coefficient R^2 was > 0.95 , concentrations of the samples were calculated.

2.2.4.4.3 Protein quantification by SDS-PAGE

The protein quantification on a SDS-PAGE gel was performed according to the Coomassie Brilliant Blue G method by Smith B.J. *et al.*¹³⁷, derived from Reisner A.H. *et al.*¹³⁸ The assay is sensitive in the range of 10ng/mm² to 5µg/mm² protein.

The BSA standard was diluted to 0, 5, 10, 20, 50, 100 and 200µg/ml and samples were diluted in water to a concentration in the range of the standard.

10µl standard and sample dilutions were mixed with 5µl non-reducing sample buffer 3x (120mM TrisHCl, 37.5% glycerol, 5% SDS, 0.009% bromophenol blue, pH 6.8) and were boiled for 5min at 95°C, while shaking with 1'200rpm.

The non-reducing SDS-PAGE was run, following the protocol in Section 2.2.4.2.2.

The run PAGE gel was incubated in 50ml fixation buffer (20% ethanol, 5% glacial acetic acid) for 20min, while shaking with 70rpm, and then was three times washed with about 200ml water for 5min. After staining for 90min in 50ml dye solution (0.01% Coomassie Brilliant Blue G250, 10% phosphoric acid 85%, 5% ethanol) while shaking with 70rpm, the stained gel was washed in water that contained some cotton wool until complete distain of background.

Using the GelDoc2000 and Quantity One 4.1 software, the gel was photographed (white mode) and the standard calibration curve was drawn to calculate the amounts of sample protein.

2.2.5 H1-CRD expression and purification

2.2.5.1 H1-CRD expression

The H1-CRD was expressed in pET3H1 transformed *E.coli* clones (see Section 2.2.3.4) as described in the pET System Manual.¹¹⁹

3ml starter cultures (see Section 2.2.2.2.1) of *E.coli* expression clones in LB or TB medium with appropriate antibiotics (see Table 4) and with glucose (1%) were incubated at 37°C overnight. After centrifugation at 3'000rcf for 5min, cells were resuspended in 3ml fresh medium, prior to the dilution into 50ml fresh medium to get an OD₆₀₀ of 0.1 (5·10⁷cells/ml). The culture was incubated at 37°C, while shaking with 300rpm, until an OD₆₀₀ of 0.8-1.0 was reached. The expression was induced by addition of 0.4mM IPTG followed by incubation for another 5h at 37°C, while shaking with 300rpm. After cooling on ice for 5min, cells were harvested at 3'000rcf for 10min at 4°C and the pellet was stored at 4°C overnight or at -20°C for several days.

2.2.5.2 Optimization of the H1-CRD expression

2.2.5.2.1 Selection of the *E.coli* expression strain and clone

The H1-CRD was expressed (see Section 2.2.5.1) in a number of pET3H1-transformed clones of each *E.coli* expression strain (see Section 2.2.3.4).

Proteins of the culture pellets and media, harvested prior to and after expression, were purified and concentrated by TCA / acetone precipitation and were analyzed on a reducing SDS-PAGE gel (see Section 2.2.4.2.1).

2.2.5.2.2 Selection of expression conditions

A pET3H1 transformed *E.coli* clone (see Section 2.2.3.4) was cultured in different media. The expression was not induced for negative control or induced at different OD₆₀₀ by addition of various concentrations of IPTG.

Expression of H1-CRD in different culture medias

At the same time, the expression of H1-CRD (see Section 2.2.5.1) was performed for 5h in LB and in TB media containing suitable antibiotics and glucose (1%) or no glucose.

Expression of H1-CRD at different OD₆₀₀

Simultaneously, the H1-CRD expression (see Section 2.2.5.1) was not induced or induced at six different OD₆₀₀ in the range of 1.0-6.0 and was performed for 700min.

Induction of H1-CRD expression with different IPTG concentrations

In parallel, the H1-CRD expression (see Section 2.2.5.1) was induced with 0.2mM, 0.4mM and 0.8mM IPTG or was not induced (negative control) and was run for 700min after induction.

Expression analysis

Every 50min, the OD₆₀₀ of cultures was measured (see Section 2.2.2.1), the pH was monitored using indicator sticks, and 1ml samples were taken out. Samples were cooled on ice for 5min and were centrifuged at 16'000rcf for 5min. Pellets and media were stored separately at -20°C until analyses.

Proteins of the pellets and media were purified and concentrated by TCA / acetone precipitation and were analyzed by reducing SDS-PAGE (see Section 2.2.4.2.1). Growth curves were drawn and doubling times were calculated using the Prism4 software.

2.2.5.3 Optimization of the H1-CRD purification

2.2.5.3.1 Fraction analysis of the selected *E.coli* expression clone

The analysis of the medium, the total cell protein and its periplasmic, soluble and insoluble cytoplasmic fractions to ascertain the localization of expressed H1-CRD in a

pET3H1 transformed *E.coli* expression clone (see Section 2.2.3.4) was performed according to the pET System Manual.¹¹⁹

The *E.coli* expression clone was cultured in 100ml LB and TB medium containing antibiotics and glucose (1%). After taking out a 10ml aliquot (negative control), the H1-CRD was expressed in remaining 90ml culture for 4h (see Section 2.2.5.1).

Medium proteins and total cell proteins

1ml of the expression culture was centrifuged at 10'000rcf for 10min at 4°C. Then, the medium was transferred to a new tube and the pellet was dried by tapping the tube onto a paper towel prior to its resuspension in 1ml PBS.

Periplasmic fractions

Cells of 80ml expression culture were harvested by centrifugation at 10'000rcf for 10min at 4°C and were resuspended in 0.5 volume sucrose buffer (30mM TrisHCl (pH8.0), 20% sucrose, 1mM EDTA). After incubation for 30min, while shaking with 70rpm, cells were collected by centrifugation at 10'000rcf for 10min at 4°C, were resuspended in 0.5 volume ice-cold MgSO₄ (5mM) and placed on ice for 10min, while shaking with 70rpm. Cells were centrifuged at 10'000rcf for 10min at 4°C again before 1ml supernatant was transferred to a new tube for precipitation of periplasmic proteins.

The pellet of the periplasmic fraction was stored on ice until using for preparation of the soluble cytoplasmic fraction.

Soluble cytoplasmic fraction

The pellet of the periplasmic fraction, derived from 80ml culture, was resuspended in 0.1 volume cold TrisHCl 20mM (pH7.5) and was lysed completely by sonication with 12 bursts (20s sonication / 10s break, 80% duty) on ice. After centrifugation at 14'000rcf for 10min, 100µl supernatant were transferred to a new tube for the precipitation of cytoplasmic soluble proteins.

The pellet of the soluble cytoplasmic fraction was stored on ice until using to prepare the insoluble cytoplasmic fraction.

Insoluble cytoplasmic fraction

The pellet of the soluble cytoplasmic fraction, derived from 80ml culture, was twice washed with 0.1 volume TrisHCl 20mM (pH7.5) and centrifuged at 10'000rcf for 5min. The pellet was resuspended in 0.1 volume SDS (1%) and was boiled for 5min at 95°C, while shaking with 1'200rpm before cytoplasmic insoluble proteins were precipitated.

Analysis

Proteins of the medium, total cell proteins, periplasmic proteins cytoplasmic soluble and insoluble proteins, derived from 1ml culture, were ten times concentrated by TCA / acetone precipitation (see Section 2.2.4.1) prior to the analysis by reducing SDS-PAGE (see Section 2.2.4.2.1).

2.2.5.3.2 Inclusion bodies denaturation and reduction

Three 500ml expression cultures (see Section 2.2.5.1) of an *E.coli* clone were pooled and split to three equal aliquots to get the same starting pellet. Proteins of the inclusion bodies were denatured and reduced, comparing the “fast dilution” (FD), the “no fast dilution” (NFD) and the “inclusion body” (IB) solubilization methods in parallel.

FD solubilization method

The not preclearing FD method was performed according to Meier M. *et al.*²⁶

The pellet, derived from 500ml expression culture, was suspended in 2.5ml prechilled denaturation buffer (20mM TrisHCl, 0.01% β -mercaptoethanol, 8M urea, pH 8.0). Cells were lysed by 12 bursts of 20s sonication and 10s stops on ice, and debris was removed by ultracentrifugation at 32'800rcf for 20min at 4°C. This lysis cycle was repeated twice. The resulting 0.9 volume lysate solution was supplemented with 0.1 volume precooled high salt buffer 10x (5M NaCl, 250mM CaCl₂, 0.3% β -mercaptoethanol, denaturation buffer) prior to the incubation on ice for 1h, while shaking with 70rpm. After fast dilution with 3 volumes prechilled dilution buffer (20mM TrisHCl, 500mM NaCl, 25mM CaCl₂, pH 7.5), the diluted lysate solution was cleared by ultracentrifugation at 32'800rcf for 20min at 4°C.

Proteins of the cleared lysate solution were refolded by dialysis in different buffer systems (see Section 2.2.5.3.3).

NFD solubilization method

The not preclearing NFD method is a modification of the method by Meier M. *et al.*²⁶ and was developed empirically.

The pellet, derived from 500ml expression culture was suspended in 25ml precooled denaturation buffer (20mM TrisHCl, 0.01% β -mercaptoethanol or 1mM DTT, 8M urea, pH 8.0). Cells were lysed by 24 bursts of 20s sonication and 10s stops on ice, and debris was removed by ultracentrifugation at 32'800rcf for 20min at 4°C. This lysis cycle

was repeated twice but only using 2.5ml denaturation buffer for suspending the debris pellet. NaCl, CaCl₂ and β-mercaptoethanol or DTT were added to concentrations of 500mM, 25mM and 0.3% or 1mM, respectively. After incubation on ice for 1h, while shaking with 70rpm, followed by dilution with 0.5 volume prechilled dilution buffer (20mM TrisHCl, 500mM NaCl, 25mM CaCl₂, pH 7.5), the diluted lysate solution was cleared by ultracentrifugation at 32'800rcf for 20min at 4°C.

Proteins of the cleared lysate solution were refolded by dialysis in different buffer systems (see Section 2.2.5.3.3).

IB solubilization method

The preclearing IB method was developed empirically according to the Protein methods.¹²⁷

The pellet, derived from 500ml expression culture (about 3g bacterial pellet wet weight), was suspended in 30ml (10ml/g pellet wet weight) precooled lysis buffer (20mM TrisHCl, 500mM NaCl, 10% sucrose, pH 8.0). Cells were lysed by 24 bursts of 20s sonication and 10s stops on ice, and IB were collected by ultracentrifugation at 32'800rcf for 20min at 4°C. This lysis and washing cycle was repeated four times with 30ml prechilled lysis buffer (10ml/g pellet wet weight) and once with 5ml precooled IB washing buffer (20mM TrisHCl, 10mM EDTA, 1% TritonX-100, 1M urea, pH 8.0). Following complete removal of the supernatant by tapping dry on a paper towel, the IB pellet was weighted to get the IB wet weight. Then, it was dissolved in 100μl/mg (IB wet weight) prechilled extraction buffer (20mM TrisHCl, 1mM DTT, 8M urea, pH 8.0), 1mM PMSF) by 12 bursts of 20s sonication and 10s stops on ice. After incubation for 1h, while shaking with 700rpm, followed by dilution with 200μl/mg (IB wet weight) precooled extraction buffer to final concentrations of 1mM DTT and 8M urea, the diluted IB solution was cleared by ultracentrifugation at 32'800rcf for 20min at 4°C.

Proteins of the IB solution were refolded by dialysis in different buffer systems (see Section 2.2.5.3.3).

2.2.5.3.3 H1-CRD refolding

Cleared FD, NFD and IB lysate solutions (see Section 2.2.5.3.2) were dialyzed against different refolding buffer combinations.

Preparation of dialysis tubes

The method for the preparation of ZelluTrans 6.0 dialysis tubes was adapted from Deutscher M.P.⁵⁵ and the ZelluTrans Roth product information.

ZelluTrans Roth 6.0 dialysis tubes (25·200mm, 10 pieces) were swollen in 500ml soaking buffer (10mM NaHCO₃, 1mM EDTA, pH8.0) of 80°C to 90°C for 30min with gentle stirring magnetically. After washing three times in 500ml water of 60°C, 40°C and 20°C, respectively for 10min with gentle stirring, swollen tubes were stored at 4°C in 1mM EDTA (pH8.0).

Refolding of H1-CRD in different buffer systems

The refolding system A according to Spiess M. *et al.*²⁶ used one basic refolding buffer (20mM TrisHCl, 0.5M NaCl, 25mM CaCl₂, pH 7.5) without any refolding additives. Refolding systems B to D were adapted from A using the same basic refolding buffer but were supplemented either with 0.1mM DTT and / or 30% glycerol or with 1mM reduced / 0.2mM oxidized glutathione (GSH / GSSG) according to Table 6. The FD and the NFD lysate solution were refolded in refolding systems A and C whereas the IB lysate solution was refolded in refolding systems B and D.

Table 6: Refolding buffer systems A to D.

Refolding system	Additives to the basic refolding buffer*			Lysate solution
	Buffer change 0 and 1	Buffer change 2 and 3	Buffer change 4 and 5	
A	-	-	-	FD, NFD
B	0.1mM DTT	-	1mM GSH / 0.2mM GSSG	IB
C	-	-	1mM GSH / 0.2mM GSSG	FD, NFD
	30% glycerol	30% glycerol	-	
D	0.1mM DTT	-	1mM GSH / 0.2mM GSSG	IB
	30% glycerol	30% glycerol	-	

*: Basic refolding buffer: 20mM TrisHCl (pH 7.5), 0.5M NaCl, 25mM CaCl₂

Cleared FD, NFD and IB lysate solutions were split up and each sample (equivalent to 250ml expression culture) was transferred into swollen dialysis tubes (25·200mm tubes). All samples were dialyzed separately, each against 200ml prechilled refolding buffer (250ml measuring cylinder of same diameter and length), with gentle stirring magnetically.

Refolding buffers were replaced five times with fresh buffer according to Table 6 after dialysis for 8-13h, respectively. Following the final dialysis for 2-3h, the refolded protein samples were cleared by ultracentrifugation at 44'000rcf for 1h at 4°C and the H1-CRD of each sample was purified by affinity chromatography (see Section 2.2.5.3.4).

2.2.5.3.4 H1-CRD affinity purification on Gal-Sepharose by FPLC

Coupling of galactose to Sepharose

The galactose was coupled to activated Sepharose 6B according to the divinylsulfone method of Fornstedt N. *et al.*¹³⁹. The Gal-Sepharose and the blank Sepharose were prepared in parallel.

The packed Sepharose 6B was three times washed with 1 volume water and centrifuged at 1'100rcf for 5min. The Sepharose was suspended in 1 volume carbonate buffer (500mM Na₂CO₃, pH11.0) and was activated by addition of 0.1 volume divinylsulfone prior to the incubation for 1h, while shaking with 1'000rpm. After washing on a glass fritte (borosilicate 3.3, pore 4) with 100 volumes water, the activated Sepharose was split into two portions and was suspended in 1 part-volume Gal solution (20% galactose in 500mM Na₂CO₃, pH10.0) or blank solution (500mM Na₂CO₃, pH10.0) for coupling overnight, while shaking with 300rpm. Coupling slurries were centrifuged at 3'100rcf for 5min, were washed three times with water and resuspended in 1 part-volume carbonate buffer (500mM NaCO₃, pH8.5) before they were blocked with 0.02 part-volume β-mercaptoethanol for 2h, while shaking with 300rpm. After washing three times with 10 part-volumes water, the slurries were packed into BioScale MT-2, MT-10 or MT-20 column (2ml, 10ml or 20ml bed-volume) according to the column instruction manual using ultrafiltered water (0.45µm) and an operating flow rate of 2ml/min.

Specificity control of H1-CRD binding to Gal-Sepharose by HPLC

The specificity of the H1-CRD binding to Gal-Sepharose was controlled as described by Ricklin D¹⁴⁰.

The cleared solution of refolded proteins (see Section 2.2.5.3.3) was applied to Gal-Sepharose and blank Sepharose BioScale MT-2 columns (2ml bed-volume).

H1-CRD affinity purification on Gal-Sepharose by FPLC

H1-CRD was purified by affinity to Gal-Sepharose according to Spiess M. *et al.*²⁶ by FPLC. The purification was performed with degassed buffers at 4°C on a BioLogic workstation, using the EZLogic software.

The cleared solution of refolded proteins (see Section 2.2.5.3.3), equivalent to 100ml expression culture, was loaded onto the Gal-Sepharose BioScale MT-10 column (10ml bed-volume), equilibrated with washing buffer (20mM TrisHCl, 500mM NaCl, 25mM

CaCl₂, pH7.8 at 20°C) at a flow rate of 1ml/min. Contaminating proteins were washed out isocratically with 2 bed-volumes washing buffer at a flow rate of 1ml/min until the baseline was reached. Then, the Gal-bound H1-CRD was eluted isocratically with 2 bed-volumes elution buffer (20mM TrisHCl, 500mM NaCl, 2mM EDTA, pH7.8 at 20°C) at a flow rate of 1ml/min. The eluting protein was detected by monitoring the A₂₈₀ absorbance and was collected in fractions.

Protein Fractions were analyzed by PAGE (see Section 2.2.4.2), were pooled and quantified by Bradford assay (see Section 2.2.4.4.2).

2.2.5.4 Size exclusion chromatography of the H1-CRD by FPLC

The gel filtration method was developed according to the Amersham Handbook¹⁴¹.

The size exclusion chromatography (SEC) by FPLC was performed at 4°C on a BioLogic workstation, using the software EZLogic. Three different SEC buffers were tested: SEC₀ (20mM TrisHCl, 120mM NaCl, pH 7.8), SEC_{Ca} (20mM TrisHCl, 120mM NaCl, 2mM CaCl₂, pH7.8) and SEC_{EDTA} (20mM TrisHCl, 120mM NaCl, 2mM EDTA, pH 7.8).

When the SEC was run with SEC_{EDTA} buffer, 3mM EDTA was added to the H1-CRD solution prior to injection.

The affinity-purified H1-CRD (see Section 2.2.5.3.4) was concentrated in Centricon filter devices YM-10.000 at 4'800rcf and 4°C and was transferred into collection tubes by spinning at 650rcf for 2min at 4°C, prior to SEC.

The Bio-Prep SE100/17 column (15ml bed-volume, 8·300mm) was equilibrated with SEC buffer at a flow rate of 0.3ml/min overnight. 300µl concentrated H1-CRD solution was injected and the SEC was run isocratically at a flow rate of 0.3ml/min. Eluting proteins were detected by monitoring the A₂₈₀ absorbance, were collected in fractions and analyzed by PAGE (see Section 2.2.4.2).

300µl Biorad gel filtration standard (670kDa, 158kDa, 44kDa, 17kDa, 1.35kDa) was used for the calibration. The standard calibration curve was drawn and retention times of monomeric and dimeric H1-CRD were calculated using the Prism4 software.

2.2.5.5 Preparative scale production of the H1-CRD

The expression and the purification were ten times up-scaled for the preparative H1-CRD production.

The H1-CRD was expressed in 500ml cultures of an *E.coli* expression clone (see Section 2.2.5.1). Pellet proteins of 5'000ml expression culture were solubilized by the FD or the NFD method, using the reductant β -mercaptoethanol (see Section 2.2.5.3.2). The solution of solubilized proteins was dialyzed against 4'000ml precooled basic refolding buffer (buffer system A) in a 5'000ml beaker glass (see Section 2.2.5.3.3). The solution of refolded proteins was split to 5 portions. One portion was applied to a Gal-Sepharose BioScale MT-20 column in a single run. The column was run at a flow rate of 1ml/min and was washed with 4-5 bed-volumes washing buffer (see Section 2.2.5.3.4). The column flow through, the wash and eluting fractions were analyzed by SDS-PAGE (see Section 2.2.4.2).

The solution of pooled elution fractions, derived from 5'000ml expression culture, was transferred into swollen dialysis tubes (see Section 2.2.5.3.3) and dialyzed against 4'000ml precooled dialysis buffer (20mM TrisHCl, 120mM NaCl, 2mM CaCl₂, pH 7.8) in a 5'000ml beaker glass at 4°C, gently stirring on a magnetic stirrer. After 15h dialysis, the buffer was replaced once with prechilled fresh buffer.

The dialyzed H1-CRD solution was concentrated in Centricon filter devices YM-10.000 at 4'800rcf and 4°C and was transferred into collection tubes by spinning at 650rcf for 2min at 4°C. The concentrated H1-CRD solution was stored at -20°C in aliquots.

Concentrated H1-CRD was quantified by Bradford assay (see Section 2.2.4.4.2).

2.3 Production and purification of polyclonal antibodies

2.3.1 Hen immunization and egg handling

Immunization of hens and egg collection was performed as described by Bootz F.¹⁴²

Preparation of antigen

The galactose affinity and SEC-purified H1-CRD (see Sections 2.2.5.3.4 and 2.2.5.4) was diluted to 40µg/ml in sterile PBS. For priming 500µl antigen solution was emulsified with 500µl Complete Freund's adjuvant and for boosts 500µl antigen solution was emulsified with 500µl Incomplete Freund's adjuvant.

Antigen injection

Three 22 weeks old hybrid laying hens were primed subcutaneously with 1'000µl antigen / CFA emulsion (20µg H1-CRD) and were boosted subcutaneously with 1'000µl antigen / IFA emulsion (20µg H1-CRD) every 21-28 days.

Egg handling

Preimmune eggs were collected. Eggs of immunized hens were collected, starting day 14 after the first boost, and were stored at 4°C until IgY extraction.

2.3.2 IgY purification

2.3.2.1 Purification optimization

After separation of the egg white and the yolk, lipids were removed, trying out three different methods, and total IgY were extracted, looking at three different methods.

2.3.2.1.1 Egg white and yolk separation

The egg was broken, the yolk was separated from the egg white and rolled on a filter paper to remove traces of egg white. The yolk vitellin membrane was punctured and the yolk collected in a measuring cylinder.

2.3.2.1.2 Protein / Lipid separation methods

Lipids and some proteins were removed, comparing the freeze / thaw (F/T) method modified from Jensenius J.C. *et al.*⁹⁶ and Devi C.M *et al.*⁹⁹, the water dilution (WD)

method of Atika E.M *et al.*⁹⁸ and the PEG 3.5% precipitation (PEG) method of Polson A. *et al.*¹⁰⁰.

Freeze / Thaw method

10ml yolk was diluted to 100ml in water and the pH was adjusted to pH7.0 with NaOH (1M). The yolk solution was frozen three times at -20°C overnight and thawed at 4°C overday. Lipids were precipitated at 2'000rcf for 20min and the supernatant was cleared by centrifugation at 4'000rcf for 20min, followed by filtration using MILLEX GP filters (0.22 μm).

Water dilution method

10ml yolk was diluted to 100ml in water and the pH was adjusted to pH5.0 with HCl (3.7%). The yolk solution was incubated overnight at 4°C and cleared by ultracentrifugation at 13'000rcf for 25min at 4°C , followed by filtration using MILLEX GP filters (0.22 μm).

PEG8000 3.5% precipitation method

10ml yolk was diluted to 50ml in phosphate buffer (100mM Na_2HPO_4 , pH7.6). 3.5% PEG8000 was added and dissolved, stirring for 10min. Lipids were precipitated at 2'900rcf for 20min at 4°C and the supernatant filtered using Macherey-Nagel filters MN615.

2.3.2.1.3 Protein / total IgY separation methods

Yolk protein solutions (see Section 2.3.2.1.2) were split into three equal portions. Thereof, total IgY antibodies were extracted, comparing the ammoniumsulfate precipitation (AS) method of Swendsen L. *et al.*¹⁴³, the PEG precipitation (PEG) method of Polson A. *et al.*⁸⁴ and the PEG / ethanol precipitation (PEG/EtOH) method of Polson A. *et al.*¹⁰⁰ at the same time.

Ammoniumsulfate 50% precipitation method

Ammoniumsulfate was added to the yolk protein solution to 25% saturation and the suspension was stirred in ice-water for 20min, followed by centrifugation at 2'900rcf for 45min at 4°C . Ammoniumsulfate was dissolved in the cleared yolk solution to a final saturation of 50% and precipitated IgY were collected at 2'900rcf for 45min at 4°C .

Precipitated IgY were dissolved in 1ml (0.1 yolk volume) KPBS (1.5mM KH_2PO_4 , 8mM Na_2HPO_4 , 137mM NaCl, 2.7mM KCl).

PEG8000 12% precipitation method

PEG8000 was added to the yolk protein solution to a final saturation of 12% and the suspension was stirred for 30min, followed by centrifugation at 2'900rcf for 45min at 4°C. Precipitated IgY were dissolved in 25ml phosphate buffer (100mM Na_2HPO_4 , pH7.6) and precipitated a second time with 12% PEG8000. After spinning at 2'900rcf for 45min at 4°C, collected IgY were dissolved in 1ml (0.1 yolk volume) KPBS.

PEG8000 12% / ethanol 50% precipitation method

IgY were extracted according to the PEG 12% precipitation method but collected IgY were dissolved to 2.5ml in phosphate buffer and additionally precipitated by addition of 50% ethanol of -20°C, after cooling the IgY solution on ice to about 0°C. The IgY suspension was incubated on ice for 1h and ultracentrifuged at 13'000rcf for 25min at 0°C. The precipitated IgY were dissolved in 2.5ml (0.75 yolk volume) phosphate buffer.

2.3.2.1.4 Dialysis of IgY solutions

Dialysis tubes (ZelluTrans Roth 6.0, 25mm) were prepared as described in Section 2.2.5.3.3. 1 volume IgY solution was transferred into swollen dialysis tubes and was dialyzed against 1'000 volumes KPBS or phosphate buffer at 4°C, stirring magnetically. The buffer was twice exchanged within 30h.

After addition of 0.02% NaN_3 , the IgY solution was stored at 4°C.

2.3.2.1.5 Extraction of specific anti-H1 IgY

The antigen H1-CRD was coupled to agarose using the AminoLink® Plus Immobilization Kit according to the manufacturer instructions¹⁴⁴.

Buffer exchange of H1-CRD

The disturbing primary amine Tris of the H1-CRD solution (see Section 2.2.5.5) was removed by buffer exchange to HEPES buffer (pH7.2) using Biomax ultrafree 0.5 centrifugal devices (MWCO 10'000). The needed volume H1-CRD solution was concentrated at 10'000rcf for 10min, the buffer exchanged by spinning six times with 500µl HEPES buffer at 10'000rcf for 10min and the dialyzed H1-CRD diluted to 2ml in HEPES buffer (pH7.2) to a final concentration of 2mg/ml H1-CRD.

Coupling of H1-CRD antigen to agarose

2ml AminoLink agarose slurry 50% were equilibrated with HEPES buffer (pH7.2) and activated with 40 μ l NaCyanoborohydrid solution (5M NaCyanoborohydrid, 10mM NaOH). 2ml H1-CRD solution (2mg/ml) were added and H1-CRD was coupled by incubation overnight. The coupled agarose slurry was washed with 5ml HEPES buffer and blocked with 4ml quenching buffer (1M TrisHCl, 0.05% NaN₃, pH 7.4), while shaking over-head. Finally, coupled slurry was washed with 15ml washing buffer (1M NaCl, 0.05% NaN₃).

Anti-H1 IgY affinity purification on H1-CRD agarose

2ml dialyzed IgY solution (see Section 2.3.2.1.3) was applied onto the H1-CRD agarose column (1ml bed-volume), was equilibrated with 6 bed-volumes phosphate buffer (100mM Na₂HPO₄, pH7.6) and incubated for 1h. After washing with 12 bed-volumes phosphate buffer, bound IgY were eluted with 8 bed-volumes 100mM glycine (pH2.5-3.0). 500 μ l fractions were collected in 1.5ml tubes containing 75 μ l TrisHCl (1M, pH7.5) for neutralization. The specific IgY-containing fractions were detected by Bradford spot assay or absorbance A₂₈₀ measurement (see Section 2.2.4.4) and were pooled.

After addition of 0.02% NaN₃, the solution of specific IgY was stored at 4°C.

2.3.2.2 Preparative scale extraction of total IgY by PEG precipitation

The optimized method was ten times scaled up for preparative extraction of total IgY.

125ml yolk was diluted to 500ml in phosphate buffer and lipids were removed by the PEG3.5% method (see Section 2.3.2.1.2). Total IgY were extracted from total yolk proteins by the PEG 12% precipitation method (see Section 2.3.2.1.3). Purified IgY were dissolved in 20ml KPBS and were dialyzed against 5'000ml KPBS (see Section 2.3.2.1.4). The buffer was exchanged three times every 5-10h.

The dialyzed IgY solution was preserved with 0.02% NaN₃ and stored at 4°C.

2.3.2.3 Analysis

The purity of the total and the specific IgY were controlled by PAGE and the activity was tested by immunoblotting and AP-ELISA (see Sections 2.2.4.2, 2.2.4.3 and 2.4.2.5.1). The yield was determined by Bradford assay or A₂₈₀ measurement (see Section 2.2.4.4).

The characterization of IgY was performed according to Section 2.5.

2.4 Production and purification of monoclonal antibodies

2.4.1 Buffers and media

2.4.1.1 Buffers

KPBS (1.5mM KH_2PO_4 , 8mM Na_2HPO_4 , 137mM NaCl, 2.7mM KCl)

T-Ca20 (20mM TrisHCl, 20mM CaCl_2 , pH 7.5)

TBS (20mM TrisHCl, 120mM NaCl, pH 7.5)

TTBS (20mM TrisHCl, 120mM NaCl, 0.05% Tween20, pH 7.5)

TTBS-Ca20 (20mM TrisHCl, 120mM NaCl, 20mM CaCl_2 , 0.05% Tween20, pH 7.5)

2.4.1.2 Media

FCS was heat inactivated for 30min at 56°C in a water bath and supplemented medias (see Formulation 8) were filtered using disposable Stericup™ (0.22µm) prior to use.

DMEM-10: DMEM high-glucose with 10% FCS

	Dulbecco's Modified Eagle's medium high-glucose (4.5mg/ml glucose, NaPyruvate)
10%	FCS
2mM	L-glutamine
100U/ml	Penicilline
100µg/ml	Streptomycine

DMEM-15: DMEM high-glucose with 15% FCS

	Dulbecco's Modified Eagle's medium high-glucose (4.5mg/ml glucose, NaPyruvate)
15%	FCS
2mM	L-glutamine
100U/ml	Penicilline
100µg/ml	Streptomycine

IMDM-5: IMDM with 5% FCS

	Iscove's Modified Dulbecco's medium
5%	FCS
25mM	HEPES
2mM	GlutaMAX
50µg/ml	Gentamicin

IMDM-10: IMDM with 10% FCS

	Iscove's Modified Dulbecco's medium
10%	FCS
25mM	HEPES
2mM	GlutaMAX
50µg/ml	Gentamicin

HT-IMDM-5: IMDM with 5% FCS and HT 1x

	IMDM-5
5mM	Hypoxanthine
800µM	Thymidine

HAT-IMDM-5: IMDM with 5% FCS and HAT 1x

IMDM-5
 5mM Hypoxanthine
 20 μ M Aminopterin
 800 μ M Thymidine

RPMI-0: RPMI1640

RPMI1640 without L-glutamine
 1x NEAA
 1mM Sodium pyruvate
 2mM GlutaMAX
 100 μ g/ml Kanamycine

RPMI-6: RPMI1640 with 6% FCS (low IgG)

RPMI-0
 6% FCS (low IgG)

RPMI-10: RPMI1640 without L-glutamine with 10% FCS

RPMI-0
 10% FCS

6-RPMI-15: RPMI1640 without L-glutamine with 15% FCS and IL-6

RPMI-0
 15% FCS
 1% Human IL-6

6 β -RPMI-15: RPMI1640 without L-glutamine with 15% FCS, IL-6 and β -mercaptoethanol

RPMI-0
 15% FCS
 1% Human IL-6
 10 μ M β -mercaptoethanol

HT-RPMI-15: RPMI1640 with 15% FCS and HT 1x

RPMI-0
 15% FCS
 5mM Hypoxanthine
 800 μ M Thymidine

df-RPMI-10: RPMI1640 with 10% FCS, human IL-2 and hGMCSF

RPMI-0
 10% FCS
 8% Human IL-2 supernatant
 10% Human granulocyte-macrophage colony-stimulating factor supernatant

HAT6 β -RPMI-15: RPMI1640 with 15% FCS, IL-6, β -mercaptoethanol and HAT 1x

RPMI-0
 15% FCS
 5mM Hypoxanthine
 20 μ M Aminopterin
 800 μ M Thymidine
 1% Human IL-6
 10 μ M β -mercaptoethanol

Formulation 8: Composition of supplemented cell culture media.

Cells in a “bad shape” were temporarily cultured in medium including 1% human IL-6.

2.4.2 General methods

2.4.2.1 Viability check and cell counting by trypan blue

The cell number and the viability were verified according to the protocol of Harlow E. *et al.*¹⁰²

The cell suspension was combined with the same volume trypan blue stain 0.4% and filled into an improved Neubauer counting chamber. White living cells and blue dead cells of four big squares (1mm², volume 0.1mm³) were counted with 100 times magnification under the microscope (IM, binocular Kpl-W10x/18, objective Ph1F10/0.25, Zeiss). The cell density was calculated using Equation 7 and the viability was estimated using Equation 8.

$$C_{\text{cells/ml}} = n_{\text{viable}} \cdot \frac{d \cdot 10^4}{f} \quad (\text{Eq. 7})$$

Equation 7: Determination of the cell density, using an improved Neubauer counting chamber. The cell density (c) (cells/ml) of a cell suspension, d times diluted with trypan blue was calculated by counting the number of viable cells n_{viable} in f big squares.

$$v_{\%} = \frac{n_{\text{viable}}}{n_{\text{total}}} \cdot 100\% \quad (\text{Eq. 8})$$

Equation 8: Determination of the cell viability, using an improved Neubauer counting chamber. The cell viability v (%) of a cell suspension, stained with trypan blue was calculated by counting the number of viable cells (n_{viable}) compared to the total number of cells (n_{total}).

2.4.2.2 Cell thawing

Cells were thawed according to a protocol provided by Gober H.J.¹⁴⁵.

Cells, frozen at -185°C (see Section 2.4.2.4), were quickly thawed at 37°C in a water bath and immediately diluted with 1ml DPBS in the cryotube while pipetting carefully up and down. Cells were washed in 30ml DPBS and collected at 125rcf for 10min. Following another wash in 10ml DPBS, the cell pellet was broken by tapping the tube and suspended to about $5 \cdot 10^5$ cells/ml in supplemented culture medium. 2ml/well were dispersed into a 24-well plate and incubated at 37°C (5% CO_2 , 100% humidity).

After about 1h, the shape of the cells was controlled under the microscope and high dense cultures were split.

2.4.2.3 Cell cultivation

2.4.2.3.1 Collagen coating of culture plates and flasks

Culture flasks and plates were coated following the protocol of Stokmaier D.¹⁰³

About 10 μ l/cm² sterile collagen solution (0.25mg/ml collagen S, 500mM acetic acid (pH2.8), sterile) was spread in culture flasks and plates overnight at 4°C. The collagen coating was neutralized by washing twice with about 40 μ l/cm² DPBS. Coated flasks and plates were stored at 4°C until use.

2.4.2.3.2 Cell splitting and propagation

Cells were cultured according to Harlow E. *et al.*¹⁰² and according to the protocols of the group of De Libero G.¹⁴⁵ or of Stokmaier D.¹⁰³

Cell cultures were examined under the microscope (IM, binocular Kpl-W10x/18, objectives F2.5/0.08, Ph1F10/0.25, F-LD20/0.025, Zeiss) to look for contamination and to inspect the shape, the viability and the density of cells (see Section 2.4.2.1) prior to splitting or propagation. Different cell lines were cultured in 96-well plates (200 μ l/well), 24-well plates (2ml/well), 6-well plates (5ml/well), T²⁵ flasks (7ml) and T⁷⁵ flasks (20ml).

The detailed composition of the cell media can be found in Section 2.4.1.2.

Isolated primary cells (monocytes, dendritic cells)

Human monocytes were resuspended at 5 \cdot 10⁵cells/ml in df-RPMI-10 (see Section 2.4.1.2) and 3ml/well plated on 6-well plates. Monocytes differentiated to dendritic cells during incubation at 37°C (5% CO₂, 100% humidity) for 4 days.

Suspension cells (myelomas, hybridomas, HL-60, Jurkat, K-652, THP-1)

After diluting cells to about 5 \cdot 10⁵cells/ml in RPMI-10 (see Section 2.4.1.2), 2ml/well were distributed in 24-well plates and incubated at 37°C (5% CO₂, 100% humidity).

In dense cultures, cells were suspended by pipetting and split 1:2 to 1:4 with RPMI-10.

Adherent cells (HepG2, SK-Hep1)

Cells were resuspended at 1 \cdot 10⁶cells/ml in DMEM-10 (see Section 2.4.1.2). 5ml/well HepG2 were distributed in collagen coated 6-well plates and 5ml/well SK-Hep1 in untreated 6-well plates.

In confluent cultures, the medium was removed and cells rinsed once with DPBS. The trypsin / EDTA solution was distributed, immediately removed and cells detached during

incubation at 37°C for 2-5min. Detached cells were washed in DPBS and collected at 125rcf for 10min. The pellet was loosened by tapping the tube and resuspended in fresh DMEM-10.

HepG2 were split 1:5 to 1:10 into collagen-coated flasks or plates and SK-Hep1 were diluted 1:10 to 1:20 into untreated flasks or plates.

2.4.2.4 Cell freezing

Cells were frozen following the procedure of Harlow E. *et al.*¹⁰² modified by Fischer R.¹⁴⁶

One day before freezing, cells were split 1:2 to 1:10 in fresh medium.

Cells (4-8 wells of 24-well plates, 2 wells of 6-well plates, 1 T²⁵ flask) were counted and the viability checked (see Section 2.4.2.1). After centrifugation at 400rcf for 5min at 4°C, the cell pellet was resuspended in the remaining medium by tapping the tube and was diluted into cold freezing medium (90% FCS, 10% DMSO) to get about 3·10⁶ vital cells/ml. 0.5-1.0ml aliquots were distributed in labeled cryotubes, which were placed in a styropore support. Cells were immediately frozen, for 2h at –20°C first, then 1day at –80°C prior to storage in liquid N₂ for infinite time.

Cells were frozen following the procedure of Harlow E. *et al.*¹⁰² modified in the protocol of De Libero G.¹⁴⁵

Cells were frozen following the same procedure as described above but cells were collected at 125rcf for 2min at 4°C and diluted to about 1·10⁶ vital cells/ml in cold freezing medium. 0.5-1.0ml aliquots were immediately frozen in a styropore support for 1-10days at –80°C prior to storage in liquid N₂.

2.4.2.5 Screening ELISA

2.4.2.5.1 Alkaline phosphatase ELISA

The alkaline phosphatase ELISA was modified from Fischer R.¹⁴⁶.

The culture medium served as negative control and the serum of immunized mice (1:1'000 in blocking buffer) was used as positive control.

MaxiSorb ELISA plates were coated with 100µl/well H1-CRD solution (3µg/ml H1-CRD, 20mM CaCl₂ in TBS, pH7.5) and were incubated overnight at 4°C. After washing twice with 250µl/well washing buffer (20mM CaCl₂, 0.05% Tween20 in TBS, pH7.5) using the plate washer or the multi-dispense multi-channel pipet, remaining binding sites were blocked with 250µl/well blocking buffer (4% milk powder in TBS, pH7.5) during

incubation for 2h at RT. Wells were washed three times with 250µl/well washing buffer. 80µl supernatant samples, negative and positive controls were incubated for 2h at RT and wells were washed three times with 250µl/well washing buffer. After incubation with 80µl/well AP-labeled goat-anti-mouse antibody solution (GAM-IgG(whole molecule)-AP or GAM-Ig(polyvalent)-AP 1:1'000 to 1:5'000 in blocking buffer) for 2h at RT, wells were washed five times with 250µl/well washing buffer again. 80µl/well substrate solution (1mg/ml p-nitrophenylphosphate, 500mM MgCl₂, 10% diethanolamine, pH9.8) was distributed and the color was developed for 15-20min at RT prior to read the absorbance at 405nm in a Spectramax190 plate reader.

2.4.2.5.2 Horse radish peroxidase ELISA

The horseradish peroxidase ELISA was adapted from De Libero G.¹⁴⁵.

The culture medium served as negative control and serum of immunized mice (1:1'000 in blocking buffer) was used as positive control.

MaxiSorb ELISA plates were coated with 70µl/well coating solution (3-5µg/ml H1-CRD, 20mM CaCl₂ in TBS, pH7.5) and were incubated overnight at 4°C, covered with lid and parafilm. After washing once with 200µl/well washing buffer (20mM CaCl₂, 0.05% Tween20 in TBS, pH7.5), plates were tapped dry on paper towels and blocked with 150µl/well blocking buffer (1% BSA, 20mM CaCl₂, 0.05% Tween20 in TBS, pH7.5) during incubation for 1h at RT. Wells were washed twice with 200µl/well washing buffer, tapped dry and were incubated with 50µl/well supernatant sample (nude or diluted in blocking buffer), negative control or positive control for 1h at RT (or 30min at 37°C). After three times washing with 200µl/well washing buffer and tapping dry, 50µl/well horseradish peroxidase (HRP)-labeled anti-mouse antibody solution (GAM-Ig(polyvalent)-HRP or GAM-Ig(H+L chain)-HRP 1:5'000 in blocking buffer) were distributed and incubated for 1h at RT. Plates were washed five times with 200µl/well washing buffer, followed by incubation with 90µl/well Sigma Fast OPD substrate solution for 5min in the dark. The color development was stopped by addition of 50µl/well H₂SO₄ (10%) and the absorbance was read at 490nm in a Spectramax190 plate reader.

2.4.3 Production of hybridomas

2.4.3.1 Immunization

Mice were immunized by Fischer R.¹⁴⁶ and by De Libero G.¹⁴⁵

2.4.3.1.1 Immunization of NMRI outbred mice by Fischer R.

Preparation of antigen

For immunization of three mice, affinity-purified H1-CRD (see Section 2.2.5.5) was diluted to 400µg/ml in sterile PBS and stored at –20°C until use.

Prior to priming three mice, 300µl antigen solution was emulsified with 300µl CFA (1mg/ml heat inactivated *M. tuberculosis*, 85% paraffin oil, 15% mannide monooleat) using two Hamilton syringes connected by a valve. The water phase was first pressed into the oil phase, and then pressed from one syringe to the other to get a very thick w/o emulsion.

Just prior to boost, 300µl antigen solution was emulsified with 300µl IFA (85% paraffin oil, 15% mannide monooleat) the same way. For final boost, the antigen solution was diluted in sterile PBS to 200µg/ml.

Antigen injection

Three 8-10 weeks old female wildtype NMRI outbred mice (specific pathogen free) were primed with 100µl antigen / CFA emulsion (20µg H1-CRD) subcutaneously in the neck and boosted at least twice with 100µl antigen / IFA emulsion (20µg H1-CRD) subcutaneously in the neck every 3 weeks after immunization.

For final boosts, 200µl antigen solution (20µg H1-CRD) without adjuvant was injected subcutaneously in the neck 3, 2 and 1 day prior to fusion.

2.4.3.1.2 Immunization of Balb/c inbred mice by De Libero G.

Preparation of antigen

For immunization of three Balb/c mice, affinity-purified H1-CRD (see Section 2.2.5.5) was diluted to 2mg/ml in pyrogen-free sterile NaCl 0.9% Braun and sterile filtered. 500µl aliquots were stored at –20°C until use.

Prior to priming three mice, 500µl antigen solution was emulsified with 500µl thoroughly vortexed CFA using two syringes, connected by a two-way valve. The water phase was first pressed into the oil phase, and then pressed from one syringe into the other until a very thick white w/o emulsion was formed. After pressing into one syringe, a needle was connected to immunize mice.

Just prior to boost, 500µl antigen solution was emulsified with 500µl IFA the same way. For final boost, the antigen solution was diluted in pyrogen-free sterile NaCl 0.9% Braun to 1mg/ml.

Antigen injection

Three 7-8 weeks old female wildtype Balb/c inbred mice were primed with 200µl antigen / CFA emulsion (200µg H1-CRD) intraperitoneally and boosted at least twice with 200µl antigen / IFA emulsion (200µg H1-CRD) intraperitoneally every 2 weeks.

For final boost, 200µl antigen solution (200µg H1-CRD) without adjuvant was injected retro-ocularly intravenously or intraperitoneally 3 days prior to fusion.

2.4.3.1.3 Serum titer determination

100µl venous blood of immunized mice was taken retro-ocularly using a glass capillary.

The venous blood was coagulated in a 1.5ml tube for 20min at 37°C in a water bath. The coagulate was broken off by flicking the tube and incubated on ice for 20min prior to centrifugation at 3'000rpm for 5min at 0°C. Cleared serum was stored at -20°C.

Sera of immunized mice, of an unimmunized Balb/c mouse for negative control and of a previously immunized NMRI mouse for positive control were diluted to 10^{-2} , 10^{-3} , 10^{-4} and 10^{-5} in PBS and tested in HRP-ELISA according to the procedure described in Section 2.4.2.5.2. All samples were measured in duplicate.

2.4.3.2 Polyethylene glycol fusion

Splenocyte-myeloma hybridomas were formed following the polyethylene glycol (PEG) fusion procedure of Fischer R.¹⁴⁶ and De Libero G.¹⁴⁵ originally introduced by Köhler G. and Milstein C.⁸²

2.4.3.2.1 PEG1500 fusion of NMRI splenocytes and P3X63-Ag8.563 myeloma cells by the method of Fischer R.

The PEG1500 fusion method of Fischer R. is adapted from Harlow E. *et al.*¹⁰² originally modified from the procedure of Galfre G. *et al.*¹⁴⁷.

Myeloma cell culture

Three days prior to fusion, Balb/c myeloma cells P3X63-Ag8.563 were thawed (see Section 2.4.2.2) and cultured in IMDM-10 (see Section 2.4.1.2) at 37°C (5% CO₂, 100% humidity).

Macrophage feeder layer

Unimmunized Balb/c mice were stimulated with 20ng lipopolysaccharid intraperitoneally about 9 days prior to fusion and euthanized six days later with methoxyflurane or CO₂. The abdominal skin of ethanol-(70%)-disinfected mice was removed, using sterile tweezers and scissors, prior to injection of 10ml sterile, prechilled PBS into the peritoneal cavity. The stomach was gently moved for 5min to detach the peritoneal macrophages. The suspension was aspirated and macrophages were collected at 1'000rpm for 5min, resuspended by tapping the tube and diluted to 50ml in IMDM-5 (see Section 2.4.1.2). 100µl/well macrophage feeder suspension was plated into 96-well plates and incubated at 37°C (5% CO₂, 100% humidity) until fusion.

PEG1500 fusion

The day after the last final boost, the NMRI mouse was anaesthized with Metofane® and decapitated using scissors. The blood of the arteria carotis was collected to get the serum after coagulation and centrifugation at 16'000rcf for 5min. The serum was stored at -20°C until used as a positive control in the screening ELISA.

The spleen of the ethanol-(70%)-disinfected mouse was prepared using sterile tweezers and scissors. After removal of fat tissue and rinsing with PBS, the spleen was homogenized in a glass potter with 4ml PBS at 37°C by moving the piston five times up and down. Suspended cells were collected at 280rcf for 5min, the pellet loosened by tapping the tube and diluted to 50ml in PBS at 37°C. Splenocytes and P3X63-Ag8.563 myeloma cells were counted (see Section 2.4.2.1).

After collecting splenocytes at 280rcf for 5min, the cells were diluted in a calculated volume of myeloma cell suspension in a 50ml Falcon tube to get a ration of splenocytes : myeloma cells of 3:1. Combined cells were spun again and were washed three times with 50ml PBS at 37°C before the supernatant was removed completely.

While turning the tube manually, 1 volume PEG1500 at 37°C (1ml per $5 \cdot 10^7$ splenocytes) was added within 10s, using a syringe with needle. After incubation for 90s at 37°C, cells were slowly diluted with PBS at 37°C while turning the tube continuously, adding 1 volume within the 1st min followed by 2, 4, ..., 2^{n-1} volumes within the 2nd, 3rd, ..., nth min until a total cell suspension of 50ml was obtained. Fused cells were gently spun at 125rcf for 5min, then the pellet was resuspended by tapping the tube and cells were diluted with 40ml IMDM-5. 50µl/well cell fusion was distributed in eight 96-well

plates, which were already plated with 100µl/well macrophage feeder layer and cells were incubated at 37°C (5% CO₂, 100% humidity) in a Nuair IR autoflow incubator.

The day after fusion, 50µl/well selective IMDM-5 medium containing HAT 4x (20mM hypoxanthine, 80µM aminopterin, 3.2mM thymidine) were added to get HAT-IMDM-5 and plates were further incubated at 37°C (5% CO₂, 100% humidity) for 21 days.

2.4.3.2.2 PEG4000 fusion of Balb/c splenocytes and P3X63-Ag8.563 myeloma cells by De Libero G.

Myeloma cell culture

Balb/c myeloma cells P3X63-Ag8.563 were thawed (see Section 2.4.2.2) and cultured in RPMI-10 (see Section 2.4.1.2) at 37°C (5% CO₂, 100% humidity). When confluent and one day prior to fusion, cells were split 1:2 to 1:3.

Preparation of PEG4000 solution

In a glass tube, 2.2ml GKN (3M), 0.8ml sterile water and 40µl NaOH (100mM) were mixed and therein, 2.0g PEG4000 was solubilized till just dissolved by shaking in boiling water.

PEG4000 fusion

Three days after the final boost, the Balb/c mouse was euthanized with CO₂. The blood was collected to get the serum after coagulation and centrifugation at 800rcf for 2min. The serum was stored at -20°C until used as a positive control in the screening ELISA.

The spleen of the ethanol-(70%)-disinfected mouse was prepared using sterile tweezers and scissors. After removal of fat tissue, the spleen was pressed with the pistil through a cell sieve into a Petri dish containing a few ml MEM. Tissue clumps were homogenized using a Pasteur pipet. After a twice sedimentation of remaining clumps for 2min in 15ml Falcon tubes, splenocytes of the supernatant were collected at 1'000rpm for 10min and were resuspended in 10ml MEM. Splenocytes and P3X63-Ag8.563 myeloma cells were counted (see Section 2.4.2.1).

The splenocytes and the myeloma cells suspension were combined in a 50ml Falcon tube, to get a ratio of splenocytes : myeloma cells of 5:1, and were diluted to 50ml with MEM. The combined cells were gently spun at 125rcf for 10min and were washed once in 50ml before the supernatant was removed completely.

While shaking the tube manually in a water bath at 37°C, 1ml prewarmed PEG4000 solution was slowly added drop by drop. After incubation for 1min in the water bath at 37°C without shaking, cells were diluted slowly with about 50ml RPMI at 37°C within 10min, adding drop by drop at the beginning and gradually speeding up while gently shaking. The cell fusion was incubated at 37°C in the water bath for 5min, was centrifuged at 125rcf for 10min and was resuspended in 100ml 6β-RPMI-15 (see Section 2.4.1.2). 100μl/well cell fusion was distributed in ten 96-well plates and was incubated at 37°C (5% CO₂, 100% humidity) in a Revca ultima incubator.

The day after fusion, 100μl/well selective 6β-RPMI-15 medium containing HAT 2x (10mM hypoxanthine, 40μM aminopterin, 1.6mM thymidine) were added to get HAT6β-RPMI-15 and plates were further incubated at 37°C (5% CO₂, 100% humidity) for 14 days.

2.4.3.3 Hybridoma cultivation and screening

2.4.3.3.1 NMRI hybridoma cultivation and screening

NMRI hybridomas were cultured according to Harlow E. et al.¹⁰² and Fischer R.¹⁴⁶

The day 21 post-fusion, plates were checked for living hybridomas under the microscope. 100μl/well supernatant was replaced by fresh HAT-IMDM-5 of 37°C and tested in an AP screening ELISA (see Section 2.4.2.5.1). Fusion plates were screened by AP-ELISA again, the days 28 and 35 post-fusion.

200μl dense hybridomas in ELISA-positive wells on fusion plates were expanded to a 24-well macrophage feeder layer plate (1ml macrophages, see Section 2.4.3.2.1). 200μl cell suspension of the 24-well plate was transferred back to the fusion plate for back-up purpose.

Dense hybridomas on 24-well plates were checked by AP screening ELISA prior to expansion of still positive hybridomas to 6ml/well with fresh HT-IMDM-5 (see Section 2.4.1.2) on a 6-well plate and further to 8-10ml in T²⁵ flasks.

Hybridomas were frozen at -185°C in 2 batches of at least 3 cryotubes (see Section 2.4.2.4).

2.4.3.3.2 Balb/c hybridoma cultivation and screening

Balb/c hybridomas were cultured according to De Libero G.¹⁴⁵

The day 14 post-fusion, plates were controlled for living hybridomas under the microscope and 100µl supernatant were checked in HRP screening ELISA (see Section 2.4.2.5.2). ELISA-positive hybridomas were transferred to every odd column on a 96-well plate and were diluted to 200µl/well with HT-RPMI-15 (see Section 2.4.1.2). After expansion of dense hybridomas to the even columns, hybridomas were tested by HRP screening ELISA again. Dense and ELISA-positive hybridomas were diluted from 2 wells of the 96-well plates to 2ml HT-RPMI-15 in one well on a 24-well plate and 200µl cell suspension was transferred back to the 96-well plate for back-up purpose.

Hybridomas were expanded to 4 wells on the 24-well plate in HT-RPMI-15 for freezing at -185°C in 2 batches of at least 3 cryotubes (see Section 2.4.2.4). The supernatant at freezing time was tested again by HRP screening ELISA.

All hybridomas were stored in two different N_2 tanks.

2.4.3.4 Terasaki cloning

Hybridomas were cloned on Terasaki-plates following the method of De Libero G.¹⁴⁵

Hybridomas cloning

Hybridomas were thawed (see Section 2.4.2.2) the day before cloning and were cultured in RPMI-10 at 37°C (5% CO_2 , 100% humidity).

Cells were counted (see Section 2.4.2.1) and diluted to 500, 150, 50 and 15cells/ml in 6-RPMI-15 (see Section 2.4.1.2). 20µl/well cell suspension were distributed into labeled 60-well Terasaki-plates, using an ethanol (70%) and flame-sterilized Terasaki-pipettor. Obtained 10 cloning plates with 0.3cell/well, 6 plates with 1cell/well, 3 plates with 3cells/well and 2 plates with 10cells/well were immediately incubated at 37°C (5% CO_2 , 100% humidity) for 10-12 days without opening of the incubator.

Clone cultivation and screening

The day 10-12 post-cloning, cell-positive wells were counted under the microscope to estimate the plating efficiency (plating ratio at that 37% of wells are negative). Clones of dilutions with at least three times less cells/well were transferred to every odd column on 96-well plates, which contained already 200µl/well 6-RPMI-15.

About 19 days post-cloning, transferred clones were tested by AP or HRP screening ELISA (see Section 2.4.2.5) and positive clones were expanded to the even columns on the 96-well plates and further to 24-well plates (see Section 2.4.3.3.2).

A selected number of clones of the highest dilutions were frozen at -185°C in different N_2 tanks and in two batches of at least 2 cryotubes.

2.4.4 Production of monoclonal antibodies

2.4.4.1 Propagation of clones

Selected clones were propagated following the procedure of De Libero G.¹⁴⁵

A clone was thawed (see Section 2.4.2.2) and expanded step by step by diluting 1:2 to 1:4 in RPMI-10 at 37°C (5% CO_2 , 100% humidity). As soon as dense cell growth was established, the pooled cells of one entire 24-well plate were counted (see Section 2.4.2.1) and $2 \cdot 10^6$ cells were frozen in 2 cryotubes at -185°C (see Section 2.4.2.4). The remaining cells were collected at 400rcf for 5min, were suspended in 36ml RPMI-6 (see Section 2.4.1.2) and 6ml/well were distributed in a 6-well plate.

Dense cells of one full 6-well plate were diluted to 75ml in RPMI-6 in a T^{175} flask. After 3-4 days, cells were expanded to 125ml in RPMI-6 and another 3-4 days later, they were diluted to 250ml in RPMI-0 to a final FCS (low IgG) concentration of 3%. The yellowish supernatant of still living cells was harvested at 400rcf for 5min and cleared by filtration using StericupTM (0.22 μm). After addition of 0.02% NaN_3 , the cleared supernatant was stored at 4°C until affinity purification (see Section 2.4.4.2).

The cell pellet was resuspended in 75ml fresh RPMI-6 in a T^{175} flask and the cells were propagated another time following the same procedure.

2.4.4.2 Affinity purification

2.4.4.2.1 Ig κ purification on Protein L-Sepharose spinning columns

Monoclonal Ig were affinity-purified analytically on Nab Protein L spin columns according to the manufacturer instructions.

10ml cleared supernatant (mAb in RPMI -10) was applied to a 0.1ml Protein L spin column in aliquots of 500 μl . Loaded column was incubated for 30min or overnight at 4°C , while shaking with 100rpm, followed by spinning at 5'000rcf for 1min. After washing twice with 400 μl PBS (pH7.5), bound antibodies were eluted four times with 200 μl

elution buffer into a 1.5ml tube containing 20 μ l 1M TrisHCl (pH8.0). Then, the spin columns were three times washed with 400 μ l PBS for neutralization. Collected fractions were analyzed (see Section 2.4.4.2.5).

After addition of 0.02% NaN₃, the antibody solution was stored at 4°C.

2.4.4.2.2 IgG1 purification on a Protein A-agarose column (FPLC)

Monoclonal IgG1 were purified on an AffiGel Protein A-agarose cartridge, following the high-salt method of Harlow E. *et al.*¹⁰², originally adapted from Ey P.L. *et al.*¹⁴⁸. The Protein A-agarose cartridge was run at 4°C by FPLC on a BioLogic work station with the EZLogic software using degassed buffers of 4°C.

NaCl and glycine were dissolved in the cleared supernatant to 3.3M NaCl and 1.5M glycine (see Section 2.4.4.1) and the pH was adjusted to pH9.0 with 1M NaBorat (pH9.0) prior to filtration with Stericup™ (0.22 μ m).

100ml high-salt supernatant was loaded onto the AffiGel Protein A cartridge (1ml bed-volume), which was equilibrated with washing buffer 1 (50mM NaBorate, 3M NaCl, pH 9.0) at a flow rate of 1ml/min. The column was first washed with 5 volumes washing buffer 1, then with 10 volumes using a gradient from washing buffer 1 (100%) to washing buffer 2 (10mM NaBorate, 3M NaCl, pH 9.0, 100%) and finally with 5 volumes washing buffer 2 at a flow rate of 1ml/min. The antibodies were eluted with 10 volumes glycine (100mM, pH4.0). Eluting antibodies, which were detected by absorbance A₂₈₀ measurement, were collected in fractions of 1ml into 1.5ml tubes that contained 50 μ l TrisHCl (1M, pH8.8) for neutralization. The column was neutralized by washing with 5ml washing buffer 2 and 5ml water at a flow rate of 1ml/min. The collected fractions were analyzed (see Section 2.4.4.2.5) and pooled for quantification.

After addition of 0.02% NaN₃, the antibody solution was stored at 4°C.

2.4.4.2.3 IgG1 and IgG2a purification on a Protein G-Sepharose column (FPLC)

Monoclonal IgG1 and IgG2a were affinity-purified on a HiTrap Protein G-Sepharose column, according to a method modified from the manufacturer instructions and Nelson P.N.¹⁴⁹. The Protein G-Sepharose column was run at 4°C by FPLC on a BioLogic workstation with the EZLogic software using degassed buffers of 4°C.

100ml or 200ml cleared supernatant (see Section 2.4.4.1) was loaded onto one or two coupled HiTrap Protein G HP columns (1ml bed-volume), equilibrated with 5ml PBS (pH7.5), at a flow rate of 0.2ml/min. After washing with 10 volumes PBS (pH7.5) at a

flow rate of 0.2ml, bound antibodies were eluted with 10 volumes glycine (100mM, pH3.0) at a flow rate of 0.4-1ml/min. Eluting antibodies were detected by monitoring of A_{280} absorbance and 1ml fractions were collected in 1.5ml tubes, which contained 50 μ l TrisHCl (1M, pH8.8) for neutralization. The column was neutralized, by washing with 5ml washing buffer and 5ml water, at a flow rate of 1ml/min. The collected fractions were analyzed (see Section 2.4.4.2.5) and pooled for quantification.

After addition of 0.02% NaN₃, the antibody solution was stored at 4°C.

2.4.4.2.4 IgM purification on a H1-CRD-Sepharose column (FPLC)

H1-CRD was coupled to Sepharose using Pierce AminoLink Plus kit (see Section 2.3.2.1.5), packed into a BioScale MT-1 (1ml) column and used for affinity purification of monoclonal IgM. The H1-CRD-Sepharose column was run at 4°C by FPLC on a BioLogic workstation using the EZLogic software following a method modified from the manufacturer instructions. All buffers were degassed by filtration (0.45 μ m) and of 4°C.

100ml cleared supernatant (see Section 2.4.4.1) was loaded onto the H1-CRD-Sepharose column (1ml bed-volume), equilibrated with washing buffer (20mM TrisHCl, 500mM NaCl, 20mM CaCl₂, pH7.5 at 20°C), at a flow rate of 0.2ml/min. Contaminating proteins were washed out isocratically with 10 volumes washing buffer at a flow rate of 0.2ml/min, until the baseline was reached. The antibodies were eluted isocratically with 10 volumes glycine (100mM, pH3.0) and were detected by absorbance A_{280} measurement. The antibody peak was collected in 1ml fractions into 1.5ml tubes, which contained 50 μ l TrisHCl (1M, pH8.8) for neutralization. The column was neutralized, by washing with 5ml TBS-Ca20 and with 5ml water. Antibody fractions were analyzed (see Section 2.4.4.2.5) and pooled for quantification.

After addition of 0.02% NaN₃, the antibody solution was stored at 4°C.

2.4.4.2.5 Analysis

The purity of antibody fractions was analyzed by SDS-PAGE (see Section 2.2.4.2) and the activity of diluted antibodies was controlled by HRP-ELISA (see Section 2.4.2.5.2).

The antibody concentration was determined by absorbance A_{280} measurement, by Bradford assay and by SDS-PAGE quantification (see Section 2.2.4.4).

2.5 Antibody characterization

2.5.1 Protein assays

2.5.1.1 Polyacrylamide-gel Electrophoresis

Anti-H1 mAb and plgY were controlled by reducing, non-reducing SDS-PAGE and native PAGE (see Section 2.2.4.2).

2.5.1.2 Immunoblotting

2.5.1.2.1 Immunoblotting of antibodies

Purified monoclonal anti-H1 antibodies were run by PAGE, blotted to a nitrocellulose membrane and were stained (see Section 2.2.4.3). After blocking and washing, the mAb were directly immunostained with a secondary antibody.

2.5.1.2.2 Immunoblotting of the H1-CRD

The native and reduced-alkylated H1-CRD (see Section 2.5.1.4.1) were run by reducing SDS-PAGE, the native and native-alkylated H1-CRD were applied to non-reducing SDS-PAGE and in addition, the native H1-CRD was separated by native PAGE. The H1-CRD bands on the PAGE gels were blotted to a nitrocellulose membrane (see Section 2.2.4.3).

After blocking and washing, the membrane was cut into pieces, which represented each antigen sample once. Pieces were incubated separately in 2ml antibody solution (0.5µg-5.0µg/ml purified anti-H1 mAb, 1% BSA, in TTBS-Ca20) in small Petri dishes (diameter 60mm) or in 5ml antibody solution (100µg/ml purified anti-H1 total plgY, 1% BSA in TTBS-Ca20 or anti-H1 mAb supernatant) in large Petri dishes (diameter 1'000mm), covered with parafilm, overnight at 4°C, while shaking with 70rpm. Then, the pieces were three times washed in TTBS-Ca20, before they were incubated separately in 3-5ml secondary antibody solution (GAM-IgG(whole)-AP, GAM-Ig(polyvalent)-AP or RACH-IgY(whole)-AP 1:2'000 to 1:5'000, 1% BSA in TTBS-Ca20) in large Petri dishes (diameter 100mm), covered with parafilm for 2h at RT, while shaking with 70rpm. The pieces were washed twice in TTBS-Ca20 and once in TBS, prior to casting in 3-5ml substrate solution (100mM TrisHCl, 100mM NaCl, 5mM MgCl₂, 0.4% NBT/CIP, pH 8.8) in large Petri dishes. Finally, the color development was stopped in 5mM EDTA (pH8.0).

2.5.1.3 Colorimetric assay

2.5.1.3.1 Isotyping ELISA

The isotype of the monoclonal anti-H1 antibodies was determined with the SBA Isotyping Kit according to the HRP screening ELISA (see Section 2.4.2.5.2) but using different isotype-specific HRP-labeled antibodies GAM-Ig(isotype M, G1, G2a, G2b, κ or λ)-HRP (1:300) and polyvalent HRP-labeled antibody GAM-Ig(H+L)-HRP (1:300).

2.5.1.3.2 Titration ELISA

Anti-H1 mAb and pIgY were titrated following a slightly modified method of the HRP screening ELISA (see Section 2.4.2.5.2). All incubation steps were performed in plates, which were covered with a lid and parafilm or were placed in a humidified chamber.

MaxiSorb ELISA plates were coated with 70 μ l/well coating solution (3-6 μ g/ml H1-CRD, 20mM CaCl₂ in TBS, pH7.5) overnight at 4°C, were once washed with 200 μ l/well TTBS-Ca20 (20mM CaCl₂, 0.05% Tween20 in TBS, pH7.5), TTBS-Ca2 (2mM CaCl₂, 0.05% Tween20 in TBS, pH7.5) or TTBS-Ca0 (10mM EDTA, 0.05% Tween20 in TBS, pH7.5) and were blocked with 150 μ l/well blocking buffer (1% BSA in TTBS-Ca) for 2h at RT. After washing twice with 200 μ l/well TTBS-Ca and thoroughly tapping dry on paper towels, 50 μ l/well purified anti-H1 mAb solutions (range of 0.001-30 μ g/ml anti-H1 mAb, 1% BSA in TTBS-Ca) or blank (1% BSA in TTBS-Ca) were distributed in duplicate or triplicate and were incubated for 2h at RT. The plates were washed three times with 200 μ l/well TTBS-Ca and were tapped dry on paper towels followed by the detection with 50 μ l/well HRP-labeled antibody solution (GAM-Ig(H+L)-HRP 1:1'000, 1% BSA in TTBS-Ca) for 2h at RT. After thoroughly washing five times with 200 μ l/well TTBS-Ca and tapping dry, 90 μ l/well OPD Sigma Fast substrate solution was added and the plate was incubated in the dark for 10min. The color development was stopped with 50 μ l/well HCl (3.6%) and the absorbance was read at 490nm in a Spectramax190 plate reader.

2.5.1.3.3 Competitive GalNAc-polymer assay

The competition of anti-H1 mAb and GalNAc for binding to the H1-CRD was tested in the GalNAc-polymer assay of Stokmaier D.¹⁰³ based on Weitz-Schmidt G. *et al.*¹⁵⁰.

Formation of β -GalNAc-polymer-biotin-streptavidin-POD complex

20 μ l biotinylated β -GalNAc-polymer (1mg/ml, 5mol% biotin, 20mol% GalNAc), 80 μ l streptavidin-POD-conjugate (500U/ml), 20 μ l FCS and 80 μ l HAB-Ca (20mM HEPES),

150mM NaCl, 1mM CaCl₂, pH 7.4) were mixed in a 1.5ml tube and the complex was formed during incubation for 2h at 37°C. The β-GalNAc-polymer complex solution (100μg/ml) was stored at 4°C in the dark.

Polymer assay

The evaporation was prevented by incubation in a humidified chamber during assay.

MaxiSorb ELISA plates were coated with 100μl/well coating solution (3μg/ml H1-CRD in HAB-Ca) overnight at 4°C. The coating was discarded, the plates were tapped dry on paper towels and the wells were blocked with 150μl/well blocking buffer (3% BSA in HAB-Ca) for 1h at 4°C. After washing three times with 200μl/well HAB-Ca and tapping dry on paper towels, 50μl/well β-GalNAc-polymer complex (0.6μg/ml in HAB-Ca) solution, followed by 50μl/well purified anti-H1 mAb solutions (range of 2-200μg/ml anti-H1 mAb in HAB-Ca), HAB-Ca or EDTA solution (5mM EDTA in HAB-Ca) were distributed in triplicate and incubated for 1h at 37°C. The plates were washed twice with 200μl/well HAB-Ca and were tapped dry on paper towels before 100μl/well Sigma Fast OPD solution or Biorad ABTS solution were added. After an incubation of 10min in the dark, the color development was stopped with 100μl/well acid (HCl 3.6%, OPD or 2% oxalic acid, ABTS) and the absorbance was read at 490nm (OPD) or 415nm (ABTS) in a Spectramax190 plate reader.

The titration curve was drawn and the EC₅₀ was calculated using the Prism4 software.

2.5.1.4 Epitope mapping

The epitopes of anti-H1 mAb were mapped by matrix-assisted laser desorption ionization Fourier-transformation cyclotron resonance (MALDI-FT-ICR) following the epitope excision and extraction method of Przybylski M.¹⁵¹ based on Macht M. *et al.*¹⁰⁶

2.5.1.4.1 Reduction and alkylation of the H1-CRD

The native H1-CRD (see Section 2.2.5.5) was diluted to 1mg/ml (equivalent to 412μM Cys) in T-Ca20 (50mM TrisHCl, 20mM CaCl₂, pH 8.0) and was reduced with a 50-fold molar excess of dithiothreitol (equivalent to 20.6mM DTT) to Cys during incubation for 1h at 56°C, while shaking with 1'200rpm.

The native H1-CRD (1mg/ml H1-CRD in T-Ca20) and the reduced H1-CRD (1mg/ml H1-CRD, 20.6mM DTT in T-Ca20) were alkylated with 2.5-fold molar excesses of iodoacetamide (IAA, equivalent to 51.5mM IAA) to DTT for 1h in the dark.

2.5.1.4.2 Preparation of the anti-H1 mAb-Sepharose column

Buffer exchange of anti-H1 mAb

Disturbing primary amines Tris and glycine in anti-H1 mAb solutions (100mM glycine, TrisHCl buffered, see Section 2.4.4.2) were removed by buffer exchange to coupling buffer (200mM NaHCO₃, 500mM NaCl, pH 8.3) using Microcon YM-10 spin devices (MWCO 10'000). The volume of the purified mAb solution that contained 300µg mAb, was concentrated at 14'000rcf for 30min and the buffer was exchanged by spinning three times with 500µl coupling buffer at 14'000rcf for 30min. The mAb concentrate was diluted to 100µl in coupling buffer and was spun out of the device at 1'000rcf for 3min. The device membrane was three times extracted with 100µl coupling buffer and was spun into the same 1.5ml tube to get 400µl mAb solution (750µg/ml).

Coupling of anti-H1 mAb to Sepharose

133.3mg cyanobromide-activated Sepharose 4B (1mg swells to 3µl) were swollen in 400µl anti-H1 mAb solution (750µg/ml in coupling buffer) and were coupled during incubation for 1h, while shaking at 1'200rpm.

The coupled mAb-Sepharose slurry was packed into a 1ml Mobicol column containing a lower filter, and an upper filter was placed in the luer cap. The remaining activated sites were quenched with 5ml blocking buffer by washing drop by drop. After rinsing three times sequentially with 5ml acetic buffer (200mM NaCH₃COO, 500mM NaCl, pH 4.0) and 5ml blocking buffer, the column was incubated for 1h, while shaking with 600rpm. Then, the packed column was three times washed the same way with 5ml acetic buffer and 5ml blocking buffer, followed by the neutralization with 5ml T-Ca20.

2.5.1.4.3 Epitope extraction of digested H1-CRD

Trypsine digest of H1-CRD

20µl native H1-CRD (1mg/ml H1-CRD in T-Ca20) or reduced and alkylated H1-CRD (1mg/ml H1-CRD, 20.6mM DTT, 51.5mM IAA in T-Ca20) was digested with 0.4µl trypsin (100µg/ml trypsin in T-Ca20, 0.02mg/mg H1-CRD), for 5h at 37°C, while shaking with 700rpm.

Epitope extraction of trypsin-digested H1-CRD

The anti-H1 mAb-Sepharose column was equilibrated with 10ml T-Ca20 before 20µl trypsin-digested H1-CRD (1mg/ml, to get a molar ratio of antibody : H1-CRD of 2:1) solution was loaded by direct application to the Sepharose, and then was incubated for 2h, while shaking with 700rpm. The column was rinsed drop by drop with 40ml T-Ca20 and the bound epitope fragment was eluted once or twice by incubation with 500µl TFA (0.1%) for 15min, while shaking with 700rpm.

The flow through, wash and elution samples were lyophilized and desalted prior to MS analysis (see Section 2.5.1.4.5).

ZipTip desalting

The lyophilized sample was dissolved in 15µl TFA (0.1%), was sonicated in a water bath for 5min and spun down. The ZipTip C18 (Millipore) was wet three times with acetonitrile (50%) by slow aspiration followed by complete extrusion. The ZipTip was equilibrated five times with TFA (0.1%) before the sample was loaded by twenty cycles of slow aspiration and extrusion. After washing twice with TFA (0.1%), the desalted sample was eluted with 4µl elution solution (0.1% TFA, 50% acetonitrile) by five cycles of aspiration and extrusion.

2.5.1.4.4 Epitope excision of mAb-bound H1-CRD

Epitope excision of mAb-bound H1-CRD by digesting with trypsin

The anti-H1 mAb-Sepharose column was equilibrated with 10ml T-Ca20, loaded with 20µl native H1-CRD (1mg/ml in T-Ca20) or alkylated H1-CRD (see Section 2.5.1.4.1) solution to get a molar ratio of antibody : H1-CRD of 2:1. The H1-CRD was directly administered onto the Sepharose and incubated for 2h, while shaking with 700rpm. The column was rinsed drop by drop with 10ml T-Ca20 and bound H1-CRD was digested with 20µl trypsin solution (0.02mg/ml in T-Ca20, 0.02mg/mg H1-CRD) for 5h at 37°C, while shaking with 700rpm. After washing the column drop by drop with 40ml T-Ca20, bound epitope fragments were eluted once or twice by incubation 500µl TFA (0.1%) for 15min.

The column was regenerated, by washing with 10ml TFA (0.1%) and with 20ml T-Ca20 and samples (wash, flow through, elution) were lyophilized and desalted (see Section 2.5.1.4.3) prior to MS analysis (see Section 2.5.1.4.5).

Epitope excision of mAb-bound H1-CRD by digesting with proteinase K

The epitope excision followed the same procedure, but bound H1-CRD was digested with 40 μ l proteinase K solution (0.05mg/ml in T-Ca20, 0.1mg/mg H1-CRD) for 4h at 37°C, while shaking with 700rpm.

Epitope excision of mAb bound H1-CRD by digesting with α -chymotrypsine

The epitope excision was performed following the procedure above, but bound H1-CRD was digested with 20 μ l α -chymotrypsine solution (0.02mg/ml in T-Ca20, 0.02mg/mg H1-CRD) for 2-4h at 30°C, while shaking with 700rpm.

Epitope excision of mAb-bound trypsin-digested H1-CRD by double digesting with pronase K

The epitope excision was performed according to the procedure above, but 20 μ l solution of trypsin-digested H1-CRD (see Section 2.5.1.4.3) was loaded and after washing, was additionally digested with 200 μ l pronase solution (0.5mg/ml in T-Ca20, 5mg/mg H1-CRD) for 18h at 40°C, while shaking with 700rpm.

2.5.1.4.5 MS measurement

Desalted samples were measured as described by Stefanescu R.¹⁵¹ using MALDI-FT-ICR or electro-spray ionization Fourier-transformation cyclotron resonance (ESI-FT-ICR).

2.5.1.4.6 Solid phase synthesis of acylated epitope fragments and biotin labeling

The solid phase synthesis of epitope fragments and the purification by C18 reverse phase HPLC (0% acetonitrile / 100% TFA 0.1% gradient to 80% acetonitrile / 20% TFA 0.1%) was performed as described by Stefanescu R.¹⁵¹

Fragments were C-terminal acetylated and for ELISA experiments they were additionally N-terminal biotinylated.

2.5.1.4.7 Extraction of acetylated epitope fragments

The extraction of acetylated epitope fragments (see Section 2.5.1.4.6) was carried out following the procedure in Section 2.5.1.4.3. 50 μ l epitope fragment solution (10nM fragment in T-Ca20) was loaded.

2.5.1.4.8 Epitope ELISA with acetylated biotin-labeled epitope fragments

Epitope ELISA was performed according to the protocol of Przybylski M.¹⁵¹

Anti-H1 mAb-capturing ELISA

MaxiSorb ELISA plates were coated with 100µl/well streptavidine solution (5µg/ml streptavidine in T-Ca20) for 2h at RT, were washed four times with 200µl/well TTBS-Ca20, dried by aspiration and 100µl/well biotinylated epitope fragments (range of 0.0001-20µM in T-Ca20) were bound for 2h at RT. Coated wells were washed four times with 200µl/well TTBS-Ca20, dried by aspiration and were blocked with 200µl/well blocking buffer (5% BSA in TTBS-Ca20) for 2h at RT. After incubation with 100µl/well anti-H1 mAb solution (1µg/ml anti-H1 mAb, 1% BSA in T-Ca20) for 2h and washing four times with 200µl/well TTBS-Ca20, bound mAb was detected with 100µl/well HRP-labeled antibody (GAM-Ig(H+L)-HRP 1:1'000, 1% BSA in T-Ca20). The plates were thoroughly washed four times with 200µl/well TTBS-Ca20, dried by aspiration prior to addition of 90µl/well OPD Sigma Fast substrate solution and incubation for 10min in the dark. The color development was stopped with 50µl/well HCl (3.6%) and the absorbance was read at 490nm in a Spectramax190 plate reader.

Epitope-capturing ELISA

MaxiSorb ELISA plates were coated with 100µl/well anti-H1 mAb solution (2µg/ml anti-H1 mAb in T-Ca20) overnight at 4°C, were washed four times with 200µl/well TTBS-Ca20, dried by aspiration and were blocked with 200µl/well blocking buffer (5% BSA in TTBS-Ca20) for 2h at RT. After washing once with 200µl/well TTBS-Ca20, the coated plates were incubated with 100µl/well biotinylated epitope fragments (40µM biotinylated fragment in T-Ca20) for 2h at RT. Wells were washed four times with 200µl/well TTBS-Ca20, dried by aspiration and the fragment were tagged with 100µl/well HRP-labeled antibody (1µg/ml anti-biotin IgG-HRP 1:1'000, 1% BSA in TTBS-Ca20) for 2h at RT. The plates were thoroughly washed four times with 200µl/well TTBS-Ca20, dried by aspiration prior to addition of 90µl/well OPD Sigma Fast substrate solution and incubation for 10min in the dark. The color development was stopped with 50µl/well HCl (3.6%) and the absorbance was read at 490nm in a Spectramax190 plate reader.

2.5.1.5 Surface plasmon resonance

Kinetics of the anti-H1 mAb binding to monomeric and dimeric H1-CRD surfaces were measured by surface plasmon resonance (SPR, Biacore) as described by Ricklin D.¹⁴⁰

2.5.2 Cell assays

2.5.2.1 Fluorescence flow cytometry

2.5.2.1.1 Intracellular flow cytometry of fixed cells

The intracellular immunofluorescence staining of hybridoma cells was performed after blocking secretion of antibodies, following the protocol of De Libero G.¹⁴⁵

The screening ELISA-positive hybridoma B01 was used as positive control, the ELISA-negative hybridoma A12 as negative control and unstained cells served as blank.

Blocking of antibody secretion

10µg/ml Brefeldin A was added to the hybridoma cultures 12h prior to staining.

Preparation of cells

The cells were counted (see Section 2.4.2.1) and collected at 280rcf for 5min. After dilution to $5 \cdot 10^6$ cells/ml in DPBS, 100µl/well cell suspension was distributed in a 96-well U bottom plate to get $5 \cdot 10^5$ cells/well.

Paraformaldehyde fixation of cells

The cells were spun at 1'500rpm for 2min and the supernatant was discarded by fast flicking the plate. After washing twice with 200µl/well DPBS, the cells were fixed with 200µl/well paraformaldehyde (2%) buffer during incubation for 15min.

Intracellular fluorescence staining

The fixed cells were collected at 280rcf for 2min, were washed twice with 200µl/well FACS buffer 1 (0.5% HSA, 0.02% NaN_3 in DPBS) and twice with 200µl/well FACS buffer 2 (0.1% saponine in FACS buffer 1) followed by permeabilization during an incubation with 20µl/well Fluorescein isothiocyanate (FITC)-labeled goat anti-mouse antibody solution (GAM-IgG(H+L)-FITC, 1:50 in FACS buffer 2) for 25min in the dark. Stained cells were washed three times with 200µl/well FACS buffer 2 and were resuspended in 200µl/well FACS buffer 1 before they were transferred into FACS tubes for measurement of the emission in FL-1 at 530nm after excitation at 488nm using a FACScan reader.

2.5.2.1.2 Extracellular flow cytometry of not fixed or fixed cells

The extracellular immunofluorescence staining on different human cell lines was performed according to the protocol of De Libero G.¹⁴⁵

C15sn or the positive hybridoma B01 and the monoclonal anti-ASGPR1 (Calbiochem) were used for positive controls B3sn, mcl2 or the negative hybridomas A12 for negative control and unstained cells were used for blank.

Detachment of adherent HepG2 and SK-Hep1 and of weak adherent dendritic cells

Cells were detached according to Seow Y.Y.¹¹

The adherent cells HepG2 and SK-Hep1 were washed once with DPBS and were detached by incubation with EDTA solution (2.5mM EDTA in DPBS, pH 8.0) for 5min at 37°C or on ice by enforced pipetting and scratching.

Weak adherent dendritic cells were detached by incubation on ice for 5min and enforced pipetting.

Blocking of monocytes and THP-1 cells

THP-1 and monocytes were collected at 400rcf for 5min and were washed once with FACS buffer (0.5% BSA, 0.02% NaN₃ in DPBS) before they were incubated with 100-500µl human serum for 20min on ice.

Preparation of cells

The detached adherent cells, blocked suspension cells and HL-60, JS-7, Jurkat, K-652 suspension cells were collected with 400rcf for 5min and were resuspended in DPBS for counting (see Section 2.4.2.1). After washing once in FACS buffer (0.5% BSA or HSA, 0.02% NaN₃ in DPBS), the cell pellet was broken by tapping the tube. Washed cells were diluted to $5 \cdot 10^5$ cell/ml in FACS buffer and 200µl/well cell suspension was distributed in a 96-well U bottom plate to get $1 \cdot 10^5$ cells/well. The plate was spun at 1'500rpm for 2min at 4°C, and the supernatant was discarded by fast flicking followed by washing twice with 200µl/well DPBS.

Optional paraformaldehyde fixation of cells

The cells were fixed with 200µl/well paraformaldehyde (2%) buffer during incubation for 15min at RT. After spinning the plate at 1'500rpm for 2min at 4°C, the cells were washed twice with 200µl/well prechilled FACS buffer.

Extracellular fluorescence staining

The not fixed or optionally fixed cells were incubated with 50µl/well prechilled supernatant or with 20µl/well precooled purified monoclonal antibody solution (20µg/ml mAb in FACS buffer) for 20min on ice followed by washing twice with 200µl/well precooled FACS buffer and spinning at 1'500rpm for 2min at 4°C. The cells were stained with 20µl/well R-phycoerythrin (RPE) or FITC-labeled goat anti-mouse antibody solution (GAM-Ig(H+L)-RPE or GAM-Ig(H+L)-FITC, 1:50 in precooled FACS buffer) during incubation for 20min at 4°C in the dark. The stained cells were washed three times with 200µl/well precooled FACS buffer, were resuspended in 200µl/well FACS buffer, which contained 5ng/ml propidium iodide and were transferred to FACS tubes on ice. The emission was measured in FL-1 at 530nm for FITC-stained and in FL-2 at 585nm for RPE-stained cells after excitation at 488nm using a FACScan reader. The propidium-stained dead cells that were detected in FL-3 at 670nm were excluded.

2.5.2.2 Immunofluorescence microscopy with HepG2 and SK-Hep1 cells

The immunofluorescence microscopy of HepG2 and SK-Hep1 cells was performed following the optimized protocol of Stokmaier D.¹⁰³

2.5.2.2.1 Labeling of antibodies and asialofetuin with Texas Red fluorochrome

The anti-H1 mAb and pIgY were labeled with Texas Red (TR) using FluoReporter[®] Texas Red-X protein labeling Kit according to the kit instruction manual.

The disturbing primary amines glycine and Tris in the mAb solution (100mM glycine, TrisHCl buffered, see Section 2.4.4.2) were removed by exchanging the buffer to PBS using Microcon YM10 centrifugal filter devices (MWCO 10'000).

The needed volume of dye solution was calculated using the following Equation 9.

$$V_{\text{dye}} = \frac{c_{\text{Ab}} \cdot V_{\text{Ab}} \cdot 817 \cdot 200 \cdot 5}{145000} \quad (\text{Eq. 9})$$

Equation 9: Calculation of the needed volume dye solution V_{dye} for the defined volume antibody solution V_{Ab} with an antibody concentration c_{Ab} above 1mg/ml.

20µl NaHCO₃ buffer (1M, pH8.3) was mixed with 200µl antibody solution (2mg/ml antibody in KPBS) or asialofetuin solution (2mg/ml asialofetuin in KPBS) before calculated volume dye stock solution (1 vial dye dissolved in 100µl DMSO) was slowly added to the buffered antibody solution, while magnetically stirring. After incubation for

1h in the dark, the solution of labeled antibody was dialyzed in Slide-A-Lyzer[®] mini dialysis units (MWCO 10'000) against 100ml KPBS overnight at 4°C in the dark. Particles were removed by centrifugation at 16'000rcf for 5min and the solution of labeled antibody was stored at 4°C in the dark.

2.5.2.2.2 Preparation of cell cultures on coverslips

Paraformaldehyde fixation buffer

The paraformaldehyde solution (0.3g paraformaldehyde, 8.8ml water, 10 μ l NaOH 1M) in a closed 15ml tube was heated in a water bath of 60°C until the solution cleared up. After cooling to RT, 1ml KPBS 10x (15mM KH₂PO₄, 80mM Na₂HPO₄, 1.37M NaCl, 27mM KCl) and 20 μ l HCl (1M) were added and the pH was checked with indicator sticks to be pH7.0-7.5.

The fixation buffer (3% paraformaldehyde in KPBS, pH 7.0-7.5) was always prepared freshly.

Mowiol mounting buffer

25g Mowiol was dissolved in 100ml KPBS and was combined with 50ml glycerol and *N*-propylgallate (0.75%). After stirring for 8h, the mounting buffer was cleared by ultracentrifugation at 13'000rcf for 15min and was stored airtight at 4°C in the dark.

Collagen coating of coverslips

Coverslips were cleaned, degreased and roughened according to the protocol of Salmons Lab¹⁵².

The single coverslips were washed in water and were treated in HCl (1M) for 4h at 50-60°C. After cooling down to RT, the coverslips were sonicated three times for 30min in in a bath of water and three times for 30min in a bath of 50%, 70% and 95% ethanol, respectively.

The coverslips were stored in ethanol (95%) until use.

The pretreated coverslips were dried and briefly flamed over a Bunsen burner. 1coverslip/well were placed into a 12-well plate using sterile tweezers and were coated with 60 μ l/well collagen solution (1mg/ml collagen S, 500mM acetic acid, pH2.8) overnight at 4°C. After washing the collagen-coated coverslips once with 1ml/well DPBS, they were stored in 1ml/well DPBS at 4°C until use.

Cell cultivation on collagen-coated coverslips

$2 \cdot 10^5$ cells were seeded into a well with a collagen-coated coverslip and were incubated in 1ml/well DMEM-15 (see Section 2.4.1.2) at 37°C (5% CO₂, 100% humidity).

2.5.2.2.3 Immunodetection of anti-H1 antibody binding to fixed cells

The immunostaining was adapted from Novikoff P.¹⁵³ and Seow Y.Y.¹¹

Direct immunodetection of binding with Texas Red-labeled antibodies

After a one-day culture period, the cells on coverslips were carefully washed once or twice with 1ml/coverslip DPBS and were fixed with fixation buffer for 30min or overnight at 4°C. The fixed cells were washed three times with 1ml/coverslip DPBS and were permeabilized with 1ml/coverslip permeabilization solution (1% Triton-X100 in DPBS) for 15min. After washing once with 1ml/coverslip DPBS, the autofluorescence of the permeabilized cells was quenched with NaBorohydride solution (10mg/ml NaBorohydride in DPBS) for 15min on ice. The quenched cells were washed abundantly with 1ml/coverslip DPBS until bubbles disappeared and were FCS-starved in 1ml/coverslip DPBS for 1h followed by incubation with 100-200µl/coverslip TR-labeled anti-H1 antibody (10-40µg/ml anti-H1 mAb-TR or plgY-TR in DPBS) or asialofetuin (5-20µg/ml asialofetuin-TR in DPBS) for 2h in the dark. After washing three times with 1ml/coverslip DPBS, the coverslips were mounted onto glass slides.

Indirect immunodetection of binding with labeled secondary antibodies

The cells were prepared as described above but after FCS starvation, the cells were incubated with 100-200µl/coverslip anti-H1 antibody (10-20µg/ml anti-H1 mAb in DPBS or supernatant) for 2h, were washed twice with 1ml/coverslip DPBS and were stained with 100-200µl/coverslip labeled secondary antibody (DAM-IgG(H+L)-Cy3 1:3'000 or GAM-IgG(H+L)-AlexaFluor488 1:800 in KPBS) for 1h in the dark. After washing three times with 1ml/coverslip DPBS, the coverslips were mounted onto glass slides.

Mounting of coverslips onto glass slides

The coverslips were rinsed with water, were tapped dry with a Kimberly clark paper towel and were mounted with one drop Mowiol mounting buffer onto glass slides. After drying for 30min in the dark, the mounted slides were stored at 4°C in the dark until microscopy.

Fluorescence microscopy and photography of the slides

The fluorescence-stained cells were examined under an Apofluorescence microscope (Zeiss) with 630 times magnification (binocular 10x/20, objective 63x/1.25oil (Ph3plan-neofluor 440481). The red fluorescence filter (BP546, FT580, LP590) and the green fluorescence filter (450-490, FT510, 515-565) were used for investigation of slides.

The pictures of the slides were taken on a Kodak ELITE 400 film for dia-positives (1600 ASA) and were scanned with a Canon PI CS-U4.1X flat bed scanner.

2.5.2.2.4 Immunodetection of anti-H1 antibody internalization into cells prior to fixation

The immunostaining was adapted from Novikoff P.¹⁵³ and Seow Y.Y.¹¹

Direct immunodetection of internalized Texas Red-labeled anti-H1 antibodies

The cells on coverslips were carefully washed once or twice with 1ml/coverslip DMEM and were FCS-starved in DMEM for 1h at 37°C (5% CO₂, 100% humidity). The starved cells were incubated with 200µl/coverslip TR-labeled anti-H1 antibody (10-40µg/ml anti-H1 mAb-TR or pIgY-TR in DPBS) or asialofetuin (5-20µg/ml asialofetuin-TR in DPBS) and for 40min at 37°C (5% CO₂, 100% humidity) in the dark. After washing three times with 1ml/coverslip DPBS, the stained cells were fixed with 500µl/coverslip fixation buffer for 30min in the dark. The fixed cells were washed three times with 1ml/coverslip PBS again before the coverslips were mounted onto glass slides and were analyzed under the fluorescence microscope as described in Section 2.5.2.2.3

Indirect immunodetection of internalized labeled secondary antibodies

The cells were prepared as described above but after FCS starvation, the cells were incubated with 200µl/coverslip anti-H1 antibody (10-20µg/ml anti-H1 mAb in KPBS or supernatant) for 40min at 37°C (5% CO₂, 100% humidity), were washed three times with 1ml/coverslip DPBS and additionally were permeabilized with 1ml/coverslip Triton-X100 (0.1% Triton-X100, PBS) for 15min in the dark. Permeabilized cells were washed three times with 1ml/coverslip DPBS and were stained with 200µl/coverslip labeled secondary antibody (GAM-IgG(H+L)-Cy3 1:3'000 in KPBS) for 1h in the dark. After washing three times with 1ml/coverslip DPBS, the coverslips were mounted onto glass slides and were analyzed under the fluorescence microscope as described in Section 2.5.2.2.3.

2.5.3 Tissue assays

2.5.3.1 Immunostaining of liver tissue

The immunostaining of human liver tissue was performed by Terracciano L.¹⁵⁴.

Briefly, the sections of paraformaldehyde-fixed, paraffin-embedded human liver tissue were dewaxed. The antigen of dewaxed sections in PBS was retrieved by various treatments: the microwaving in citrate buffer (pH 6.0) at 98°C for 30min or 60min, the steaming in citrate buffer (pH 6.0, pH 1-2 and pH 10-11) at 120°C for 5min, the proteinase K treatment with 3 drops within 5min, the pronase XIV (1mg/ml) treatment at 37°C for 15min or at 4°C for 30min and the trypsin (1mg/ml) treatment at RT for 30min. Optionally, the endogenous avidin/biotin activity was blocked. The sections were dehydrated in methanol-peroxide for 30min and were blocked with murine serum for 30min, followed by incubation in primary antibody solution (200-300µg/ml purified anti-H1 IgG, 1:50, 1:100, 1:200 and 1:400). The primary antibody was captured with avidin-labeled anti-mouse Ig for 30min and with biotin-labeled HRP for 30min. The sections were finally stained with diaminobenzidine (DAB) substrate and were counterstained with Harris' hematoxylin, prior to mounting.

3 Result

3.1 ASGPR database research

3.1.1 ASGPR and H1-CRD alignments

The amino acid sequence alignment of the human asialoglycoprotein 1 (ASGPR-1) with the mouse and chicken hepatic lectins (MHL-1 and ChHL-1) resulted in 80% sequence identity or 87% similarity to the MHL-1 and only 39% identity or 47% similarity to the ChHL-1. The area of the binding site showed higher homologies with 93% identical or 96% similar amino acids to the MHL-1 and 55% identical or 60% similar amino acids to the ChHL-1 (see Figure 21).

```

seqLech_human   MTKEYQDLQHLNNEE--SDHHQLRKGPPLPQLRLCSGPRLLLLSLGLSLLLLLVVVCVI
seqLech_mouse   MTKDYQDFQHLND--NDHHQLRRGPPPTPRLQLCSGSRLLLSSLSILLLVVVCVI
seqLech_chicken -----MDEERLSDNVRLYKGGIRQGLRSFAAVYVLLALSFLLLTLLSSVSLARI
                *: : . *: : * . * . * * * : : * * : . *

seqLech_human   GSQNSQLQEELRGLRETFNFTASTEAVKGLSTQGGNVGRKMKSLQLEKQKDLSED
seqLech_mouse   TSQNSQLREDLLALRQNFNLTVSTEDQVKALSTQGSVGRKMKLVESKLEKQKDLTED
seqLech_chicken AALSSKLSTLQSEPKHNFSS-----
                : . * : *          : . . * .

seqLech_human   HSSLLLHVQKQFVSDLRSLSCQMAALQNGSERTCCPVNWEHERSCYWFERSGKAWADAD
seqLech_mouse   HSSLLLHVQKQLVSDVRSLSQMAAFRNGSERICCPINWVEYEGSCYWFSSSVRPWTEAD
seqLech_chicken RDSLLFPC-----GAQSR----QWEYFEGRCYFSLSRMSWHKAK
                : . * :          * : :          : * . * * : * * * . * .

seqLech_human   NYCRLEDAHLVVVTSWEEQKVFVQHHIGPVNTWMLHDQN--GPWKVDGTDYETGFKNWR
seqLech_mouse   KYCQLEN AHLVVVTSRDEQNF LQRHMGPLNTWIGLTDQN--GPWKVDGTDYETGFQNWR
seqLech_chicken AECEEMHSHLIIIDSYAKQNFVMPFRTRNERFWIGLTDENQEGEWQVDGTDTRSSFTFWK
                * . . : * : : * . * : : . * : * * * * * : * * * :

seqLech_human   PEQPDDWYGHGLGGGEDCAHFTD DGRWDDVCQRPYRWCETELDKASQEPPLL
seqLech_mouse   PEQPDN WYGHGLGGGEDCAHFTD DGRWDDVCRPYRWCETKLDKAN-----
seqLech_chicken EGEPNNR-----GFNEDCAHVWTS GQWNDVYCTYECYVCEKPLPK-----
                * : :          * . * * * . . * : * * *          : * * . * *

```

Figure 21: T-COFFEE alignment of Lech_human (ASGPR-1) with Lech_mouse (MHL-1) and Lech_chicken (ChHL-1). Identical amino acids are indicated with stars, similar amino acids with points. The sequence of the CRD is written in bold and the binding site is shaded in grey.

The H1-CRD of the human ASGPR-1 was aligned with the CRD of the asialoglycoprotein receptor 1 of the species, which were selected for the antibody productions: the mouse (*mus musculus*) to produce monoclonal and the chicken (*gallus gallus*) to get polyclonal antibodies. Furthermore, the H1-CRD amino acid sequence was compared with the amino acid sequences of homologous receptors in human (*homo*

sapiens), mouse and chicken: the asialoglycoprotein receptor 2 (ASGPR-2), the macrophage Gal/GalNAc-specific lectin (Mmgl) on macrophages, the Kupffer cell receptor on Kupffer cells and the dendritic cell-specific ICAM-3-grabbing nonintegrin (DC-SIGN, CD209) on dendritic cells.

Table 7: Amino acid sequence homologies. Alignment of the human ASGPR-1, the H1-CRD or the binding site of the H1-CRD with the same and homologous receptors in human, mouse and chicken.

No	Sequence ID	Identity (similarity)		
		Receptor	CRD	Binding site
1	Lech_human	100%	100%	100%
2	Lech_chicken	37% (51%)	37% (51%)	42%
3	Lech_mouse	64% (73%)	79% (91%)	93% (96%)
4	Leci_human	48% (59%)	67% (78%)	66% (72%)
5	Leci_mouse	43% (55%)	60% (71%)	63% (69%)
6	Mmgl_human	52% (66%)	71% (81%)	84% (87%)
7	Mmgl_mouse	50% (65%)	67% (80%)	78% (84%)
8	Kucr_human			
9	Kucr_mouse	28% (45%)	41% (52%)	-
10	209_human	38% (51%)	38% (51%)	36% (42%)
11	209_mouse	38% (55%)	38% (55%)	36% (36%)

The comparison showed, that the CRD domains of these receptors on its own exhibited higher homologies with 37-79% identical or 51-91% similar amino acids than the entire receptors with 37-64% identical or 41-73% similar amino acids. When only the sequences of the binding site were aligned, the homologies are further increased to 63-93% identity or 69-96% similarity compared to the ASGPR-1, ASGPR-2 and Mmgl in human and mouse. No significant homologies were found for Kucl and DC-SIGN in human and mouse and for ChHL-1 (see Table 7, Figure 22).

```

seqLech_human      --GNGSERTCCPVNWVEHERSCYWFSSRSKAWADADNYCRLEDAHLVVVTSWEEQKFVQ-
seqLech_chicken    -----CGAQSQRQWEYFEGRCYFSLSRMSWHKAKAECEEMHSHLIIIDSYAKQNFVM-
seqLech_mouse      --GNGSERICCPINWVEYEGSCYWFSSVRPWTEADKYCQLENAHLVVVTSRDEQNFLO-
seqLeci_human      --SNGSQRTCCPVNWVEHQGSCYWFSSHGKAWAEAEKYCQLENAHLVVINSWEEQKFIV-
seqLeci_mouse      ----SNGTECCPVNWVEFGGSCYWFSSRDGLTWAEDQYCQLENAHLVINSREEQDFV-
seqMmgl_human      --NASTEGTCCPVNWVEHQDSCYWFSSGMSWAEAEKYCQLKNAHLVVINSREEQNFVQ-
seqMmgl_mouse      --NNGSEVACCPHWTHEHGSCYWFSSSEKSWPEADKYCLENLHVVVNSLEEQNFLO-
seqKucr_mouse      --TQNQVLQLIAQNWKYFNNGFYFSSRDKPPWREAEKFCSTSQGAHLASVTSQEEQAFV-
seq209_human       -AAVERLCHPCPWEWTFQGNCFMSNSQRNWHDSITACKEVGAQLVVIKSAAEQNFLO-
seq209A_mouse      -AGVDRLCRSCPWDWTFHQGSCYFFSVAQKSWNDSATACHNVGAQLVVIKSDEEQNFLO-
seq209B_mouse      -TEFLRLCRLCPWDWTFLLGNCYFFSKSQRNWINDAVTACKEVKAQLVIINSDEEQTFLO-
seq209C_mouse      -SQINRLCRPCPWDWTFVQGNCFYFFSKFQNWNSVNACRKLDAQLVVIKSDDEQSFLO-
seq209D_mouse      -AEVHDGLCQPCARDWTFNNGSCYFFSKSQRNWHNSTTACQELGAQLVIETDEEQTFLO-
seq209E_mouse      -SEVDRLCRLCPWDWTFNNGNCYFFSKSQRDWHDSTACKEMGAQLVVIKSHEEQSFLO-
                    . *           * : : *      * . : *      : : * : : * * :

```

```

seqLech_human      HHIGPVN-TWMGLHD--QNGPWKVVWDGTDYETGF--KNWRPEQPDDWYGHGLGGGEDCAH
seqLech_chicken    FRTRNER-FWIGLTDENQEGEWQVWDGTDTRS--SFTFWKEGEPNN-----RGFNEDCAH
seqLech_mouse      RHMGPLN-TWIGLTD--QNGPWKVVWDGTDYETGF--QNWRPEQPDNWWYGHGLGGGEDCAH
seqLeci_human      QHTNPFN-TWIGLTD--SDGSWKVVWDGTDYRHN--KNWAVTQPDNWHGHELGGSEDCVE
seqLeci_mouse      KHRSQFH-IWIGLTD--RDGSWKVVWDGTDYRSNY--RNWAFQPDNWWQHEQGGGEDCAE
seqMngl_human      KYLGSAY-TWMGLSD--PEGAWKVVWDGTDYATGF--QNWKPGQPDDWQGHGLGGGEDCAH
seqMngl_mouse      NRLANVV-SWIGLTD--QNGPWRVVWDGTFEKGFF--KNWAPLQPDNWFVGHGLGGGEDCAH
seqKucr_mouse      QTTSSGD-HWIGLTDQGTQTEGIWRVVWDGTFNNAQSKGFVWGNQPDNWR--HRNGEREDCVH
seq209_human       QSSRSNRFQWGLSDLNQEGTWQVWDGSPLLPSFK-QYWNRRGEPNNV-----GEEDCAE
seq209A_mouse      QTSKRGYTWGLIDMSKESTWYVWDGSPLLSFM-KYWSKGEPPNNL-----GEEDCAE
seq209B_mouse      QTSKAKGPTWGLSDLKKEATWLWVWDGSTLSSRFQ-KYWNRRGEPNNI-----GEEDCVE
seq209C_mouse      QTSKEKGYAWGLSDLKHEGRWVWDGSHLLFSFM-KYWNRRGEPNNE-----WEEDCAE
seq209D_mouse      QTSKARGPTWGLSDMHNEATWVWVWDGSPSPSFT-RYWNRRGEPNNV-----GDEDCAE
seq209E_mouse      QTSKKNSTWGLSDLNKEGEWVWLDGSPSLSFE-KYWKKGQPPNNV-----GGQDCVE
                    *:* *  :. * *:*: *  :*: :  :*:.
seqLech_human      FTDDGRWDDVCQRPYRWVCETELDK-ASQEPPLL-----
seqLech_chicken    VWTSGQWNDVYCTYECYVVECKPLPK-----
seqLech_mouse      FTTDGRWDDVCRRPYRWVCETKLDK-AN-----
seqLeci_human      VQPDGRWDDFCLOVYRWVCEKRRNA-TGEVA-----
seqLeci_mouse      ILSDGHWNDNFCQVNRWVCEKRRNI-TH-----
seqMngl_human      FHPDGRWDDVCQRPYHWVCEAGLQ-TSQE-----
seqMngl_mouse      ITTGGPWDDVCQRTFRWICEMKLAK-ES-----
seqKucr_mouse      VRQ--QWNDMACGSSYPWVCKKSTGW-SAAVVG-----
seq209_human       FSGNG-WNDDKCNLAKFWICKKSAAS-CSRDEEQFLSPAPATPNPPPA
seq209A_mouse      FRDDG-WNDTKCTNKKFWICKKLSST-CP SK-----
seq209B_mouse      FAGDG-WNDSKCELKFWICKKSATP-CTEG-----
seq209C_mouse      FRGDG-WNDAPCTIKKYWICKKSAMS-CTEK-----
seq209D_mouse      FSGDG-WNDLSCDKLLFWICKKVS'TSSCTTK-----
seq209E_mouse      FRDNG-WNDAKCEQRKFWICKKIATT-CLSKW-----
                    .      *** *  : * :

```

Figure 22: T-COFFEE alignment of Lech_human (ASGPR-1) with the same receptor in mouse (Lech_mouse, MHL-1) and chicken (Lech_chicken, ChHL-1) and in addition with homologous receptors on the surface of macrophages (Mngl_mouse, Mngl_human = CLE14_HUMAN), Kupffer cells (Kucr_mouse, Kucl_human not known) and dendritic cells (209A-E_mouse, 209_human). Identical amino acids are indicated with stars, similar amino acids with points. The sequence of the binding site is shaded in grey.

3.1.2 H1-CRD epitope prediction

The antigenicity, hydrophobicity and accessibility of amino acid residues were estimated and superimposed in plots to predict the putative epitope sequences of the H1-CRD.

The highest antigenicities were suggested for the amino acids 13-17, 26-31, 34-37 and 133-140, which lie outside of the binding site, but also for 91-98 and 109-120, which are positioned in the binding site of the H1-CRD. In these putative antigenic areas, the amino acid sequences are hydrophobic and accessible. This is especially true for amino acids 91-95 and 115-119 of the binding site, and these have therefore a good chance to be recognized as epitopes (see Figure 23).

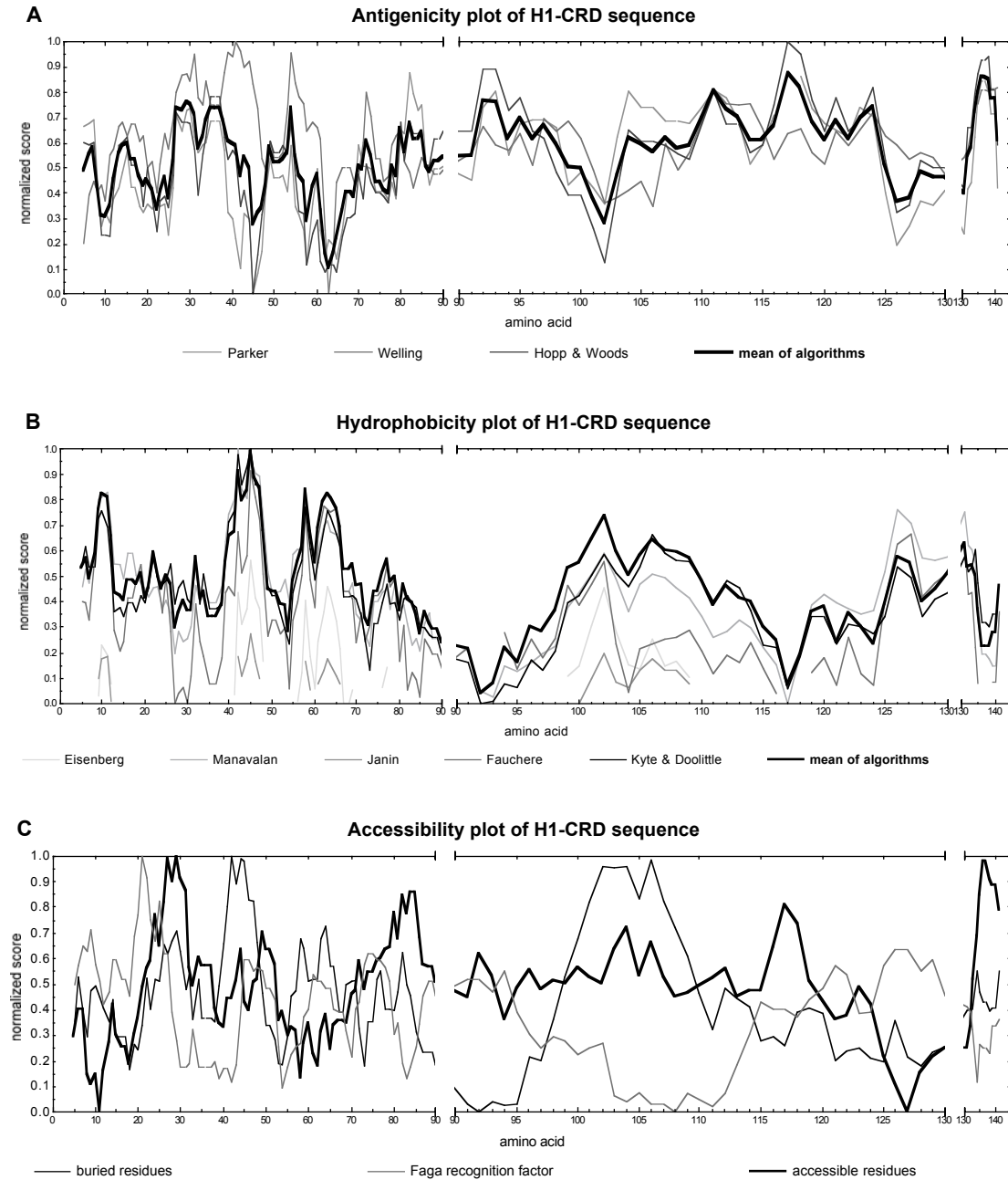


Figure 23: Epitope prediction using program ProScale (ExpASy, window 9, weighting 100%). Values of each score set were normalized (highest value 1.0, lowest value 0). The normalized score sets were superimposed to calculate the mean blot curve. A: Antigenicity algorithms from Woods *et al*, Parker and Welling. B: Hydrophobicity algorithms from Kyte *et al*, Janine, Manavalan and Fauchere. C: Accessibility algorithms.

3.2 Cloning, expression and purification of H1-CRD

Mg amounts of the H1-CRD were necessary for immunization first, and then for the screening and characterization of the obtained antibodies.

3.2.1 Preparative scale expression in *E.coli* JM109pET3H1

The yield of the H1-CRD, determined by Bradford assay, was very low with only 128-164µg/L JMpET3H1 culture in LB medium.

As a consequence, the antigen production has had to be optimized first. To reach a highly efficient H1-CRD production, four different *E.coli* expression strains and two vectors were tested first to identify an optimal production clone. In a second step, various conditions of the H1-CRD expression in the selected production clone were investigated and finally, the H1-CRD purification procedure was improved.

3.2.2 Optimization of the *E.coli* expression system

3.2.2.1 Plasmid pET3H1 expression system

The recombinant pET3b vector that codes for the H1-CRD cDNA (pET3H1) was amplified in the *E.coli* cloning strain JM109 prior to its transformation into DE3-lysogenic *E.coli* expression strains JM109(DE3), AD494(DE3) and Rosetta-gami(DE3)TM.

The selected clones of all pET3H1 plasmid-transformed strains JMpET3H1, ADpET3H1 and RGPET3H1 were controlled by standard PCR and by restriction digest with *Nde* I and *Bam*H I to confirm the correct integrity of the pET3H1.

In standard PCR, a 450bp fragment that corresponds to the 447bp cDNA of H1-CRD was specifically amplified from the plasmid DNA of all picked clones (see Figure 24A).

The undigested plasmid DNA of JMpET3H1 and ADpET3H1 clones showed the two fragments of the not linearized circular and the supercoiled pET3H1 plasmid of approximately 5'000bp. The plasmid DNA of RGPET3H1 clones resulted in four bands, which derived from unlinearized circular and supercoiled forms of pET3H1 and pRARE.

In the single digest with *Nde* I, the plasmid DNA of clones from all *E.coli* strains was linearized to the 5'054bp fragment of the pET3H1. In the double digest with *Nde* I and *Bam*H I, the plasmid was further cut into the 447bp H1-CRD cDNA fragment and the 4'607bp fragment of the pET3 vector. For RGPET3H1 clones, the additional fragments of

4'700bp in the single and of 1'000bp and 3'700bp in the double digest were found. These originated from pRARE (see Figure 24B).

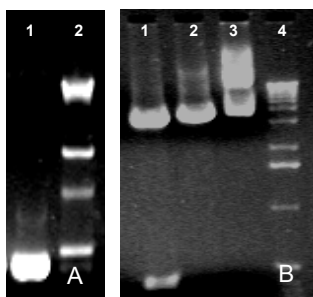


Figure 24: Transformation control of clones from *E. coli* JMpET3H1 (not shown), ADpET3H1 and RgpET3H1 (not shown) on ethidium-stained agarose-gels. A: Standard PCR. The DNA was 10-1000 times diluted for the amplification with primers H1fw and H1bw and the *Taq* DNA polymerase or *Taq* / *Pfu* DNA polymerases. Amplified fragment (1) and marker (2) B: Restriction digest. The single digest of pET3H1 with *Nde* I (2) should result in the 5'054bp fragment of linearized pET3H1 and for double digest with *Nde* I and *Bam*H I (1) in fragments of 447bp and 4'607bp. The undigested circular and supercoiled plasmid DNA (3) and the marker (4).

The standard PCR as well as the restriction digest confirmed the correct transformation of the clones and therefore provided three different pET3H1 expression systems: the JMpET3H1, the ADpET3H1 and the RgpET3H1.

3.2.2.2 Plasmid pEZZ18H1 expression system

Two strategies for cloning the H1-CRD cDNA into the multiple cloning site of vector pEZZ18 were tried: a 3'-blunt / 5'-blunt-ended ligation and a 3'-sticky / 5'-blunt-ended ligation. Both should result in a recombinant pEZZ18H1 plasmid, which carries the H1-CRD cDNA in the correct open reading frame and contains the restriction sites of *Nde* I and *Bam*H I, followed by two stop codons. Only in the 3'-blunt / 5'-blunt-ended ligation, the cDNA can be ligated in inverse orientation.

The H1-CRD cDNA was amplified using *Pfu* DNA polymerase and was ligated 3'-blunt / 5'-blunt-ended into the *Sma* I-digested and dephosphorylated pEZZ18. For 3'-sticky / 5'-blunt-ended ligation, the amplified H1-CRD cDNA was cut with *Bam*H I prior to its introduction into the *Sma* I and *Bam*H I double-digested and dephosphorylated pEZZ18 vector. Both recombinant plasmids were transformed into the *E. coli* cloning host JM109 and the *E. coli* expression and cloning host Top10.

All clones were screened by colony PCR using *Taq* DNA polymerase and two different primer pairs: the presence of the cDNA was confirmed with cDNA-specific primers H1fw and H1bw, whereas the orientation of the cDNA was verified with the cDNA-specific primer H1fw combined with the plasmid-specific primer M13 standard. The amplification

of the H1-CRD cDNA failed for all clones. Therefore, it was presumed, that JM109 and Top10 were transformed with recircularized original pEZZ18.

This was confirmed by the restriction digest of the plasmid DNA using *Nde* I. The recombinant pEZZ18H1 should result in three fragments of 459bp, 1465bp and 3118bp, but only two fragments of 450bp and 4100bp were obtained, identical to the *Nde* I-digested pEZZ18 vector (458bp, 4133bp).

In the context of the promising results with pET3H1 transformants, the strategy of this expression system was no longer pursued.

3.2.2.3 Selection of a high expressing *E.coli* production clone

The different clones of JMpET3H1, ADpET3H1 and RGpET3H1 were cultured in LB and TB medium, containing antibiotics and 1% glucose. The expression of H1-CRD was induced with 1mM IPTG.

On a reducing SDS-PAGE gel, the total cell proteins were compared prior to after 5h expression. An additional huge orange 17kDa band of the H1-CRD was observed for clones of ADpET3H1, especially for ADpET3H1.4. Only a weak additional band was visible for clones of RGpET3H1, but none was detected for clones of JMpET3H1. For all five clones, no H1-CRD was present in the expression culture media (see Figure 25).

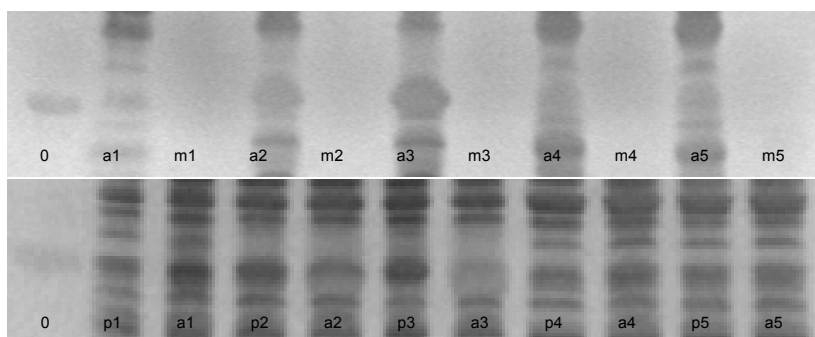


Figure 25: Silver-stained reducing SDS-PAGE gel 15 % of the TCA / acetone precipitated total proteins from clones of JMpET3H1, ADpET3H1 and RGpET3H1. Total TB medium proteins (m) and total pellet proteins prior (p) and after (a) 5h expression. H1-CRD (0) and clones JMpET3H1.1 (1), ADpET3H1.1 (2), ADpET3H1.4 (3), RGpET3H1.2 (4), RGpET3H1.3.

The high expression level of ADpET3H1.1 and ADpET3H1.4 was confirmed by the purification of the H1-CRD from 200ml expression cultures according to the method of Meier *et al.*²⁶ The yields, determined by Bradford assay, were excellent for both clones, but was substantially higher for ADpET3H1.4 with 1450µg/L compared to 250µg/L culture for ADpET3H1.1.

3.2.2.4 Sequence verification of the H1-CRD

Plasmid DNA sequencing and H1-CRD MS was used to verify, that the selected clone ADpET3H1.4 expresses correct full-length H1-CRD.

Plasmid pET3H1 verification by DNA sequencing

The plasmid DNA of clone ADpET3H1.4 was sequenced, starting with primer T7 for the plus strand and with primer T7term for the minus strand determination. The 583 bases sequence of the plus strand overlapped with the 417 bases sequence of the minus strand in all 417 bases. Both strands contained one uncertain nucleotide, but these were unequivocal defined by the overlap with the complementary strand.

```

PET3H1.4: 39  ggctcagaaaggacctgctgcccgggtcaactgggtggagcagcagcgcagctgctactgg 98
  |||
ASGPR-1: 614  ggctcagaaaggacctgctgcccgggtcaactgggtggagcagcagcgcagctgctactgg 673

PET3H1.4: 99  ttctctcgctccgggaaggcctgggctgacgccgacaactactgccggctggaggacgcg 158
  |||
ASGPR-1: 674  ttctctcgctccgggaaggcctgggctgacgccgacaactactgccggctggaggacgcg 733

PET3H1.4: 159  cacctggtggtggtcacgtcctgggaggagcagaaatttgtccagcaccacatagggcct 218
  |||
ASGPR-1: 734  cacctggtggtggtcacgtcctgggaggagcagaaatttgtccagcaccacatagggcct 793

PET3H1.4: 219  gtgaacacctggatgggctccacgacaaaacgggccctggaagtgggtggacgggacg 278
  |||
ASGPR-1: 794  gtgaacacctggatgggctccacgacaaaacgggccctggaagtgggtggacgggacg 853

PET3H1.4: 279  gactacgagacgggctcaagaactggaggccggagcagccggacgactggtacggccac 338
  |||
ASGPR-1: 854  gactacgagacgggctcaagaactggaggccggagcagccggacgactggtacggccac 913

PET3H1.4: 339  gggctcggaggaggcaggactgtgccacttcaccgacgacggccgctggaacgacgac 398
  |||
ASGPR-1: 914  gggctcggaggaggcaggactgtgccacttcaccgacgacggccgctggaacgacgac 973

PET3H1.4: 399  gtctgccagaggccctaccgctgggtctgcgagacagagctggacaaggccagccaggag 458
  |||
ASGPR-1: 974  gtctgccagaggccctaccgctgggtctgcgagacagagctggacaaggccagccaggag 1033

PET3H1.4: 459  ccacctctcctttaat 474
  |||
ASGPR-1: 1034  ccacctctcctttaat 1049

```

Figure 26: Blastn (NCBI, matrix 1-3) alignment of the plus strand sequence of the pET3H1 sequencing, searching databases Genbank, EMBL, DDJ, and PDB. The identity was 436/436 nucleotides (strand plus/plus) to the published sequence of the asialoglycoprotein receptor 1 with ID [HUMASGPR1] (1277bp, human asialoglycoprotein receptor H1 mRNA, complete cds).

The plus strand sequence of pET3H1 was identical to the published sequence by Meier *et al.*²⁶ and confirmed ADpET3H1 to encode correct H1-CRD (see Figure 26).

H1-CRD sequence verification by Mass Spectrometry

The translated positive strand sequence of pET3H1 plasmid (see Figure 26) aligned with the H1-CRD sequence proved the correct coding of pET3H1 in ADpET3H1.4. They were 100% identical over the entire 144 amino acids sequence of the H1-CRD in blastp (see Figure 27).

```

PET3H1:      2  GSERTCCPVNWVEHERSCYWFSRSGKAWADADNYCRLEDAHLVVVTSWEEQKFVQHHIGP  61
                GSERTCCPVNWVEHERSCYWFSRSGKAWADADNYCRLEDAHLVVVTSWEEQKFVQHHIGP
ASGPR-1: 148  GSERTCCPVNWVEHERSCYWFSRSGKAWADADNYCRLEDAHLVVVTSWEEQKFVQHHIGP  207

PET3H1:      62  VNTWMGLHDQNGPWKWDGTDYETGFKNWRPEQPDDWYGHGLGGGEDCAHFTDDGRWNDD  121
                VNTWMGLHDQNGPWKWDGTDYETGFKNWRPEQPDDWYGHGLGGGEDCAHFTDDGRWNDD
ASGPR-1: 208  VNTWMGLHDQNGPWKWDGTDYETGFKNWRPEQPDDWYGHGLGGGEDCAHFTDDGRWNDD  267

PET3H1:     122  VCQRPYRWVCETELDKASQEPPLL  145
                VCQRPYRWVCETELDKASQEPPLL
ASGPR-1: 268  VCQRPYRWVCETELDKASQEPPLL  291

```

Figure 27: Blastp (NCBI, matrix BLOSUM62) alignment of the translated plus strand sequence of the pET3H1 sequencing, searching databases non-redundant Genbank cds. The identity was 100% (144/144 residues) with 0% (0/144 residues) gaps in the alignment with sp |P07306| (291residues, human asialoglycoprotein receptor H1).

The calculated monoisotopic molecular weight (ProtParam, ExPASy) of the H1-CRD with a starting Met is 16991.5Da when all 7Cys are reduced or is 16985.5Da when 6 Cys are involved in disulfide bridges. Without the first Met, a molecular weight of 16860.3Da with reduced Cys and of 16854.3.6Da for the H1-CRD with 3 S-S bonds is calculated.

In the ESI-FT-ICR, a mass of 16930.3Da was measured. The difference to the calculated mass, when the starting Met missed and 3 S-S bonds were formed, was +76Da. Due to the elemental composition and the use of β -mercaptoethanol for reduction during H1-CRD purification, it was supposed, that one β -mercaptoethanol molecule was linked to the free Cys (see Figure 28).

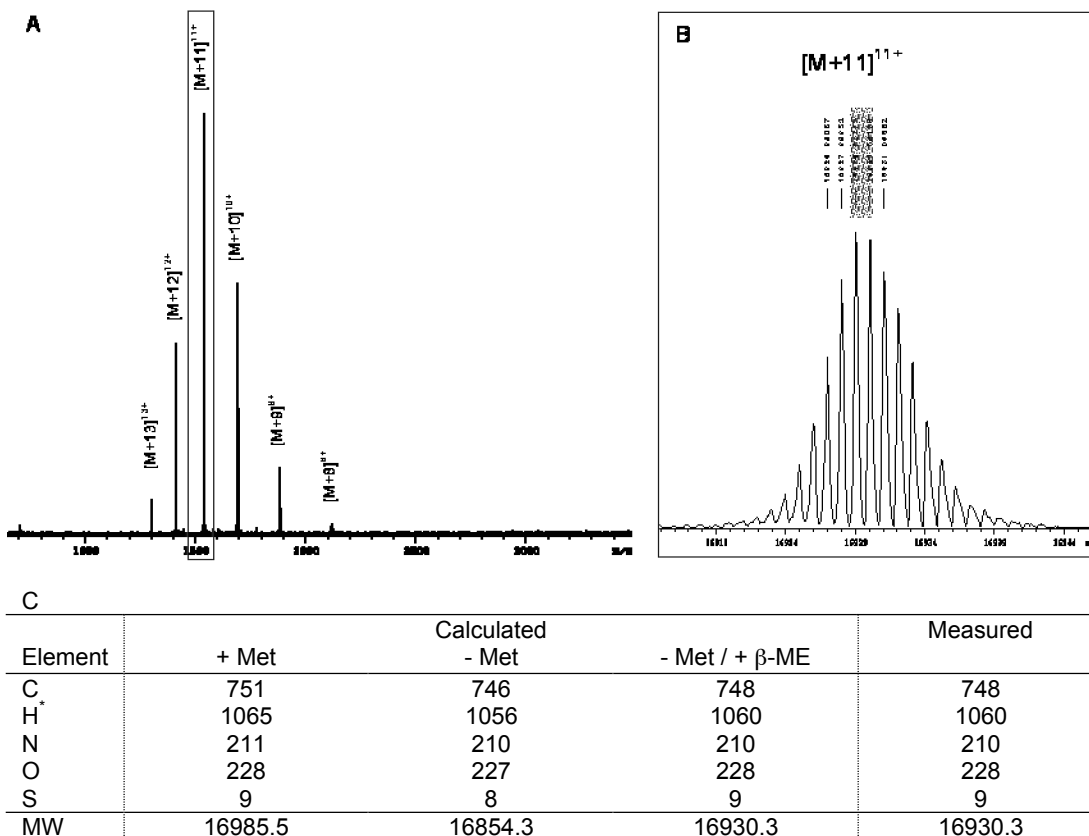


Figure 28: ESI-FT-ICR of the H1-CRD, produced in ADpET3H1.4. A: Spectrum prior to deconvolution. B: Deconvoluted spectrum. C: Molecular mass of the H1-CRD, calculated with ProtParam (ExpASY) and measured by ESI-FT-ICR.

In addition, native and reduced alkylated H1-CRD was digested with trypsin and its fragments were measured by MALDI-FT-ICR. Except for fragments F1 (residues 1-5), F4 (residues 25-27) and F12 (residues 138-145), all expected fragments were found. The three missing fragments were the smallest with molecular weights of 291.166 - 854.462Da.

Two disulfide bridges were identified, which linked Cys⁷-Cys⁸ and Cys³⁶-Cys¹³¹. The third S-S bond, linking Cys¹⁰⁹-Cys¹²³ was not detectable. Probably, this double fragment of 4719.993Da was too large for the detection in this measurement mode (see Figure 29).

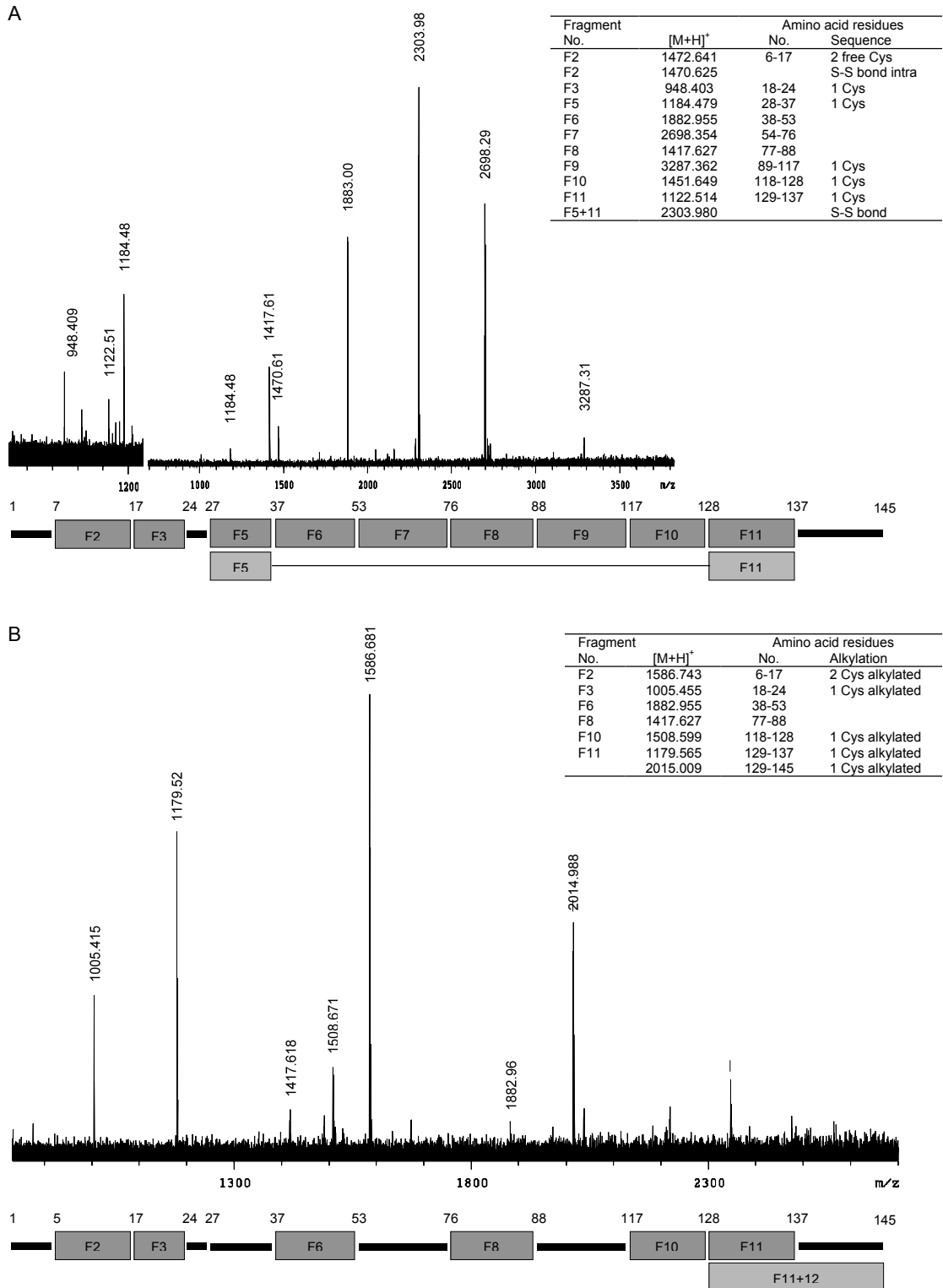


Figure 29: MALDI-FT-ICR of the H1-CRD, produced in ADpET3H1.4. Spectra, tables and schematic diagrams of found fragments are shown. A: Native H1-CRD, digested with trypsin. B: Reduced alkylated H1-CRD, digested with trypsin.

3.2.3 Optimization of expression conditions

ADpET3H1.4 was cultured in the two media, LB and TB, containing antibiotics and glucose 1%. The expression was induced at six cell densities of OD₆₀₀ of 1 - 6 with three IPTG concentrations in the range of 0.2mM - 0.8mM and was run for a period of 9h. During growth and expression, temperature and shaking were kept at 37°C and 300rpm.

3.2.3.1 IPTG concentration and expression period in *E.coli* ADpET3H1.4

The expression of the H1-CRD in ADpET3H1.4, which was cultured in 50ml TB medium, was not induced or was induced with 0.2mM, 0.4mM or 0.8mM IPTG at an OD₆₀₀ of 1.

During growth and expression, the OD₆₀₀ and pH monitoring showed, that after a lag phase of less than 50min, ApET3H1.4 grew with a mean doubling time of 46.2min until an OD₆₀₀ of about 5-6, and then entered the stationary phase, with a plateau at OD₆₀₀ of about 8. When the H1-CRD was induced, the growth of ADpET3H1.4 immediately stopped. The OD₆₀₀ even slightly decreased in the first 5h after induction, but then started a second slower growth phase with a mean doubling time of 140min.

The transition from log phase to stationary phase in the not induced ADpET3H1.4 culture was accompanied by a decrease of the pH to 4.5, whereas in induced cultures, the pH remained constantly at pH 7.5 (see Figure 30).

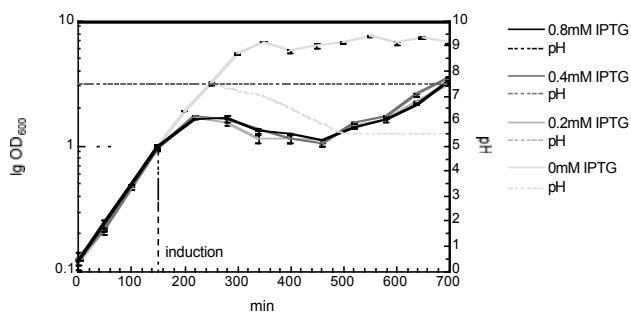


Figure 30: Growth and pH curve of ADpET3H1.4 during growth and expression phase. The H1-CRD expression was induced with 0mM, 0.2mM, 0.4mM or 0.8mM IPTG at an OD₆₀₀ of 1.

On a reducing SDS-PAGE gel, the total cell proteins of ADpET3H1.4 before to during expression were compared. The gel showed, that the H1-CRD was not baseline-produced preliminary to the induction. No significant 17kDa band was detected for not induced ADpET3H1.4. In contrast, for induced ADpET3H1.4, the additional 17kDa band of H1-CRD appeared with increasing intensity during the first 3h of the expression, and then remained constant until 5-6h after induction. In the following 3h till the end of the

expression, the intensity of the 17kDa band decreased, while simultaneously the bands of other cell proteins became more prominent. This is in agreement with the up going OD_{600} . No H1-CRD was detected in the concentrated media of the expression cultures (see Figure 31).

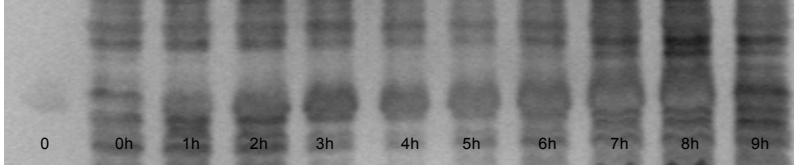


Figure 31: Silver-stained reducing SDS-PAGE gel 15% of precipitated and concentrated total cell proteins from ADpET3H1.4 prior to (0h) and after 1-9h expression and of pure H1-CRD (0).

The intensity of the H1-CRD band was slightly stronger for ADpET3H1.4 induced with 0.4mM, compared to 0.2mM and 0.8mM.

In conclusion, the highest H1-CRD yield was obtained when the H1-CRD expression was induced with 0.4mM IPTG and was run for 5h.

3.2.3.2 ADpET3H1.4 cell density at induction time

The expression of the H1-CRD in ADpET3H1.4 TB cultures was induced with 0.4mM IPTG at different OD_{600} of 1, 2, 3, 4 and 5 during log phase and at an OD_{600} of 5.5 after the exponential growth phase.

The OD_{600} measurement confirmed the same growth behavior of ADpET3H1.4 as described in the previous section, with a first log phase, followed by the plateau phase after induction and a second growth phase. However, when induced at an OD_{600} of 3 or higher, the pH decreased down to 6.5 during expression (see Figure 32).

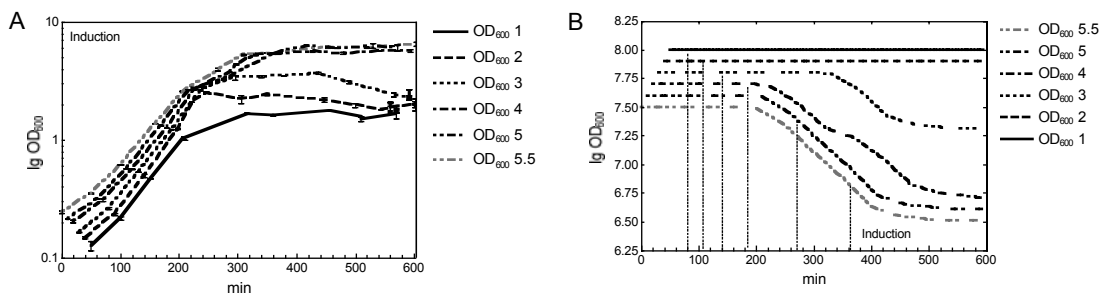


Figure 32: Growth of, and H1-CRD expression in *E.coli* production clone ADpET3H1.4. Cell densities (A) and pH (B) were compared during growth and expression, inducing with 0.4mM IPTG at OD_{600} of 1 - 6.

To sum up, the H1-CRD expression was optimal when started at a cell density of below an OD_{600} of 3.

3.2.3.3 Growth medium of ADpET3H1.4

ADpET3H1.4 was cultured in LB and TB medium with or without glucose 1%. The expression of the H1-CRD was not induced or induced with 0.4mM IPTG.

The OD₆₀₀ measurement showed, that the doubling time in TB medium was shorter than in LB medium, with calculated doubling times of 44.4min compared to 50.8min. Furthermore, the stationary phase was reached at a higher OD₆₀₀ of 5 in TB medium compared to LB (see Figure 33A).

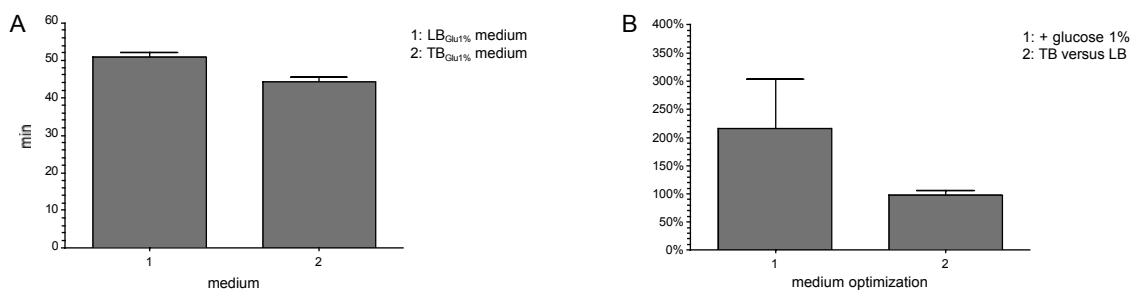


Figure 33: A: Doubling times of ADpET3H1.4 in LB or TB medium, containing glucose 1%. The doubling time was 50.8min (SEM 1.2min) in LB and 44.3min (SEM 1.3min) in TB medium, calculated using nonlinear regression fit (equation exponential growth). B: H1-CRD yield in ADpET3H1.4 TB and LB cultures with or without glucose 1%. Compared to LB medium, the yield in TB medium was 98.2% (SEM 6.2%) and in LB medium with 1% glucose 214.4% (SEM 88.2%).

When H1-CRD expression was induced at the same OD₆₀₀, no difference in the yields was detected on a reducing SDS-PAGE gel. But the addition of 1% glucose seemed to have a variable, but positive effect onto the H1-CRD yield (see Figure 33B).

3.2.4 Optimization of purification procedures

The H1-CRD location within the bacterial cell was identified first. Dependent on this, the purification procedure was adapted and optimized.

3.2.4.1 Identification of the H1-CRD localization in *E.coli* ADpET3H1.4

An ADpET3H1.4 culture, which was induced with 0.4mM IPTG at an OD₆₀₀ of 1 after 5h expression, was split into the medium, the periplasmic, the soluble cytoplasmic and the insoluble cytoplasmic fraction.

A reducing SDS-PAGE gel showed, that the 17kDa H1-CRD band was only present in the insoluble cytoplasmic fraction and as intense as in the total cell proteins. Therefore, the H1-CRD is exclusively present in the form of inclusion bodies (see Figure 34).

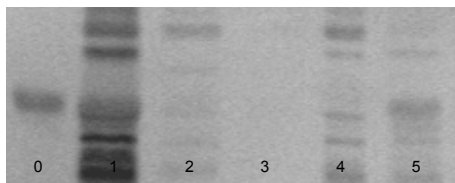


Figure 34: Silver-stained reducing SDS-PAGE gel 15% of fractions from an ADpET3H1.4 expression culture. Concentrated (equivalent / normalized to the same culture volume) total proteins of the medium (2) and the pellet (1) with its fractions: periplasmic (3), soluble cytoplasmic (4) and insoluble cytoplasmic fraction (5).

3.2.4.2 Renaturation and affinity chromatography of the H1-CRD

The H1-CRD was expressed for 5h in 500ml ADpET3H1.4 LB cultures, containing 1% glucose, after induction with 0.4mM IPTG at an OD_{600} of 1. Harvested cultures were combined and split to three equal aliquots to get the same starting material for all purification procedures.

The inclusion body proteins were solubilized in three parallel procedures: the “fast dilution” (FD) method, the “non fast dilution” (NFD) method and the “inclusion body” (IB) method. Obtained denatured and reduced proteins of each procedure were split into two equal aliquots: proteins of the FD and NFD portions were refolded in the two refolding systems, A and C (FD_A , NFD_A , FD_C , NFD_C), and proteins of the IB portions were renatured in two other refolding systems, B and D (IB_B , IB_D). The buffer compositions differed in the content of glycerol, reductant DTT and reshuffling glutathione. The portions of refolded H1-CRD were separately extracted by Gal-Sepharose affinity FPLC.

The FD solubilization in combination with refolding system A (FD_A) was identical to the published method by Meier *et al.*²⁶

3.2.4.2.1 Denaturation and reduction by the FD, NFD and IB method

On a silver-stained reducing SDS-PAGE gel, no H1-CRD was detected in the FD-solubilized pellets of the clearing ultracentrifugation after solubilization and after refolding. The same band pattern was obtained for NFD-solubilized pellets, on a PAGE gel. The IB solubilization showed traces of H1-CRD in inclusion body washes. Furthermore, the ultracentrifugation pellets after reductive denaturation and after refolding were almost pure H1-CRD.

3.2.4.2.2 Refolding in buffer systems A to D

The protein solutions prior to refolding differed in the content of reductant and denaturing agents. The concentration was lower for FD-treated than for NFD-treated proteins.

Furthermore, the protein concentrations varied, whereas the highest was determined in the lysate solution after FD solubilization and lowest after IB solubilization. The volume of the FD lysate solution was 1.3-fold smaller compared to the NFD and the IB lysate solution. As a consequence, the buffer exchange rate and the dilution rate of reducing and denaturing agents during refolding were not identical, when dialyzing against the same volume of refolding buffer (see Table 8).

Table 8: Final concentration of additives to the basic refolding buffer (20mM TrisHCl (pH7.5), 0.5M NaCl, 25mM CaCl₂) after 6 refolding steps.

Method	Buffer system	dilution step	Dilution in total	Concentration of additives, denaturants and reductants	
				Refolding start	Refolding end
FD	A and C*	8.4	$5.3 \cdot 10^5$ (8.4^6)	2M urea 0.01% β -mercaptoethanol	$5.7 \cdot 10^{-6}$ M urea $2.8 \cdot 10^{-8}$ % β -mercaptoethanol 1mM GSH / 0,2mM GSSG* 0.4% glycerol*
NFD	A and C*	6.3	$6.3 \cdot 10^4$ (6.3^6)	4.8M urea 0.02% β -mercaptoethanol	$7.6 \cdot 10^{-5}$ M urea $3.2 \cdot 10^{-7}$ % β -mercaptoethanol 1mM GSH / 0,2mM GSSG* 0.4% glycerol*
NFD	A and C*	6.3	$6.3 \cdot 10^4$ (6.3^6)	4.8M urea 2mM DTT	$7.6 \cdot 10^{-5}$ M urea $3.2 \cdot 10^{-5}$ mM DTT 1mM GSH / 0,2mM GSSG* 0.4% glycerol*
IB	B and D*	6.4	$6.9 \cdot 10^4$ (6.4^6)	8M urea 1mM DTT	$1.2 \cdot 10^{-4}$ M urea $1.5 \cdot 10^{-5}$ mM DTT 1mM GSH / 0,2mM GSSG 0.4% glycerol*

$$\frac{\text{dilution}}{\text{step}} = \frac{(V_{\text{lysate}} + V_{\text{buffer}})}{V_{\text{lysate}}}; \quad \text{dilution in total} = \left(\frac{\text{dilution}}{\text{step}} \right)^{\text{numberofsteps}}$$

During the first refolding step, considerable amounts of proteins precipitated in the FD_A and the FD_C solution. The same happened in the NFD_A and the NFD_C solution, when proteins had been reduced with DTT for solubilization before. In contrast, in the IB_B and the IB_D solution and in the NFD_A and the NFD_C solution, when reduced with β -mercaptoethanol before, just about no precipitate was formed. Additionally, a more than 8 times dilution in less than 10h also provoked protein precipitation. If no precipitate occurred in the first refolding step, no precipitate formed during the following steps.

3.2.4.2.3 Affinity chromatography

The refolded active H1-CRD was extracted from the different solutions, i.e. the FD_A, the FD_C, the NFD_A, the NFD_C, the IB_B and the IB_D, by affinity to the Gal-Sepharose. Volumes, equivalent to the same volume of ADpET3H1.4 expression culture were applied to the column in one run.

Yield

The comparison of the areas under the elution peak clearly showed, that the yield of the FD-renatured H1-CRD was significantly lower than of the NFD and IB-renatured H1-CRD (see Figure 35).

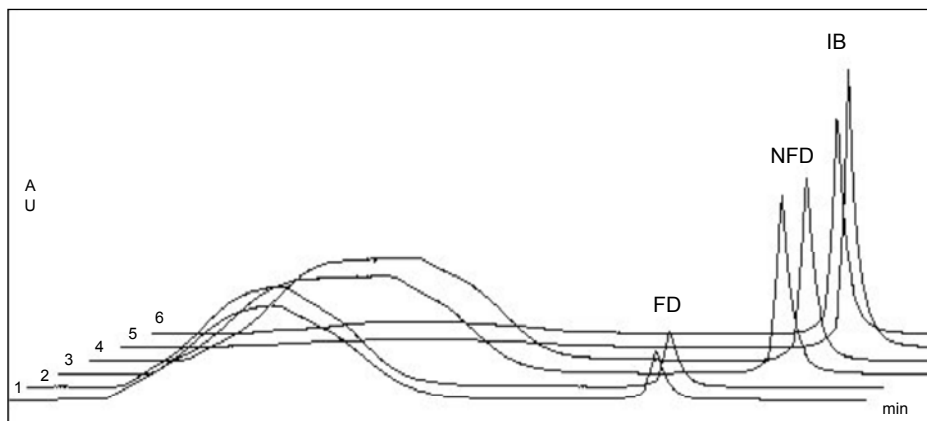


Figure 35: Overlay of Gal-Sepharose FPLC chromatograms. The volumes of FD_A (1), FD_C (2), NFD_A (3), NFD_C (4), IB_B (5) and IB_D (6) equivalent to 100ml ADpET3H1.4 expression culture were applied to the 10ml Gal-Sepharose column.

This agreed with the analysis on reducing SDS-PAGE gels and with the quantification of the eluted H1-CRD by Bradford assay.

In the FD-derived H1-CRD, the 17kDa H1-CRD band not only appeared in the elution, but also significantly in the flow through. Comparing the amount of H1-CRD in the flow through to the amount in the protein solution prior to FPLC, a substantial portion of the H1-CRD was inactive. In contrast, the NFD-derived H1-CRD was mainly active. The intense 17kDa band was visible in the elution, while only traces were detected in the flow through. Similarly, the IB-derived H1-CRD was predominantly present in the elution. In the flow through, only a minor portion of inactive H1-CRD remained and almost no other proteins were present due to the inclusion body wash prior to reduction (see Figure 36).

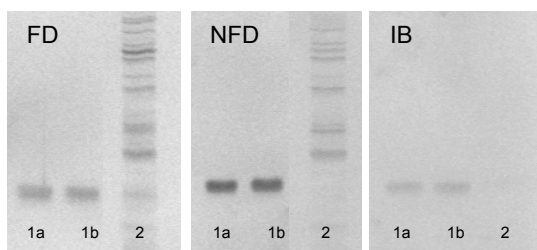


Figure 36: Silver-stained reducing SDS-PAGE gel 15% of the H1-CRD purification following six different procedures: three denaturation methods FD, NFD and IB in combination with refolding buffer systems A and C or B and D showing raising (a) and falling (b) fraction of the elution peak (1) and column flow through (2).

The IB methods provided the highest yields of active H1-CRD with 22mg/L ADpET3H1.4 culture followed by the NFD methods with similar yields of 20mg/L. Only half of this yielded the FD methods with 11mg/L in mean (see Figure 37).

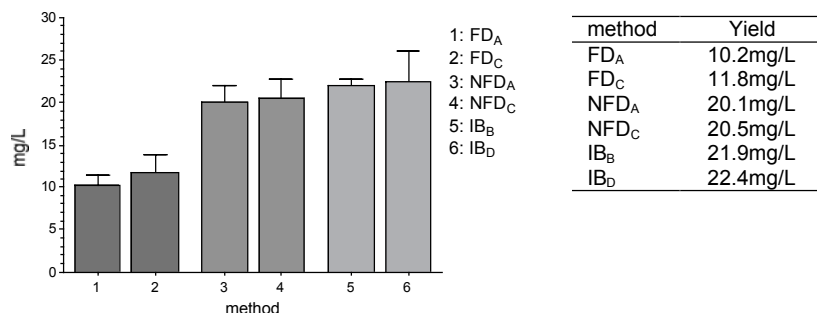


Figure 37: Comparison of the H1-CRD yields from an ADpET3H1.4 expression culture, derived after purification following the six different procedures. FD_A yielded 10.2mg/L (SEM 1.2mg/L), FD_C 11.8mg/L (SEM 2.2mg/L), NFD_A 20.1mg/L (SEM 2.0mg/L), NFD_C 20.5mg/L (SEM 2.2mg/L), IB_B 21.9mg/L (SEM 0.7mg/L) and IB_D 22.4mg/L (SEM 3.6mg/L).

Purity

The reducing and non-reducing SDS-PAGE gel confirmed the high purity of the active H1-CRD independent of the used purification method.

Interestingly, the conformity of the active H1-CRD was only fairly dependent on the denaturation method, but was significantly influenced by the used refolding system. When H1-CRD was refolded in the refolding system A (FD_A and NFD_A) double bands of 14kDa and 17kDa for monomeric species and of 28kDa and 34kDa for dimeric species were visible. In contrast, when refolded in the other refolding systems (FD_C, NFD_C, IB_B and IB_D) monomeric and dimeric H1-CRD only appeared as a single band of 17kDa and 34kDa, respectively (see Figure 38).

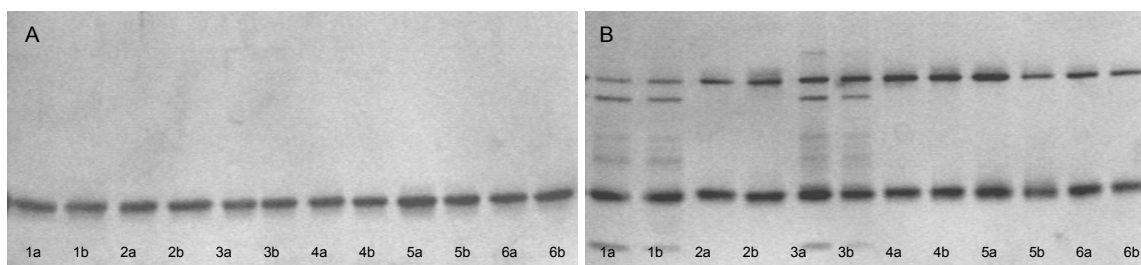


Figure 38: Silver-stained reducing (A) and non-reducing (B) SDS-PAGE gel 15% of the H1-CRD, eluted from the Gal-Sepharose affinity column, showing the protein of the rising (a) and falling (b) peak. Comparison of the six purification procedures: FD_A (1), FD_C (2), NFD_A (3), NFD_C (4), IB_B (5) and IB_D (6).

Furthermore, the H1-CRD, which was derived from the different renaturation procedures, varied in the ratio of monomeric to dimeric H1-CRD. The portion of dimeric species was highest for the FD-treated and lowest for the IB-treated H1-CRD.

3.2.4.2.4 Effect of reductants

The NFD solubilization was performed using the two reductants β -mercaptoethanol (NFD $_{\beta\text{-ME}}$) and DTT (NFD $_{\text{DTT}}$). Unexpectedly during refolding, the NFD $_{\beta\text{-ME}}$ -derived proteins remained soluble in the form of a slightly turbid solution, while the NFD $_{\text{DTT}}$ -treated proteins precipitated nearly quantitatively.

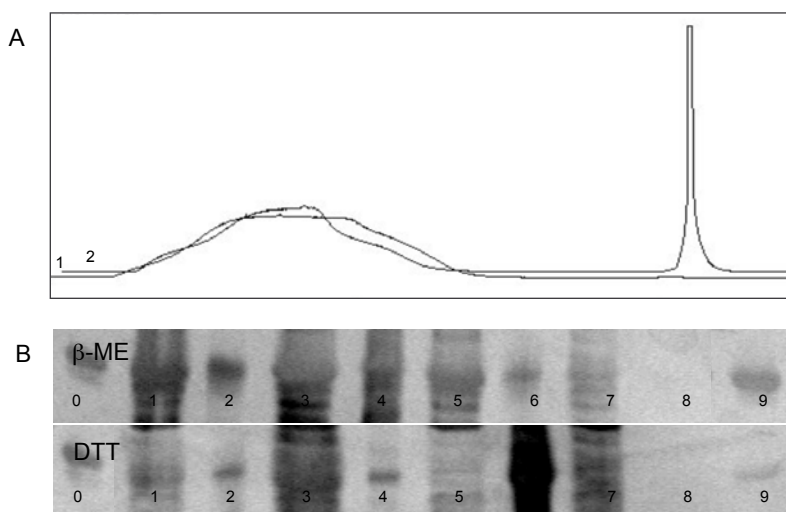


Figure 39: A: Overlay of Gal-Sepharose FPLC chromatograms of the NFD $_{\beta\text{-ME}}$ (2) and NFD $_{\text{DTT}}$ (1) derived H1-CRD. B: Silver-stained reducing SDS-PAGE gel 15% of the NFD $_{\beta\text{-ME}}$ and NFD $_{\text{DTT}}$, showing pure H1-CRD reference (0), cleared protein solution (1) and pellet (2) prior to dilution, cleared protein solution (3) and pellet (4) prior to refolding, cleared protein solution (5) and pellet (6) after refolding, column flow through (7), wash (8) and elution fractions (9-12).

In the Gal-Sepharose extraction almost no H1-CRD elution peak was detected for NFD $_{\text{DTT}}$, but an immense peak for NFD $_{\beta\text{-ME}}$ appeared. The reducing SDS-PAGE gel confirmed, that the precipitate of the NFD $_{\text{DTT}}$ refolding almost uniquely consisted of H1-CRD. As a consequence, only traces of H1-CRD were detected in the cleared protein solution after refolding and in the elution (see Figure 39).

3.2.4.2.5 Control of Gal-Sepharose binding specificity

The purified active H1-CRD clearly bound to Gal-Sepharose and did not elute until EDTA was added. In contrast, the H1-CRD not interacted with blank Sepharose. No elution peak was detected and therefore, the binding of the H1-CRD was proved to be specific for galactose (see Figure 40).

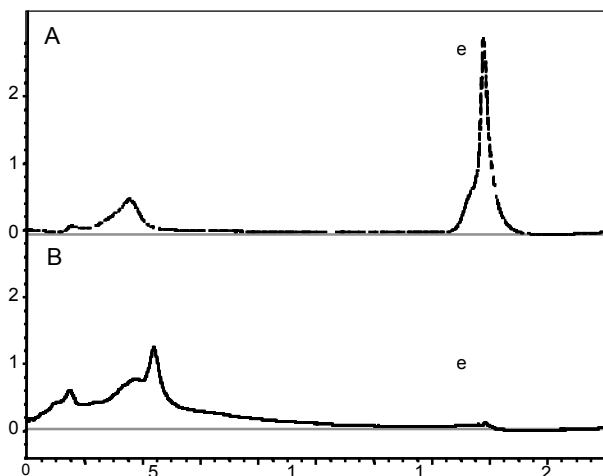


Figure 40: HPLC chromatograms of the H1-CRD binding to Gal-Sepharose (A) and to blank Sepharose (B) with elution peak (e).

To sum up, the highest yield was achieved, when the H1-CRD was expressed for 5h in an ADpET3H1.4 TB or LB culture with glucose 1%, after induction with 0.4mM IPTG at an OD_{600} below 3. The active H1-CRD, which accumulated in the form of inclusion bodies, was most successfully purified, when the proteins were denatured by the NFD method and were refolded in the buffer systems A or C before the H1-CRD was extracted by affinity to Gal-Sepharose.

3.2.5 Preparative scale expression in *E.coli* ADpET3H1.4

The expression conditions were optimized for 50ml cultures. Adaptations during scale up were not necessary. Stepwise scale up, starting with 200ml and going up to 500ml culture volumes showed, that yields/L expression culture remained constant.

The preparative production of H1-CRD in ADpET3H1.4 was started in parallel to the optimization of the production. Therefore, the H1-CRD was purified, following partially optimized methods (see Table 9).

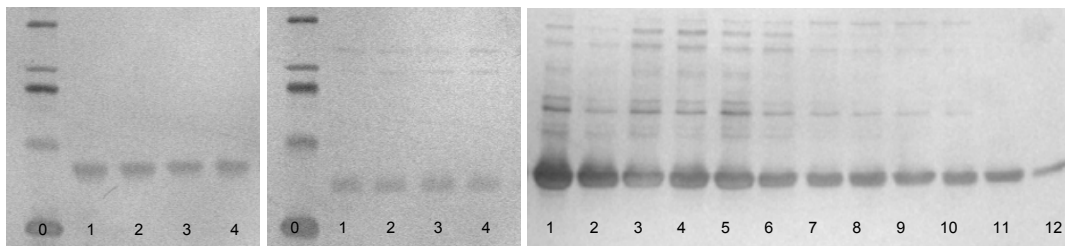


Figure 41: Silver-stained reducing SDS-PAGE gel 15% of the purified active H1-CRD after FPLC and concentrating by Centricon. Higher molecular bands than the 17kDa band were supposed to be due to incomplete reduction of the H1-CRD.

The reducing SDS-PAGE gel confirmed the high H1-CRD purity of all batches, after extraction by Gal-Sepharose FPLC (see Figure 41).

The H1-CRD yields after purification by the FD_A method were 0.9mg/L ADpET3H1.4 LB culture, 3.3mg/L LB culture with and 2.7mg/L TB culture with 1% glucose, determined by Bradford assay. After H1-CRD purification by the NFD_A method, higher yields of 5.9mg/L in LB with 1% glucose and of 6.1mg/L in TB with 1% glucose were obtained (see Table 9).

Table 9: Yields of the preparative expressions in JMpET3H1.4 and ADpET3H1.4, determined by Bradford assay.

Clone	Medium	Method	Culture	Yield/batch	Yield/L
JMpET3H1.4	LB	FD	15L	2.302mg	0.153mg/L
Total			15L	2.302mg	0.153mg/L
ADpET3H1.4	LB	FD	2L	1.827mg	0.914mg/L
	LB / 1% glucose	FD	6L	19.642mg	3.274mg/L
	LB / 1% glucose	NFD	5L	29.437mg	5.887mg/L
ADpET3H1.4	TB / 1% glucose	FD	0.5L	1.366mg	2.672mg/L
ADpET3H1.4	TB / 1% glucose	NFD	0.5L	3.080mg	6.160mg/L
Total			14L	55.352mg	3.954mg/L
Overall			29L	57.654mg	1.988mg/L

H1-CRD stability and storage

Periodically thawed and refrozen H1-CRD was compared to H1-CRD, which was continuously kept frozen. The silver-stained reducing SDS-PAGE gel showed the same band pattern, identical to the pattern prior to freezing. The H1-CRD was not degraded at -20°C and was not sensitive to repeated freezing.

3.2.6 Size exclusion chromatography

The purified active H1-CRD was applied to a Sephadex SEC column to remove traces of other proteins and to separate monomeric and dimeric H1-CRD. Interestingly, the SEC separation of the H1-CRD in buffer with 20mM calcium (SEC_{Ca}), no calcium (SEC₀) and 1mM EDTA (SEC_{EDTA}) produced completely different results (see Figure 42, Figure 43).

Buffer with 20mM calcium

In SEC_{Ca} buffer, only traces of protein eluted at the calculated time, but the main peak came, when the buffer was switched to water and the ionic strength approximated to zero. The non-reducing SDS-PAGE gel showed, that monomeric and dimeric H1-CRD eluted together.

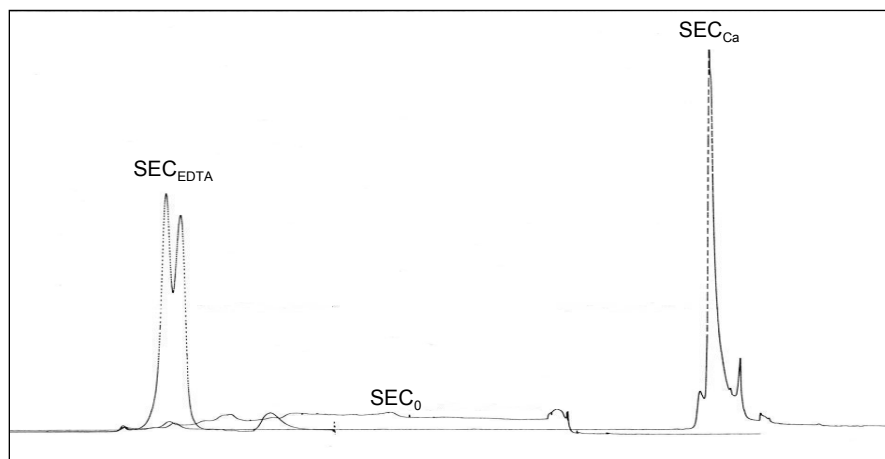


Figure 42: FPLC chromatograms of the SEC experiment using different buffers. The buffer of SEC_{Ca} contained 20mM calcium, the buffer of SEC₀ no calcium and the buffer of SEC_{EDTA} included 2mM EDTA. Determined elution times for dimeric and monomeric H1-CRD were 28min and 32min respectively. Recoveries of H1-CRD were 78% for the SEC_{Ca}, 87% for the SEC₀ and 80% for the SEC_{EDTA}.

Buffer without calcium

In SEC₀ buffer, the H1-CRD started to elute at the determined elution time. Several small peaks overlapped and eluted over a long period of time. The non-reducing SDS-PAGE gel confirmed, that all peaks were composed of monomeric and dimeric species of H1-CRD, but in different ratios. In peak 1, the 14kDa and the 28kDa bands of H1-CRD were visible together with traces of other proteins. Peaks 2-4 additionally showed the 17kDa and the 34kDa proteins and peak 5 only contained the 17kDa and the 34kDa proteins, expected for the H1-CRD.

Buffer with 1mM EDTA

In SEC_{EDTA} buffer, proteins eluted in one main, but incompletely separated double peak at the expected elution time. Additionally, two small peaks appeared, one prior and one after the double peak. The non-reducing SDS-PAGE gel indicated, that the two small peaks contained irrelevant proteins. At least, the double peak was pure H1-CRD with a mainly dimeric H1-CRD fraction at the bottom of peak 1, a mixed fraction in the area of the peak overlap and only monomeric H1-CRD in the descendent branch of peak 2.

The purity of the H1-CRD was highly improved by SEC. The main impurities of 14kDa, 22kDa, 40-45kDa and 66kDa were removed. Only traces of a 36kDa protein were detected, which can probably be deduced to the incomplete reduction of H1-CRD.

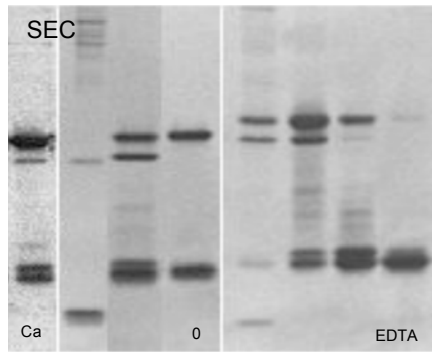


Figure 43: Silver-stained reducing and non-reducing SDS-PAGE gel 15% and native PAGE gel 15% of the SEC-purified active H1-CRD used for immunization. Hen 1, hen 2 and hen 3 were immunized with H1-CRD of the last fractions of SEC_{Ca} with 20mM calcium, SEC₀ without calcium and SEC_{EDTA} with 1mM EDTA, respectively. The gel shows fractions of the SEC_{Ca}, SEC₀ and SEC_{EDTA} over the time course.

The SEC_{Ca} allowed the extraction of other proteins. The SEC₀ was neither suitable for the separation of monomeric and dimeric species nor for the removal of other proteins. Finally, the SEC_{EDTA} was partially successful in the separation of monomeric and dimeric species.

In conclusion, having a stock of more than 50mg affinity-purified active H1-CRD and 1.15mg affinity and SEC-purified active H1-CRD, the basis was established to start the production of monoclonal and polyclonal anti-H1 antibodies, respectively.

3.3 Production and purification of polyclonal antibodies

3.3.1 Production of IgY

The highly pure active H1-CRD, which was purified by affinity to Gal-Sepharose and by SEC (see Figure 43), was emulsified with Complete Freund's Adjuvant or Incomplete Freund's Adjuvant. Three hybrid leg hens were primed with 20 μ g H1-CRD/CFA emulsion sc at day 1 and were boosted with 20 μ g H1-CRD/IFA emulsion sc at days 20, 59, 84, 133. From day 34 to 224, 271 eggs were collected and pooled prior to purification.

3.3.2 Purification of IgY

There exists no standard method for the extraction of IgY from yolks, but most procedures are composed of two main steps: the removal of lipids, followed by the separation of IgY from total yolk proteins.

3.3.2.1 Optimization of the total IgY extraction

Three methods for each step were selected and combined. The lipids were removed by the "freeze / thaw" (FT), the "water dilution" (WD) or the PEG 3.5% (PEG) method, and the total IgY were precipitated with ammoniumsulfate (AS), PEG 12% (PEG) or PEG 12% / ethanol (PEG/ETOH). The total IgY, which were derived from the nine procedures, were compared in terms of their purity, yield and activity.

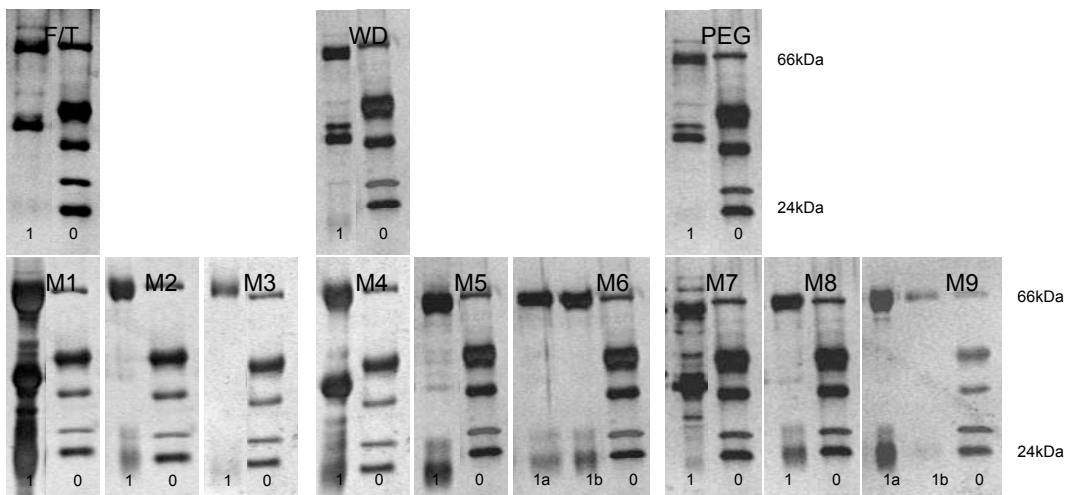


Figure 44: Silver-stained reducing SDS-PAGE gel 12% of extracted polyclonal total IgY (1), purified by the 9 different procedures M1-M9 and the LMW marker (0). The amounts of IgY per band on gel were normalized to 20 μ l yolk (0.0015 egg).

Purity

The F/T, the WD and the PEG method precipitated lipids quantitatively. The following extraction of the total IgY with PEG and PEG/EtOH methods yielded highly pure IgY antibodies. On the reducing SDS-PAGE gel, the 24kDa and 66kDa bands of the light and heavy chains were intensely stained and only traces of 36kDa and 45kDa proteins were detected in the PEG-derived, but not in the PEG/EtOH-derived total IgY. In contrast, the AS-derived total IgY were contaminated with substantial amounts of other yolk proteins (see Figure 44).

Yield

The total yolk proteins and the total IgY antibodies were quantified by Bradford micro-assay and the yields were normalized to the amount/egg. Comparing the lipid and the total IgY precipitation separately, the PEG method provided highest amount of total yolk proteins with 792mg/egg, followed by the WD method with 323mg/egg and the F/T method with 195mg/egg in mean (see Figure 45). The highest total IgY yield resulted from the AS method with a 23% portion of the total yolk proteins. This was substantially more than from the PEG method with a 6% and the PEG/EtOH method with only a 2% portion of the total yolk proteins in mean (see Figure 46).

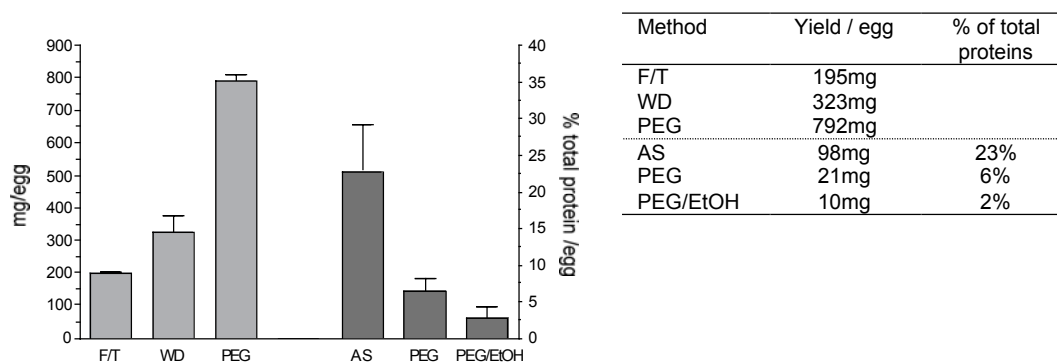


Figure 45: Extraction of the total yolk proteins and total IgY. The yield/egg of total yolk proteins extracted by the F/T, the WD or the PEG method and % IgY of total yolk proteins extracted by the AS, the PEG or the PEG/EtOH method were compared. The yield of total yolk proteins by the F/T method was 195mg/egg (SEM 6mg/egg) by the WD method 323mg/egg (SEM 53mg/egg) and by the PEG method 792mg/egg (SEM 18mg/egg). The yield of total IgY received by the AS method was 98mg/egg (SEM 33/egg), by the PEG method 21mg/egg (SEM 6mg/egg) and by the PEG/EtOH method 10mg/egg (SEM 5mg/egg). The yield of IgY normalized to the yield of total yolk proteins resulted in 23% (SEM 6%) for the AS method, 6% (SEM 2%) for the PEG method and 3% (SEM 2%) for the PEG/EtOH method.

Overall, the highest yield with 149mg/egg IgY resulted from procedure M4, which was composed of the WD and the AS method, followed by 108mg/egg IgY from procedure M7 that consisted of the PEG and the AS method (see Figure 49).

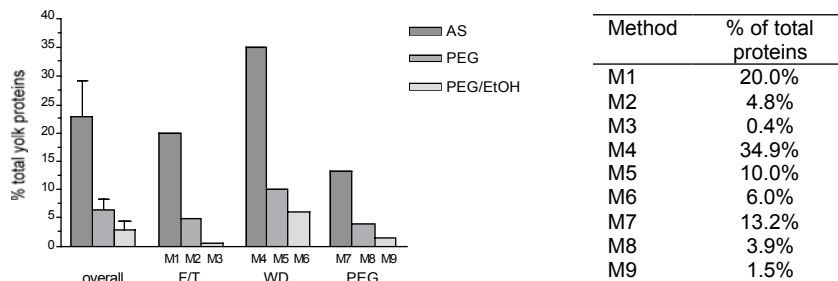


Figure 46: Comparison of the nine IgY purification procedures. The yield of the IgY in % of the total yolk proteins was arranged by the lipid precipitation methods.

Activity

The activities of the total yolk proteins and of the total IgY antibodies were tested in an AP-ELISA and the absorbances were normalized to the activity/egg. Looking the lipid and the IgY precipitation separately, the highest activity of the total yolk proteins was retained by the WD method with 2897AU/egg, followed by the PEG method with 2297AU/egg and the lowest by the F/T method with 1925AU/egg (see Figure 47). The highest activity of the total IgY was obtained by the PEG method with a 13.6% portion of the total protein activity. This was only slightly higher than by the AS method with a 11.8% portion. A substantially lower activity remained by the PEG/EtOH method with a 9.0% portion of the total protein activity (see Figure 48).

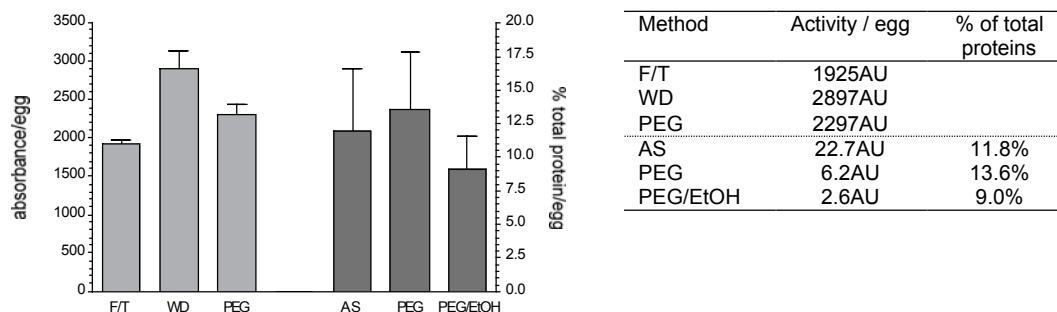


Figure 47: Activity of the IgY after lipid precipitation with F/T, WD and PEG and after IgY precipitation with AS, PEG and PEG/EtOH. The total yolk protein activity was 1925AU/egg (SEM 44/egg) after F/T, 2897AU/egg (SEM 236/egg) after WD and 2297AU/egg (SEM 137/egg) after PEG. The total IgY activity reached, was by the AS method 22.7AU/egg (SEM 6.4/egg), by the PEG method 6.2AU/egg (SEM 1.9/egg) and by the PEG/EtOH method 2.6AU/egg (SEM 1.7/egg). The total IgY activity in percentage of the activity of the total yolk proteins was by the AS method 11.8% (SEM 4.7%), by the PEG method 13.6% (SEM 4.1%) and by PEG/EtOH 9.0% (SEM 2.5%).

Overall, the highest activity provided procedure M7 with 484AU/egg, closely followed by procedure M8, which was composed of PEG and PEG, with 448AU/egg. The lowest activity remained with procedure M1 that consisted of F/T and AS, with 94AU/egg.

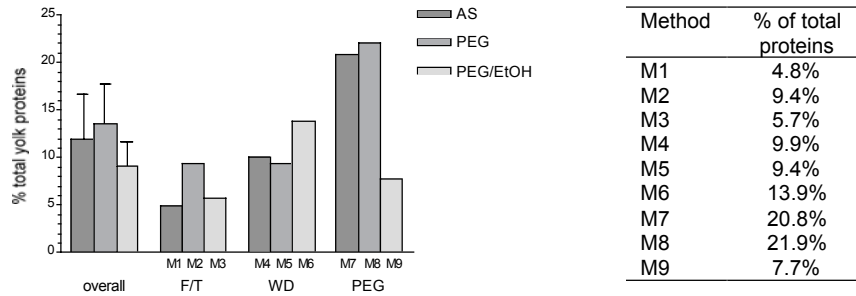


Figure 48: Activity of the yolk proteins and of the polyclonal total IgY in AP-ELISA, detected with an AP-labeled rabbit anti-chicken IgG (whole molecule) and in percentage of the total protein activity. The activities were normalized to the activity per one egg (13.4ml yolk).

In conclusion, the highest H1-CRD binding activity was obtained with M7-derived IgY, but the reducing SDS-PAGE indicated, that the AS precipitation was only partially effective (see Figure 49). The resulting polyclonal IgY were of low purity. As a consequence, M8 was the procedure of choice. M8-derived IgY were nearly as active as M7-derived IgY, but were highly pure. Alternatively, procedure M6, composed of W/D and PEG/EtOH could be preferable, if traces of PEG in the M8-derived IgY would disturb the IgY interaction. The second precipitation of the total IgY with EtOH removed PEG effectively.

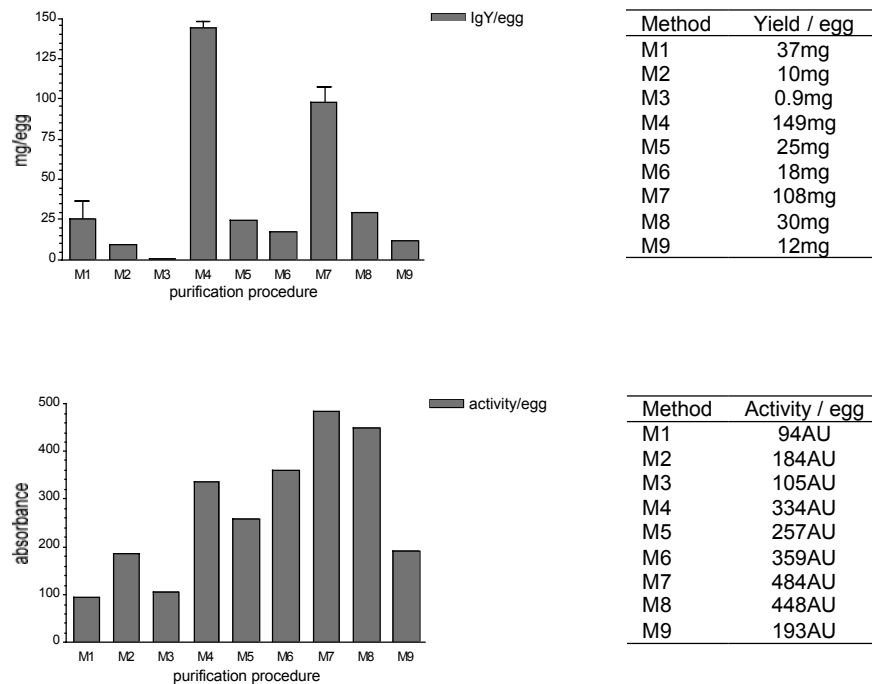


Figure 49: Comparison of the nine different purification procedures M1-M9. The yields were determined by Bradford assay (A) and the activities were measured in an AP-ELISA (B).

3.3.2.2 Extraction of specific anti-H1 IgY

The polyclonal H1-CRD-specific (anti-H1) IgY were extracted from total polyclonal IgY by H1-CRD-Sepharose (H1-Sepharose) affinity chromatography (see Figure 50A).

The comparison of the areas under the elution peaks indicated, that the highest amount of anti-H1 IgY per egg were extracted from total IgY of M4 (M4_{H1}), followed by IgY of M8 (M8_{H1}) (see Figure 50B). No elution peak was detected when total IgY of preimmune eggs were applied to the H1-CRD column.

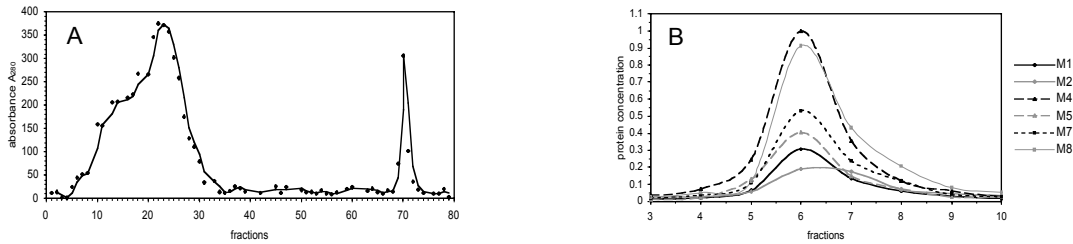


Figure 50: Extraction of specific anti-H1 IgY from total IgY of the different procedures M1-M9 (M1_{H1}-M9_{H1}) on an H1-CRD-Sepharose column, detecting proteins by A₂₈₀ measurement. A: Chromatogram of an anti-H1 IgY extraction. B: Overlaid elution peaks of the anti-H1 IgY extraction chromatograms.

Yield

The quantification of the eluted anti-H1 IgY by Bradford assay and A₂₈₀ measurement confirmed, that procedure M4_{H1} yielded the highest amount of specific IgY with 4.3mg/egg, followed by M8_{H1} and M5_{H1} with 2.1mg/egg and 2.0mg/egg, respectively. With procedures M1_{H1}, M2_{H1} and M7_{H1}, only approximately five to seven times lower anti-H1 IgY yields were received (see Figure 51).

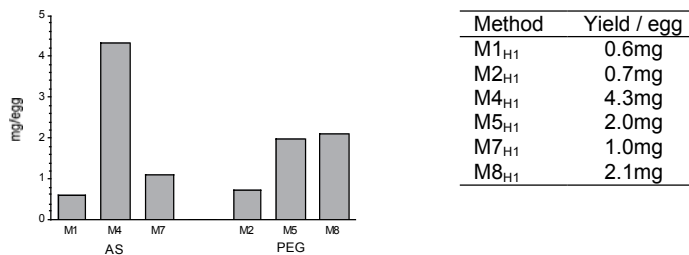


Figure 51: Yield of the specific anti-H1 IgY antibodies extracted from total IgY of M1-M9 by affinity using an H1-CRD-Sepharose column.

When looking the fraction of anti-H1 IgY in the total IgY, the highest portion of anti-H1 IgY was obtained by M2_{H1}, M5_{H1} and M8_{H1}, which all included the PEG precipitation. This agreed with the excellent total IgY purity of the PEG-derived compared to the AS-derived

IgY. The AS-based procedures M1_{H1}, M4_{H1}, and M7_{H1} included only a minute portion of 1-3% specific IgY (see Figure 52).

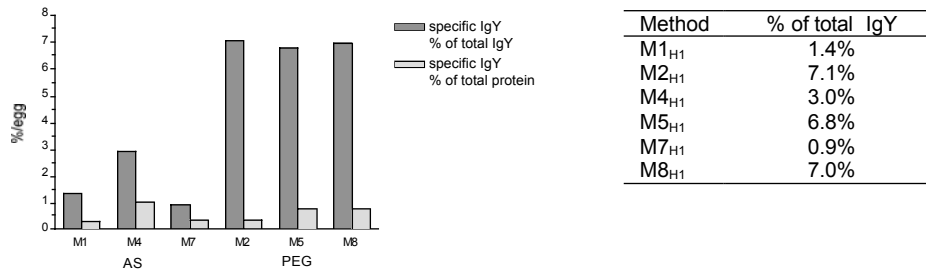


Figure 52: Fraction of the specific anti-H1 IgY in percentage of the total IgY, arranged according to the procedures M1-M9.

Purity

The reducing SDS-PAGE gel clearly indicated, that the excellent yield of M4_{H1} was caused by the presence of irrelevant proteins of mainly 36 to 45kDa. The same bands were visible in all specific IgY, extracted from AS-derived total IgY of procedures M1_{H1}, M4_{H1} and M7_{H1}. In the anti-H1 IgY, obtained from PEG-derived total IgY of procedures M2_{H1}, M5_{H1} and M8_{H1}, only the 24kDa and 66kDa bands of the light and heavy chains appeared (see Figure 53).

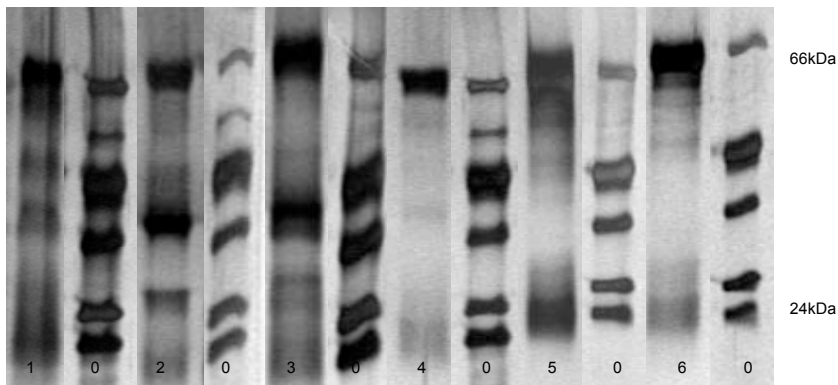


Figure 53: Silver-stained reducing SDS-PAGE gel 12%, showing the specific anti-H1 IgY of procedures M1_{H1} (1), M2_{H1} (2), M4_{H1} (3), M5_{H1} (4), M7_{H1} (5), M8_{H1} (6) and the LMW marker (0).

Activity

The high activity of the specific IgY was confirmed in the AP-ELISA. A strong absorbance was seen for specific IgY of M1_{H1} to M9_{H1}.

3.3.2.3 Optimized IgY extraction

The AS-derived procedures resulted in the highest yields, with 37-148mg/egg total IgY from procedures M1, M4 and M7 and with 4.3mg/egg specific IgY from procedure M4_{H1}, but the IgY were of low purity. Other yolk proteins were not quantitatively removed. Therefore, these methods were not suitable. Of the remaining procedures, M8 showed not only highest yield of total IgY with 30mg/egg, but also of specific IgY with 2mg/egg. Hence, the procedure M8 was selected for the preparative IgY purification (see Table 10).

Table 10: Yields of IgY from one egg, purified by nine different procedures.

Method	Protein / egg yield	IgY / egg		Specific IgY / egg		
		yield	% of protein	yield	% of IgY	% of protein
M1	183.0mg	36.6mg	20.0%	0.6mg	1.4%	0.32%
M2	200.6mg	9.6mg	4.8%	0.7mg	7.1%	0.35%
M3	201.8mg	0.9mg	0.4%	-	-	-
M4	425.2mg	148.6mg	34.9%	4.3mg	3.0%	1.02%
M5	245.4mg	24.6mg	10.0%	2.0mg	6.8%	0.80%
M6	300.3mg	18.0mg	6.0%	-	-	-
M7	310.9mg	107.7mg	13.2%	1.0mg	0.9%	0.35%
M8	818.1mg	29.8mg	10.8%	2.1mg	7.0%	0.76%
M9	274.5mg	11.9mg	4.6%	-	-	-

3.3.2.4 Preparative scale purification of total IgY

The polyclonal total IgY antibodies were purified from 25-30eggs per batch, following procedure M8. The reducing SDS-PAGE gel showed in the total IgY of all 8 batches only the light and heavy chains and no irrelevant proteins. Consequently, the purity of the total IgY antibodies was high (see Figure 54).

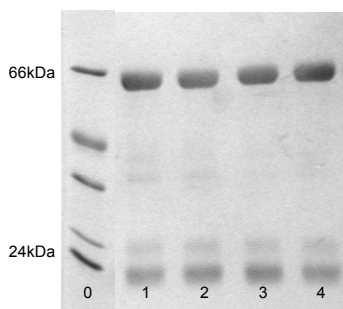


Figure 54: Silver-stained reducing SDS-PAGE gel 12% of the total IgY (1-4) extraction by procedure M8 in preparative scale and the LMW marker (0).

The overall yield was 11.8g total IgY, estimated by A_{280} measurement. Compared to the IgY yield from M8 during optimization of 30mg/egg, scale up resulted in a 1.5-fold increased extraction efficiency, with a yield of 45mg/egg.

3.3.3 IgY characterization

3.3.3.1 *In vitro* characterization

Immunoblotting

The total IgY specifically immunostained reduced, non-reduced and native H1-CRD. Interestingly, on the immunoblot of the non-reduced and native H1-CRD, the band intensity of the dimeric species was stronger than of the monomeric species. In contrary, on the non-reducing SDS-PAGE gel and native PAGE gel of the same H1-CRD batch, the ratio of dimeric and monomeric bands was stained vice versa. In addition, other bands of higher molecular weights were detected on the immunoblot, but were not seen on the corresponding PAGE. They matched in their weight to the oligomeric aggregates (trimers, tetramers, ...) of the H1-CRD (see Figure 55).

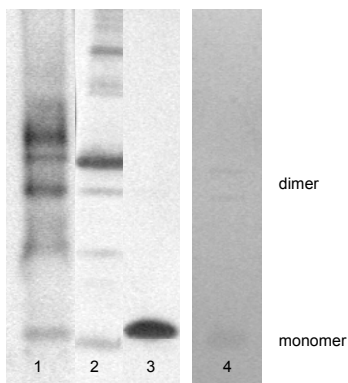


Figure 55: Immunoblot with total IgY. H1-CRD was blotted from reducing and non-reducing SDS-PAGE gels and from a native PAGE gel 15% to nitrocellulose, followed by immunostaining with 20 μ g/ml total IgY and AP-labeled rabbit anti-chicken IgG (whole molecule) in dilution 1:5000: blots of native (1), non-reduced (2) and reduced (3) H1-CRD and non-reducing (4) SDS-PAGE gel of the H1-CRD.

No cross-reaction with the LMW marker proteins was visible.

3.3.3.2 *On cell characterization*

Immunofluorescence microscopy

Texas Red-labeled IgY stained ASGPR-positive HepG2 but also ASGPR-negative SK-Hep1 cells very weakly (see Figure 56).

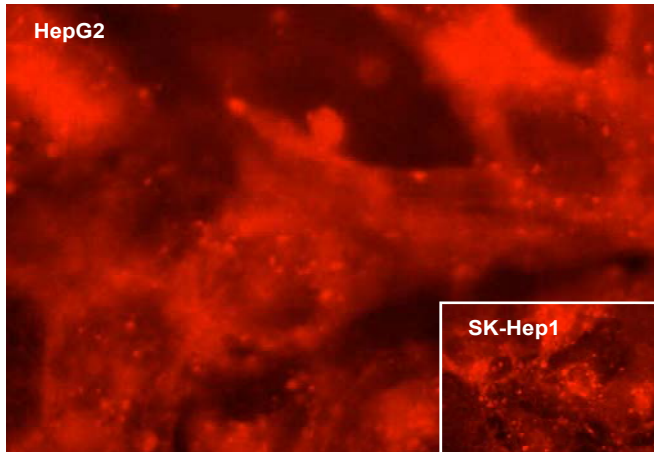


Figure 56: Immunofluorescence microscopy picture of directly stained HepG2 and SK-Hep1 cells. The Texas Red-labeled specific anti-H1 IgY (40 μ mg/ml, 220nM) was endocytosed into living cells, followed by paraformaldehyde fixation.

3.4 Production and purification of monoclonal antibodies

3.4.1 Production of hybridomas

3.4.1.1 Immunization of mice

The active H1-CRD used for immunization of mice was purified by Gal-Sepharose affinity chromatography.

3.4.1.1.1 Immunization of NMRI outbred mice

Three batches of three female 8-10 weeks old NMRI mice were primed sc in the neck, with 20µg H1-CRD in CFA, and were boosted sc at least twice, every three weeks, with 20µg H1-CRD in IFA. Mice were finally boosted with 20µg H1-CRD sc without adjuvant at days 3, 2 and 1 prior to fusion (see Table 11).

Table 11: Schedule of the NMRI mice immunizations with H1-CRD and PEG fusions of splenocytes with myeloma cells.

Immunization	Day	Mouse	Antigen injection	Remarks
Priming	1	1-3	20µg H1-CRD / CFA, sc.	
Boost 1	~ 20	1-3	20µg H1-CRD / IFA, sc.	
Boost 2	~ 40	1-3	20µg H1-CRD / IFA, sc.	
Serum titer				Not determined
Myeloma cells	77			P3X63-Ag8.563 cells ready in culture
Final boost 1	77	3	20µg H1-CRD, sc.	
Final boost 2	78	3	20µg H1-CRD, sc.	
Final boost 3	79	3	20µg H1-CRD, sc.	
Fusion 3 (RB.A)	80	3		PEG1500 fusion, NMRI feeder layer
Myeloma cells	40			P3X63-Ag8.563 cells ready in culture
Final boost 1	40	1	20µg H1-CRD, sc.	
Final boost 2	41	1	20µg H1-CRD, sc.	
Final boost 3	42	1	20µg H1-CRD, sc.	
Fusion 4 (RB.B)	43	1		PEG1500 fusion, Balb/c feeder layer

3.4.1.1.2 Immunization of Balb/c inbred mice

One batch of three female 6 weeks old Balb/c mice was primed ip, with 200µg H1-CRD in CFA, and was boosted ip, with 200µg H1-CRD in IFA, at days 21 and 60.

The serum titer of specific anti-H1 antibodies was determined by HRP-ELISA. Three days prior to fusion, the mouse with the highest titer was finally boosted iv, with 200µg H1-CRD without adjuvant. Although the antigen solution was tested to be pyrogen-free, the first two mice died after final boosting iv. As a consequence, the last mouse was finally boosted ip (see Table 12).

Table 12: Schedule of the Balb/c mice immunizations with H1-CRD and PEG fusions of splenocytes with myeloma cells.

Immunization	Day	Mouse	Antigen injection	Remarks
Priming	1	1-3	200µg H1-CRD / CFA, ip.	
Boost 1	21	1-3	200µg H1-CRD / IFA, ip.	
Boost 2	60	1-3	200µg H1-CRD / IFA, ip.	
Serum titer	72	1-3		Dilution 1:300-1:100000
Myeloma cells	77			P3X63-Ag8.563, start culture
Final boost	83	1	200µg H1-CRD, iv.	Mouse with highest serum titer, died
Fusion 1	86			Mouse dead
Final boost	87	2	200µg H1-CRD, iv.	Mouse with middle serum titer, died
Fusion 2	90			Mouse dead
Final boost	87	3	200µg H1-CRD, ip.	Mouse with lowest serum titer
Fusion 3 (RB.C)	90			PEG4000 fusion,

3.4.1.2 Fusion and hybridoma screening

3.4.1.2.1 PEG fusion of NMRI splenocytes with myeloma cells

The splenocytes of an immunized NMRI mouse were fused with murine myeloma cells P3X63-Ag8.563 using PEG1500. Two of nine fusions (fusion A and B) succeeded, while the others failed.

Fusion A

The fusion A was performed at day 80 after priming and the fused cells were distributed in plates, which contained a feeder-layer of NMRI macrophages.

After 21 days incubation in selective HAT medium without feeding, the supernatants of all wells on the fusion plates were screened by AP-ELISA, every 7 days. The first screen at day 22 post fusion resulted in 31, the second screen at day 29 post fusion in additional 16 and the third screen at day 36 post fusion in 5 new positive hybridomas.

During expansion of these 52 ELISA-positive hybridomas, 34 stopped growing and further 12 stopped the secretion of antibodies. The remaining 6 hybridomas of fusion A were successfully expanded from macrophage-coated 96-well to coated 24-well plates and further to 6-well plates without coating, they were frozen in liquid nitrogen (see Table 13). While cultivating, the selective HAT-supplemented medium was replaced with HT-supplemented and further with nonselective medium.

Table 13: Reasons for the loss of positive hybridomas from fusions A and B, during transfer and expansion, until freezing in liquid nitrogen.

Reason	Hybridomas
Stop growth	A01, A02, A03, A05, A06, A07, A08, A09, A10, A13, A14, A15, A21, A22, A23, A27, A29, A30, A31, A32, A34, A35, A36, A37, A38, A39, A40, A44, A46, A48, A49, A50, A51, A52
Stop Ab production	A12, A16, A17, A18, A19, A20, A26, A28, A33, A42, A43, A45
Instable positive hybridomas	A04, A11, A24, A25
Positive hybridomas	A41, A47 B01, B02

Fusion B

Cells of fusion B were fused at day 39 and were distributed on plates with Balb/c macrophage feeder-layer. The fusion B resulted in 2 positive hybridomas, which were expanded for freezing (see Table 13).

3.4.1.2.2 PEG fusion of Balb/c splenocytes with myeloma cells

Splenocytes of an immunized Balb/c mouse were fused with myeloma cells P3X63-Ag8.563 at day 90 after priming and cells were plated without feeder-layer, but in IL-6-supplemented medium.

Hybrid cells were incubated in selective HAT-containing medium for 14 days without feeding. At day 15 post fusion, the supernatants of all wells on the fusion plates were screened by HRP-ELISA, showing 63 of 480 wells to be positive. 48 hybridomas were expanded to 24-well plates, but thereof 8 gave up growing and 21 stopped the antibody production. From remaining 19 hybridomas of fusion C, 8 stayed slightly and 11 were clearly positive in ELISA, until freezing in liquid nitrogen. During cultivation, the medium was switched to HT-containing medium for a period of 2 weeks, and then to nonselective medium (see Table 14).

Table 14: Reasons for the loss of positive hybridomas from fusions C, during transfer and expansion, until freezing in liquid nitrogen.

Reason	Hybridomas
Stop growth	C02, C06, C07, C08, C36, C38, C40, C45
Stop Ab production	C01, C03, C04, C05, C10, C12, C13, C15, C20, C24, C25, C29-32, C37, C39, C41-44
Instable positive hybridomas	C26, C27, C28, C33, C34, C35, C46, C47
Positive hybridomas	C09, C11, C14, C16, C17, C18, C19, C21, C22, C23, C48

3.4.1.3 Fingerprint characterization of hybridomas

3.4.1.3.1 Isotyping

The heavy chain isotypes of the 18 hybridomas included all subclasses of antibodies. 38% belonged to IgM and 61% to IgG. These were subdivided into 44% of IgG1, 11% of IgG2a and 6% of IgG2b (see Figure 57). The light chain isotype was always κ .

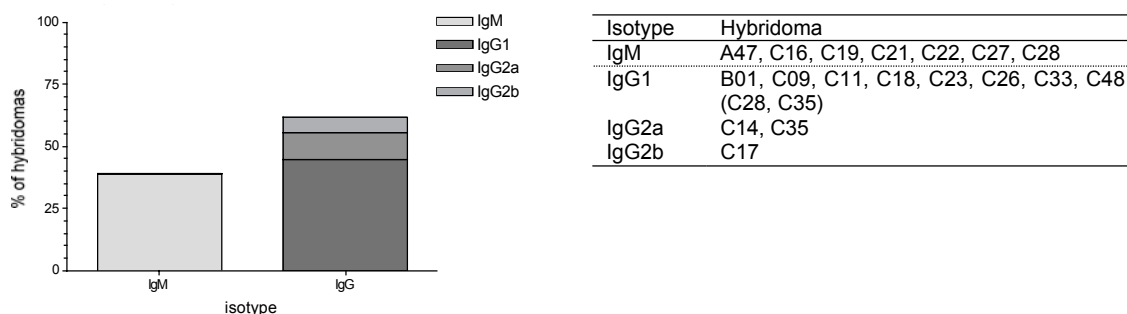


Figure 57: Isotyping of the 18 hybridomas from fusions A to C.

3.4.1.3.2 Immunoblotting

The blots of reduced, non-reduced and native H1-CRD were stained in supernatants of the 20 different hybridomas, i.e. the A47, B01, C09, C11, C14, C16, C17, C18, C19, C21, C22, C23, C26, C27, C28, C33, C35, C39, C46 and the C48.

The antibodies of the 6 hybridomas B01, C09, C11, C14, C18, C23 and C48 bound to reduced, non-reduced as well as native H1-CRD. In contrast to C11, C18, C23 and C48, which showed similar band intensities with H1-CRD in all three states, B01, C09 and C14 preferentially recognized reduced H1-CRD. Furthermore, for all hybridomas except for C14, a stronger signal was obtained with dimeric compared to monomeric H1-CRD species on the non-reducing blot, although on the corresponding SDS-PAGE gel, signal intensities of both species were vice versa.

Interestingly, the antibodies of hybridoma C17 interacted with reduced and native, but not with non-reduced H1-CRD. In contrary, the antibodies of the 7 hybridomas A47, C16, C19, C21, C22, C33 and C35 exceptionally stained H1-CRD in reduced, but not in non-reduced and native state. Finally, no band was detected neither on the reducing, non-reducing nor the native immunoblot, when stained with supernatants of the 4 hybridomas C26, C27, C28 and C46 (see Figure 58).

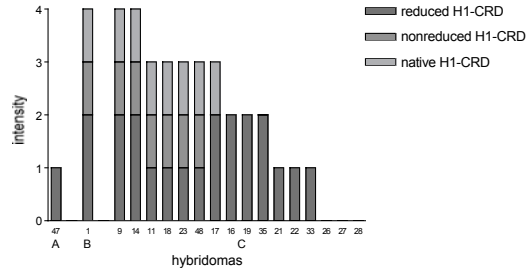


Figure 58: Immunoblot of the H1-CRD, staining in supernatant of the 20 hybridomas and with AP-labeled goat anti-mouse Ig (whole molecule). The reducing, non-reducing and native blots were stained in the same batches of supernatant.

3.4.1.3.3 ELISA

Specificity to H1-CRD and H2-CRD

Identical amounts of H1-CRD and H2-CRD were coated on the same plate and differences in binding to the antibodies of the hybridoma supernatants were detected by HRP-ELISA.

All supernatants were positive with H1-CRD and H2-CRD but differed in the signal intensities. The antibodies in the supernatant of the 13 hybridomas C09, C14, C16, C17, C18, C19, C21, C22, C23, C27, C28, C33 and C46 recognized the H1-CRD and the H2-CRD to a similar extent. In contrast, the 5 hybridomas A47, B01, C11, C26 and C48 and the sera of H1-immunized mice preferentially bound to H1-CRD. Compared to the H2-CRD, the absorbance increased more than 10% (see Figure 59).

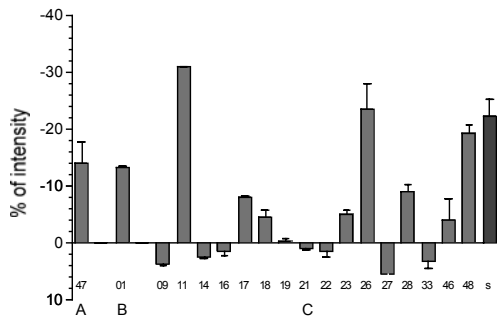


Figure 59: Differences in the binding of the H1-CRD and the H2-CRD to hybridoma antibodies. The murine serum of an immunized mouse (s) and the supernatants of hybridomas from fusion A to C were tested in duplicate by HRP-ELISA on the same plate.

Calcium sensitivity

The binding of hybridoma antibodies to the H1-CRD in the presence and absence of calcium was tested in a HRP-ELISA. All antibodies interacted with the H1-CRD in high

and low concentrated calcium buffers as well as in buffer with EDTA. The binding of B01, C09, C14, C16, C18 and C21 antibodies was not calcium-dependent. In contrast, the affinity of A47, C23, C26 and C48 to the H1-CRD was substantially and of C11 and C22 slightly increased in the presence of 20mM calcium. A negative calcium-dependence, showing a stronger binding in the presence of 2mM EDTA, was observed for C19. Finally, for C17 antibodies, the lowest signal was obtained in the presence of 2mM calcium compared to 20mM calcium and 2mM EDTA, while for C35 antibodies, the highest signal resulted in the presence of 2mM calcium (see Figure 60).

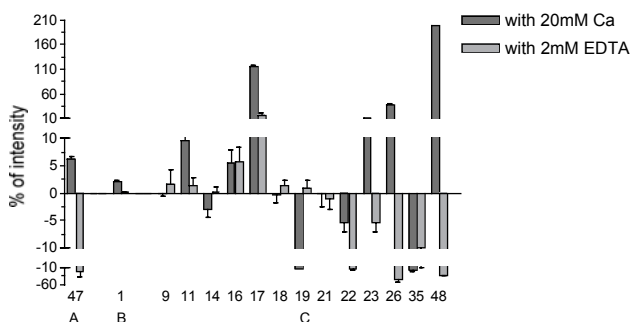


Figure 60: Differences in the binding of the H1-CRD to hybridoma antibodies in the presence or absence of calcium. The supernatants of hybridomas from fusion A to C were tested in duplicate in an HRP-ELISA on the same plate.

3.4.1.3.4 Fluorescence flow cytometry

Extracellular flow cytometry with HL-60, Jurkat, K-562, THP-1 and HepG2 cells

HL-60, Jurkat, K-562 and THP-1 and HepG2 cells were extracellularly stained with hybridoma supernatants and FITC-labeled goat anti-mouse Ig (polyvalent), without cell fixation.

The antibodies of all 17 hybridomas A47, B01, C09, C11, C16, C17, C18, C19, C21, C22, C23, C26, C27, C28, C33, C46 and C48, were not bound to the surface of HL-60, Jurkat, K-562 and THP-1. Exceptions were C35, which recognized THP-1 cells and C14, which in addition interacted with HL-60 cells.

All, but not the 7 hybridomas C19, C26, C27, C28, C33, C35 and C46, stained the ASGPR-positive HepG2 cells. The fixation of the HepG2 cells with paraformaldehyde however, prevented the binding of A47, C14, C16, C21 and C22 antibodies, whereas stains were still observed with B01, C09, C11, C17, C18, C23 and C48 antibodies (see Figure 61).

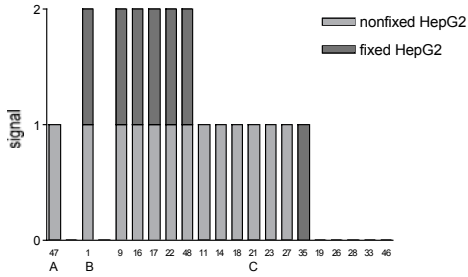


Figure 61: Binding of the antibodies in the hybridoma supernatants to the surface of fixed or not fixed HepG2 cells.

Intracellular flow cytometry of hybridomas

The hybridomas A04, A11, A12, A17, A24, A25, A41 and B01 were taken into culture two days before they were screened by intracellular fluorescence flow cytometry to examine their ability to produce antibodies.

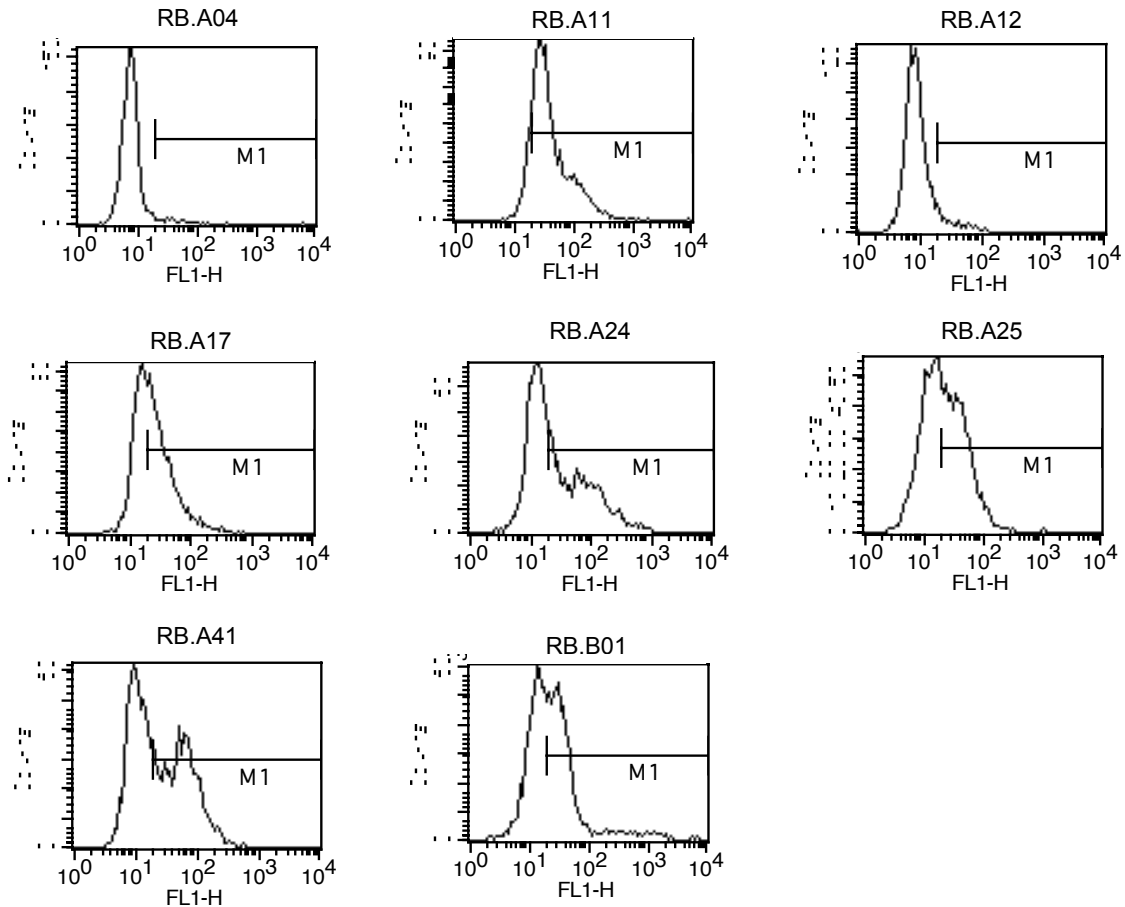


Figure 62: Intracellular FACS of the hybridomas A04, A11, A17, A24 and A25 after a preincubation with Brefeldin.

The in intracellular staining of Brefeldin-treated hybridomas showed, that only the hybridomas A11 and B01 preserved the antibodies production, with a clear shift of the cell population in FL1-H. A minute shift was still detected for the hybridomas A17 and A25, but no shift appeared in hybridomas A04 and A12. Interestingly, the hybridomas A24 and A41 were composed of two cell populations, a positive and a negative one (see Figure 62).

In contrary, in the AP-ELISA, all hybridoma supernatants were negative and contained no anti-H1 antibodies, except the B01 supernatant of the positive control.

Dependent on the fingerprint characterization, hybridomas were selected for cloning and further investigation of the monoclonal antibody characteristics. All hybridomas, which failed in the staining of HepG2 cells, were excluded.

Selected 12 hybridomas, i.e. the A11, A24, A41, A47, B01, C09, C11, C14, C17, C18, C23 and the C48, represented mainly IgG1, but each isotype class and subclass was considered once, at least. The hybridomas C11, C18 and C23 were regarded as highly promising candidates to be blocking antibodies. They preferentially bound to native H1-CRD and in a calcium-dependent manner (see Table 15).

Table 15: Summary of the fingerprint characterization of the different hybridomas from fusions A to C The FACS-negative hybridomas are written in italic, selected hybridomas are shaded in grey and most promising hybridomas are written in bold.

Hybridoma	Isotype	IB			HRP-ELISA			Extracellular FACS	
		red	non-red	native	H1	H1>>H2	Ca>>EDTA	not fixed HepG2	fixed HepG2
A41		-	+	+					
A47	IgM	+	-	-	+	+	+	+	-
B01	IgG1	++	+		+	+	-	+	+
C09	IgG1	++	+	+	+	-	-	+	+
C11	IgG1	+	+	+	+	+	+	+	+
C14	IgG2a	++	+	+	+	-	-	+	-
C16	IgM	++	-	-	+	-	-	+	-
C17	IgG2b	++	-	+	+	-	-	+	+
C18	IgG1	+	+	+	+	-	-	+	+
<i>C19</i>	<i>IgM</i>	++	-	-	+	-	-	-	-
C21	IgM	+	-	-	+	-	-	+	-
C22	IgM	+	-	-	+	-	+	+	-
C23	IgG1	+	+	+	+	-	++	+	+
C26	<i>IgG1</i>	-	-	-	+	+	++	-	-
C27	IgM	-	-	-	+	-		+	-
C28	<i>IgM</i> (<i>IgG1</i>)	-	-	-	+	-		-	-
C33	<i>IgG1</i>	+	-	-	+	-		-	-
C35	<i>IgG2a</i> (<i>IgG1</i>)	++	-		+		-	-	-
C46			-		+	-		-	
C48	IgG1	+	-	+	+	+	++	+	+

3.4.2 Production and propagation of clones

3.4.2.1 Terasaki single-cell cloning of hybridomas

The selected 12 hybridomas, i.e. the A11, A24, A41, A47, B01, C09, C11, C14, C17, C18, C23 and the C48 were cloned in dilutions 10cells/well, 3cells/well, 1cell/well and 0.3cell/well on special 60-well Terasaki-plates in IL-6-supplemented medium.

The hybridomas A11, A24 and A41 were all cloned twice successfully, with cloning efficiencies of 1.1-1.7cells/well. But all 298 clones of A11 stopped the antibody production during expansion, all 87 clones of A24 never produced antibodies and all 169 clones of A41 stopped growing.

The hybridoma A47 of fusion A was cloned with a cloning efficiency of 21.0cells/well. All 48 clones of the cloning in dilutions 0.3 and 1cell/well were positive in the AP-ELISA. Thereof, 12 clones (A47.1 to A47.12) were expanded. The antibodies of all clones were of the IgM isotype, identical to the antibodies of the hybridoma A47 (see Figure 63).

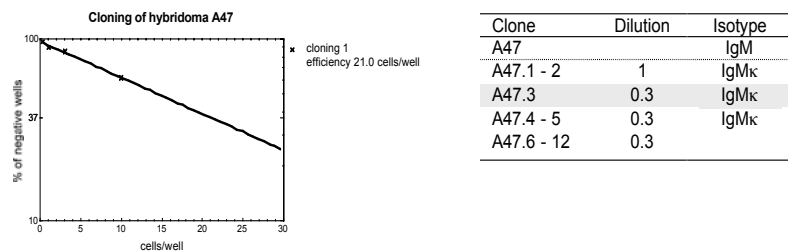


Figure 63: Terasaki cloning of hybridoma A47. A: The cloning efficiency of A47 (21.0cells/well, top 96.7, K 0.046, r^2 0.98). B: Positive clones with its cloning dilution and the isotype of the produced antibodies. The selected clone for the characterization is shaded in grey.

The hybridoma B01 of fusion B was cloned with a cloning efficiency of 24.2cells/well. All 81 clones were ELISA-positive. Selected 6 clones (B01.1 to B01.6) of the cloning in dilutions 0.3 to 3 were expanded. The clone B01.4 was isotyped, showing the same subclass IgG1 as the originating hybridoma B01 (see Figure 64).

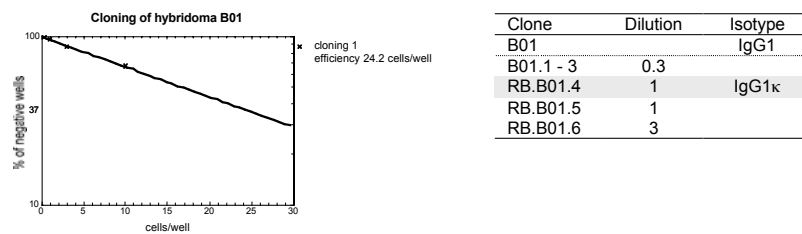


Figure 64: Terasaki cloning of hybridoma B01. A: The cloning efficiency of B01 (24.2cells/well, top 100.1, K 0.041, r^2 1.00). B: Positive clones with its cloning dilution and the isotype of the produced antibodies. The selected clone for the characterization is shaded in grey.

All hybridomas of fusion C, i.e. the C09, C11, C14, C18, C23 and the C48, were cloned and positive clones were expanded successfully, except hybridoma C17.

Hybridomas C09, C11, C14, C18 and C23 were cloned with cloning efficiencies of 8.9cells/well, 4.0cells/well, 26.3cells/well, 14.8cells/well and 5.2cells/well, respectively. Dependent on this, all clones of the cloning in dilutions 0.3-1cell/well, 0.3cell/well, 0.3-10cells/well, 0.3-3cells/well and 0.3-1cell/well were picked and screened by HRP-ELISA, showing all clones to produce anti-H1 antibodies. The selected 4 of 15 clones from C09 (C09.1-C09.4), 4 of 33 clones from C11 (C11.1-C11.4), 6 of 74 clones from C14 (C14.1-C14.6), 4 of 44 clones from C18 (C18.1-C18.4) and 8 of 48 clones from C23 (C23.1-C23.8) were expanded for freezing. All clones produced antibodies of the same isotype subclass as the originating hybridoma. All clones of C09, C11, C18 and C23 were of the IgG1 class and all clones C14 were of the IgG2a class (see Figure 66).

The hybridoma C48 was cloned with an efficiency of 8.3cells/well and 48 clones of the cloning in dilutions 0.3 and 1cell/well were transferred. The screening of the supernatant indicated, that only 17 produced antibodies. During expansion of 9 selected positive clones (C48.1 to C48.9), 44% of this clones (C48.1, C48.2, C48.5, C48.7) stopped the antibody secretion (see Figure 65).



Figure 65: Terasaki cloning of hybridoma C48. A: The cloning efficiency of C48 (8.3cells/well, top 100.3, K 0.120, r^2 0.99). B: Positive clones with its cloning dilution and the isotype of the produced antibodies. The selected clones for the antibody characterization are shaded in grey.

The hybridoma C17 was cloned twice with efficiencies of 37.3cells/well and 79.2cells/well, but no anti-H1 antibody-producing clone was received. Only 2 of 73 clones were positive in HRP-ELISA, but lost the ability to produce antibodies during expansion for freezing.

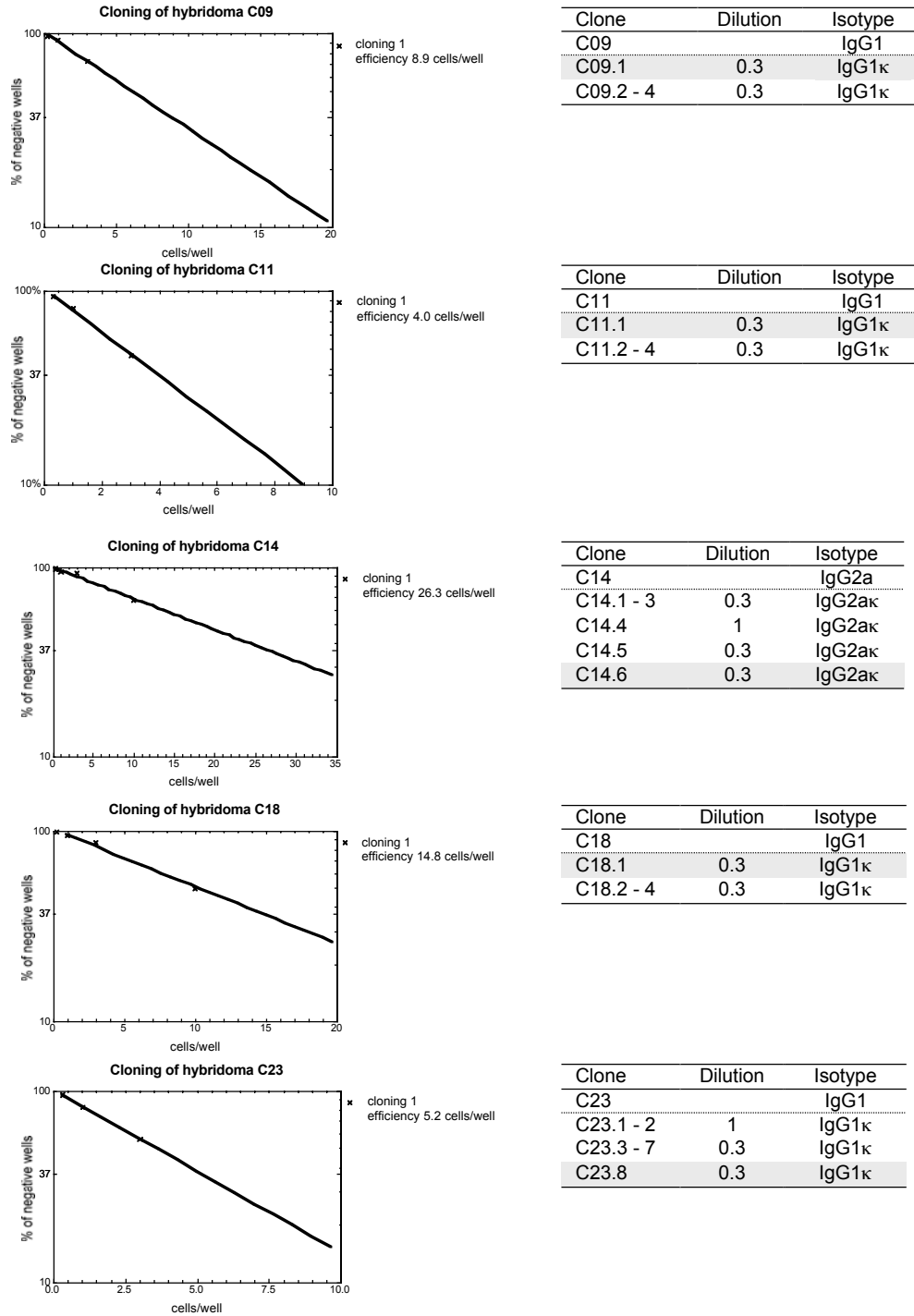


Figure 66: Terasaki cloning of hybridomas C09, C11, C14, C18 and C23. A: The cloning efficiency of hybridoma C09 (8.9cells/well, top 9102.8, K 0.115, r^2 0.98), C11 (4.0cells/well, top 103.6, K 0.259, r^2 0.99), C14 (26.3cells/well, top 101.0, K 0.038, r^2 0.96), C18 (14.8cells/well, top 103.0, K 0.069, r^2 0.99) and C23 (5.2cells/well, top 101.2, K 0.195, r^2 1.00). B: Positive clones with their cloning dilution and the isotype of the produced antibodies. Selected clones for the antibody characterization are shaded in grey.

3.4.2.2 Propagation of clones

The clone A47.3 was propagated in RPMI enriched with 10% FCS, and 500ml supernatant was harvested after 4 weeks. In contrast, the clone B01.4 was propagated in RPMI supplemented with 3% FCS (low IgG), and 500ml supernatant were harvested twice after 4 and 5 weeks, respectively. Similarly, the clones C09.1, C11.1, C14.6, C18.1, C23.8 and C48.9 were propagated in RPMI with 3% FCS (low IgG), but only 250ml supernatant were harvested twice, 4-6 weeks after propagation start.

The clone C14.6 cells tended to clump during propagation, when the FCS concentration was lowered. The clones C23.8 and C48.9 were very sensitive to low cell densities and a low FCS concentration and therefore, they stopped cell division. Both hybridomas tended to be instable in their antibody production, as tested in a HRP-ELISA.

3.5 Antibody characterization

3.5.1 Monoclonal A47.3 IgM

3.5.1.1 Purification of A47.3 IgM

Murine IgM antibodies neither bind to Protein A nor to Protein G. Therefore, the purification of A47.3 IgM by affinity chromatography using Protein L-Sepharose and H1-Sepharose was tested.

Purification by Protein L spin chromatography

The IgM purification from culture supernatant of A47.3, containing 10% FCS, using a Protein L-Sepharose spin column was not suitable. On the one hand, the purity was low, showing a high content of BSA on the silver-stained reducing SDS-PAGE gel. On the other hand, also the yield was minute. The HRP-ELISA let to conclude, that only a minor fraction of A47.3 was extracted, because the column flow through showed still approximately the same absorbance as the supernatant.

Purification by H1-CRD FPLC

The A47.3 IgM were also extracted from 10% FCS-containing culture supernatant, using an H1-Sepharose column. Due to precipitation problems, the baseline was very instable during loading. The supernatant was loaded onto the column twice. The IgM, which were eluted at a pH of 3, were highly pure. Only the 25kDa and 80kDa bands of the light and heavy chains were visible on a reducing SDS-PAGE gel (see Figure 67).

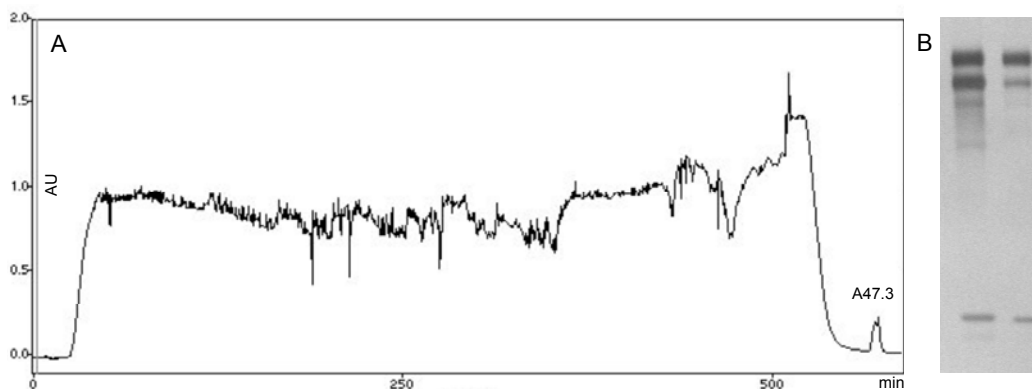


Figure 67: IgM purification from culture supernatant of clone A47.3, containing 10% FCS. A: H1-CRD FPLC chromatogram. B: Silver-stained reducing SDS-PAGE gel 10% of eluted A47.3 IgM, showing the 25kDa light chain band and the about 80kDa heavy chain double band.

The yield, determined by Bradford assay and absorbance A_{280} measurement, was substantially better with 0.77mg A47.3 IgM in mean, equivalent to 7.7mg/L supernatant. Thereof, the first extraction yielded 4.3mg/L and the second extraction 3.4mg/L supernatant (see Figure 68). Also the H1-CRD affinity chromatography allowed only the extraction of an A47.3 antibody fraction. Hence, the flow through was still positive in the HRP-ELISA after twice clearing the supernatant.

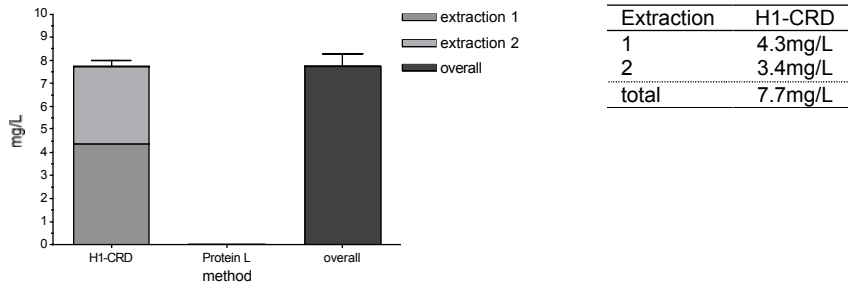


Figure 68: Yield of A47.3 IgM, purified by affinity to Protein L and H1-CRD and quantified by Bradford micro-assay and absorbance A_{280} measurement. Overall yield was 7.734mg/L (SEM 0.569mg/L) culture supernatant of clone A47.3.

3.5.1.2 In vitro characterization

3.5.1.2.1 Immunoblotting

Identical amounts of the reduced, non-reduced and native H1-CRD as well as of the reduced-alkylated and native-alkylated H1-CRD were blotted to nitrocellulose and were stained, using A47.3 IgM in concentrations of 5 μ g/ml or 0.5 μ g/ml (see Figure 69).

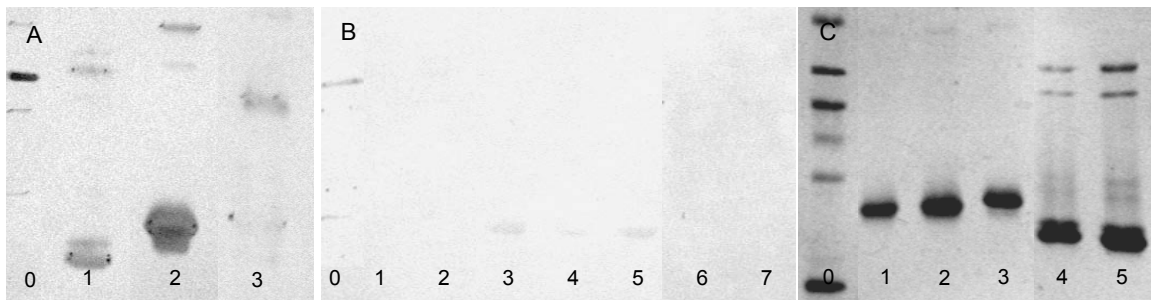


Figure 69: Immunoblot of the H1-CRD, stained using monoclonal A47.3 IgM. 1 μ g/band H1-CRD on PAGE gels 15% under reducing, non-reducing denatured or native conditions were blotted to nitrocellulose and were immunostained with A47.3 IgM, followed by detection with AP-labeled goat anti-mouse Ig (whole molecule) in dilution 1:5000. A: Blot stained with 5 μ g/ml A47.3 IgM, showing the LMW marker (0), the reduced (1), non-reduced (2) and native (3) H1-CRD. B: Blot stained with 0.5 μ g/ml A47.3 IgM, showing the LMW marker (0), reduced (1), the reduced state of reduced-alkylated (2), the reduced state of native-alkylated (3), non-reduced (4), the non-reduced state of native-alkylated (5), native (6) and the native state of the native-alkylated (7) H1-CRD. C: Silver-stained reducing and non-reducing SDS-PAGE gel 15% of the same probes used in B (0-5).

On a Ponceau S-casted blot, the bands pattern was identical to the bands on the PAGE gel (see Figure 69C). The intensities of the monomeric H1-CRD species were about the same, independent of their alkylation state and much stronger than of dimeric H1-CRD.

The monoclonal A47.3 IgM specifically recognized monomeric and dimeric H1-CRD in reduced, non-reduced and native state, but they also cross-reacted with the carbonic anhydrase (bovine erythrocytes) of the LMW marker. The binding to native H1-CRD was much weaker than to non-reduced and reduced H1-CRD.

With the lower A47.3 IgM concentration of 0.5 μ g/ml, the reduced H1-CRD appeared only fairly in the stain, whereas neither non-reduced nor native H1-CRD was detected. The alkylation of H1-CRD did not affect the binding on the reducing blot.

3.5.1.2.2 ELISA

The binding of the monoclonal A47.3 IgM to the H1-CRD (5 μ g/ml, 300 μ M) was titrated in the concentration range of 0 - 10nM in a HRP-ELISA, using HRP-labeled goat anti-mouse Ig (H+L) diluted 1:1000 for detection. For half maximal binding of the A47.3 IgM, an EC₅₀ of 12.20nM was calculated. However, this concentration lied out of the titrated range (see Figure 70).

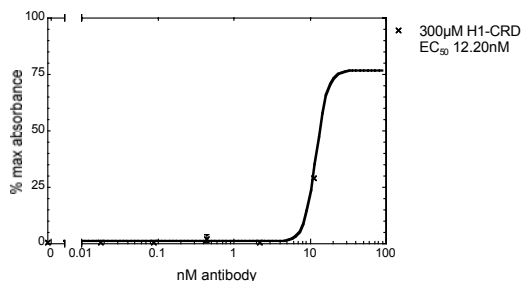


Figure 70: Binding of the A47.3 IgM to H1-CRD in a HRP-ELISA. The A47.3 was titrated in the range of 0.017-10nM in duplicate (exponential dilution row) in the presence of 20mM calcium. The plate was coated with 5 μ g/ml (300 μ M) H1-CRD and A47.3 detected with HRP-labeled goat anti-mouse Ig (H+L) diluted 1:1000. The EC₅₀ was calculated, using a nonlinear regression fit (equation sigmoid dose-response, variable slope, r^2 0.99) of Prism4 software.

The calcium sensitivity of the A47.3 IgM binding to the H1-CRD in the HRP-ELISA was tested. Therefore, A47.3 was caught in the presence of 20mM calcium or 1mM calcium and in the absence of calcium, when calcium was chelated with 10mM EDTA. During all other incubation steps, the same buffers were used, which included 1mM calcium prior and 20mM calcium after the A47.3 capturing.

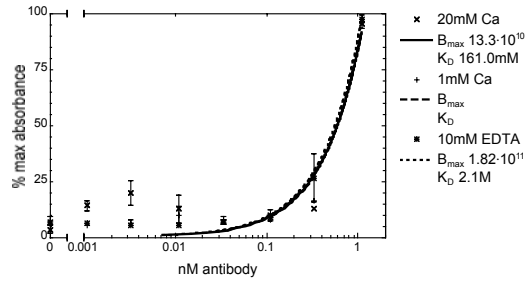


Figure 71: Ca sensitivity of the A47.3 IgM binding to the H1-CRD in a HRP-ELISA in the presence of 20mM calcium, 1mM calcium or in the absence of calcium, chelated with 10mM EDTA. The plate was coated with 3 μ g/ml H1-CRD (175 μ M) and the A47.3 IgM was titrated in the range of 0.001 – 1nM in triplicate. B_{max} and K_D were calculated, using a nonlinear regression fit (equation one site binding, hyperbola, r^2 0.82 and 0.94) of Prism4 software.

A47.3 IgM bound only very weak and independent of calcium in the titrated range. A lower K_D of 161mM and B_{max} of $1.3 \cdot 10^{11}\%$ were calculated in the presence of 20mM calcium compared to a K_D of 2.1M and B_{max} of $1.8 \cdot 10^{11}\%$ in the presence of 10mM EDTA. But as the K_D lied outside of the titrated range, this can only be regarded as a finger hint (see Figure 71).

3.5.1.2.3 GalNAc-polymer assay

The competition of the A47.3 IgM with POD-labeled streptavidin-biotin β -GalNAc-polymer for binding to the H1-CRD was investigated in HAB buffer, containing 1mM calcium.

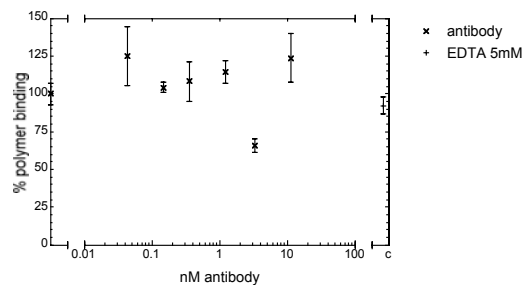


Figure 72: Competition of the A47.3 IgM and the GalNAc-polymer for binding to the H1-CRD in the polymer assay. The plate was coated with 3 μ g/ml (175 μ M) H1-CRD. A47.3 IgM in the range of 0.04 – 10nM (exponential dilution) in triplicate or tetruplicate, competed with 0.3 μ g/ml GalNAc-complex for binding. Nonlinear regression fit (equation, one site competition).

Independent of the A47.3 concentration in the range of 0 – 10nM, the β -GalNAc-complex was not displaced. Therefore, A47.3 IgM and β -GalNAc did not compete for binding to H1-CRD (see Figure 72).

3.5.1.3 On cell characterization

3.5.1.3.1 Immunofluorescence flow cytometry

ASGPR-positive hepatic HepG2 cells, ASGPR-negative hepatic SK-Hep1 cells, macrophage-like THP-1 cells and primary human macrophages and dendritic cells were indirectly extracellularly stained with A47.3 IgM, without fixation of the cells.

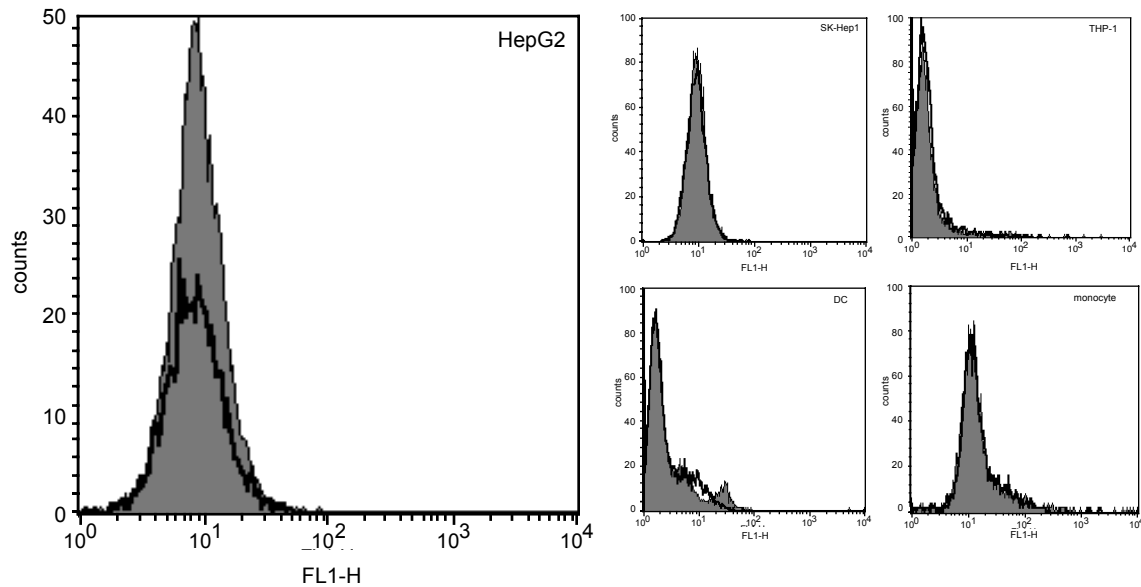


Figure 73: Flow cytometry of not fixed ASGPR-positive HepG2, ASGPR-negative SK-Hep1, THP-1, macrophages and dendritic cells. Cells were indirectly extracellularly stained with A47.3 IgM and FITC-labeled goat anti-mouse Ig (H+L). The dead propidium-stained cells were excluded. The histogram shows an overlay with the negative control (irrelevant IgG!).

The A47.3 IgM did not stain the HepG2, SK-Hep1, THP-1, macrophages and dendritic cells. Hence, the A47.3 did not bind to the ASGPR on cells (see Figure 73).

3.5.1.3.2 Immunofluorescence microscopy

The internalization of the Texas Red-labeled A47.3 IgM into HepG2 cells via the ASGPR was investigated, using SK-Hep1 cells for negative control.

No fluorescent flats were visible in HepG2 and in SK-Hep1 cells, which confirmed, that the A47.3 were not internalized (see Figure 74).

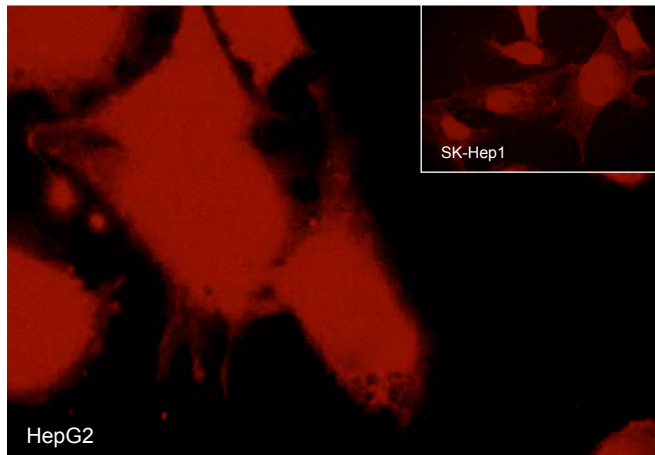


Figure 74: Immunofluorescence microscopy of the HepG2 and SK-Hep1 cells, stained with TR-labeled A47.3 IgM (40 μ g/ml, 45nM), followed by paraformaldehyde fixation.

3.5.2 Monoclonal B01.4 IgG1

3.5.2.1 Purification of B01.4 IgG1

Murine IgG1 antibodies stronger bind to Protein G than to Protein A. For purification of the monoclonal B01.4 IgG1 both, Protein A and G affinity chromatography, were tested.

Purification by Protein A FPLC

The salt concentration in the culture supernatant of clone B01.4, supplemented with 3% FCS (low IgG), was increased to 3.3M NaCl and 1.5M glycine, before the antibodies were extracted twice, using a Protein A-Sepharose column. The baseline was very instable, when loading the supernatant. The B01.4 IgG1 eluted in a very broad peak. The slow dissociation was probably due to a slightly too high elution pH of 4.

Purification by Protein G FPLC

The B01.4 IgG1 were three times extracted from culture supernatant of clone B01.4, containing 3% FCS (low IgG), using a Protein G-Sepharose column. The loading baseline was very stable, and the antibodies eluted at a pH of 3 in a narrow concentrated peak (see Figure 75). The activity of the purified B01.4 IgG1 antibodies after elution was verified by HRP-ELISA.

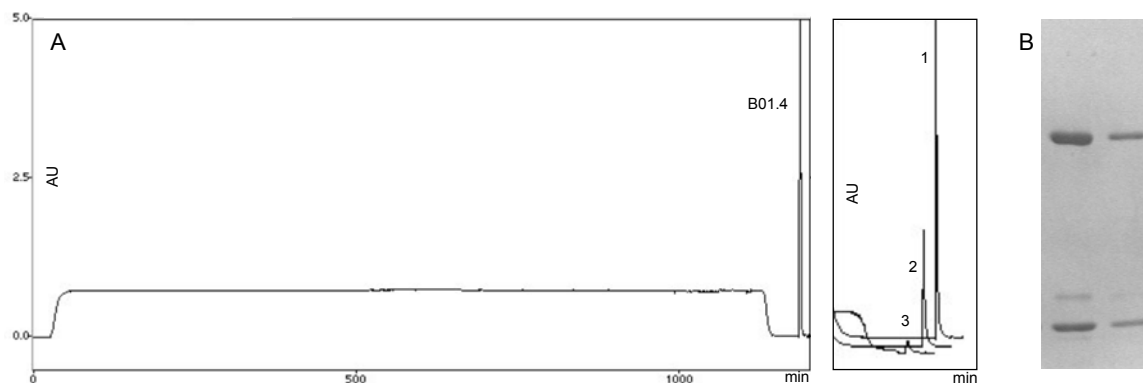


Figure 75: IgG1 purification from culture supernatant of clone B01.4, containing 3% FCS (low IgG). A: Protein G FPLC chromatogram with elution peaks of the first (1), the second (2) and the third (3) extraction and B: Silver-stained reducing SDS-PAGE gel 12% of the eluted B01.4 IgG1, showing the 25kDa light and the 55kDa heavy chain band.

The reducing SDS-PAGE gel confirmed the high purity of the B01.4 IgG1 for both methods, showing only the 25kDa and 55kDa band of the light and heavy chain, without BSA contamination (see Figure 75A and B).

The yield, estimated by Bradford micro-assay, SDS-PAGE quantification and A_{280} measurement, was higher for Protein G chromatography with 26.0mg/L, than for Protein A chromatography with 20.8mg/L supernatant. But this was the effect of the additional third extraction step. The yield of each extraction was approximately the same with 11.2 – 11.8mg/L in the first extraction, 9.6 – 9.8mg/L in the second extraction and 4.4mg/L in the third extraction (see Figure 76).

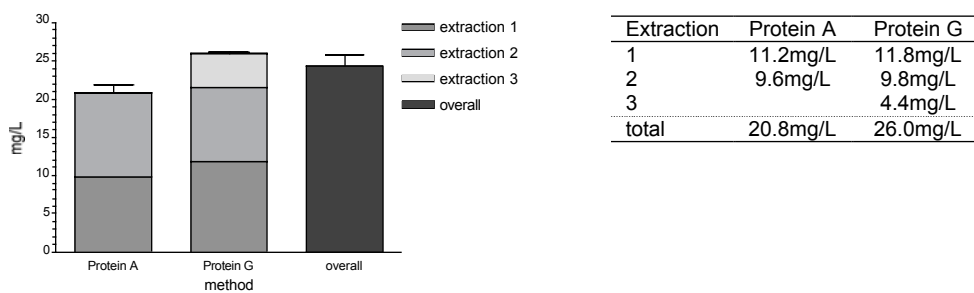


Figure 76: Yield of the B01.4 IgG1, purified by affinity to Protein A and Protein G and quantified by Bradford micro-assay, SDS-PAGE quantification and absorbance A_{280} measurement. The overall yield was 24.280mg/L (SEM 1.539mg/L) culture supernatant of B01.4, in mean.

Overall, 24.3mg B01.4 IgG1 antibodies were purified from 1000ml culture supernatant of clone B01.4. This is equivalent to a yield of 24.4mg/L supernatant. Multiple extractions were crucial for high-yield IgG1 purification.

3.5.2.2 *In vitro* characterization

3.5.2.2.1 Immunoblotting

Identical amounts of the reduced, non-reduced and native H1-CRD as well as of the reduced-alkylated and native-alkylated H1-CRD were blotted to nitrocellulose and were stained with 5 μ g/ml and 0.5 μ g/ml B01.4 IgG1 (see Figure 77).

The Ponceau S-stained membrane and the silver-stained PAGE gel showed identical bands pattern (see Figure 77C). The intensity of the monomeric H1-CRD species was higher than of the dimeric species, but was independent of the H1-CRD to be alkylated or not.

Monoclonal B01.4 IgG1 specifically recognized monomeric and dimeric H1-CRD in reduced, non-reduced and native state. Even when using the high IgG1 concentration of 5 μ g/ml, no cross-reactions with LMW marker proteins were detected.

Already at the lower B01.4 IgG1 concentration, the reduced, non-reduced and native H1-CRD were immunostained, but the intensities varied dependent on the alkylation state.

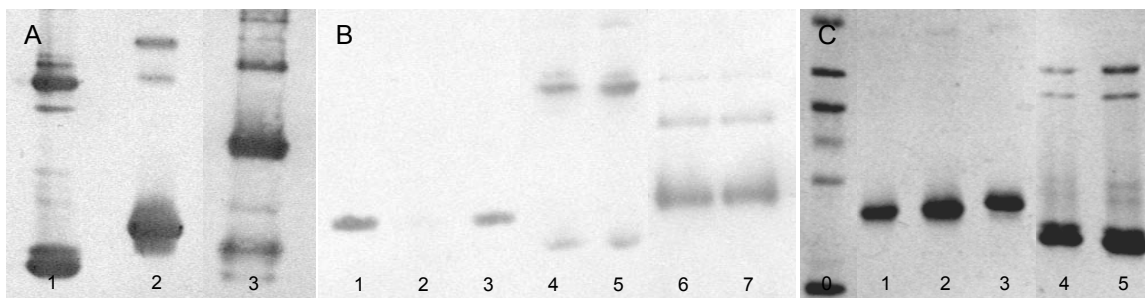


Figure 77: Immunoblot of the H1-CRD, stained with the monoclonal B01.4 IgG1. 1 μ g/band H1-CRD on PAGE gels 15% under reducing, non-reducing denatured or native conditions were blotted to nitrocellulose and were immunostained with B01.4 IgG1, followed by the detection with AP-labeled goat anti-mouse IgG (whole molecule) in dilution 1:5000. A: Blot stained with 5 μ g/ml B01.4 IgG1, showing non-reduced (1), reduced (2) and native (3) H1-CRD. B: Blot stained with 0.5 μ g/ml B01.4 IgG1, showing reduced (1), the reduced state of reduced-alkylated (2), the reduced state of native-alkylated (3), non-reduced (4), the non-reduced state of native-alkylated (5), native (6) and the native state of native-alkylated (7) H1-CRD. C: Silver-stained reducing and non-reducing SDS-PAGE gel 15%, the same probes (B, 1-5). LMW marker (0).

The reduced-alkylated (alkylated after reduction) H1-CRD was only minute stained, whereas strong bands were obtained for the not alkylated and native-alkylated (alkylated without prior reduction) H1-CRD. Similarly, B01.4 recognized the native-alkylated and the not alkylated H1-CRD in non-reduced or native state, respectively with identical signal intensities.

Furthermore, a stronger staining was observed for dimeric H1-CRD species than for monomeric, although band intensities were vice versa on silver-stained PAGE gels. This effect was seen for non-reduced, but much stronger for native H1-CRD.

3.5.2.2.2 ELISA

The monoclonal B01.4 IgG1 was titrated in the concentration range of 0.1 - 300nM in an HRP-ELISA. The binding to plates, which were coated with 5 μ g/ml (300 μ M) H1-CRD was detected with HRP-labeled goat anti-mouse Ig (H+L) diluted 1:1000.

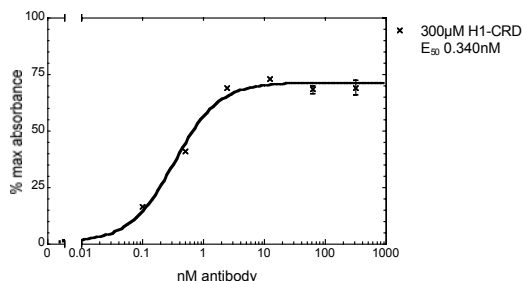


Figure 78: Binding of the B01.4 IgG1 to the H1-CRD in a HRP-ELISA. B01.4 was titrated in the range of 0.1-300nM in duplicate (exponential dilution row) in the presence of 20mM calcium. The plate was coated with 5 μ g/ml (300 μ M, 0.4 μ g/well) H1-CRD and B01.4 was detected with HRP-labeled goat anti-mouse Ig (H+L), diluted 1:1000. The EC_{50} was calculated, using a nonlinear regression fit (equation sigmoid dose-response, variable slope, r^2 0.99) of Prism4 software.

An EC_{50} of 0.340nM was calculated for half maximal binding (see Figure 78).

In an HRP-ELISA, the calcium sensitivity of the B01.4 IgG1 binding to the H1-CRD was tested in the presence of 20mM calcium, 1mM calcium or 10mM EDTA to chelate all calcium. Beside in this B01.4 antibody-capturing step, all buffers were composed identically, containing the lower concentration of 1mM calcium before and the higher concentration of 20mM calcium after this step.

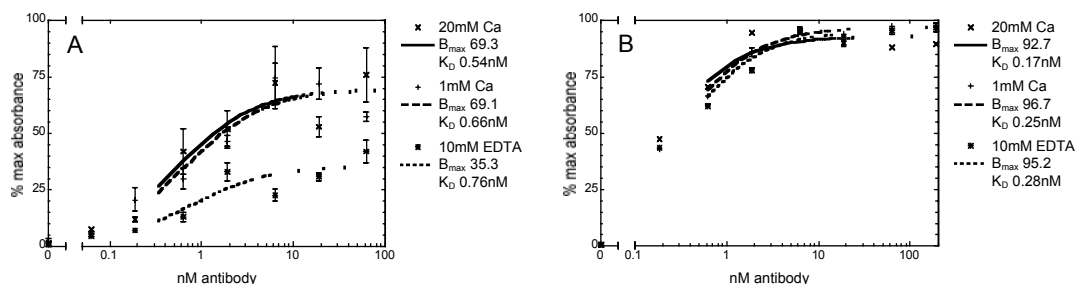


Figure 79: Ca sensitivity of the B01.4 IgG1 binding to H1-CRD in HRP-ELISA in the presence of 20mM calcium, 1mM calcium or in the absence of calcium, chelated with 10mM EDTA. Plates were coated with 3µg/ml (175µM) (A) or 6µg/ml (350µM) (B) H1-CRD and B01.4 IgG1 was titrated in the range of 0.0625-6.25nM (A) or 0.1875-187.5nM (B) in triplicate. B_{max} and K_D were calculated, using a nonlinear regression fit (equation one site binding, hyperbola, r^2 0.80 – 1.00).

When coating with 175µM H1-CRD, the B01.4 binding was slightly increased in the presence of calcium, compared to no calcium, but was not influenced by the height of the calcium concentration. The K_D of 0.54nM and B_{max} of 69.3% in 20mM calcium and K_D of 0.66nM and B_{max} of 69.1% in 1mM calcium were about the same, compared to K_D of 0.76nM and B_{max} of 35.3% in 10mM EDTA. In contrary, when coating with 350µM H1-CRD, about the same K_D in the range of 0.17-0.28nM and B_{max} in the range of 92.7-96.7% were received, not dependent on the presence of calcium (see Figure 79).

3.5.2.2.3 GalNAc-polymer assay

The competition of the POD-labeled streptavidin-biotin β -GalNAc-polymer and the B01.4 IgG1 for binding to the H1-CRD was tested in the presence of 1mM calcium. The B01.4 antibodies, which were titrated in the range of 0-625nM, competed against 0.3µg/ml β -GalNAc-complex for binding to the H1-CRD (see Figure 80).

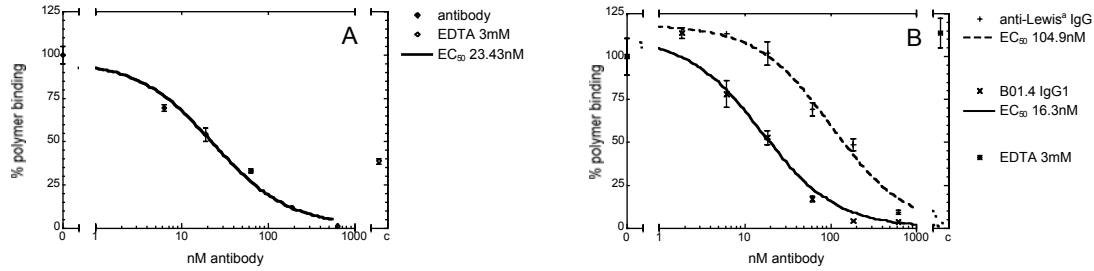


Figure 80: Competition of the GalNAc-polymer and the B01.4 (A) or the anti-Lewis^a (B) IgG1 for binding to the H1-CRD in the polymer assay. The plate was coated with 3 μ g/ml (175 μ M) H1-CRD. The B01.4 and the anti-Lewis^a antibodies, in the range of 0-625nM (exponential dilution) in triplicate or tetruplicate, competed with 0.3 μ g/ml GalNAc-complex for binding (nonlinear regression fit: equation, one site competition).

The B01.4 IgG1 showed an EC₅₀ of 16-24nM, whereas the negative control antibody of the same isotype, a murine anti-Lewis^a IgG, had a calculated about five times higher EC₅₀ of 104.9. Hence, the blocking effect was not only the consequence of a high antibody concentration but of steric or functional competition for binding to the H1-CRD.

3.5.2.2.4 Biacore

The binding constants and kinetics of the B01.4 IgG1 interaction with monomeric and dimeric H1-CRD were examined and determined by Biacore assay (see Figure 81A).

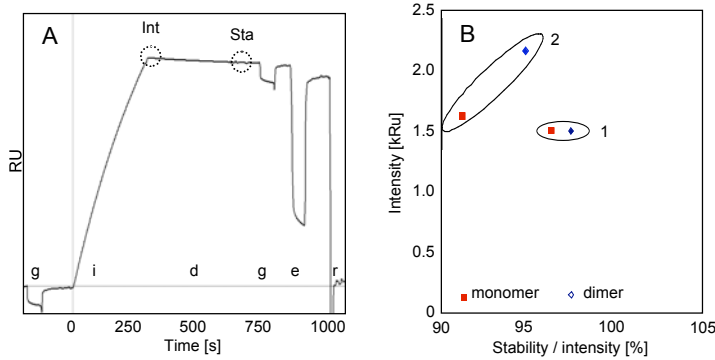


Figure 81: Biacore assay of the B01.4 IgG1 binding to monomeric and dimeric H1-CRD. A: Sensogram, with a preliminary injection of 5mM galactose (g), B01.4 IgG1 injection (i), dissociation phase (d), followed by a second 5mM galactose injection and an EDTA pulse (e), prior to regeneration with HCl (r). Data points used for blotting (Int, Sta) are indicated by circles. B: Intensity after 5min injection (Int), blotted against the quotient of the stability after 5min dissociation (Sta) and the intensity in buffer with 50mM calcium (1) or 3mM EDTA (2).

B01.4 at a constant concentration did not interfere with galactose binding and therefore did not block the binding site. The difference between the first and the second galactose signal was below 10%.¹⁴⁰ The binding was slightly calcium-sensitive. Particularly, the stability of the B01.4 binding to the H1-CRD decreased when EDTA was present. The strength of the B01.4 interaction with dimeric H1-CRD however increased, indicated by

the shift to the upper left. The intensity of the B01.4 binding to the H1-CRD in the presence of calcium and to the monomeric H1-CRD in the presence of EDTA was similar. Independent of calcium and EDTA, the interaction with dimeric H1-CRD was stronger than with monomeric (see Figure 81B).

In the absence of calcium, due to 3mM EDTA, B01.4 IgG1 at different concentrations in the range of 0.14-140nM bound fast, tight and in a concentration-dependent manner. The dissociation was very slow. The dissociation constants K_D of monomeric H1-CRD with 308pM and dimeric H1-CRD with 334pM were similar, but when looking at k_{on} and k_{off} separately, both rate constants were approximately twice as high for binding to monomeric H1-CRD with k_{on} of $5.32 \cdot 10^5 M^{-1} s^{-1}$ and k_{off} of $1.64 \cdot 10^{-4} s^{-1}$ compared to the binding to dimeric H1-CRD with k_{on} of $2.69 \cdot 10^5 M^{-1} s^{-1}$ and k_{off} of $0.90 \cdot 10^{-4} s^{-1}$ (see Figure 82).

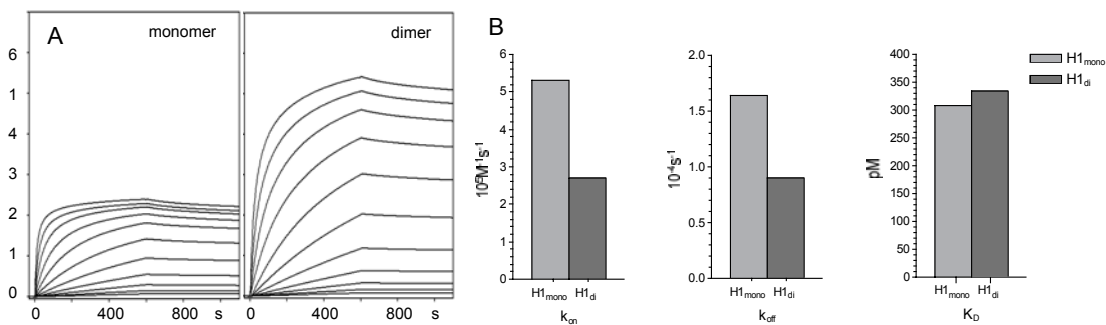


Figure 82: Comparison of kinetic rates k_{on} and k_{off} of the B01.4 IgG1 binding to a monomeric and dimeric H1-CRD species surface, after fitting to a Langmuir 1:1 binding model. A: Sensogram of the B01.4 IgG1 binding to H1-CRD in calcium-free buffer. B: calculated k_{on} , k_{off} and calculated K_D .

3.5.2.2.5 Epitope excision and extraction

The epitope excision and extraction were performed with native and with alkylated H1-CRD. In the extraction, using native trypsin-digested H1-CRD, fragments F2 (T^6-R^{17}) and F3 ($S^{18}-R^{24}$) were found in the MS elution spectrum. In the corresponding excision with trypsin, using alkylated H1-CRD, additional peaks of the double fragments F2+3 (T^6-R^{24}) and F4+5 ($S^{25}-R^{37}$) were visible (see Figure 83).

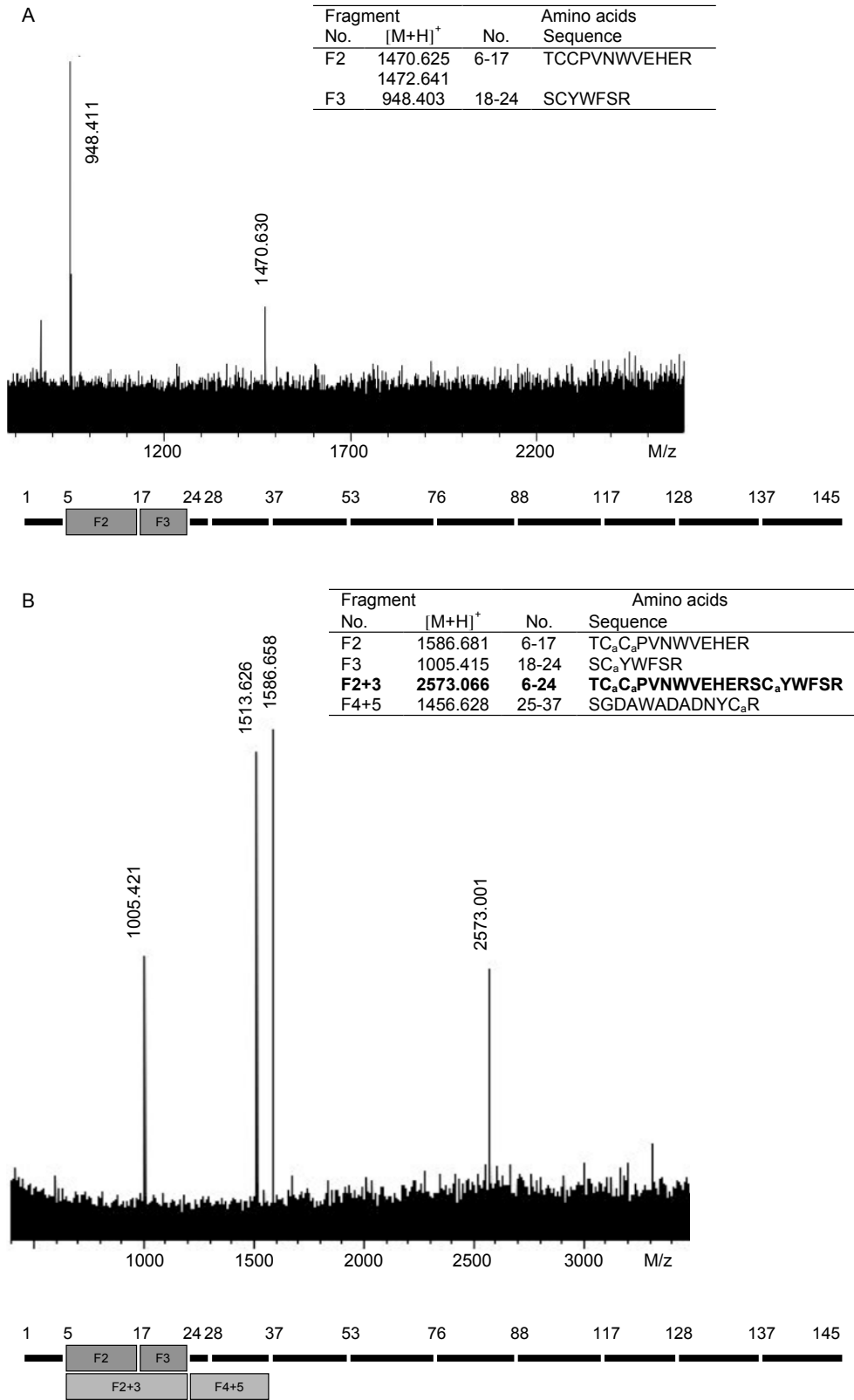


Figure 83: MS elution spectra of the epitope extraction using native trypsin-digested H1-CRD (A) and of the excision with trypsin, using alkylated H1-CRD (B). The wash spectra were clean (spectra not shown).

The binding of the B01.4 to an epitope on this partial H1-CRD sequence was proved twice. First in an HRP-ELISA, the B01.4 bound to biotin-labeled synthetic peptides F2 and F3, which were linked to streptavidin-coated plates. Second, in the epitope extraction using the acetylated synthetic F2 and F3 peptides, these peptides were recovered in the elution, but not in the wash spectra prior to elution (see Figure 84).

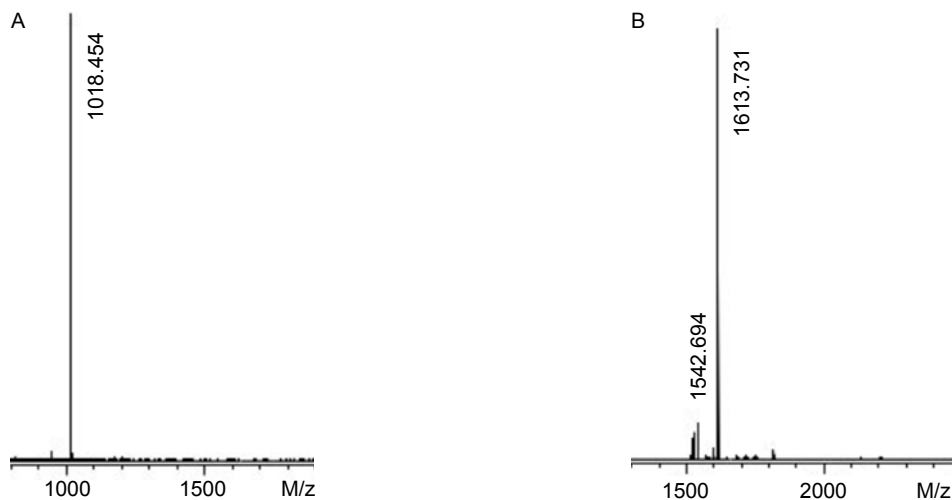


Figure 84: MALDI-FT-ICR elution spectra from epitope extraction of the synthetic acetylated peptide F2 ($\text{TC}_{\text{ac}}\text{C}_{\text{ac}}\text{PVNWVEHER}$, $[\text{M}+\text{H}]^+$ 1018.49) and F3 ($\text{SC}_{\text{ac}}\text{YWFSR}$, $[\text{M}+\text{H}]^+$ 1613.72). No fragments were found in the wash spectra (spectra not shown). A: MS elution spectrum of F2. B: MS elution spectrum of F3.

In the epitope excision of B01.4-bound H1-CRD with proteinase K, the epitope was diminished. Partial sequences of F2 and F3 were large enough to be recognized by B01.4. In the MS elution spectrum, fragments corresponding to amino acid sequences $\text{V}^{13}\text{-S}^{18}$ and $\text{C}^{19}\text{-S}^{23}$ appeared uniquely in the elution, whereas fragments of all other peaks were also present in the wash spectrum (see Figure 85).

Fragment No.	$[\text{M}+\text{H}]^+$	Amino acids No.	Sequence
F2'		13-19	VEHERS
F3'		19-23	C_aYWFS



Figure 85: Elution spectrum from epitope excision of alkylated H1-CRD, digesting with proteinase K. The wash spectrum was clean (spectra not shown).

The B01.4 IgG1 epitope sequence VEHERSCYWFS exhibited homologies to sequences of other C-type lectins in *homo sapiens*, i.e. the ASGPR-2a-c, the HBxAg-binding protein (Hepatitis B antigen binding protein) and the macrophage lectin 2. Furthermore, similar epitopes are also present in lectins of other mammals, i.e. in the ASGPR of *canis*

familiaris, *marmota monax*, *mus musculus*, *rattus norvegicus* and in the macrophage lectin of *mus musculus* and *rattus norvegicus* (see Table 16).

Table 16: Blastp of the B01.4 epitope sequence VEHERSCYWFS against the database non-redundant GenBank CDS (matrix PAM30). Identical amino acid residues are shaded and written in bold, and similar residues are written in bold.

Sequence	Identity	Similarity	Protein	Species
VEHER SCYWFS			B01.4 epitope	<i>Homo sapiens</i>
VEHER SCYWFS	100%	100%	ASGPR-1	<i>Homo sapiens</i>
VEHQG SCYWFS	81%	90%	ASGPR-2a-c	<i>Homo sapiens</i>
VEHQG SCYWFS	81%	90%	HBxAg-binding protein	<i>Homo sapiens</i>
VEHQD SCYWFS	81%	90%	Macrophage lectin 2 (CLE14)	<i>Homo sapiens</i>
VEHQD SCYWFS	81%	90%	CLEC10A protein (pancreas, spleen)	<i>Homo sapiens</i>
VEHEG SCYWFS	90%	90%	ASGPR-1	<i>Marmota monax</i>
VEYEG SCYWFS	81%	90%	ASGPR-1	<i>Mus musculus</i>
VEYEG SCYWFS	81%	90%	ASGPR-1	<i>Rattus norvegicus</i>
EYEG SCYWFS	80%	90%	ASGPR-1	<i>Canis familiaris</i>
SCYWFS	100%	100%	ASGPR-1	<i>Bos Taurus</i>
VEHEG SCYWFS	90%	90%	ASGPR-2	<i>Marmota monax</i>
SCYWFS	100%	100%	ASGPR-2	<i>Mus musculus</i>
SCYWFS	100%	100%	ASGPR-2/3	<i>Rattus norvegicus</i>
EHEG SCYWFS	90%	90%	Macrophage lectin 1/2	<i>Mus musculus</i>
EHEG SCYWFS	90%	90%	Macrophage lectin	<i>Rattus norvegicus</i>
EHVQ RCYWF	66%	77%	Variant-specific antigen	<i>Plasmodium falciparum</i>
R ICYWFS	85%	85%	Hypothetical protein	<i>Trypanosoma brucei</i>

3.5.2.3 On cell characterization

3.5.2.3.1 Immunofluorescence flow cytometry

The specific binding of the B01.4 IgG1 to the native entire ASGPR and the cross-reactivity with similar receptors were tested by extracellular flow cytometry. HepG2, SK-Hep1, THP-1, macrophages and dendritic cells were examined without fixation of the cells (see Figure 86).

The B01.4 IgG1 stained the ASGPR-positive HepG2 cells, but not the ASGPR-negative SK-Hep1 cells. Also the THP-1 cells, macrophages and dendritic cells that carry a homologous receptor, failed in staining. Therefore, B01.4 IgG1 bound specifically to the ASGPR.

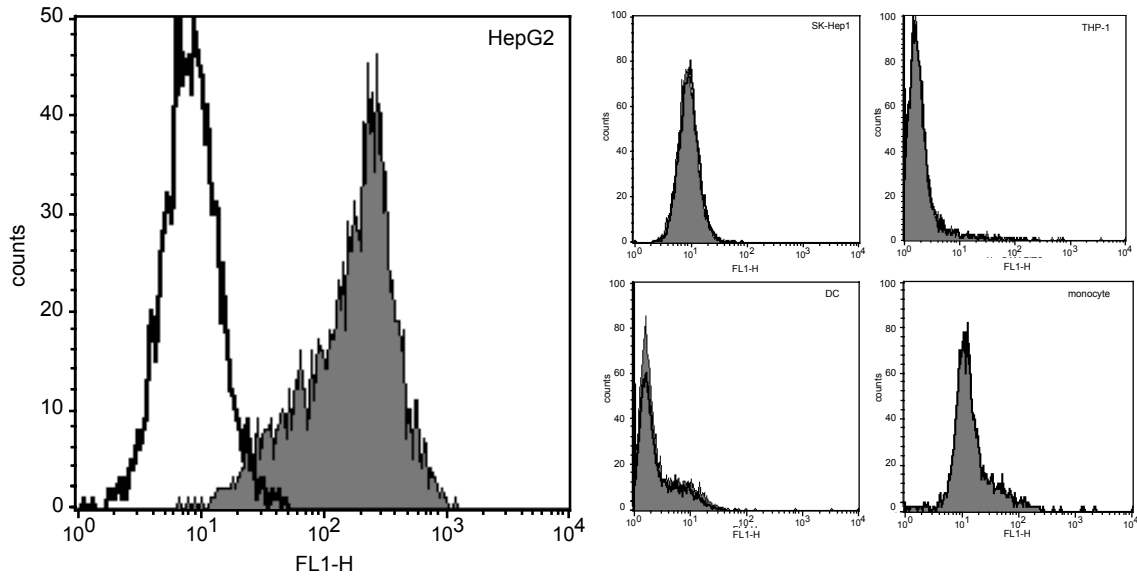


Figure 86: Flow cytometry of not fixed HepG2, SK-Hep1, THP-1, macrophages and dendritic cells, indirectly extracellular stained with B01.4 IgG1 and FITC-labeled goat anti-mouse Ig (H+L). The dead propidium-stained cells were excluded. The histogram shows an overlay with the negative control (irrelevant IgG).

3.5.2.3.2 Immunofluorescence microscopy

The internalization of the Texas Red-labeled B01.4 IgG1 into HepG2 cells was investigated by immunofluorescence microscopy. To control the specificity of the endocytosis via the ASGPR, the staining was also performed with SK-Hep1 cells.

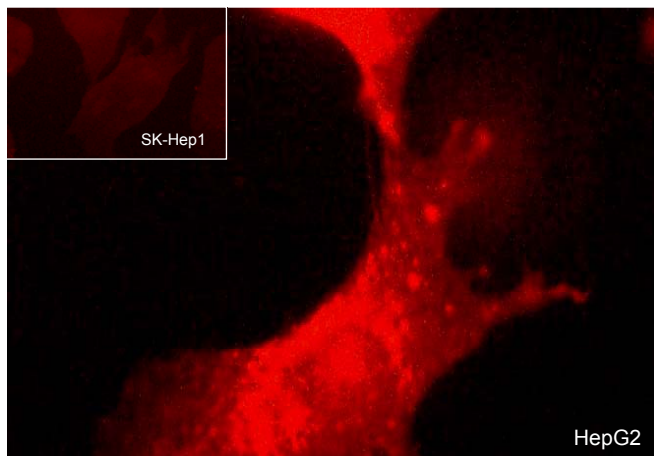


Figure 87: Immunofluorescence microscopy picture of the B01.4 IgG1 (40 μ g/ml, 250nM) endocytosis into HepG2 and SK-Hep1 cells. Direct staining with TR-labeled B01.4 IgG1, followed by paraformaldehyde fixation of the cells.

The HepG2 cells were intense stained and were strewn with very bright fluorescent spots. In contrast, the SK-Hep1 showed only some or no single spots (see Figure 87).

Hence, B01.4 was actively internalized by living HepG2 cells and the main fraction of the B01.4 specifically via the ASGPR.

3.5.2.4 *On tissue characterization*

3.5.2.4.1 Immunohistochemistry

Non-pathological human paraffin-embedded liver tissue sections were indirectly stained with DAB, to test the binding ability of B01.4. The antigen was retrieved with various steamer, microwave and enzymatic methods.

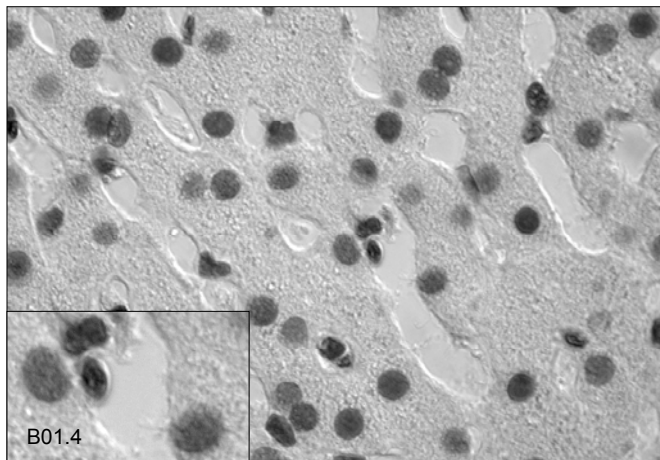


Figure 88: Indirect staining of paraffin-embedded non-pathological liver tissue (antigen retrieval with microwave at 98°C for 30min and staining with B01.4 at 4µg/ml, DAB).

No binding of the B01.4 to the hepatocyte surface was visible, independent of the tissue pretreatment for antigen retrieval (see Figure 88).

3.5.3 Monoclonal C09.1 IgG1

3.5.3.1 Purification of C09.1 IgG1

Murine C09.1 IgG1 were attempted to purification by Protein L and Protein G affinity chromatography.

Purification by Protein L spin chromatography

The IgG1 κ were purified from culture supernatant of clone C09.1, containing 10% FCS. But on the silver-stained reducing SDS-PAGE gel, only minute amounts of antibodies were visible, and above all were of insufficient purity. The HRP-ELISA confirmed, that the low yield was caused by low extraction efficiency. The supernatant and the column flow through exhibited approximately the same absorbance. Therefore, this method was not appropriate for the purification of C09.1 IgG1 κ .

Purification by Protein G FPLC

The IgG1 antibodies were purified from culture supernatant of C09.1, containing 3% FCS (low IgG) by FPLC, using a Protein G-Sepharose column. The supernatant was twice extracted, because the IgG1 binding to Protein G was not quantitative. The antibodies eluted in a sharp peak and were of high purity (see Figure 89).

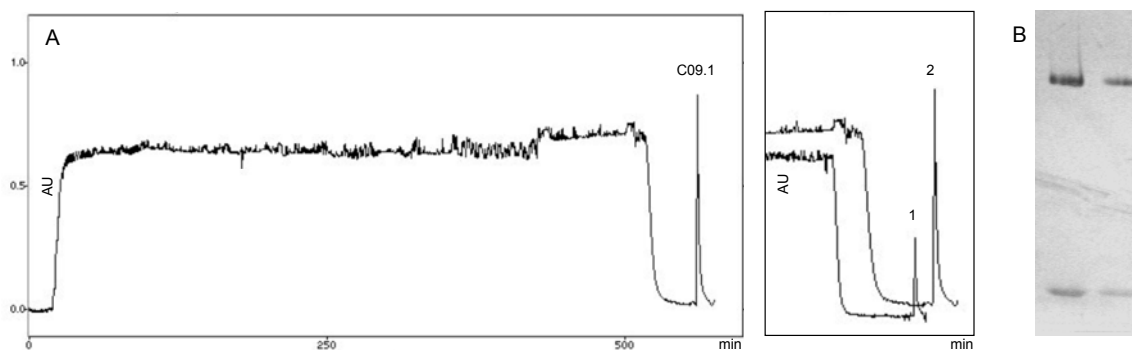


Figure 89: Purification of the IgG1 from 200ml culture supernatant of clone C09.1, containing 3% FCS (low IgG). A: Protein G FPLC chromatogram with elution peaks of the first (1) and the second (2) extraction. B: Silver-stained reducing SDS-PAGE gel 12% of the eluted antibodies, showing the 25kDa light chain and the 55kDa heavy chain band.

The C09.1 IgG1 antibodies were quantified by A_{280} measurement, SDS-PAGE quantification and by Bradford micro-assay. The yield of 11.9mg/L in the first and of 1.1mg/L in the second extraction indicated, that a double extraction is worthwhile (see Figure 90).

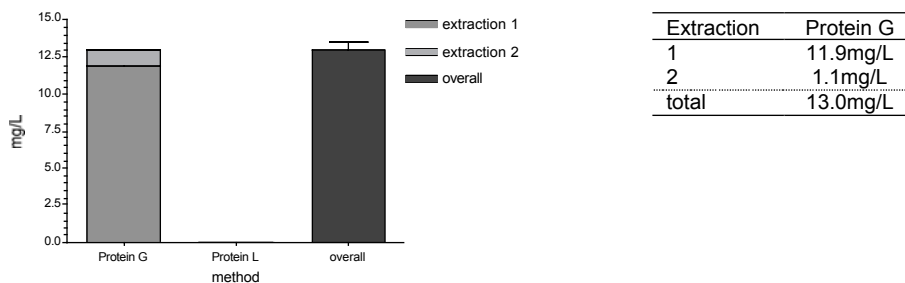


Figure 90: Yield of the C09.1 IgG1, purified by affinity to Protein G and Protein L and quantified by Bradford micro-assay, SDS-PAGE quantification and absorbance A_{280} measurement. An overall yield of 12.968mg/L (SEM 0.602mg/L) C09.1 culture supernatant was obtained.

Overall, 6.5mg IgG1 were purified from 500ml culture supernatant. This is equivalent to a yield of 13mg/L supernatant.

3.5.3.2 *In vitro* characterization

3.5.3.2.1 Immunoblotting

Identical amounts of the reduced, non-reduced and native H1-CRD as well as of the reduced-alkylated and native-alkylated H1-CRD were blotted to nitrocellulose and were caught with 5 μ g/ml or 0.5 μ g/ml C09.1 IgG1 during immunostaining (see Figure 91).

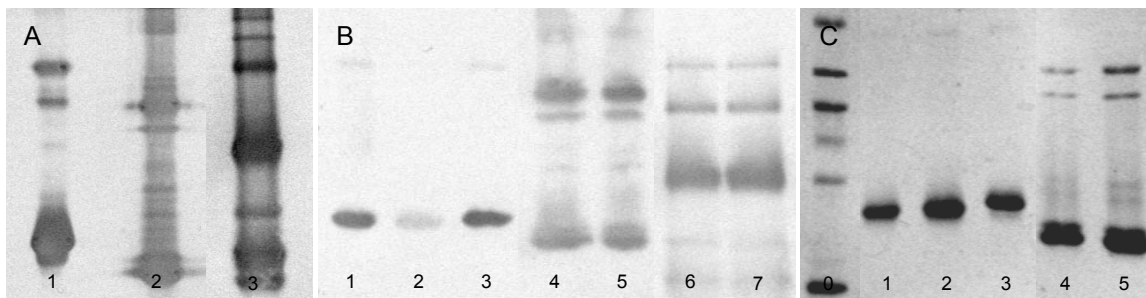


Figure 91: Immunoblot of the H1-CRD, captured with the monoclonal C09.1 IgG1. 1 μ g/band H1-CRD on PAGE gels 15% under reducing, non-reducing denatured or native conditions were blotted to nitrocellulose and were immunostained with C09.1 IgG1 followed by the detection with AP-labeled goat anti-mouse IgG (whole molecule) in dilution 1:5000. A: Blot stained with 5 μ g/ml C09.1 IgG1, showing reduced (1), non-reduced (2) and native (3) H1-CRD. B: Blot stained with 0.5 μ g/ml C09.1 IgG1, showing reduced (1), the reduced state of reduced-alkylated (2), the reduced state of native-alkylated (3), non-reduced (4), the non-reduced state of native-alkylated (5), native (6) and the native state of native-alkylated (7) H1-CRD. C: Silver-stained reducing and non-reducing SDS-PAGE gel 15% of the same probes used in B (1-5) and the LMW marker (0).

The bands pattern on a Ponceau S-stained membrane was identical to the silver-stained PAGE gel (see Figure 91C). The monomeric H1-CRD species were stained more intense than dimeric species, but the stain was independent of the H1-CRD alkylation.

The monomeric and dimeric species of reduced, non-reduced and native H1-CRD were specifically immunostained. No cross-reactions with other proteins of the LMW marker were visible, even not after staining with the higher 5µg/ml antibody concentration.

When 0.5µg/ml C09.1 IgG1 were used, the band intensities varied, dependent on the alkylation state. The C09.1 antibodies bound strongly to not alkylated or native-alkylated H1-CRD in reduced state, but recognized only minor reduced-alkylated H1-CRD in reduced state.

The dimeric species of non-reduced and much clearer of native H1-CRD were stronger immunostained than monomeric species, although on the corresponding silver-stained PAGE gel, the stain was vice versa.

3.5.3.2.2 ELISA

In an HRP-ELISA, the monoclonal C09.1 IgG1 in the concentration range of 0.1 - 300nM were titrated to examine their binding to the H1-CRD (5µg/ml H1-CRD, 300µM). For half maximal binding, an EC_{50} of 0.717nM was determined (see Figure 92).

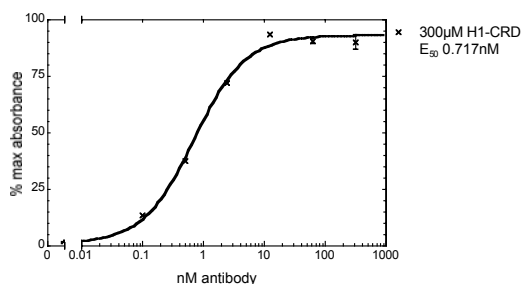


Figure 92: Binding of the C09.1 IgG1 to the H1-CRD in an HRP-ELISA. The C09.1 was titrated in the range of 0.1-300nM in duplicate (exponential dilution row) in the presence of 20mM calcium. The plate was coated with 5µg/ml (300µM) H1-CRD and C09.1 was detected with HRP-labeled goat anti-mouse Ig (H+L), diluted 1:1000. The EC_{50} was calculated, using a nonlinear regression fit (equation sigmoid dose-response, variable slope, r^2 1.00) of Prism4 software.

20mM calcium, 1mM calcium or 10mM EDTA were added during the capturing step of the C09.1 IgG1 in an HRP-ELISA, to test the calcium sensitivity. All other assay steps were identical and were performed in the presence of 1mM calcium prior to and in the presence of 20mM calcium after the C09.1 binding.

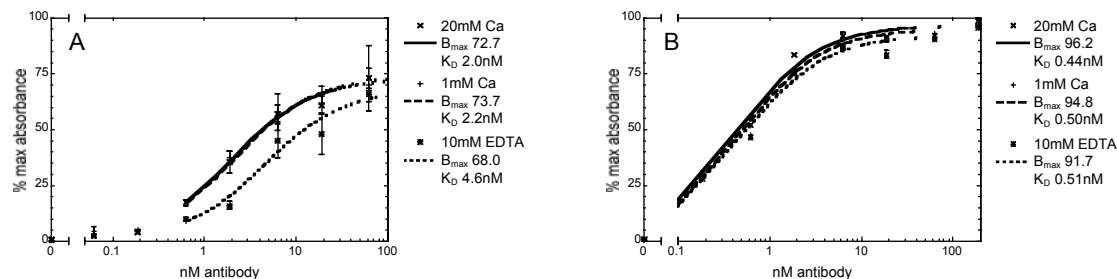


Figure 93: Ca sensitivity of the C09.1 IgG1 binding to the H1-CRD in an HRP-ELISA in the presence of 20mM calcium, 1mM calcium or of 10mM EDTA. The plates were coated with 3 μ g/ml (175 μ M) (A) or 6 μ g/ml (350 μ M) (B) H1-CRD and the C09.1 IgG1 was titrated, in the range of 0.0625-62.5nM (A) or 0.1875-187.5nM (B) in triplicate. B_{max} and K_D were calculated, using a nonlinear regression fit (equation one site binding, hyperbola, r^2 0.91 – 0.99).

At the low coating concentration of 175 μ M H1-CRD, the binding of C09.1 IgG1 in the range of 0 - 62.5 μ M was slightly calcium-sensitive, showing an about twice as high K_D of 4.6nM in the absence of calcium compared to a K_D of 2.0-2.2nM in the presence of calcium. Calculated maximal bindings B_{max} were similar. At the higher coating concentration of 350 μ M H1-CRD, the binding of C09.1 IgG1 in the range of 0 - 187.5 μ M was independent of calcium (see Figure 93).

3.5.3.2.3 GalNAc-polymer assay

The competition of the C09.1 IgG1 antibodies and the POD-labeled streptavidin-biotin β -GalNAc-polymer for binding to the H1-CRD, in the presence of 1mM calcium, was investigated (see Figure 94).

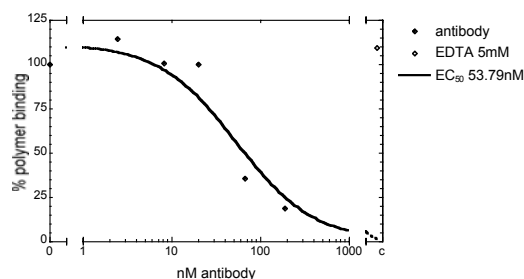


Figure 94: Competition of the GalNAc-polymer and the C09.1 IgG1 antibodies for binding to the H1-CRD in the polymer assay. The plate was coated with 3 μ g/ml (175 μ M) H1-CRD. The C09.1 in the range of 0-625nM (exponential dilution) in triplicate or tetruplicate, competed with 0.3 μ g/ml GalNAc-complex for binding (nonlinear regression fit: equation, one site competition).

The C09.1 IgG1 competed with the GalNAc-polymer for binding to the H1-CRD. A half maximal effective concentration EC₅₀ of 53.8nM was calculated.

3.5.3.2.4 Biacore

In a Biacore assay, the binding of galactose to monomeric and dimeric H1-CRD was not affected in the presence of a constant concentration of C09.1 IgG1. The first and the second galactose signal differed less than 10% (see Figure 95A).

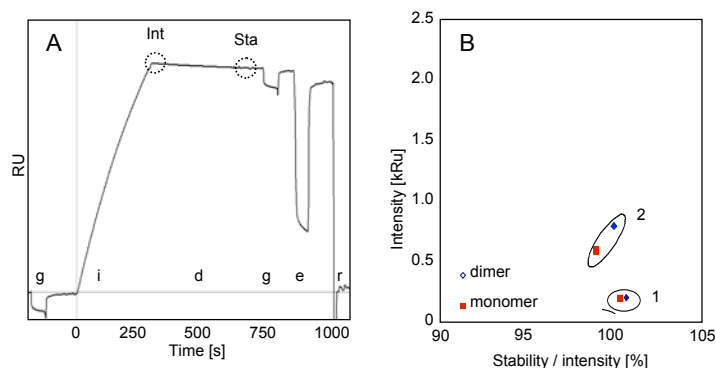


Figure 95: Biacore assay of the C09.1 IgG1 binding to monomeric and dimeric H1-CRD. A: Sensogram with a preliminary injection of 5mM galactose (g), C09.1 IgG1 injection (i), dissociation phase (d), followed by a second 5mM galactose injection and an EDTA pulse (e), prior to regeneration with HCl (r). Data points used for blotting (Int, Sta) are indicated by circles. B: Intensity after 5min injection (Int), blotted against the quotient of the stability after 5min dissociation (Sta) and the intensity, in buffer with 50mM calcium (1) or 3mM EDTA (2).

The binding of the C09.1 was slightly calcium-sensitive, showing a slightly increased intensity in the presence of 3mM EDTA. The stability and the intensity of the binding to monomeric and to dimeric H1-CRD were similar (see Figure 95B).

3.5.3.3 On cell characterization

3.5.3.3.1 Immunofluorescence flow cytometry

The specific binding of the C09.1 IgG1 to the full length ASGPR on not fixed cells was examined by extracellular flow cytometry of the receptor-positive HepG2 cells and the receptor-negative SK-Hep1 cells. Furthermore, THP-1, macrophages and dendritic cells were immunostained, to control the cross-reactivity with ASGPR-homologous receptors.

The C09.1 antibodies stained HepG2 but not SK-Hep1 cells, which indicated, that C09.1 IgG1 specifically recognized the ASGPR. In addition, they cross-reacted with no similar receptors on the surface of THP-1, macrophages and dendritic cells (see Figure 96).

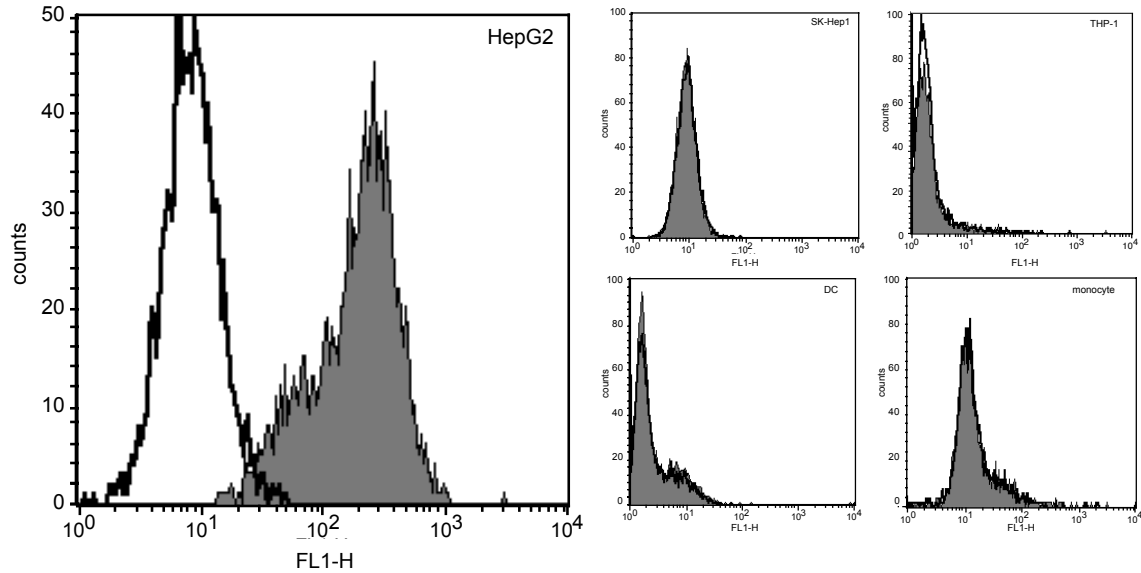


Figure 96: Flow cytometry of not fixed HepG2, SK-Hep1, THP-1, macrophages and dendritic cells, which were indirectly extracellularly stained with C09.1 IgG1 and FITC-labeled goat anti-mouse Ig (H+L). The dead propidium-stained cells were excluded. The histogram shows an overlay with the negative control (irrelevant IgG).

3.5.3.3.2 Immunofluorescence microscopy

The specific endocytosis of the Texas Red-labeled C09.1 IgG1 into HepG2 cells via the ASGPR was analyzed. To exclude the unspecific internalization, SK-Hep1 cells were stained in parallel (see Figure 97).

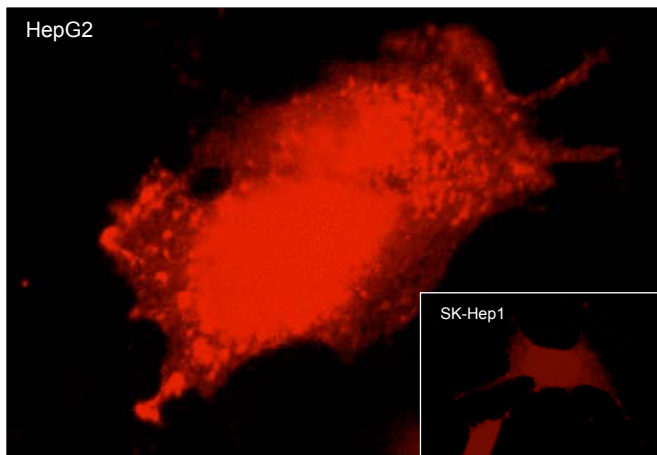


Figure 97: Immunofluorescence microscopy picture of the directly stained HepG2 and SK-Hep1 cells. The TR-labeled C09.1 IgG1 (40 µg/ml, 45 nM) were internalized into living cells, followed by paraformaldehyde fixation of cells.

The HepG2 cells were strewn with very bright large spots, but the SK-Hep1 showed only some single spots. This indicated, that the labeled C09.1 was internalized and exclusively by the ASGPR-mediated endocytosis.

3.5.3.4 *On tissue characterization*

3.5.3.4.1 Immunohistochemistry

Non-pathological human paraffin-embedded liver tissue sections were indirectly stained with DAB, to test the binding ability of C09.1. The antigen was retrieved with various steamer, microwave and enzymatic methods.

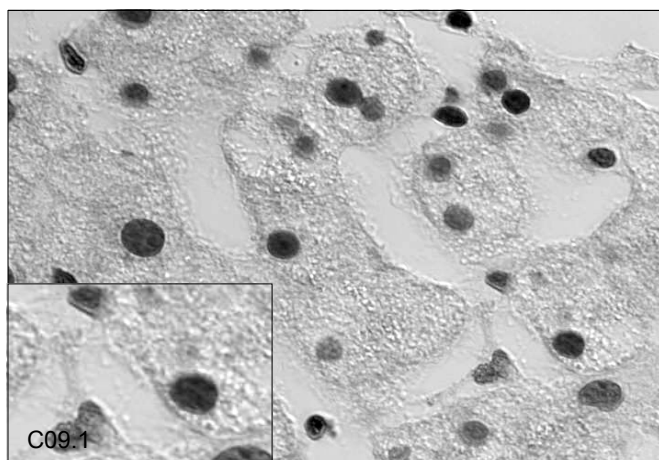


Figure 98: Indirect stained non-pathological paraffin-embedded liver tissue (antigen retrieval with microwave at 98°C for 30min and staining with C09.1 at 4µg/ml, DAB).

No binding of the C09.1 was visible, independent of the tissue pretreatment for antigen retrieval (see Figure 98).

3.5.4 Monoclonal C11.1 IgG1

3.5.4.1 Purification of C11.1 IgG1

The extraction of murine C11.1 IgG1 by Protein L and Protein G chromatography was tested.

Purification by Protein L spin chromatography

The IgG1 κ antibodies were purified from culture supernatant of C11.1, supplemented with 10% FCS, using Protein L-Sepharose spin columns. However, almost no antibodies were eluted. On a silver-stained reducing SDS-PAGE gel, hardly any 25kDa and 55kDa bands were detectable and in the HRP-ELISA, the supernatant and the flow through showed about the same absorbance, whereas the elution was negative. Therefore this method was unsuitable for the C11.1 IgG1 κ extraction.

Purification by Protein G FPLC

The IgG1 were also extracted from culture supernatant of C11.1, supplemented with 3% FCS (low IgG) by FPLC, using a Protein G-Sepharose column. The extraction was not quantitative and therefore, the supernatant was cleared twice. The antibodies eluted in a sharp peak and were highly pure. On a reducing SDS-PAGE gel, only the 25kDa and the 55kDa band of the light and heavy chain were visible (see Figure 99).

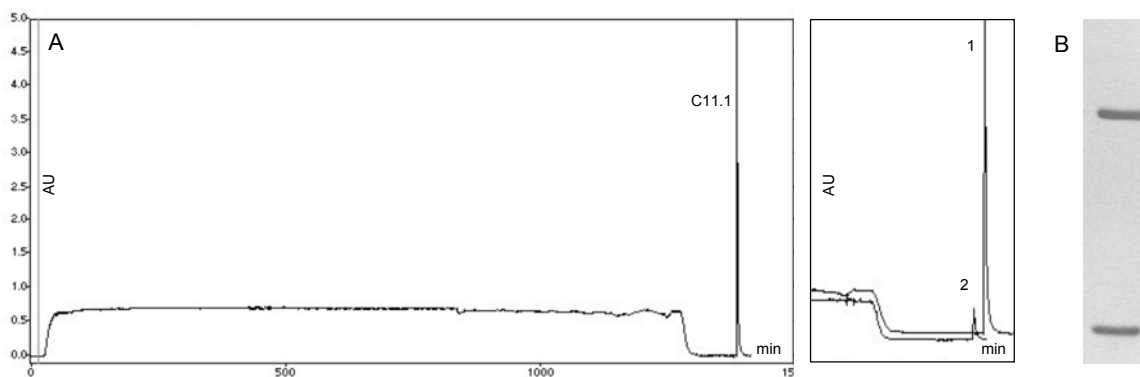


Figure 99: Extraction of the IgG1 from 250ml culture supernatant of C11.1, which contained 3% FCS (low IgG). A: Protein G FPLC chromatogram with elution peaks of the first (1) and the second (2) extraction. B: Silver-stained reducing SDS-PAGE gel 12% of the eluted antibodies, showing the 25kDa and the 55kDa bands of the light and the heavy chain.

The yield was determined by A_{280} measurement, by SDS-PAGE quantification and by Bradford micro-assay. 6.45mg C11.1 IgG1 antibodies were purified from 500ml culture supernatant. That is equivalent to a yield of 12.9mg/L supernatant (see Figure 100).

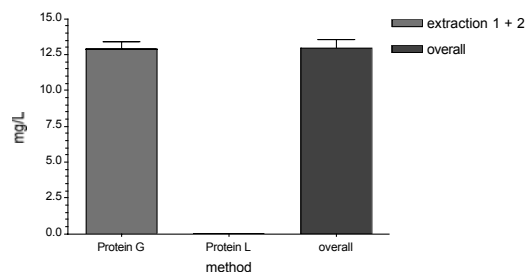


Figure 100: Yield of the C11.1 IgG1, purified by affinity to Protein G and Protein L and quantified by Bradford micro-assay, SDS-PAGE quantification and absorbance A_{280} measurement. Overall, the obtained yield was 12.867mg/L (SEM 0.521mg/L) culture supernatant of C11.1.

3.5.4.2 *In vitro* characterization

3.5.4.2.1 Immunoblotting

Identical amounts of the reduced, non-reduced and native H1-CRD as well as of the reduced-alkylated and native-alkylated H1-CRD were blotted to nitrocellulose and were immunostained with 5 μ g/ml and 0.5 μ g/ml C11.1 IgG1 (see Figure 101).

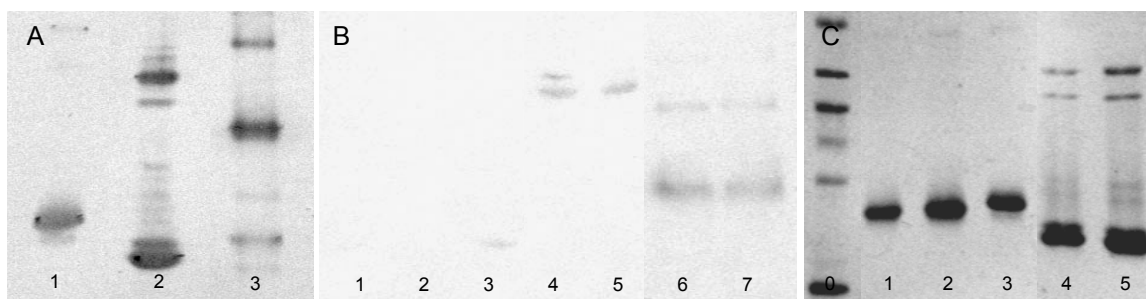


Figure 101: Immunoblot of the H1-CRD, caught with the monoclonal C11.1 IgG1. 1 μ g/band H1-CRD on PAGE gels 15% under reducing, non-reducing denatured or native conditions were blotted to nitrocellulose and were immunostained with C11.1 IgG1, followed by the detection with AP-labeled goat anti-mouse IgG (whole molecule), in dilution 1:5000. A: Blot, stained with 5 μ g/ml C11.1 IgG1, showing the reduced (1), non-reduced (2) and native (3) H1-CRD. B: Blot, stained with 0.5 μ g/ml C11.1 IgG1, showing reduced (1), the reduced state of reduced-alkylated (2), the reduced state of native-alkylated (3), non-reduced (4), the non-reduced state of native-alkylated (5), native (6) and the native state of native-alkylated (7) H1-CRD. C: Silver-stained reducing and non-reducing SDS-PAGE gel 15% of the same probes used in B (1-5) and the LMW marker (0).

The bands pattern and the relative intensities of bands were identical on the Ponceau S-stained membrane and on the silver-stained PAGE gel (see Figure 101C). The bands of the dimeric H1-CRD species were less stained on the gel than the monomeric species, independent of their alkylation state.

The C11.1 IgG1 antibodies specifically recognized monomeric and dimeric H1-CRD species. No cross-reaction occurred with the LMW marker proteins, even not at the higher C11.1 concentration of 5 μ g/ml. Also 0.5 μ g/ml C11.1 IgG1 still stained reduced,

non-reduced and native H1-CRD, although the reduced form only fair. Looking at the non-reduced and native blot, the bands of the dimeric species resulted in a stronger signal than of the monomeric species, in contrast to the PAGE gel, which showed vice versa staining intensities.

Overall, the C11.1 binding depended on the H1-CRD conformation and disulfide bridges. The strongest bands were obtained for binding to the native, decreasing to the non-reduced and the reduced H1-CRD. Furthermore, the recognition was influenced by the alkylation. The reduced H1-CRD, which was previously not alkylated or native-alkylated was stained, whereas with the reduced H1-CRD, which was reduced-alkylated before, no staining was observed.

3.5.4.2.2 ELISA

In an HRP-ELISA, the monoclonal C11.1 IgG1, in the concentration range of 0.1 - 300nM, were titrated to 5 μ g/ml H1-CRD (300 μ M) and were detected with HRP-labeled goat anti-mouse Ig (H+L) in dilution 1:1000. For the half maximal binding, an EC₅₀ of 0.304nM was calculated (see Figure 102).

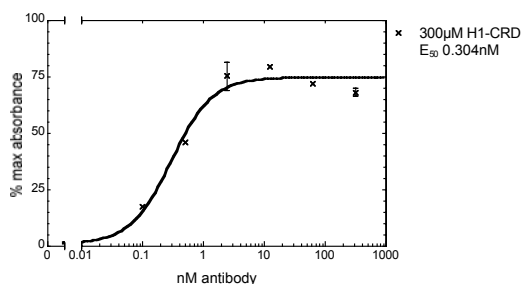


Figure 102: Binding of the C11.1 IgG1 to the H1-CRD in an HRP-ELISA. C11.1 was titrated in the range of 0.1-300nM in duplicate (exponential dilution row), in the presence of 20mM calcium. The plate was coated with 5 μ g/ml (300 μ M) H1-CRD and C11.1 was detected with HRP-labeled goat anti-mouse Ig (H+L), diluted 1:1000. The EC₅₀ was calculated, using a nonlinear regression fit (equation sigmoid dose-response, variable slope, r^2 0.98) of Prism4 software.

The calcium sensitivity of the C11.1 IgG1 binding to the H1-CRD in an HRP-ELISA was checked. C11.1 was caught in the presence of 20mM calcium, 1mM calcium or 10mM EDTA. In the buffer of all prior steps 1mM calcium, and of all following steps 20mM calcium was included.

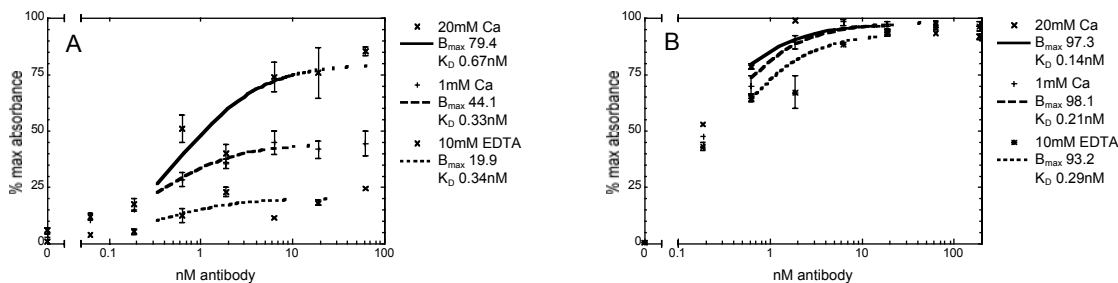


Figure 103: Ca sensitivity of the C11.1 IgG1 binding to the H1-CRD in an HRP-ELISA in the presence of 20mM calcium, 1mM calcium or of 10mM EDTA. The plates were coated with 3µg/ml (175µM) (A) or 6µg/ml (350µM) (B) H1-CRD and the C11.1 IgG1 was titrated in the range of 0.0625-62.5nM (A) or 0.1875-187.5nM (B) in triplicate. B_{max} and K_D were calculated, using a nonlinear regression fit (equation one site binding, hyperbola, r^2 0.67 – 0.99).

At the detection limit of the HRP-ELISA, when coating with 175µM H1-CRD to catch C11.1 IgG1 in the concentration range of 0 - 62.5nM, the binding was not only dependent on the presence, but also on the concentration of calcium. With 20mM calcium, a maximal binding B_{max} of 79.4% was obtained, nearly double the B_{max} of 44.1% with 1mM calcium or four times the B_{max} of 19.9% with 10mM EDTA (see Figure 103A).

In contrast, at the higher coating concentration of 350µM H1-CRD and titrating C11.1 in the range of 0 - 187.5nM, the same maximal bindings B_{max} of 97-98% with 1mM and 20mM calcium, and only a slightly lower B_{max} of 93% with 10mM EDTA were received. In addition K_D differed, showing the lowest K_D of 0.14nM for binding with 20mM calcium followed by a K_D of 0.21nM with 1mM calcium and a K_D of 0.29nM with 10mM EDTA (see Figure 103B). All in all it can be supposed, that the binding of C11.1 to the H1-CRD is calcium-sensitive, and that the binding decreases without calcium.

3.5.4.2.3 GalNAc-polymer assay

In the GalNAc-polymer assay, 0 - 625nM C11.1 IgG1 competed against 0.3µg/ml POD-labeled β -GalNAc-biotin-streptavidin-polymer, for binding to the H1-CRD, in the presence of 1mM calcium (see Figure 104).

The high effective concentration EC_{50} of 790nM indicated, that the C11.1 IgG1 not or fairly competed with the GalNAc-complex for binding to the binding site, but more probable sterically hindered the binding at a higher antibody concentration.

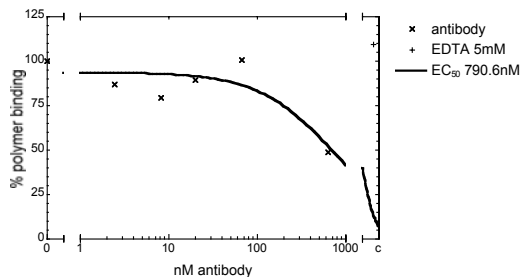


Figure 104: Competition of the GalNAc-polymer and the C11.1 IgG1 antibodies for binding to the H1-CRD in the polymer assay. The plate was coated with 3 μ g/ml (175 μ M) H1-CRD. The C11.1 in the range of 0-625nM (exponential dilution) in triplicates competed with 0.3 μ g/ml GalNAc-complex (nonlinear regression fit: equation, one site competition, r^2 0.81).

3.5.4.2.4 Biacore

The binding of galactose to the monomeric and the dimeric H1-CRD species was not affected by the presence of a constant concentration of C11.1 IgG1, in a Biacore assay. The first galactose signal prior to the C11.1 application and the second signal after C11.1 binding differed less than 10% (see Figure 105A).

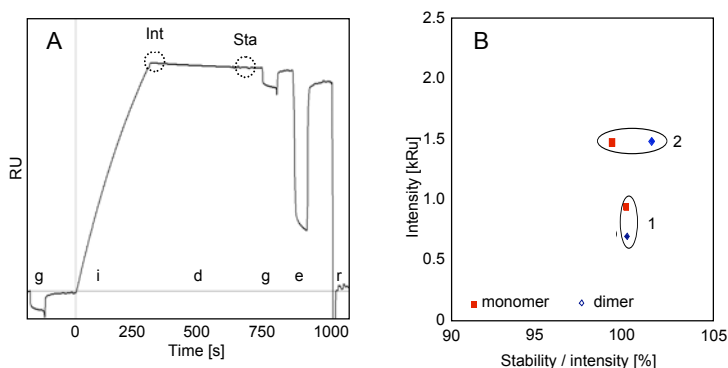


Figure 105: Biacore assay of the C11.1 IgG1 binding to monomeric and dimeric H1-CRD. A: Sensogram with a preliminary injection of 5mM galactose (g), C11.1 IgG1 injection (i), dissociation phase (d), followed by a second 5mM galactose injection and an EDTA pulse (e), prior to the regeneration with HCl (r). The data points, used for blotting (Int, Sta) are circled. B: Intensity after 5min injection (Int), blotted against the quotient of the stability after 5min dissociation (Sta) and the intensity in buffer with 50mM calcium (1) or 3mM EDTA (2).

The C11.1 binding to the H1-CRD was negative calcium-sensitive, showing an identical stability, but only half the intensity in the presence of calcium. Dependent on calcium and EDTA, the interaction of C11.1 with monomeric and dimeric H1-CRD differed. In the presence of calcium, the binding intensity of dimeric H1-CRD was lower than of monomeric H1-CRD, with identical stabilities. In contrast, in the presence of EDTA, the binding stability was higher with identical intensities (see Figure 105B).

In the absence of calcium, C11.1 IgG1 at different concentrations in the range of 0.14 - 140nM bound concentration-dependent, fast and tight. The association rate to the monomeric H1-CRD surface with a k_{on} of $3.29 \cdot 10^5 M^{-1} s^{-1}$ was faster than to the dimeric H1-CRD surface with a k_{on} of $1.92 \cdot 10^5 M^{-1} s^{-1}$. The dissociation was extremely slow, especially from the dimeric surface. As a consequence, the dissociation rate and the K_D could only be calculated for binding of monomeric H1-CRD with a k_{off} of $2.58 \cdot 10^{-5} s^{-1}$ and a K_D of 78pM. Lower on and off rates of the C11.1 interaction with monomeric compared to dimeric H1-CRD species indicated a slower but tighter binding, resulting in an increased affinity (see Figure 106A and B).

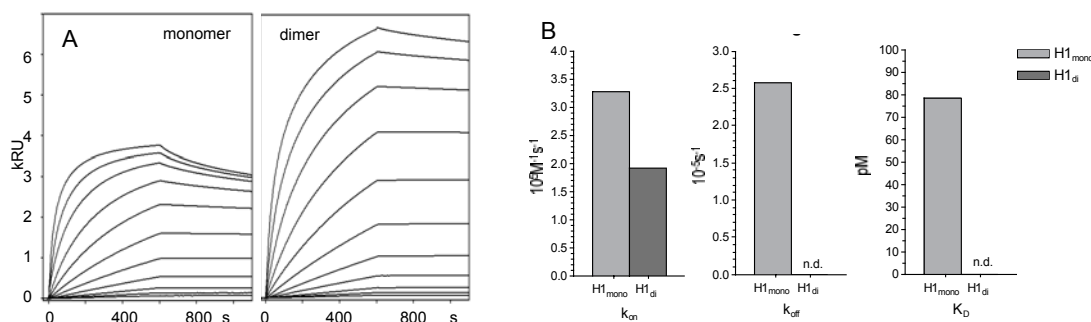


Figure 106: Comparison of the kinetic on and off rates of the C11.1 IgG1 binding to the monomeric and dimeric H1-CRD species surface, after fitting to a Langmuir 1:1 binding model. A: Sensogram of the C11.1 IgG1 binding to the H1-CRD in calcium-free buffer. B: calculated k_{on} , k_{off} and calculated K_D .

3.5.4.2.5 Epitope excision and extraction

The C11.1 epitope extraction from reduced-alkylated and trypsin-digested H1-CRD showed mainly the two fragments F2 (T⁶-R¹⁷) and F7 (F⁵⁴-K⁷⁶), but also F9 (N⁸⁹-R¹¹⁷) in the MS elution spectrum. All other peaks, which originated from H1-CRD, appeared in the wash too (see Figure 107).

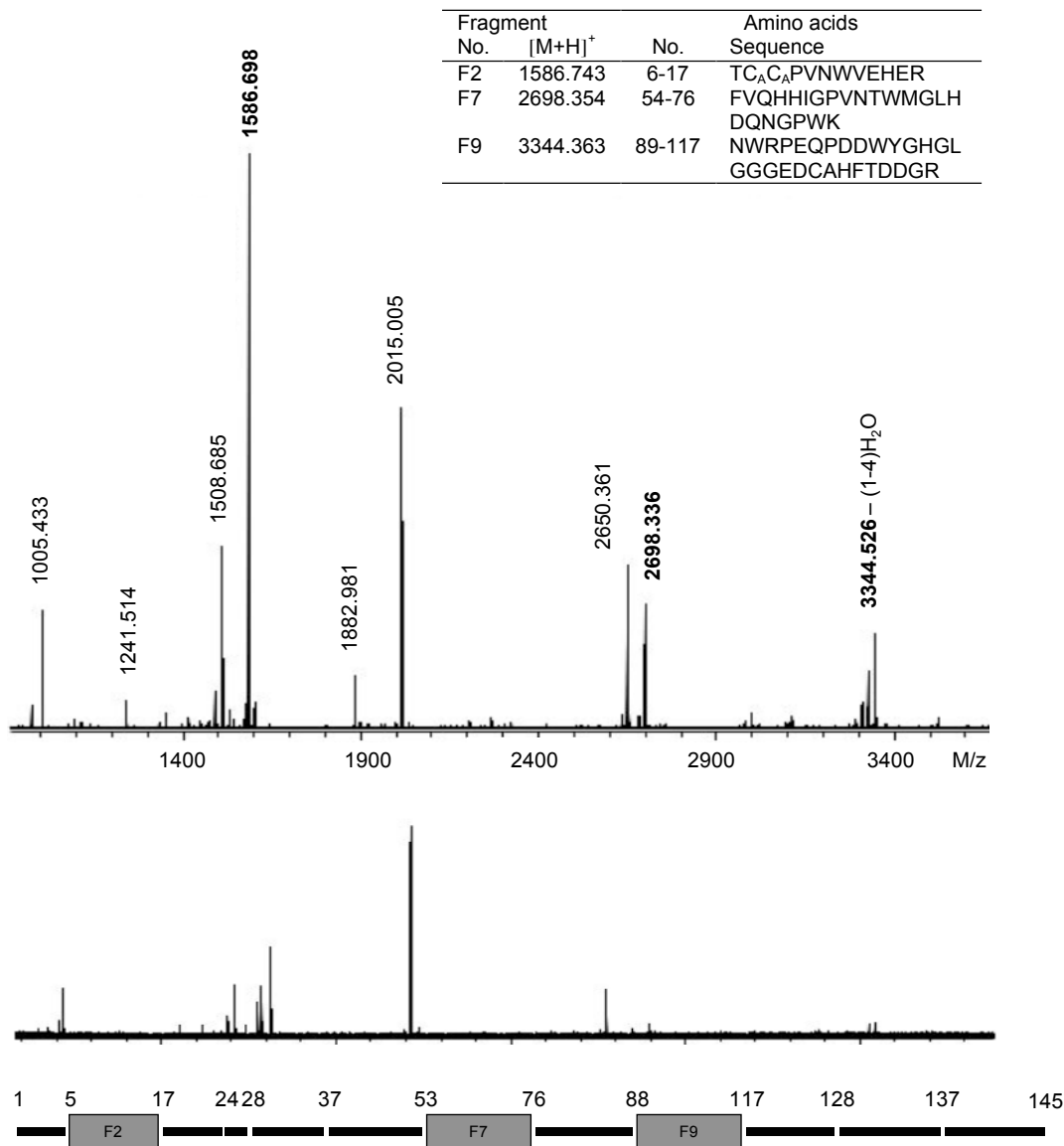


Figure 107: MALDI-FT-ICR of the elution spectrum (A) and the wash spectrum (B) in the epitope extraction of reduced-alkylated and trypsin-digested H1-CRD, using a C11.1-Sepharose column.

In an additional experiment, after binding of reduced-alkylated trypsin-digested H1-CRD fragments to immobilized C11.1, the epitope was further excised with pronase K. Among many peaks in the MS elution spectrum, some peaks were identified that corresponded to partial sequences of fragment F9 and overlapped in the residues W⁹⁰-D⁹⁶ (see Figure 108).

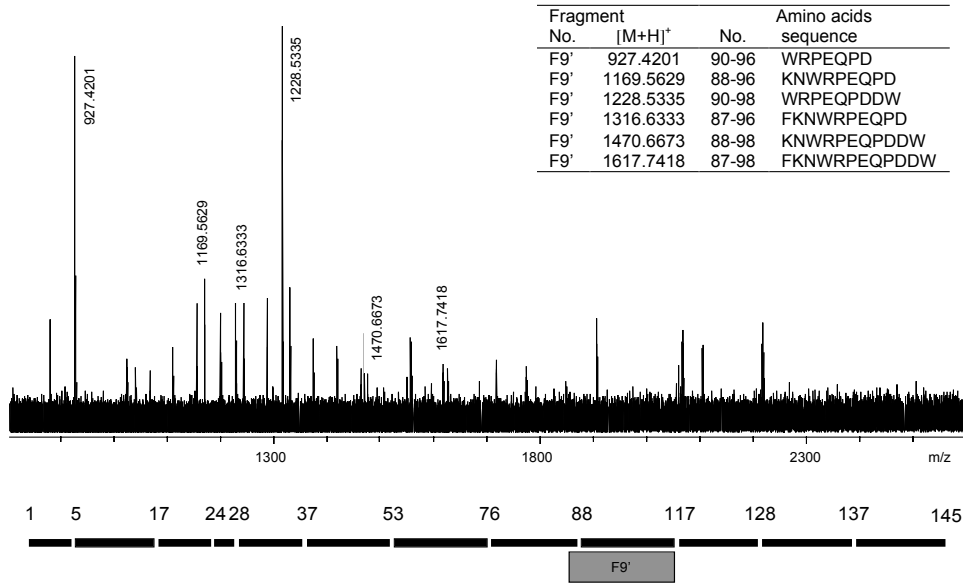


Figure 108: MALDI-FT-ICR of the elution spectrum in the epitope extraction of trypsin-digested H1-CRD, excised with pronase K on column. The wash spectrum was clean (spectrum not shown).

3.5.4.3 On cell characterization

3.5.4.3.1 Immunofluorescence flow cytometry

The ASGPR-positive HepG2 cells, the ASGPR-negative SK-Hep1 cells, THP-1 cells, primary human macrophages and dendritic cells were indirectly extracellularly stained with C11.1 IgG1 and FITC-labeled goat anti-mouse Ig (see Figure 109).

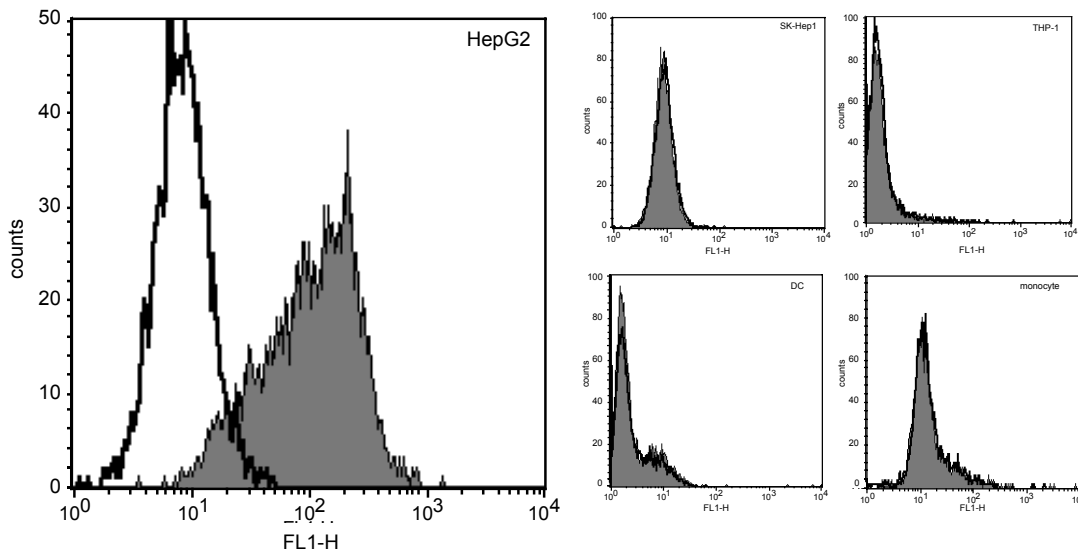


Figure 109: Flow cytometry of not fixed HepG2, SK-Hep1, THP-1, macrophages and dendritic cells, which were indirectly extracellularly stained with C11.1 IgG1 and FITC-labeled goat anti-mouse Ig(H+L). The dead propidium-stained cells were excluded. The histogram shows the overlay with an irrelevant IgG (negative control).

The C11.1 IgG1 specifically bound to the entire ASGPR. Only the HepG2, but not the SK-Hep1 cells, were stained. In addition, they did not cross-react with THP-1, macrophages or dendritic cells, which are known to carry a homologous receptor.

3.5.4.3.2 Immunofluorescence microscopy

The endocytosis of the Texas Red-labeled C11.1 IgG1 into living HepG2 cells was investigated by immunofluorescence microscopy, after paraformaldehyde fixation of the cells. SK-Hep1 cells were stained in parallel to control the internalization, specifically to be mediated via the ASGPR.

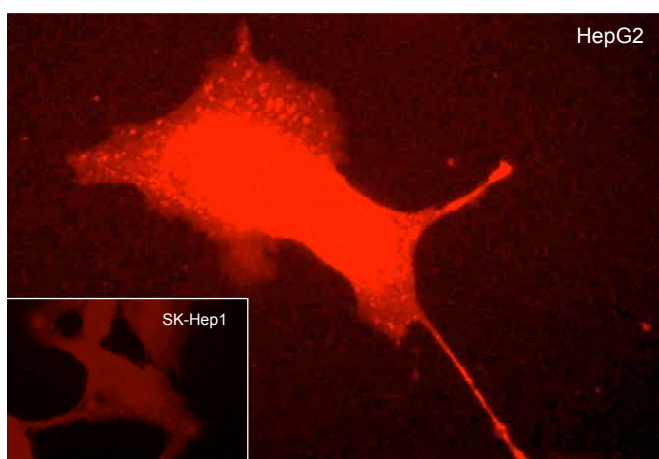


Figure 110: Immunofluorescence microscopy picture of the directly stained HepG2 and SK-Hep1 cells. The TR-labeled C11.1 IgG1 (40 μ g/ml, 45nM) was endocytosed into living cells, followed by paraformaldehyde fixation of the cells.

The HepG2 cells were strewn with very bright spots, whereas the SK-Hep1 showed only some or no single spots. Hence, the TR-C11.1 was internalized mainly via the ASGPR (see Figure 110).

3.5.4.4 *On tissue characterization*

3.5.4.4.1 Immunohepatochemistry

Non-pathological human paraffin-embedded liver tissue sections were indirectly stained with DAB, to test the binding ability of C11.1. The antigen was retrieved with various steamer, microwave and enzymatic methods.

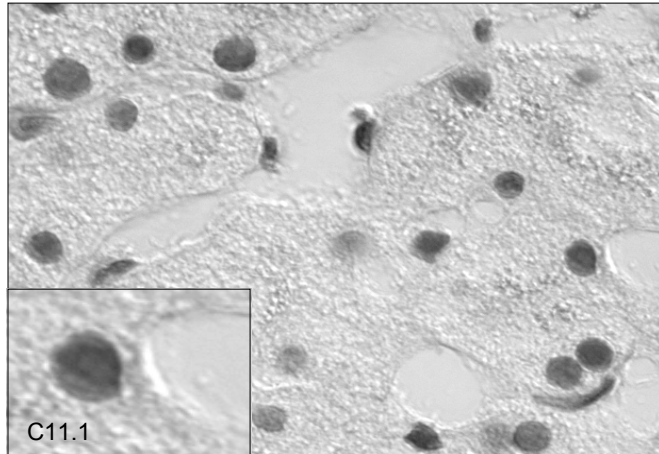


Figure 111: Indirect staining of non-pathological paraffin-embedded liver tissue (antigen retrieval with microwave at 98°C for 30min and staining with C11.1 at 4 μ g/ml, DAB).

No binding of the C11.1 to the hepatocytes surface was visible, independent of the tissue pretreatment for antigen retrieval (see Figure 111).

3.5.5 Monoclonal C14.6 IgG2a

3.5.5.1 Purification of C14.6 IgG2a

The purification of C14.6 IgG2a by affinity chromatography on Protein L and Protein G-Sepharose was investigated.

Purification by Protein L spin chromatography

The purification of IgG2a κ from culture supernatant of C14.6, which contained 10% FCS, using a Protein L-Sepharose spin column, was not suitable. A silver-stained reducing SDS-PAGE gel showed, that the yield was minute and the purity low.

Purification by Protein G FPLC

The purification of IgG2a from culture supernatant of C14.6, which contained 3% FCS (low IgG), by FPLC using a Protein G-Sepharose column, was very effective and nearly quantitative in one extraction step. The eluted antibodies were high concentrated and of excellent purity. On a reducing SDS-PAGE gel only the 25kDa light chain and the 55kDa heavy chain bands were detected (see Figure 112).

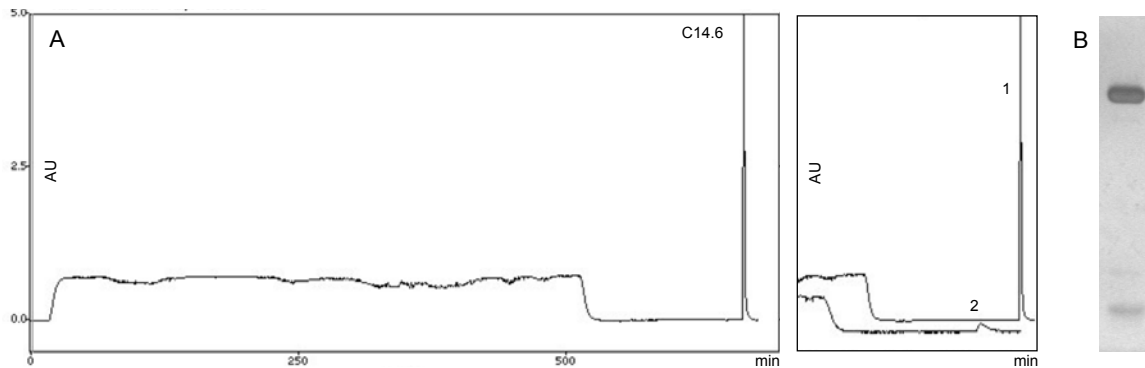


Figure 112: Purification of the IgG2a from 200ml culture supernatant of clone 14.6, containing 3% FCS (low IgG). A: Protein G FPLC chromatogram and the elution peak of extraction 1 (1) and 2 (2). B: Silver-stained reducing SDS-PAGE gel 12% of the eluted antibodies, showing the 25kDa and 55kDa bands of the light and heavy chain.

The quantification by A_{280} measurement, by SDS-PAGE and by Bradford micro-assay, resulted in a yield of 20.7mg/L for the first extraction and of only 0.3mg/L for the second extraction from culture supernatant of clone C14.6 (see Figure 113).

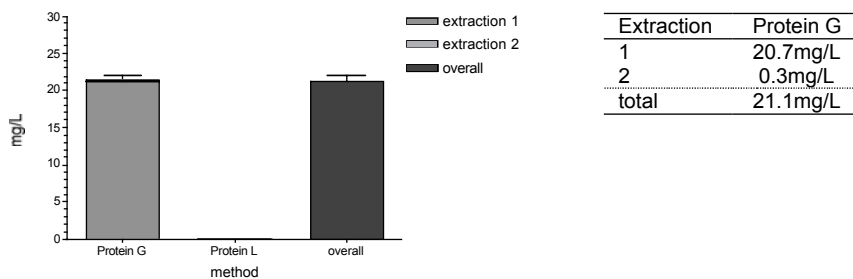


Figure 113: Yield of the C14.6 IgG2a, purified by affinity to Protein G and Protein L and quantified by Bradford micro-assay, SDS-PAGE quantification and absorbance A_{280} measurement. Overall, obtained yield was 21.098mg/L (SEM 1.086mg/L) culture supernatant of C14.6.

Overall, 10.6mg C14.6 IgG2a were purified from 500ml culture supernatant. This is equivalent to a yield of 21.1mg/L culture supernatant.

3.5.5.2 *In vitro* characterization

3.5.5.2.1 Immunoblotting

Identical amounts of the reduced, non-reduced and native H1-CRD as well as of the reduced-alkylated and native-alkylated H1-CRD were blotted to nitrocellulose and were stained, using 5 μ g/ml and 0.5 μ g/ml C14.6 IgG2a.

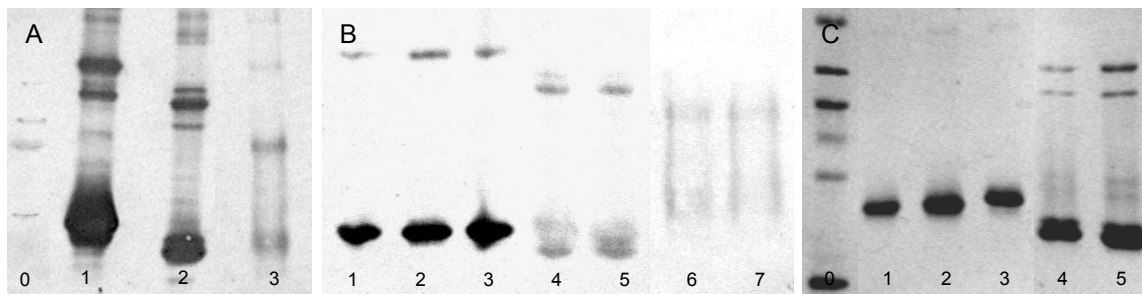


Figure 114: Immunoblot of the H1-CRD, caught with the monoclonal C14.6 IgG2a. 1 μ g/band H1-CRD on PAGE gels 15% under reducing, non-reducing denatured or native conditions were blotted to nitrocellulose and were immunostained with C14.6 IgG2a, followed by the detection with AP-labeled goat anti-mouse IgG (whole molecule), in dilution 1:5000. A: Blot, stained with 5 μ g/ml C14.6 IgG2a, showing the reduced (1), non-reduced (2) and native (3) H1-CRD. B: Blot stained with 0.5 μ g/ml C14.6 IgG2a, showing reduced (1), the reduced state of reduced-alkylated (2), the reduced state of native-alkylated (3), non-reduced (4), the non-reduced state of native-alkylated (5), native (6) and the native state of native-alkylated (7) H1-CRD. C: Silver-stained reducing and non-reducing SDS-PAGE gel 15% of the same probes used in B (1-5) and of the LMW marker (0).

The Ponceau S-stained membrane and the silver-stained PAGE gel of H1-CRD showed the same bands pattern. On both, the band intensities of the dimeric species were higher than of the monomeric species (see Figure 114C). The staining was independent of the H1-CRD alkylation state.

The monoclonal C14.6 IgG2a specifically recognized the monomeric and dimeric H1-CRD in reduced, non-reduced and native state, but also cross-reacted with trypsinogen of the LMW marker. When using C14.6 IgG2a at a concentration of 0.5 μ g/ml, the strongest stain was obtained with the reduced H1-CRD, followed by the non-reduced and native H1-CRD, which both showed approximately the same intensities. Furthermore, the binding was not dependent on the alkylation. No differences in the bands pattern and intensities were ascertained, when the alkylated forms were compared to the not alkylated forms within the reduced, non-reduced or native H1-CRD, respectively. The monomeric and dimeric species of the non-reduced and native H1-CRD showed about the same signal intensities (see Figure 114A and B).

3.5.5.2.2 ELISA

The C14.6 IgG2a antibodies were titrated in the concentration range of 0.1 - 300nM in an HRP-ELISA. When the plate was coated with 5 μ g/ml (300 μ M) H1-CRD and IgG2a was detected with HRP-labeled goat anti-mouse Ig (H+L), diluted 1:1000, an EC₅₀ of 9.7nM was calculated (see Figure 115).

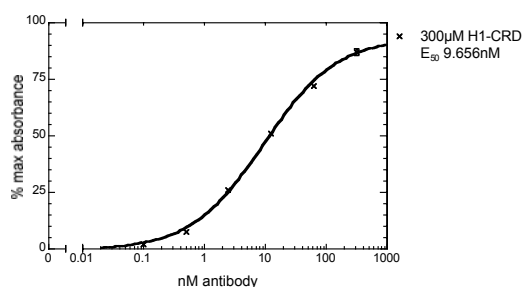


Figure 115: Binding of the C14.6 IgG2a to the H1-CRD in an HRP-ELISA. C14.6 was titrated in the range of 0.1-300nM, in duplicate (exponential dilution row), in the presence of 20mM calcium. The plate was coated with 5 μ g/ml (300 μ M) H1-CRD and C14.6 was detected with HRP-labeled goat anti-mouse Ig (H+L), diluted 1:1000. The EC₅₀ was calculated, using a nonlinear regression fit (equation sigmoid dose-response, variable slope, r^2 1.00) of Prism4 software.

To test the calcium sensitivity of the binding to the H1-CRD, the C14.6 IgG2a antibodies were titrated in the presence of 20mM calcium, 1mM calcium and 10mM EDTA. All incubation steps prior to the C14.6 capturing included 1mM calcium and all following steps contained 20mM calcium.

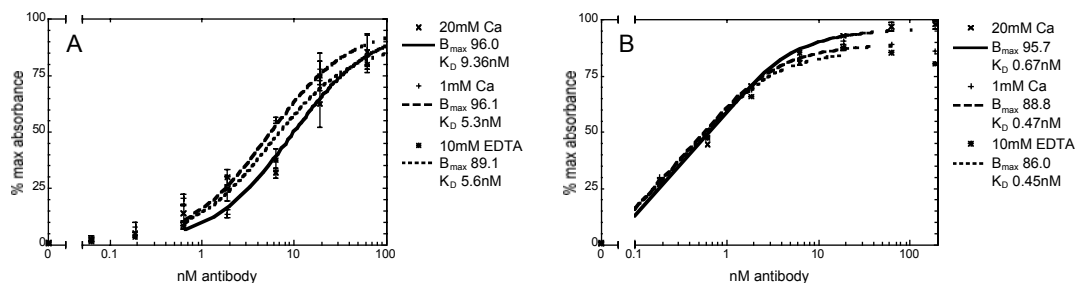


Figure 116: Ca sensitivity of the C14.6 IgG2a binding to the H1-CRD in an HRP-ELISA in the presence of 20mM calcium, 1mM calcium or of 10mM EDTA. The plates were coated with 3µg/ml (175µM) (A) or 6µg/ml (350µM) (B) H1-CRD and the C14.6 IgG2a was titrated in the range of 0.0625-62.5nM (A) or 0.1875-187.5nM (B) in triplicate. B_{max} and K_D were calculated, using a nonlinear regression fit (equation one site binding, hyperbola, r^2 0.91 – 0.99).

The binding of C14.6 IgG2a in concentrations of 0 – 187.5nM was not calcium-sensitive, neither when coating with 175µM nor with 350µM H1-CRD. In the first case, the estimated K_D varied only slightly in the range of 5.3-9.4nM and B_{max} of 90-96%. In the second case, a K_D in the range of 0.45-0.67nM and B_{max} of 86-96% were assessed (see Figure 116A and B).

3.5.5.2.3 GalNAc-polymer assay

The competition of 0 - 625nM C14.6 IgG2a and 0.3µg/ml POD-labeled streptavidin-biotin β-GalNAc-polymer for the binding to the H1-CRD was investigated in the presence of 1mM calcium.

The C14.6 IgG2a prevented the binding of the GalNAc-complex to the H1-CRD. The calculated concentration for the half maximal effect EC_{50} was low with 22.5nM (see Figure 117).

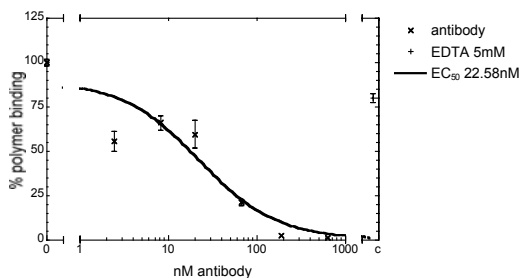


Figure 117: Competition of the GalNAc-polymer and the C14.6 IgG2a antibodies for binding to the H1-CRD in a polymer assay. The plate was coated with 3µg/ml (175µM) H1-CRD. C14.6 in the range of 0-625nM (exponential dilution) in triplicate or tetruplicate, competed with 0.3µg/ml GalNAc-complex for binding (nonlinear regression fit: equation, one site competition, r^2 0.86).

3.5.5.3 On cell characterization

3.5.5.3.1 Immunofluorescence flow cytometry

The C14.6 IgG2a binding to the whole ASGPR was controlled by extracellular flow cytometry of HepG2 and the cross-reactivity was checked by immunofluorescence staining of SK-Hep1, THP-1, human macrophages and human dendritic cells.

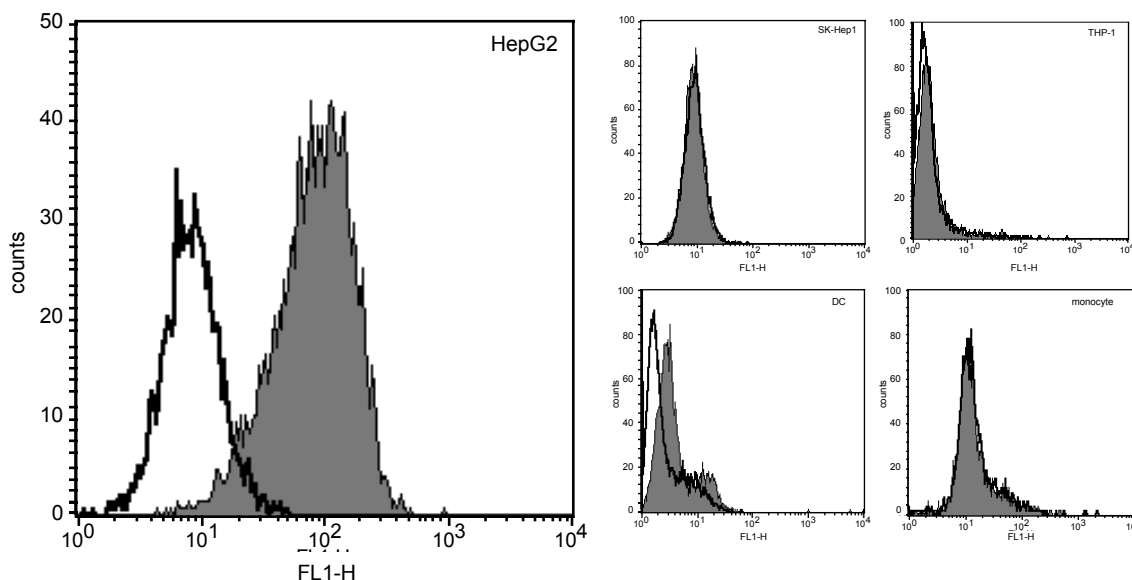


Figure 118: Flow cytometry of not fixed HepG2, SK-Hep1, THP-1, macrophages and dendritic cells, when indirectly extracellularly stained with C14.6 IgG2a and FITC-labeled goat anti-mouse Ig (H+L). The dead propidium-stained cells were excluded. The histogram shows an overlay with the negative control (irrelevant IgG).

C14.6 IgG2a specifically stained the ASGPR-positive HepG2 cells, but not the ASGPR-negative SK-Hep1 cells. However, they also slightly cross-reacted with epitopes on the surface of human dendritic cells, which carry a homologous receptor. Human macrophages were not stained (see Figure 118).

3.5.5.3.2 Immunofluorescence microscopy

The specific endocytosis of Texas Red-labeled C14.6 IgG2a into living cells via the ASGPR was investigated with HepG2 cells, using SK-Hep1 cells for the detection of unspecific internalization. After internalization, cells were fixed with paraformaldehyde.

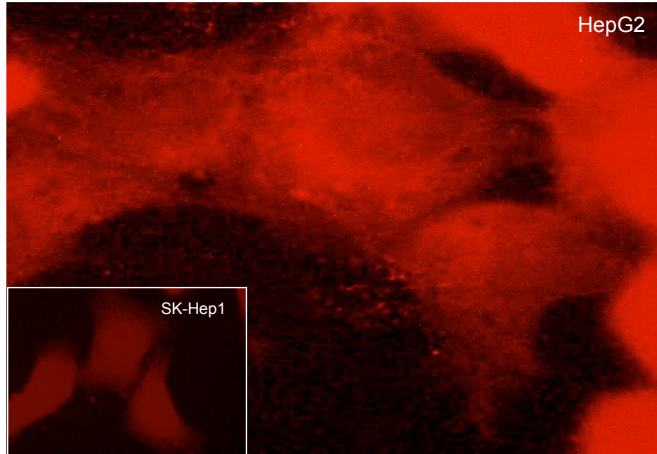


Figure 119: Immunofluorescence microscopy picture of the directly stained HepG2 and SK-Hep1 cells. , The TR-labeled C14.6 IgG2a (40 μ g/ml, 45nM) were internalized into living cells, followed by paraformaldehyde fixation of cells.

The HepG2 cells were highly strewn with very bright spots, whereas the SK-Hep1 showed only some spots. Therefore, the labeled C14.6 seemed to be internalized and this mainly by the ASGPR (see Figure 119).

3.5.5.4 *On tissue characterization*

3.5.5.4.1 Immunohepatochemistry

Non-pathological human paraffin-embedded liver tissue sections were indirectly stained with DAB to test the binding ability of C14.6. The antigen was retrieved with various steamer, microwave and enzymatic methods.

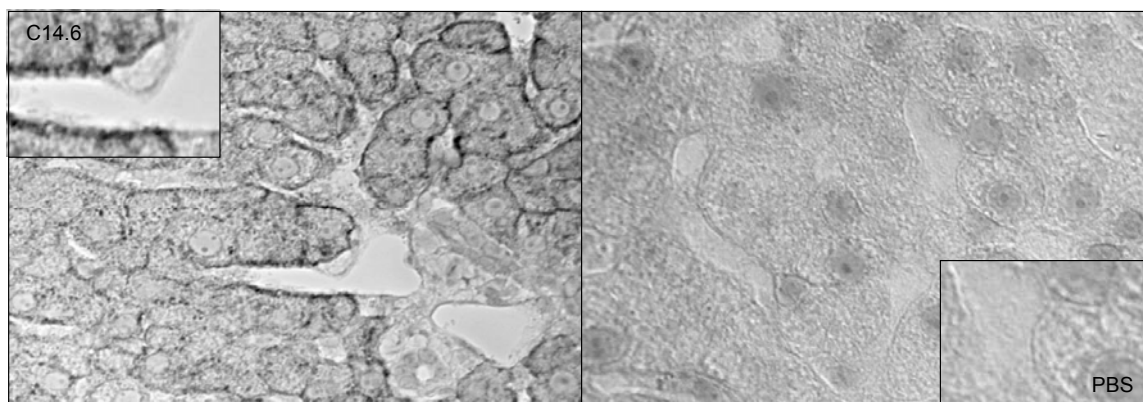


Figure 120: Indirect staining of paraffin-embedded non-pathological liver tissue (antigen retrieval with microwave at 98 $^{\circ}$ C for 30min and staining with C14.6 at 6 μ g/ml, DAB).

C14.6 specifically stained the sinusoidal surface of hepatocytes (see Figure 120).

3.5.6 Monoclonal C18.1 IgG1

3.5.6.1 Purification of C18.1 IgG1

The murine C18.1 IgG1 purification by Protein L and Protein G affinity chromatography was tested.

Purification by Protein L spin chromatography

The IgG1 κ purification from culture supernatant of clone 18.1, which contained 10% FCS, using Protein L-Sepharose spin columns, was not effective. The silver-stained reducing SDS-PAGE gel showed, that the yield was minute and the purity low. In an HRP-ELISA, it was confirmed, that the extraction failed as the supernatant and the flow through exhibited approximately the same absorbance.

Purification by Protein G FPLC

The IgG1 purification from culture supernatant of clone 18.1, which contained 3% FCS (low IgG) by FPLC, using Protein G-Sepharose, was successful (see Figure 121A). The supernatant was cleared twice, although in the first extraction already 95% of the antibodies were bound. Eluted IgG1 were highly pure. On a reducing SDS-PAGE gel only the 25kDa and the 55kDa band of light and heavy chains were visible (see Figure 121B).

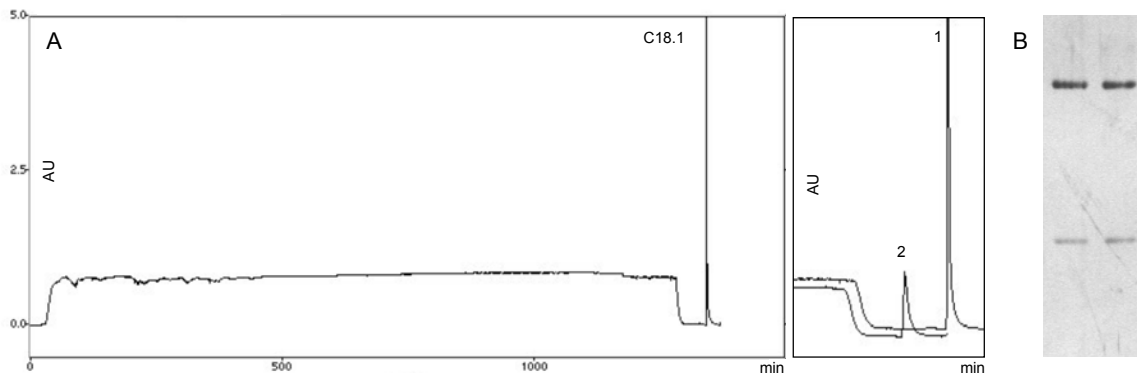


Figure 121: Extraction of the IgG1 from 250ml culture supernatant of clone C18.1, containing 3% FCS (low IgG). A: Protein G FPLC chromatogram with elution peaks of the first (1) and the second (2) extraction. B: Silver-stained reducing SDS-PAGE gel 12% of the eluted antibodies, showing the 25kDa light and the 55kDa heavy chain band.

A reliable quantification was achieved with a triple determination by A_{280} measurement, by SDS-PAGE and by Bradford micro-assay. The yield was 20.8mg/L culture

supernatant, with 19.8mg/L for the first extraction and 1.0mg/L for the second extraction (see Figure 122).

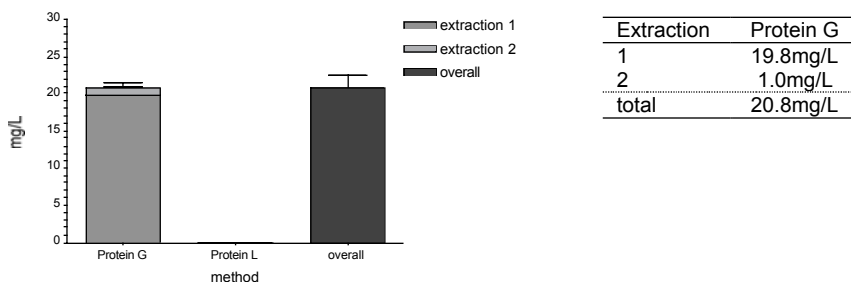


Figure 122: Yield of C18.1 the IgG1, purified by affinity to Protein G and Protein L and quantified by Bradford micro-assay, SDS-PAGE quantification and absorbance A_{280} measurement. Overall, a yield of 20.814mg/L (SEM 1.733mg/L) culture supernatant of C18.1 was obtained.

Overall, 10.4mg IgG1 were purified from 500ml culture supernatant of clone C18.1.

3.5.6.2 *In vitro* characterization

3.5.6.2.1 Immunoblotting

Identical amounts of the reduced, non-reduced and native H1-CRD as well as of the reduced-alkylated and native-alkylated H1-CRD were blotted to nitrocellulose and were caught with 5 μ g/ml and 0.5 μ g/ml C18.1 IgG1 during immunostaining.

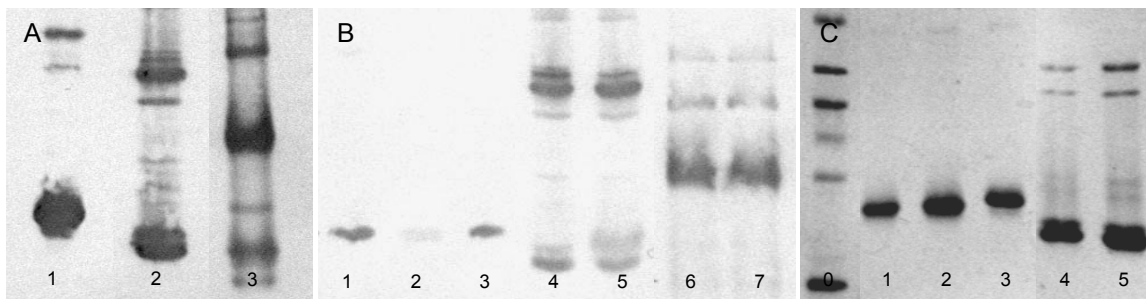


Figure 123: Immunoblot of the H1-CRD, caught with the monoclonal C18.1 IgG1. 1 μ g/band H1-CRD on PAGE gels 15% under reducing, non-reducing denatured or native conditions were blotted to nitrocellulose and were immunostained with C18.1 IgG1, followed by the detection with AP-labeled goat anti-mouse IgG (whole molecule), in dilution 1:5000. A: Blot, stained with 5 μ g/ml C18.1 IgG1, showing the reduced (1), non-reduced (2) and native (3) H1-CRD. B: Blot, stained with 0.5 μ g/ml C18.1 IgG1, showing reduced (1), The reduced state of reduced-alkylated (2), the reduced state of native-alkylated (3), non-reduced (4), The non-reduced state of native-alkylated (5), native (6) and the native state of native-alkylated (7) H1-CRD. C: Silver-stained reducing and non-reducing SDS-PAGE gel 15% of the same probes used in B (1-5) and of the LMW marker (0).

The bands pattern and the relative intensities of bands were identical on the Ponceau S-stained membrane and on the silver-stained PAGE gel. The monomeric H1-CRD

species were stronger stained than the dimeric species. The stain was independent of the H1-CRD alkylation (see Figure 123C).

The monoclonal C18.1 IgG1 specifically interacted with the monomeric and dimeric H1-CRD in reduced, non-reduced and native state. Even at the high IgG1 concentration of 5µg/ml, no cross-reactions with LMW marker proteins were visible.

On blots, which were stained with 0.5µg/ml C18.1 IgG1, the antibody recognized the reduced, non-reduced and native H1-CRD. However, the stain intensities varied in dependence of the H1-CRD alkylation. Interestingly, the reduced H1-CRD, which was previously reduced-alkylated was minute stained, whereas the interaction of C18.1 with reduced H1-CRD, which was not alkylated or native-alkylated before was strong. The previously not alkylated or native-alkylated non-reduced and native H1-CRD, respectively were bound to a similar extent.

In contrast to the band intensities on the silver-stained PAGE gel, the dimeric H1-CRD species on the blots were more intensely stained than monomeric species (see Figure 123).

3.5.6.2.2 ELISA

The C18.1 IgG1 were titrated in a HRP-ELISA in the concentration range of 0 - 300nM, after coating the plate with 5µg/ml (300µM) H1-CRD. An effective concentration EC_{50} of 0.495nM was calculated for the half maximal binding (see Figure 124).

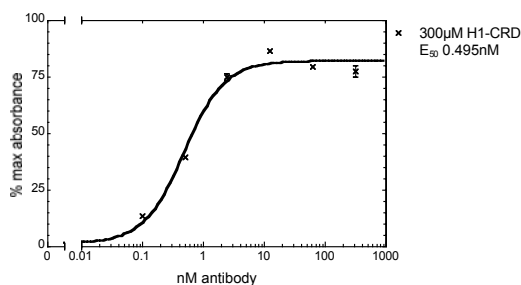


Figure 124: Binding of the C18.1 IgG1 to the H1-CRD in an HRP-ELISA. C18.1 was titrated in the range of 0.1-300nM, in duplicate (exponential dilution row) in the presence of 20mM calcium. The plate was coated with 5µg/ml (300µM) H1-CRD and C18.1 was detected with HRP-labeled goat anti-mouse Ig (H+L) diluted 1:1000. The EC_{50} was calculated, using a nonlinear regression fit (equation sigmoid dose-response, variable slope, r^2 0.99) of Prism4 software.

The calcium sensitivity of the C18.1 IgG1 binding to the H1-CRD in an HRP-ELISA was investigated. All incubation steps were identical, except the C18.1 capturing step, which was performed in the presence of 20mM calcium, 1mM calcium or 10mM EDTA. In all preceding steps 1mM calcium and in all following steps 20mM calcium were included.

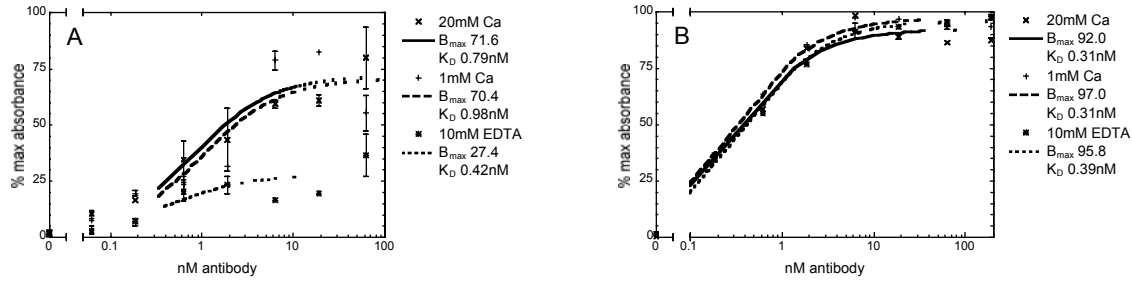


Figure 125: Ca sensitivity of the C18.1 IgG1 binding to the H1-CRD in an HRP-ELISA in the presence of 20mM calcium, 1mM calcium or 10mM EDTA. The plates were coated with 3µg/ml (175µM) (A) or 6µg/ml (350µM) (B) H1-CRD and the C18.1 IgG1 was titrated in the range of 0.0625-62.5nM (A) or 0.1875-187.5nM (B) in triplicate. B_{max} and K_D were calculated, using a nonlinear regression fit (equation one site binding, hyperbola, r^2 0.82 – 0.99).

When coating only with 175µM H1-CRD, the interaction with C18.1 IgG1 in concentrations of 0 - 62.5nM was calcium-sensitive, but independent of calcium concentration level. In the presence of calcium, B_{max} of 70-72% and K_D of 0.76-0.98nM were higher compared to B_{max} 27% and K_D 0.42nM, in the absence of calcium (see Figure 125A). In contrast, when a higher amount of 350mM H1-CRD was used for coating, the binding to C18.1 in the range of 0 - 87.5nM differed neither in B_{max} nor K_D , independent of calcium (see Figure 125B).

3.5.6.2.3 GalNAc-polymer assay

In the GalNAc-polymer assay, 0.3µg/ml POD-labeled streptavidin-biotin β -GalNAc-polymer and 0 - 625nM C18.1 IgG1 competed for binding to the H1-CRD in the presence of 1mM calcium.

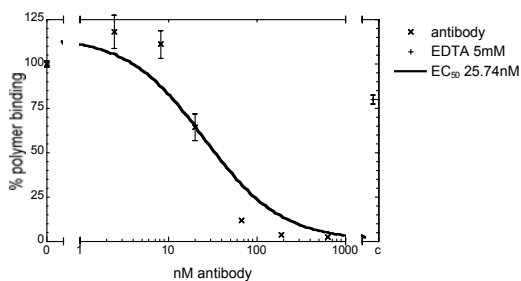


Figure 126: Competition of the GalNAc-polymer and the C18.1 IgG1 antibodies for the binding to the H1-CRD in a polymer assay. The plate was coated with 3µg/ml (175µM) H1-CRD. The C14.6 in the range of 0-625nM (exponential dilution) in triplicate or tetricate competed with 0.3µg/ml GalNAc-complex for binding (nonlinear regression fit: equation, one site competition, r^2 0.88).

The C18.1 IgG1 antibodies hindered the binding of the GalNAc-complex to the H1-CRD in a concentration-dependent manner. The calculated concentration for the half maximal effect EC_{50} was 25.7nM (see Figure 126).

3.5.6.2.4 Biacore

In a Biacore assay, the C18.1 IgG1 at a constant concentration did not affect the galactose binding to monomeric and dimeric H1-CRD, and therefore, did not block the binding site. The difference between the first galactose signal prior to the antibody capturing, and the second galactose signal when antibodies were bound, was below 10% (see Figure 127A).¹⁴⁰

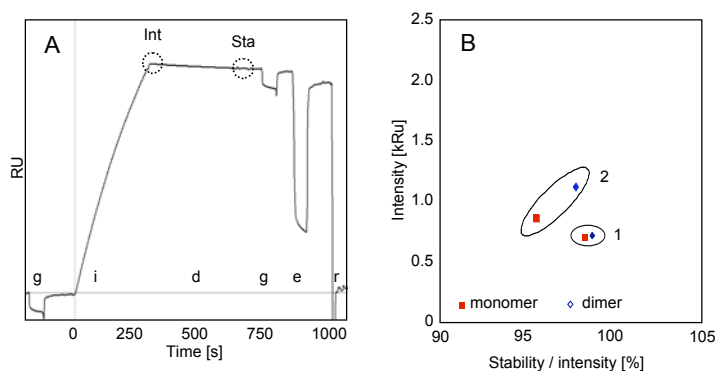


Figure 127: Biacore assay of the C18.1 IgG1 binding to the monomeric and the dimeric H1-CRD. A: Sensogram, with a preliminary injection of 5mM galactose (g), C18.1 IgG1 injection (i), dissociation phase (d), followed by a second 5mM galactose injection and an EDTA pulse (e), prior to the regeneration with HCl (r). Data points, used for blotting (Int, Sta), are indicated by circles. B: Intensity after 5min injection (Int), blotted against the quotient of the stability after 5min dissociation (Sta) and the intensity in buffer with 50mM calcium (1) or 3mM EDTA (2).

The binding was slightly calcium-sensitive. Especially the binding stability of C18.1 to the H1-CRD decreased, when EDTA was present. The strengths of the C18.1 interactions were similar and calcium-independent, except with dimeric H1-CRD, which showed an increased intensity in the presence of EDTA (see Figure 127B).

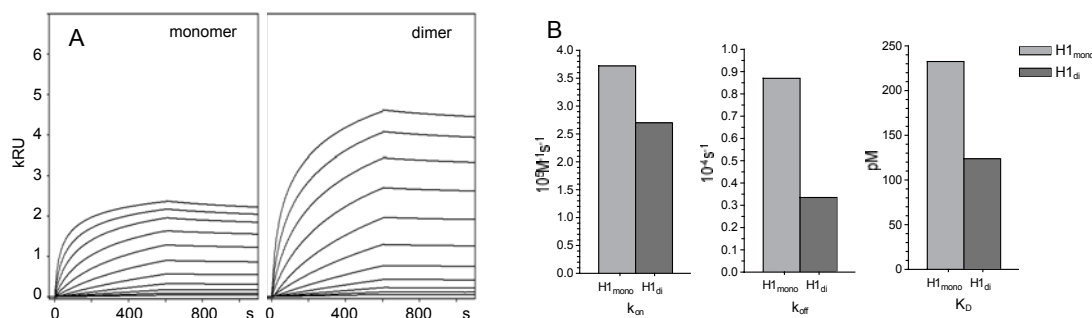


Figure 128: Comparison of the kinetic on and off rates of the C18.1 IgG1 binding to the monomeric and the dimeric H1-CRD species surface, after fitting to a Langmuir 1:1 binding model. A: Sensogram of the C18.1 IgG1 binding to H1-CRD in calcium-free buffer. B: Calculated k_{on} , k_{off} and calculated K_D .

In the presence of 3mM EDTA, the C18.1 IgG1 injected at concentrations 0.14 to 140nM interacted fast, tight and in a concentration-dependent manner with dimeric and monomeric H1-CRD (see Figure 128A).

The affinity of C18.1 IgG1 to the dimeric H1-CRD with a K_D of 124pM was nearly double than to the monomeric H1-CRD with a K_D of 233pM (see Figure 128B). This was mainly caused by the much lower off-rate of the dimer binding (k_{on} $2.70 \cdot 10^5 M^{-1} s^{-1}$ and k_{off} $3.34 \cdot 10^{-5} s^{-1}$) compared to monomer binding (k_{on} $3.73 \cdot 10^5 M^{-1} s^{-1}$ and k_{off} $8.69 \cdot 10^{-5} s^{-1}$).

3.5.6.2.5 Epitope excision and extraction

The C18.1 epitope extraction and excision failed with native as well as with reduced-alkylated H1-CRD. The change of the proteolytic enzyme, using α -chymotrypsine instead of trypsin did not improve the results too. Hence, the results were not reliable.

3.5.6.3 On cell characterization

3.5.6.3.1 Immunofluorescence flow cytometry

The interaction of C18.1 IgG1 with the native entire ASGPR, and the cross-reactivity with similar receptors was tested by extracellular flow cytometry. Not fixed HepG2, SK-Hep1, THP-1, macrophages and dendritic cells were indirectly stained with FITC.

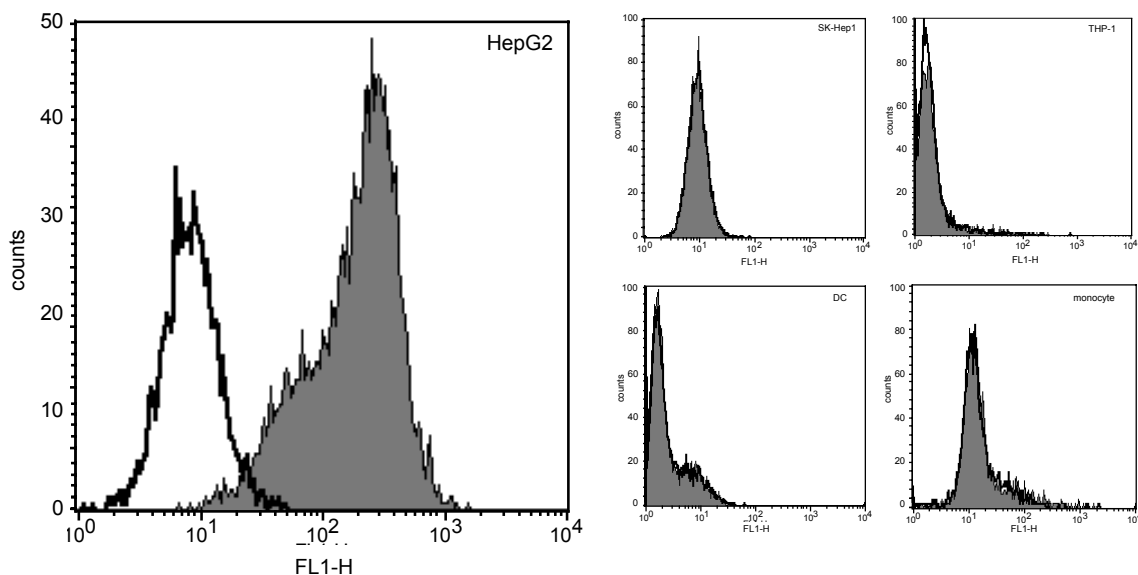


Figure 129: Flow cytometry of not fixed HepG2, SK-Hep1, THP-1, macrophages and dendritic cells, which were indirectly extracellularly stained with C18.1 IgG1 and FITC-labeled goat anti-mouse Ig (H+L). The dead propidium-stained cells were excluded. The histogram shows an overlay with the negative control (irrelevant IgG).

The C18.1 antibodies specifically stained the ASGPR-positive HepG2 cells, but not the ASGPR-negative SK-Hep1 cells. No binding to the surface of THP-1 cells, macrophages or dendritic cells, which are known to carry a homologous receptor, was detected (see Figure 129).

3.5.6.3.2 Immunofluorescence microscopy

The specific endocytosis of Texas Red-labeled C18.1 IgG1 into living HepG2 cells via the ASGPR was tested by immunofluorescence microscopy. SK-Hep1 cells were stained in parallel, to distinguish the specific and the unspecific internalization.

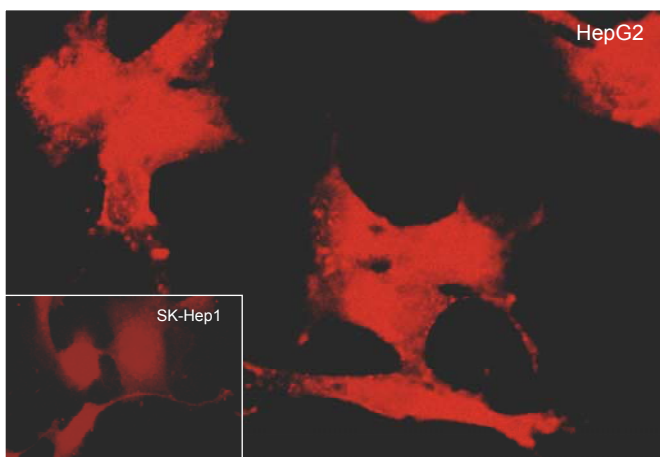


Figure 130: Immunofluorescence microscopy picture of the directly stained HepG2 and SK-Hep1 cells. The TR-labeled C18.1 IgG1 (40 μ g/ml, 45nM) was internalized into living cells, followed by paraformaldehyde fixation of cells.

The C18.1 was internalized and this primarily by the ASGPR. The HepG2 cells were strewn with very bright spots, whereas in the SK-Hep1, only some single or no spots were visible (see Figure 130).

3.5.6.4 *On tissue characterization*

3.5.6.4.1 Immunohepatochemistry

Non-pathological human paraffin-embedded liver tissue sections were indirectly stained with DAB, to test the binding ability of C18.1. The antigen was retrieved with various steamer, microwave and enzymatic methods.

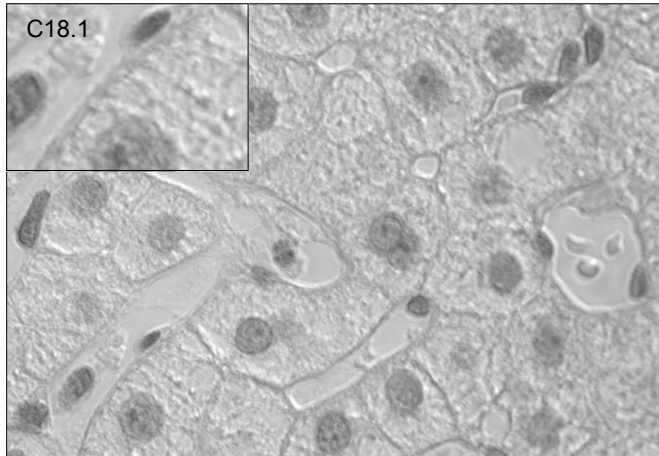


Figure 131: Indirectly stained paraffin-embedded non-pathological liver tissue section (antigen retrieval with microwave at 98°C for 30min and staining with C18.1 at 4 μ g/ml, DAB).

No binding of C18.1 to the hepatocyte surface was visible, independent of the tissue pretreatment for the antigen retrieval (see Figure 131).

3.5.7 Monoclonal C23.8 IgG1

3.5.7.1 Purification of C23.8 IgG1

The purification of C23.8 IgG1 by different affinity chromatographic methods, using Protein L, Protein G and H1-Sepharose, were tested.

Purification by Protein L spin chromatography

The IgG1 κ extraction from culture supernatant of clone C23.8, containing 10% FCS, using Protein L-Sepharose spin columns resulted in only partially pure antibodies. On the silver-stained reducing SDS-PAGE gel, beside the 25kDa light and the 55kDa heavy chain band, mainly a 66kDa band was visible, which was supposed to originate from BSA of the FCS (see Figure 132B). The HRP-ELISA confirmed, that only a fraction of C23.8 IgG1 κ was extracted. Approximately the same absorbances were obtained for the supernatant and the flow through.

Purification by H1-CRD FPLC

The IgG1 were purified from culture supernatant of clone C23.8, which contained 10% FCS, by FPLC, using an H1-Sepharose column. The antibodies were only partially pure. In addition to the 25kDa and 55kDa bands of the light and heavy chains, a double band of an approximately 66kDa protein was visible on the reducing SDS-PAGE gel (see Figure 132). An HRP-ELISA confirmed, that the antibody extraction had been effective, as the flow through was only slightly positive, compared to the supernatant.

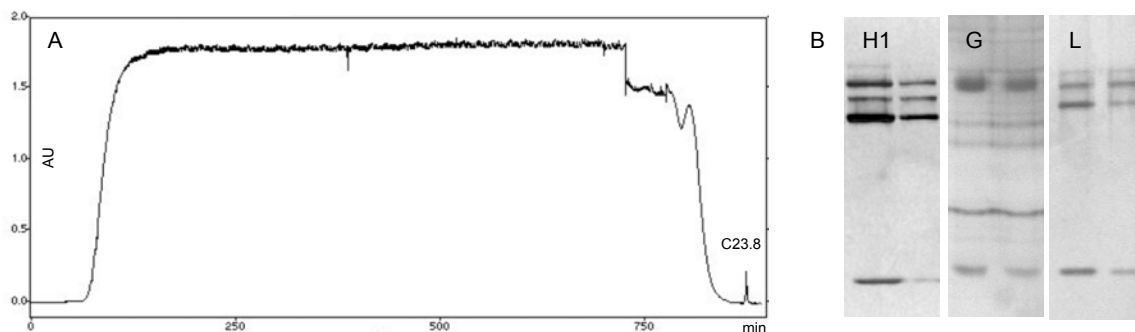


Figure 132: Extraction of the IgG1 from culture supernatant of clone C23.8, containing 10% FCS. A: H1-CRD FPLC chromatogram. B: Silver-stained reducing SDS-PAGE gel 12% of the eluted antibodies from H1-CRD FPLC (H1), from Protein G FPLC (G) and from Protein L spin columns (L), showing the 25kDa light chain band, three bands of impurities in Protein G-purified antibodies, the 55kDa heavy chain band and one or two other bands of about 66kDa in H1 and Protein L-purified antibodies, probably also glycosylated heavy chains.

Purification by Protein G FPLC

The purification of IgG1 from culture supernatant of C23.8, containing 3% FCS (low IgG), by FPLC, using a Protein G-Sepharose column, was not successful. Only a minute elution peak was detected, but an additional prepeak appeared at the end of the loading, when the column flow was stopped for an instant to change from loading to the washing buffer. The purity of the eluted antibodies was good (see Figure 132). The HRP-ELISA indicated, that the bad yield was mainly due to an extremely low C23.8 IgG1 concentration in the culture supernatant and not due to a weak extraction efficiency.

The purified C23.8 IgG1 antibodies were quantified by SDS-PAGE and by Bradford micro-assay. The highest yield was obtained, when C23.8 IgG1 were purified by H1-CRD FPLC with 4.6mg/L supernatant, followed by extraction on Protein L with 3.1mg/L supernatant. The Protein G chromatography of C23.8 yielded only 1.0mg/L supernatant (see Figure 133).

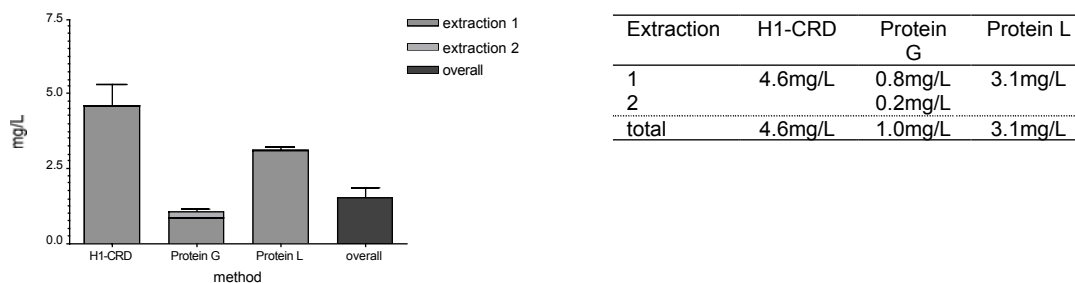


Figure 133: Yield of the C23.8 IgG1, purified by affinity to H1-CRD, Protein G and Protein L and quantified by Bradford micro-assay and SDS-PAGE quantification. Overall yield received was 1.516mg/L (SEM 0.330mg/L) culture supernatant of C23.8.

Overall, 0.55mg C23.8 IgG1 were purified, which is equivalent to a yield of 1.5mg/L supernatant.

3.5.7.2 *In vitro* characterization

3.5.7.2.1 Immunoblotting

Identical amounts of the reduced, non-reduced and native H1-CRD as well as of the reduced-alkylated and native-alkylated H1-CRD were blotted to nitrocellulose and were captured with 5µg/ml or 0.5µg/ml C23.8 IgG1 antibodies during immunostaining.

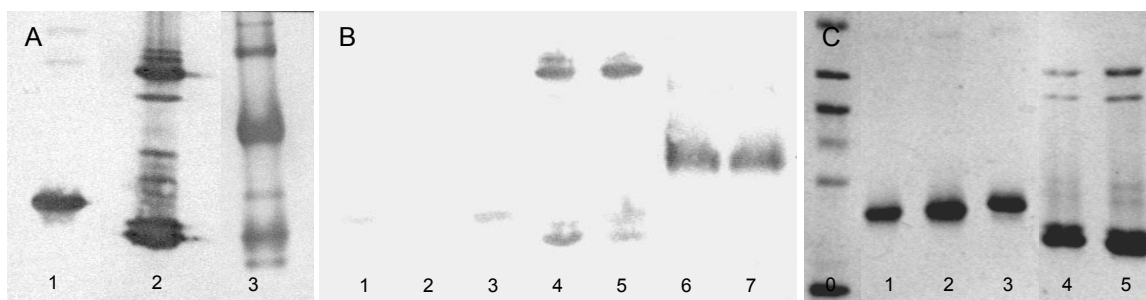


Figure 134: Immunoblot of the H1-CRD, caught with the monoclonal C23.8 IgG1. 1µg/band H1-CRD on PAGE gels 15% under reducing, non-reducing denatured or native conditions were blotted to nitrocellulose and were immunostained with C23.8 IgG1, followed by the detection with AP-labeled goat anti-mouse IgG (whole molecule), in dilution 1:5000. A: Blot, stained with 5µg/ml C23.8 IgG1, showing the reduced (1), non-reduced (2) and native (3) H1-CRD. B: Blot, stained with 0.5µg/ml C23.8 IgG1, showing reduced (1), the reduced state of reduced-alkylated (2), the reduced state of native-alkylated (3), non-reduced (4), the non-reduced state of native alkylated (5), native (6) and the native state of native-alkylated (7) H1-CRD. C: Silver-stained reducing and non-reducing SDS-PAGE gel 15% of the same probes used in B (1-5) and the LMW marker (0).

The Ponceau S-stained membrane and the silver-stained PAGE showed the same bands pattern and relative band intensities (see Figure 134C). The main fraction was monomeric H1-CRD species and only a minor fraction was dimeric species. Within reduced, non-reduced or native H1-CRD, respectively, the staining was independent of the H1-CRD alkylation state.

The C23.8 IgG1 specifically bound reduced, non-reduced and native H1-CRD, with increasing intensities in this order. Even at a high IgG1 concentration of 5µg/ml, no cross-reactions with proteins of the LMW were detected.

When capturing the H1-CRD with only 0.5µg/ml IgG1, the antibodies still bound to the H1-CRD, but with varying intensities in dependence of the alkylation state. The reduced H1-CRD, which was reduced-alkylated before was only minute recognized. In contrast, the binding of reduced, non-reduced and native H1-CRD was not affected by the alkylation, as a similar and strong staining was obtained with not alkylated and native-alkylated states of the H1-CRD.

Interestingly, although the main fraction of the H1-CRD was monomeric, the bands of the dimeric species were stronger immunostained than of the monomeric species. This effect was obvious for non-reduced H1-CRD, and much stronger for native H1-CRD (see Figure 134).

3.5.7.2.2 ELISA

In an HRP-ELISA the C23.8 IgG1 antibodies in concentrations of 0 - 300nM were bound to H1-CRD (5µg/ml, 300µM) and were detected with HRP-labeled goat anti-mouse Ig

(H+L) diluted 1:1000. The calculated concentration for the half maximal effect EC_{50} was 0.457nM (see Figure 135).

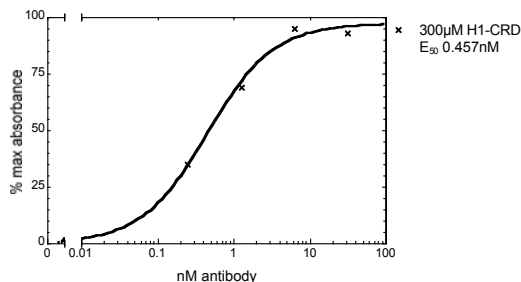


Figure 135: Binding of the C23.8 IgG1 to the H1-CRD in an HRP-ELISA. The C23.8 antibodies were titrated in the range of 0.1-300nM, in duplicate (exponential dilution row) in the presence of 20mM calcium. The plate was coated with 5µg/ml (300µM) H1-CRD and C23.8 was detected with HRP-labeled goat anti-mouse Ig (H+L), diluted 1:1000. The EC_{50} was calculated, using a nonlinear regression fit (equation sigmoid dose-response, variable slope, r^2 1.00) of Prism4 software.

The calcium sensitivity of the C23.8 IgG1 binding to the H1-CRD was checked in an HRP-ELISA. The C23.8-capturing step was performed in the presence of 20mM calcium, 1mM calcium or 10mM EDTA, whereas all other steps were identical. The preceding incubations were run in the presence of 1mM calcium, whereas following steps included 20mM calcium.

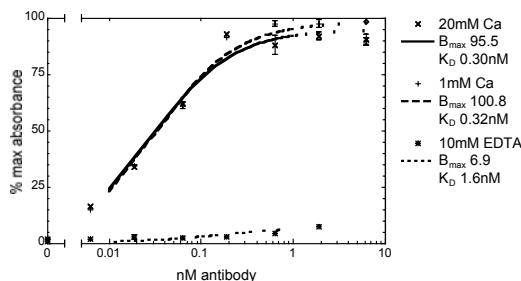


Figure 136: Ca sensitivity of the C23.8 IgG1 binding to the H1-CRD in an HRP-ELISA in the presence of 20mM calcium, 1mM calcium or 10mM EDTA. The plates were coated with 3µg/ml H1-CRD and the C23.8 IgG1 was titrated in the range of 0.0625-6.25nM in triplicate. B_{max} and K_D were calculated, using a nonlinear regression fit (equation one site binding, hyperbola, r^2 0.95-0.98).

On plates, coated only with 175µM H1-CRD, the binding of the C23.8 IgG1 in the range of 0 - 6.25nM to the H1-CRD was calcium-sensitive. However, the interaction was not dependent on the calcium concentration level, as the same binding behavior was obtained in the presence of 20mM and of 1mM calcium, showing a K_D of 0.3 and B_{max} of 96- 101%. In contrast, in the absence of calcium, in 10mM EDTA, C18.1 bound extremely weak with a K_D of 1.6nM and B_{max} of 7% (see Figure 136).

3.5.7.2.3 GalNAc-polymer assay

0.3 μ g/ml POD-labeled streptavidin-biotin β -GalNAc-polymer and C23.8 IgG1 antibodies in concentrations of 0 - 18.75nM competed for binding to H1-CRD in the presence of 1mM calcium.

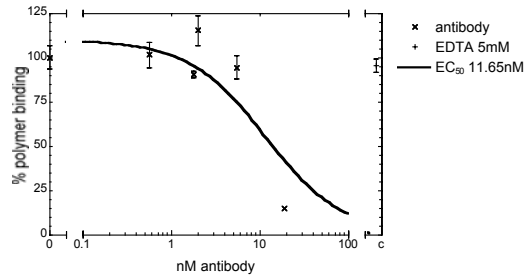


Figure 137: Competition of the GalNAc-complex and the C23.8 IgG1 antibodies for binding to the H1-CRD in a polymer assay. The plate was coated with 3 μ g/ml (175 μ M) H1-CRD. The C23.8 in the range of 0-18.75nM (exponential dilution) in triplicate or tetruplicate competed with 0.3 μ g/ml GalNAc-complex for binding (nonlinear regression fit: equation, one site competition, r^2 0.72).

With a calculated concentration for the half maximal effect EC_{50} of 12nM, C23.8 IgG1 affected the binding of the GalNAc-conjugate in a concentration-dependent manner (see Figure 137).

3.5.7.2.4 Biacore

The binding of the galactose to the monomeric and the dimeric H1-CRD surfaces in a Biacore assay was not affected, when C23.8 IgG1 were captured. The first galactose signal, prior to the antibody injection, and the second signal, after the IgG1 binding, varied less than 10% (see Figure 138A).

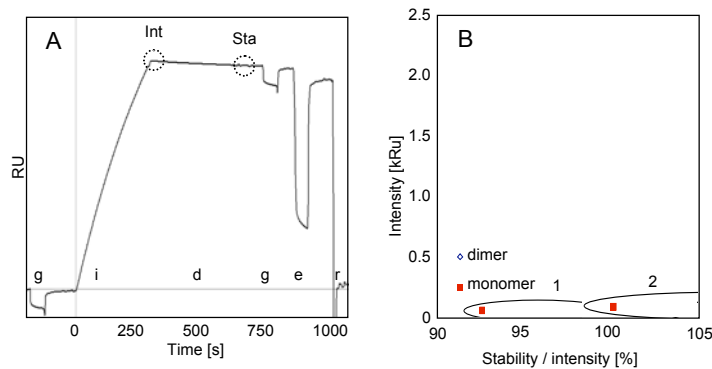


Figure 138: Biacore assay of the C23.8 IgG1 binding to the monomeric and the dimeric H1-CRD. A: Sensogram, with a preliminary injection of 5mM galactose (g), C23.8 IgG1 injection (i), dissociation phase (d), followed by a second 5mM galactose injection and an EDTA pulse (e), prior to the regeneration with HCl (r). Data points, used for blotting (Int, Sta), are indicated by circles. B: Intensity after 5min injection (Int) blotted against the quotient of the stability after 5min dissociation (Sta) and the intensity in buffer with 50mM calcium (1) or 3mM EDTA (2).

A marginal calcium sensitivity was detected, showing an increased stability of the C23.8 binding to the H1-CRD in the presence of EDTA. In addition, the binding stability to dimeric H1 CRD was higher than to monomeric H1-CRD. However, the intensity of the C23.8 interaction with H1-CRD was identical and independent of calcium or EDTA (see Figure 138B).

3.5.7.3 *On cell characterization*

3.5.7.3.1 Immunofluorescence flow cytometry

The binding of C23.8 IgG1 to the entire ASGPR on HepG2 cells and to the surface of ASGPR-negative SK-Hep1 cells was investigated by extracellular flow cytometry. Additionally, the cross-reactivity with homologous receptors on the surface of macrophages, dendritic cells and THP-1 was tested. Not fixed cells were indirectly stained with FITC.

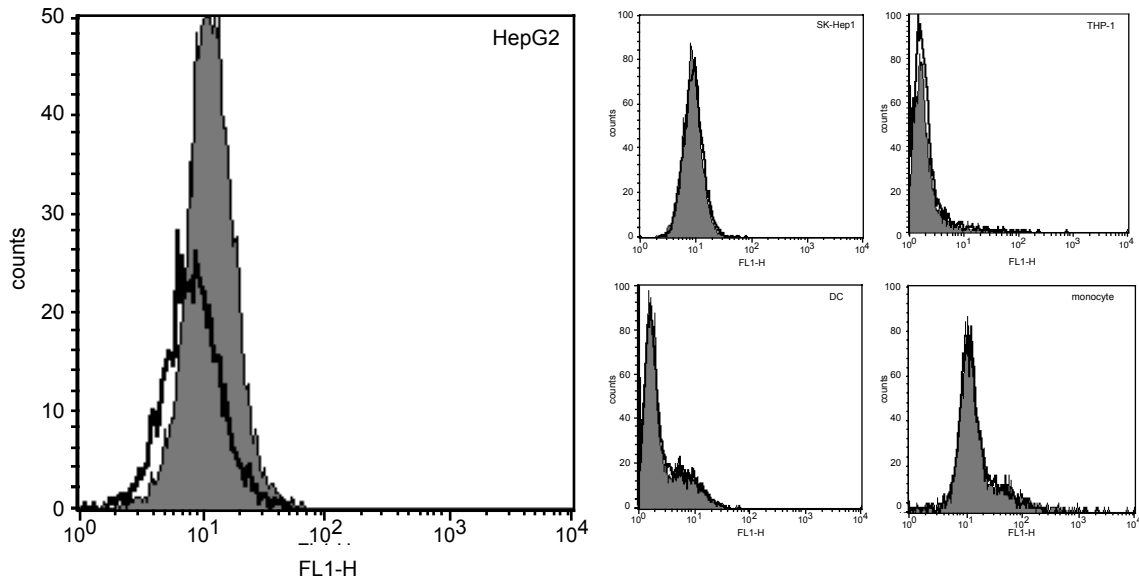


Figure 139: Flow cytometry of not fixed HepG2, SK-Hep1, THP-1, macrophages and dendritic cells, which were indirectly extracellularly stained with C23.8 IgG1 and FITC-labeled goat anti-mouse Ig (H+L). The dead propidium-stained cells were excluded. The histogram shows an overlay with the negative control (irrelevant IgG).

The C23.8 IgG1 specifically interacted with HepG2 cells and did not cross-react with SK-Hep1, THP-1, macrophages and dendritic cells. Only the HepG2 cells were fluorescence-stained (see Figure 139).

3.5.7.3.2 Immunofluorescence microscopy

The endocytosis of the C23.8 IgG1 into HepG2 and SK-Hep1 was investigated by immunofluorescence microscopy, to distinguish the specific and the unspecific internalization. The cells were indirectly fluorostained with Cy3-labeled donkey anti-mouse antibodies, after endocytosis, paraformaldehyde and permeabilization.

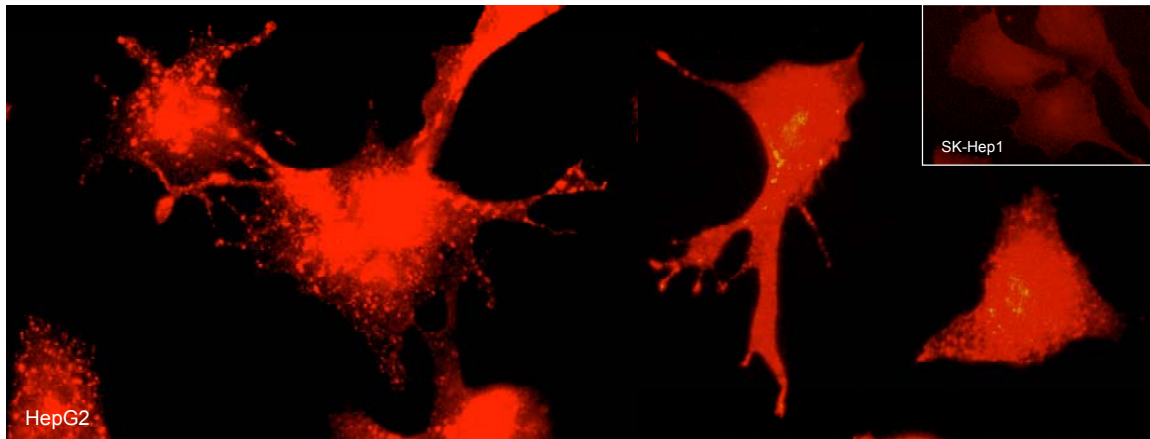


Figure 140: Immunofluorescence microscopy picture of the indirectly stained HepG2 and SK-Hep1 cells. The IgG1 in the culture supernatant of clone C23.8 were internalized into living cells, followed by the detection with Cy3-labeled donkey anti-mouse antibodies, after paraformaldehyde fixation and permeabilization of the cells.

The C23.8 IgG1 were specifically endocytosed via the ASGPR. The HepG2 cells were strewn with extremely bright spots, whereas the SK-Hep1 showed no spots. The HepG2 cells, which were only incubated with the Cy3-labeled detecting antibody, but not with C23.8 IgG1, were not stained too (see Figure 140).

3.5.8 Monoclonal C48.9 IgG1

3.5.8.1 Purification of C48.9 IgG1

The extraction of the C48.9 IgG1 by affinity chromatography was tried, testing Protein L, Protein G and H1-Sepharose.

Purification by Protein L spin chromatography

The purification of IgG1 κ from culture supernatant of C48.9, containing 10% FCS, using Protein L-Sepharose spin columns, was not successful. The silver-stained reducing SDS-PAGE gel showed, that the antibodies were of low purity and, that the yield was minute. In the HRP-ELISA, the supernatant as well as the flow through was positive.

Purification by H1-CRD FPLC

The C48.9 IgG1 antibodies were extracted from culture supernatant, containing 10% FCS by FPLC, using an H1-Sepharose column. The baseline of the FPLC chromatogram during loading was very unstable (see Figure 141A). The eluted antibodies still contained impurities. On a reducing SDS-PAGE gel, two main other proteins of about 66kDa were visible beside the 25kDa light chain band and the 55kDa heavy chain band (see Figure 141B). The extraction was quantitative, as the supernatant exhibited a strong and the flow through only a weak absorbance in the HRP-ELISA.

Purification by Protein G FPLC

The purification of C48.9 IgG1 antibodies from culture supernatant containing 3% FCS (low IgG), by FPLC, using a Protein G-Sepharose column, was not successful. During elution only a minute peak was detected, but at the end of the loading when stopping the flow to change the buffer, an unexpected prepeak appeared. On a reducing SDS-PAGE gel, hardly any antibodies, but also no other proteins were detected. Therefore, the purity seemed to be good (see Figure 141B). The HRP-ELISA indicated on the one hand, that the concentration of C48.9 IgG1 in the culture supernatant was already low and on the other hand, that the extraction was not complete. Both, the supernatant and the flow through showed a similar and low absorbance.

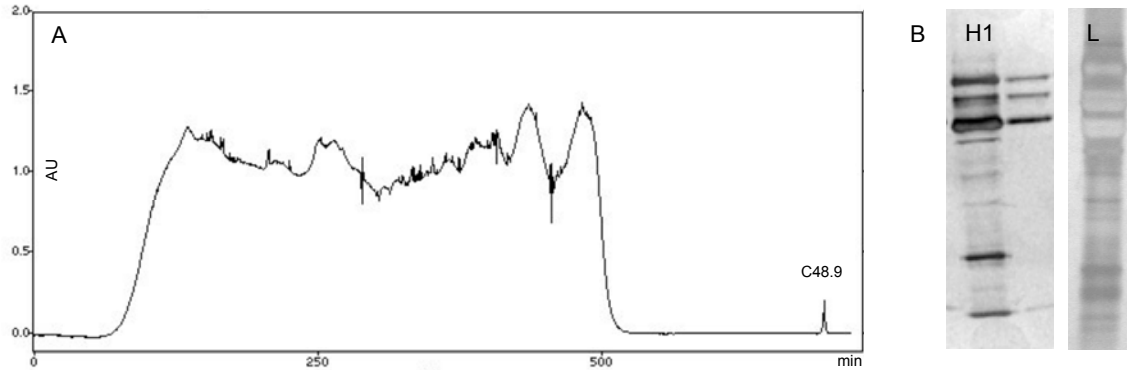


Figure 141: IgG1 extraction from culture supernatant of clone C48.9 containing 3% FCS (low IgG) A: FPLC chromatogram using H1-Sepharose. B: Corresponding silver-stained reducing SDS-PAGE gel 12% of the eluted antibodies of the H1-CRD (H1) and the Protein L (L) FPLC, showing mainly a double band for the light chain and a triple band for the heavy chain.

A reliable quantification was achieved with a double estimation by SDS-PAGE quantification and by Bradford micro-assay.

The highest C48.9 IgG1 yield was obtained by the H1-Sepharose chromatography, with 6.1mg/L supernatant, and the lowest by the extraction on Protein L-Sepharose, with 0.15mg/L supernatant. The Protein G-Sepharose affinity purification of C48.9 IgG1 from culture supernatant yielded only 0.6mg/L supernatant, too (see Figure 142).

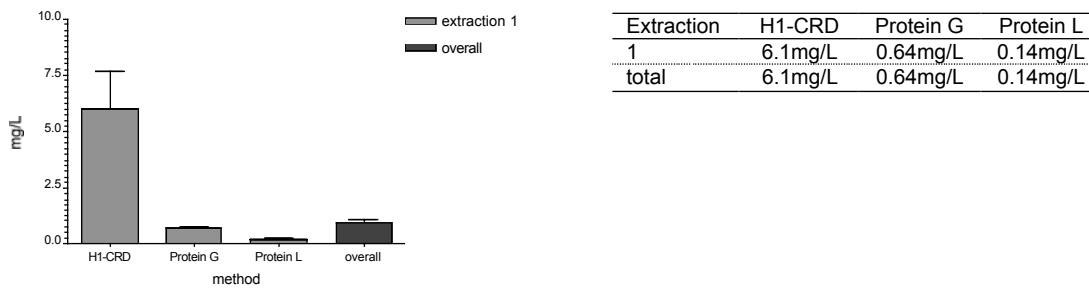


Figure 142: Yield of the C48.9 IgG1, purified by affinity to H1-CRD, Protein G and Protein L and quantified by Bradford micro-assay and SDS-PAGE quantification. Overall yield received was 0.885mg/L (SEM 0.149mg/L) culture supernatant of C48.9.

Overall, 0.47mg C48.9 IgG1 were purified from about 500ml culture supernatant, equivalent to a yield of 0.9mg/L.

3.5.8.2 *In vitro* characterization

3.5.8.2.1 Immunoblotting

Identical amounts of the reduced, non-reduced and native H1-CRD as well as of the reduced-alkylated and native-alkylated H1-CRD were blotted to nitrocellulose and were immunostained with 5 μ g/ml or 0.5 μ g/ml C48.9 IgG1, followed by an AP-labeled goat anti-mouse IgG (whole molecule).

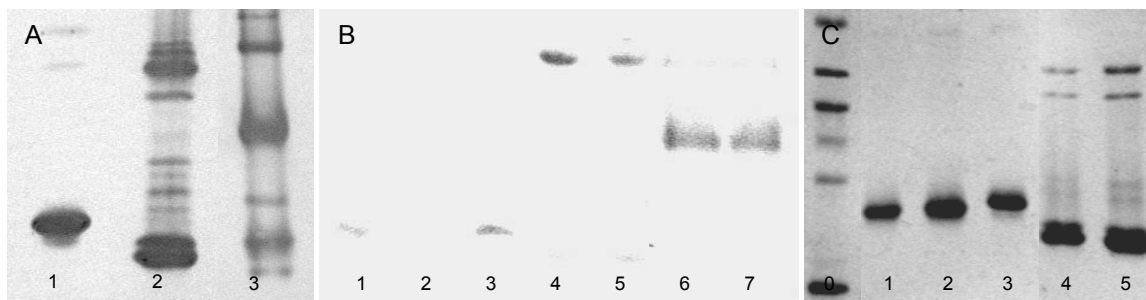


Figure 143: Immunoblot of the H1-CRD, caught with the monoclonal C48.9 IgG1. 1 μ g/band H1-CRD on PAGE gels 15% under reducing, non-reducing denatured or native conditions were blotted to nitrocellulose and were immunostained with C48.9 IgG1, followed by the detection with AP-labeled goat anti-mouse IgG (whole molecule), in dilution 1:5000. A: Blot, stained with 5 μ g/ml C23.8 IgG1, showing the reduced (1), non-reduced (2) and native (3) H1-CRD. B: Blot, stained with 0.5 μ g/ml C48.9 IgG1, showing reduced (1), the reduced state of reduced-alkylated (2), the reduced state of native-alkylated (3), non-reduced (4), the non-reduced state of native-alkylated (5), native (6) and the native state of native-alkylated (7) H1-CRD. C: Silver-stained reducing and non-reducing SDS-PAGE gel 15% of the same probes used in B (1-5) and the LMW marker (0).

The silver-stained PAGE gel and the Ponceau S-stained membrane showed the same bands pattern and same relative band intensities. The dimeric H1-CRD species were minor stained compared to the monomeric species. The different alkylation states of the reduced, non-reduced or native H1-CRD looked identical in their band intensities (see Figure 143C). The C48.9 specifically recognized the monomeric and the dimeric species of the reduced, non-reduced and native H1-CRD. The strongest signal was received for the binding to native H1-CRD, followed by the non-reduced and the lowest for the interaction with reduced H1-CRD. No cross-reaction with proteins of the LMW marker was detected.

Using the lower C48.9 IgG1 concentration of 0.5 μ g/ml for catching, the interaction with reduced H1-CRD was alkylation-dependent. Whereas the previously reduced-alkylated H1-CRD in reduced state was only minor recognized, the preliminary not alkylated and native-alkylated H1-CRD in reduced state as well as in non-reduced and native state were highly intense stained.

Interestingly, the relative band intensities of the monomeric and dimeric H1-CRD species on the C48.9-immunostained blot were vice versa compared to the Ponceau S-stained blot or the silver-stained PAGE gel. The C48.9 IgG1 preferred the binding to the dimer (see Figure 143).

3.5.8.2.2 ELISA

The binding of the monoclonal C48.9 IgG1 in concentrations of 0 - 300nM to the H1-CRD (5 μ g/ml, 300 μ M) was detected with an HRP-labeled goat anti-mouse Ig (H+L) diluted 1:1000, in an ELISA. An effective concentration EC_{50} of 1.9nM was calculated for the half maximal binding (see Figure 144).

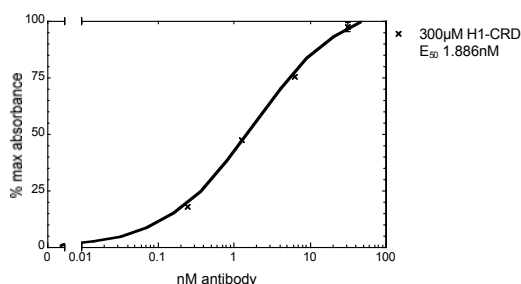


Figure 144: Binding of the C48.9 IgG1 to the H1-CRD in an HRP-ELISA. The C48.9 was titrated in the range of 0.1-300nM, in duplicate (exponential dilution row) in the presence of 20mM calcium. The plate was coated with 5 μ g/ml (300 μ M) H1-CRD and C48.9 was detected with HRP-labeled goat anti-mouse Ig (H+L), diluted 1:1000. The EC_{50} was calculated, using a nonlinear regression fit (equation sigmoid dose-response, variable slope, r^2 1.00) of Prism4 software.

The calcium sensitivity of the C48.9 IgG1 binding to the H1-CRD in the HRP-ELISA was checked. The IgG1 were caught in the presence of 2mM calcium, 1mM calcium or 10mM EDTA. All previous steps included 1mM calcium and all following steps 20mM calcium.

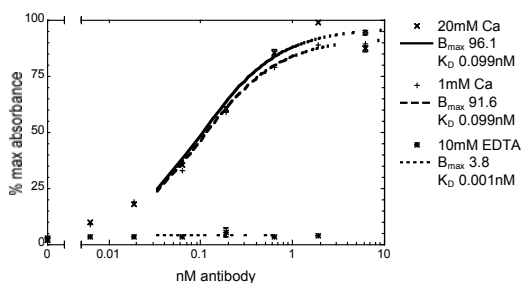


Figure 145: Ca sensitivity of the C48.9 IgG1 binding to the H1-CRD in an HRP-ELISA in the presence of 20mM calcium, 1mM calcium or of 10mM EDTA. The plates were coated with 3 μ g/ml H1-CRD and C48.9 IgG1 was titrated in the range of 0.0625-6.25nM in triplicate. B_{max} and K_D were calculated using a nonlinear regression fit (equation one site binding, hyperbola, r^2 0.98-0.99).

The binding of C48.9 in concentrations of 0 - 6.25nM to 175 μ M H1-CRD-coated plates, was substantially increased by the presence of calcium, but was independent of the

calcium concentration level. The interactions were similar in 20mM calcium, with a K_D of 0.09nM and B_{max} of 96.1% and in 1mM calcium with a K_D of 0.09nM and B_{max} of 91.6%. In contrast, in 10mM EDTA, hardly any binding was detected, showing an extremely low B_{max} of 3.8% and a K_D of 0.01nM (see Figure 145).

3.5.8.2.3 GalNAc-polymer assay

The C48.9 IgG1 in the concentration range of 0 - 18.75nM competed with 0.3 μ g/ml POD-labeled streptavidin-biotin β -GalNAc-polymer for binding to the H1-CRD, in the presence of 1mM calcium.

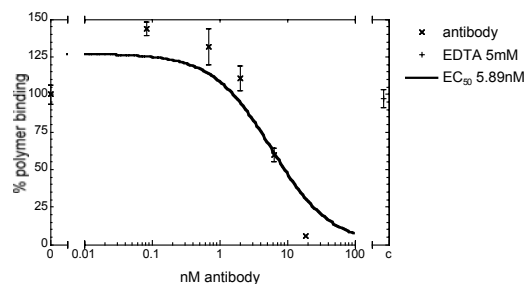


Figure 146: Competition of the GalNAc-polymer and the C48.9 IgG1 antibodies for binding to the H1-CRD in the polymer assay. The plate was coated with 3 μ g/ml (175 μ M) H1-CRD. C48.9 in the range of 0-18.75nM (exponential dilution) in triplicate or tetruplicate competed with 0.3 μ g/ml GalNAc-complex for binding (nonlinear regression fit: equation, one site competition, r^2 0.77).

The C48.9 IgG1 inhibited the binding of the GalNAc-complex to the H1-CRD effectively and concentration-dependent. The estimated concentration for the half maximal effect EC_{50} was 5.9nM (see Figure 146).

3.5.8.2.4 Biacore

In a Biacore assay, the interaction of galactose with surfaces of the monomeric and the dimeric H1-CRD species was not affected when the C48.9 IgG1 was bound. The difference of the first galactose signal prior to the C48.9 injection and the second signal after antibody capturing was below 10% (see Figure 147A).

The binding of the C48.9 IgG1 did not seem calcium-sensitive. The stability and the intensity in the presence of 50mM calcium compared to 3mM EDTA was similar.

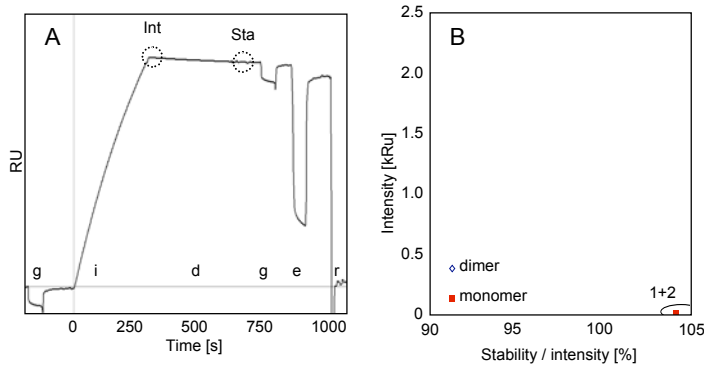


Figure 147: Biacore assay of the C48.9 IgG1 binding to the monomeric and the dimeric H1-CRD. A: Sensogram with a preliminary injection of 5mM galactose (g), C48.9 IgG1 injection (i), dissociation phase (d) followed by a second 5mM galactose injection and an EDTA pulse (e) prior to the regeneration with HCl (r). Data points used for blotting (Int, Sta) are indicated by circles. B: Intensity after 5min injection (Int) blotted against the quotient of the stability after 5min dissociation (Sta) and the intensities in buffer with 50mM calcium (1) or 3mM EDTA (2).

The binding intensity of the monomeric H1-CRD to the C48.9 was lower than of the dimeric H1-CRD (see Figure 147B).

3.5.8.3 On cell characterization

3.5.8.3.1 Immunofluorescence flow cytometry

The interaction of the C48.9 IgG1 with the entire ASGPR on HepG2 cells and with the surface of ASGPR-negative SK-Hep1 cells was checked by extracellular flow cytometry.

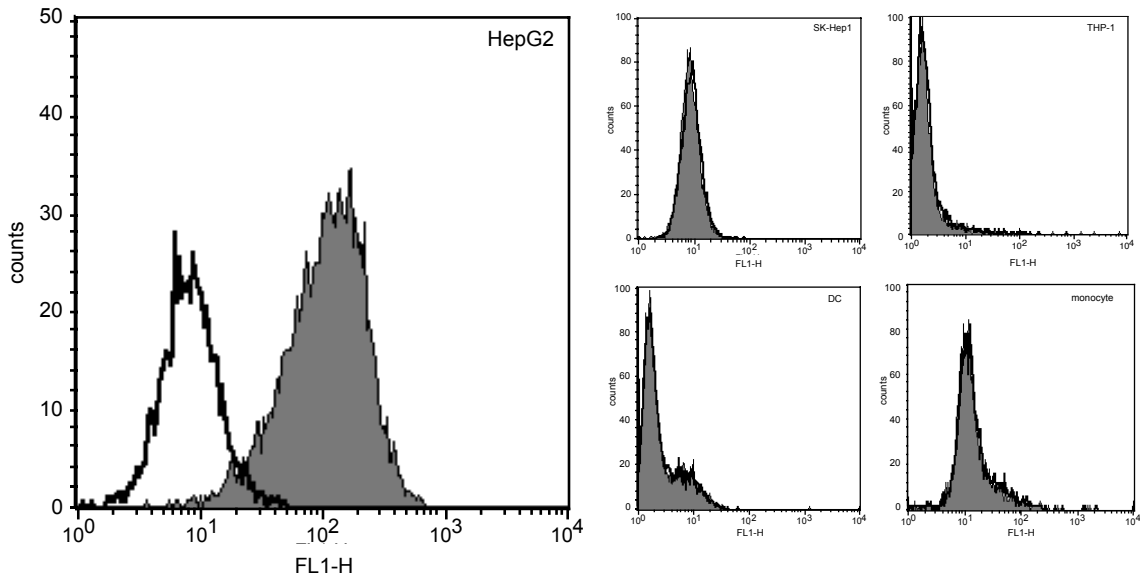


Figure 148: Flow cytometry of not fixed HepG2, SK-Hep1, THP-1, macrophages and dendritic cells, which were indirectly extracellularly stained with C48.9 IgG1 and FITC-labeled goat anti-mouse Ig (H+L). The dead propidium-stained cells were excluded. The histogram shows an overlay with the negative control (irrelevant IgG).

In addition, THP-1 cells, macrophages and dendritic cells, which are known to carry a homologous receptor, were indirectly fluorescence-stained, to spot cross-reactivity.

The C48.9 IgG1 was specifically bound to the ASGPR-positive HepG2 cells, and no cross-reaction with similar receptors on the surface of macrophages and dendritic cells was detected. Only HepG2, but none of the other tested cell lines, were positive in flow cytometry (see Figure 148).

3.5.8.3.2 Immunofluorescence microscopy

The endocytosis of C48.9 IgG1 into HepG2 and SK-Hep1 was investigated by immunofluorescence microscopy to distinguish between the specific and the unspecific internalization. The cells were indirectly stained with Cy3-labeled donkey anti-mouse antibodies after endocytosis, fixation and permeabilization.

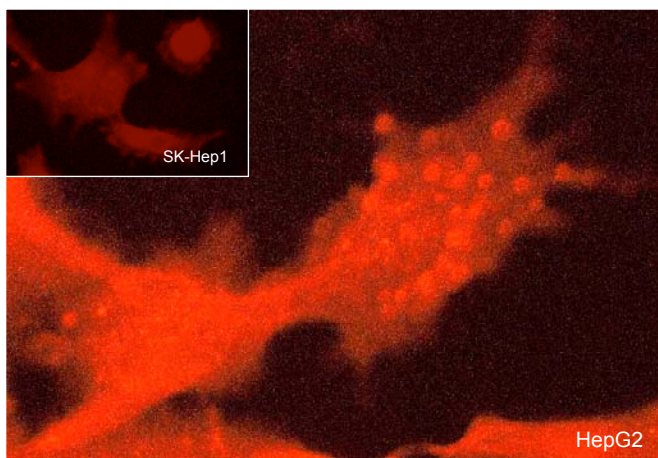


Figure 149: Immunofluorescence microscopy picture of the indirectly stained HepG2 and SK-Hep1 cells. The IgG1 in culture supernatant of clone C48.9 were internalized into living cells, followed by the detection with Cy3-labeled donkey anti-mouse antibodies, after paraformaldehyde fixation and permeabilization of cells.

The SK-Hep1 showed no spots, whereas in the HepG2 cells some bright spots were visible. Also the tubuli were only very weakly stained with anti-tubuli IgG, followed by the Cy3-labeled detecting antibody. The HepG2 cells only incubated with the detecting antibody, but not with C48.9 IgG1, were not stained. Therefore, C48.9 was internalized and mainly specifically by the ASGPR. The weak staining was supposed to be due to the weak binding of the Cy3-labeled antibody (see Figure 149).

4 Discussion

4.1 H1-CRD immunogenicity and antigenicity – a problem?

Antibodies are of primary importance in drug discovery and development, not only as analytical and diagnostic tools, but also as carriers for drug targeting. Nowadays, monoclonal and polyclonal antibodies against human target peptides and proteins are still produced in animals. Therefore, the successful preparation of antibodies is highly dependent on the antigen antigenicity and immunogenicity in the selected species. To be immunogenic, antigen-intrinsic factors and antigen-extrinsic factors, especially the phylogenetic distance to the host species are crucial.

Monoclonal antibodies are mostly produced by the hybridoma technique of Köhler and Milstein.⁸² Since mainly murine and rarely rat cells are fused, especially conserved proteins, which are highly homologous to mouse or rat proteins, may fail to induce an immune response. In this case, artificial antibodies can be produced *in vitro* by the Phage display technique of Smith¹⁵⁵ or the newer Ribosome display technique of Plückerthun *et al.*¹⁵⁶ or Taussig *et al.*¹⁵⁷.

The H1-CRD and the MHL-1 exhibit 79% sequence identity. At the Gal binding site, the homology is even higher with only 7% differing amino acids, i.e. residue D²⁴² and D²⁵⁹. Therefore, the chance of the H1-CRD to be immunogenic in mice seemed limited, and the raise of antibodies against the binding site was found to be problematic. But at least according to antigenicity, hydrophobicity and accessibility plots, the Gal binding site was predicted to be a putative epitope region.

The H1-CRD was further compared to the CRD of homologous receptors on human and mouse macrophages, dendritic cells and Kupffer cells, to assess the possibility that anti-H1 antibodies may cross-react. On the one hand, such cross-reactions can be advantageous, e.g. for the identification of homologous receptors in the same or other species. On the other hand, they may be devastating for drug targeting or the induction of an adequate immune response during immunization of mice. The moderate to high sequence similarities of up to 66% for the entire receptors, 81% for the CRD or 87% for the binding sites let assume, that cross-reactivity was probable.

In contrast to monoclonal antibodies, polyclonal antibodies for scientific application are mainly produced in rabbits or goats, but seldom in chicken. Compared to the production of rabbit IgG, the avian IgY preparation has the advantages that larger amounts of more

diverse antibodies can be produced against conserved human antigens. As chicken is phylogenetically more distant, it may respond to antigens, which are self-tolerated in rabbit. Thus, also the ChHL-1 and its CRD are only 37% and the binding site 42% identical with the ASGPR-1. Therefore, the production of polyclonal anti-H1 antibodies in chicken was much more promising.

In conclusion, the high similarity of the murine and human hepatic lectin may hamper the production of monoclonal antibodies against the H1-CRD, particularly against the Gal binding site. The chances of success seemed highest, when the full length H1-CRD in native and active state is used as antigen. On the one hand, this ensures best the binding site to be in the native conformation. On the other hand, the immunogenicity of the full length H1-CRD is expected to be higher than a part of the H1-CRD structure. Additionally, with a molecular weight of 17kDa, the H1-CRD is much above the critical antigenic size. Since avian are more distant to human than rabbit, and since IgY may bind to distinct epitopes than IgG, polyclonal antibodies against the H1-CRD were best risen in chicken.

4.2 H1-CRD production - from minute to gigantic yields

The mice and chickens immunization as well as the screening of hybridomas and the characterization of antibodies depend on sufficient amounts of antigen. Therefore, at least 50mg active H1-CRD should be recombinantly expressed in *E.coli*, before starting the production of monoclonal and polyclonal antibodies. Unfortunately, the expression and purification, according to Meier *et al.*²⁶, supplied only a minute yield of about 130µg/L culture, which was only 18% of published 688µg/L culture.

In other words, to provide 50mg, the production of H1-CRD in approximately 400L would have been required. As a consequence, the optimization of the H1-CRD production was inevitable. First, the expression was increased by variation of *E.coli* intrinsic and extrinsic factors, i.e. the expression vector, the *E.coli* strain and the expression conditions (medium, inducer concentration, cell density, expression period). Second, the purification method, mainly the solubilization and the refolding were improved (see Figure 150).

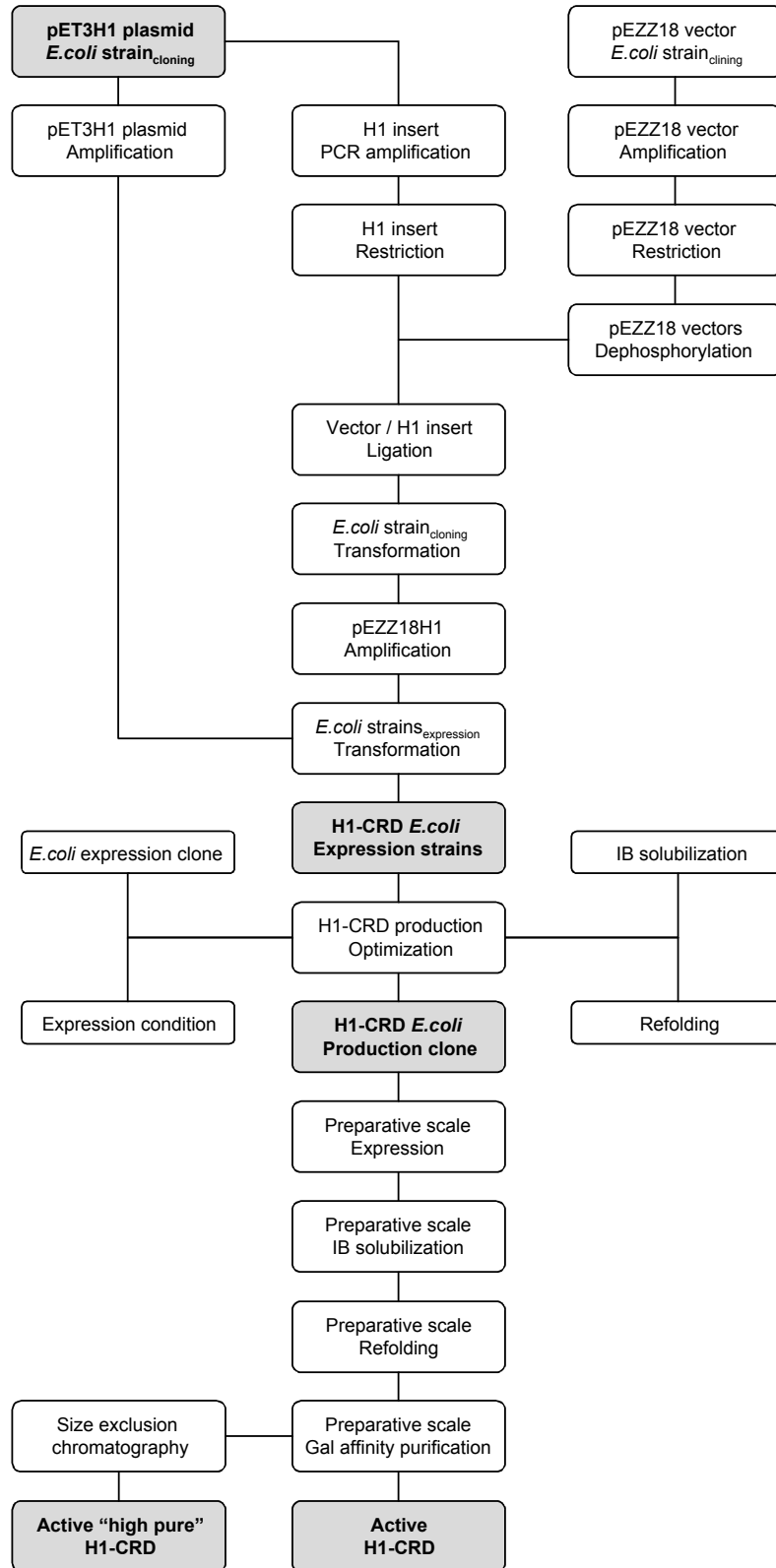


Figure 150: Overview of the H1-CRD production as antigen for the raise of monoclonal and polyclonal anti-H1 antibodies and for their characterization.

4.2.1 Optimization of *E.coli* intrinsic features – the vector-*E.coli* strain relationship

The expression level is mainly influenced by the expression conditions (temperature, pH, aeration, inducer concentration, cell density and expression period), but also by the features of the protein and the encoding cDNA, by the expression vector and the *E.coli* strain.

Therefore in a first step, *E.coli* intrinsic features were examined followed by the variation of *E.coli* extrinsic features for expression in the selected *E.coli* expression clone.

Selection of the optimal vector / E.coli partners

Beside the original pET3b expression vector, the pEZZ18 was selected for recombinant gene expression of H1-CRD (see Appendix 4, page 281). The pET3b vector encodes no tag and allows inducible cytoplasmic expression of H1-CRD in inclusion bodies.²⁶ In contrast, the pEZZ18 vector encodes the protein A signal sequence and the ZZ domain tag that allows to express the H1-CRD fused to the synthetic IgG binding domain and that directs the fusion protein to the periplasm or the medium. The periplasmic expression and the fused ZZ domain probably facilitate the native folding by enforced pairing of disulfide bridges and simplify the purification.

The pET3H1, encoding the H1-CRD, was provided by Spiess M.¹⁵⁸ To get the H1-CRD encoding pEZZ18H1, the high-fidelity *Pfu* DNA polymerase amplified H1-CRD cDNA was blunt-blunt-ended and blunt-sticky-ended introduced into pEZZ18. But no *E.coli* transformants were obtained that contained the recombinant pEZZ18H1 plasmid. The restriction probably failed, because the restriction sites of *Sma* I and *Bam*H I are only separated by 3bp.

The pEZZ18 vector strategy was no longer progressed, due to experiences with this vector system by Dragic.¹⁵⁹

There are several (DE3) *E.coli* expression strains available that are compatible with the pET3H1 plasmid. Due to the fact, that the H1-CRD sequence contains 7 Cys, which are paired in 3 S-S bonds, and that 4% of the H1-CRD cDNA encoded amino acids are rare in *E.coli*, the two strains AD494(DE3) and Rosetta-gami(DE3) promised to enhance expression levels of the H1-CRD decisively (see Appendix 3, page 280). Compared to the original expression strain JM109(DE3), AD494(DE3) facilitate disulfide pairing in the

reducing cytoplasm. Rosetta-gami(DE3) additionally encodes the rare *E.coli* amino acid residues.

The comparison of the H1-CRD expression levels in clones of JMpET3H1, ADpET3H1 and RGpET3H1 clearly indicated, that the highest yields were obtained with ADpET3H1 clones. Interestingly, the expression level did not only differ strongly between the different *E.coli* strains, but also between different clones of the same *E.coli* strain; i.e. clone ADpET3H1.4 provided an about 6-fold higher H1-CRD yield than clone ADpET3H1.1.

In conclusion, the highest expression level was assessed in *E.coli* clone ADpET3H1.4, which produced 11-fold more H1-CRD than the original expression clone of JMpET3H1. Therefore, the excellent clone ADpET3H1.4 was selected for the H1-CRD production.

Verification of H1-CRD cDNA and amino acid sequence

Prior to the preparative expression of the H1-CRD, ADpET3H1.4 was verified to express the correct peptide. On the one hand, the H1-CRD cDNA sequence contained no point mutations or frame shifts and was correct. On the other hand, the determined molecular mass in ESI-FT-ICR was 61Da higher than the calculated mass of the full length native H1-CRD.

However, the penultimate amino acid Gly at the N-terminus let to suppose, that the starting Met is posttranslationally removed¹⁶⁰. Considering this deletion (-131Da) and assuming, that 6 of 7 Cys are involved in disulfide bridges (-6Da), the mass deficit switched to a mass surplus of 76Da. Due to the circumstance, that β -mercaptoethanol was used during solubilization of the H1-CRD, it was suggested that a forth S-S bond with the remaining free Cys was formed. The β -mercaptoethanol adduct was lately proved by Ricklin.¹⁴⁰ Therefore, assuming that the H1-CRD contains three intramolecular S-S bonds, no starting Met and a β -mercaptoethanol adduct at the free Cys, the calculated and the measured masses were identical. In addition, the correct mass of the H1-CRD without starting Met was proved under reducing conditions.

Since only the positions of the two H1-CRD disulfide bridges Cys³⁶-Cys¹³¹ (Cys¹⁸¹-Cys²⁷⁶ in the H1 subunit) and Cys¹⁰⁹-Cys¹²³ (Cys²⁵⁴-Cys²⁶⁸) were determined in X-ray²⁶, but the position of the third still has to be defined, the native trypsin-digested H1-CRD was analyzed using MALDI-FT-ICR. A third S-S bond linked the vicinal Cys⁷-Cys⁸ (Cys¹⁵²-Cys¹⁵³) and therefore most probable, the Cys¹⁹ (Cys¹⁶⁴) is linked to β -mercaptoethanol or

involved in the dimerization of the H1-CRD (see Figure 151).¹⁴⁰ However, all Cys were also found in the reduced state. This was probably due to the opening of disulfide bridges, which mostly occurs under basic conditions.¹³⁷ Since the native H1-CRD was digested at neutral pH, an exchange of disulfide bridges during proteolysis cannot be excluded.



Figure 151: Disulfide bridges of the H1-CRD with a β -mercaptoethanol adduct. A: Proposed disulfide linkage according to MS (see Section 3.2.2.4). B: Suggested disulfide pairing by Meier *et al.*²⁶

In summary, the selected clone ADpET3H1.4 expressed surprisingly high amounts of correct full length H1-CRD.

4.2.2 Optimization of *E.coli* extrinsic features – the expression conditions

The maximal expression level is only achieved under optimal growth and expression condition of the defined *E.coli* expression system. The main *E.coli* extrinsic parameters, which affect the expression, are medium composition and pH, culture density, aeration, temperature, inducer concentration and the period of expression.⁵²

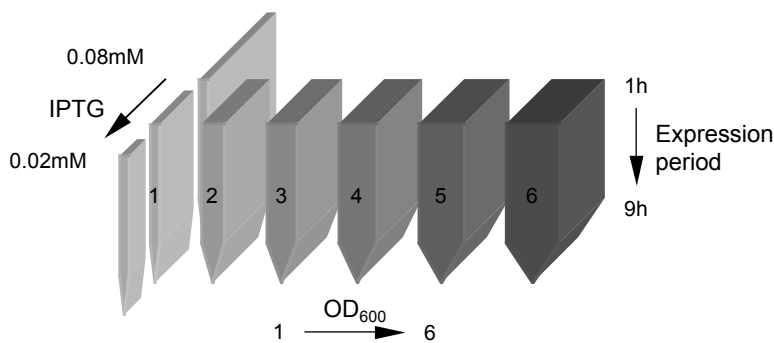


Figure 152: Setup of the experiments for the optimization of the IPTG concentration, the cell density for induction and the expression period. The expression cultures were induced at an OD₆₀₀ of 1-6 with 0.2–0.4mM IPTG, and the expressions were run for 5h, while taking samples every 1h.

In parallel-incubated ADpET3H1 expression cultures, the four determinants, i.e. medium, cell density, IPTG concentration and expression period, were systematically varied (see

Figure 152). The other important variables temperature, aeration and pH were controlled, but kept constant.

Medium – TB versus LB with or without a pinch of glucose

ADpET3H1.4 in the higher-nutrient TB medium grew slightly faster during log phase and reached a higher maximal cell density during stationary phase than in the originally used LB medium. This was not surprising, because in the richer TB medium, nutrients get later limiting. When induced at the same cell densities, similar yields were obtained in both media. The prolonged log phase in TB medium however, may enable the expression in more dense cultures, which increases the yield. Furthermore, no basal expression occurred prior to induction, even not in the absence of glucose. Although glucose was not necessary to prevent basal expression, it exhibited a variable, but positive effect onto the yield.

Cell density – expression until toxic?

Since optimal unlimited conditions are essential during expression, cells must still be in the log phase. Consequently, the protein expression is generally induced at a low cell density, at an OD₆₀₀ of 0.8 – 1. But as ADpET3H1 grew exponentially until an OD₆₀₀ of 4 - 5, the induction at a much higher density seemed possible and promising to increase the expression level. Therefore, the expression was started at various cell densities in the log phase, up to the stationary phase. Interestingly, when the cell density exceeded an OD₆₀₀ of 3, the pH decreased during expression. This indicated suboptimal culture conditions by metabolic product accumulation and that may hamper the expression. Therefore, it was assumed, that the cell densities in ADpET3H1.4 expression cultures should not exceed an OD₆₀₀ of 3.

*IPTG concentration – give *E.coli* the right “kick”*

The maximal expression may exhaust the production capacity of *E.coli*. As a consequence, lowering the expression rate, but increasing the expression period may permit to achieve higher yields.¹¹⁹ Meier *et al.*²⁶ initiated the expression with 1mM IPTG, whereas for maximal induction of pET3 vector an IPTG concentration of 0.4mM is recommended.¹¹⁹ Hence, the protein expression was started in ADpET3H1.4 by addition of half the concentration, the recommended concentration and double the concentration of IPTG, needed for maximal induction. The highest H1-CRD yields were obtained with recommended inducer concentration of 0.4mM. Since an excessive induction may cause

cell damage with release of the expressed protein, the medium was inspected, but no H1-CRD was found.

Expression period - endurance of E.coli

In general, the expression period is 3h but may be up to 20h. The highest expression level was assessed 3-5h after induction, independent of the IPTG concentration used to initiate the production. However, when the expression period was further prolonged, the observed amount of H1-CRD decreased, probably due to degradation. Interestingly, in parallel to the loss of H1-CRD, the cell density and consequently, the total cell protein mass increased. This second growth phase may be caused by IPTG depletion and as a consequence by stopped expression, or may be due to carbenicilline degradation, allowing the growth of cells that lost the plasmid. Therefore, the expression was reinduced after 5h, but no further increase of the expression level was achieved.

In conclusion, the highest expression level in ADpET3H1.4 was maintained, when the H1-CRD expression was initiated with 0.4mM IPTG at a cell density below an OD₆₀₀ of 3 and was run for 5h. Additionally, the glucose supplementation contributed to improve the H1-CRD expression.

4.2.3 Optimization of the purification procedure

The cytoplasmic expressed protein is either soluble or aggregates in insoluble inclusion bodies. The location and form of the expressed protein defines the purification procedure, needed to recover high yields of active protein.

Since H1-CRD was uniquely expressed in the insoluble and inactive form of inclusion bodies, three main purification steps were necessary to obtain active H1-CRD: the solubilization of inclusion bodies, the refolding and the isolation of active H1-CRD by affinity to galactose. To optimize the recovery of active H1-CRD, three different solubilization methods (FD, NFD, IB) in combination with four distinct refolding systems (A, B, C, D) were compared (see Figure 153).

The different purification procedures were performed in parallel, isolating H1-CRD from the same expression pellet, to exclude external factors best.

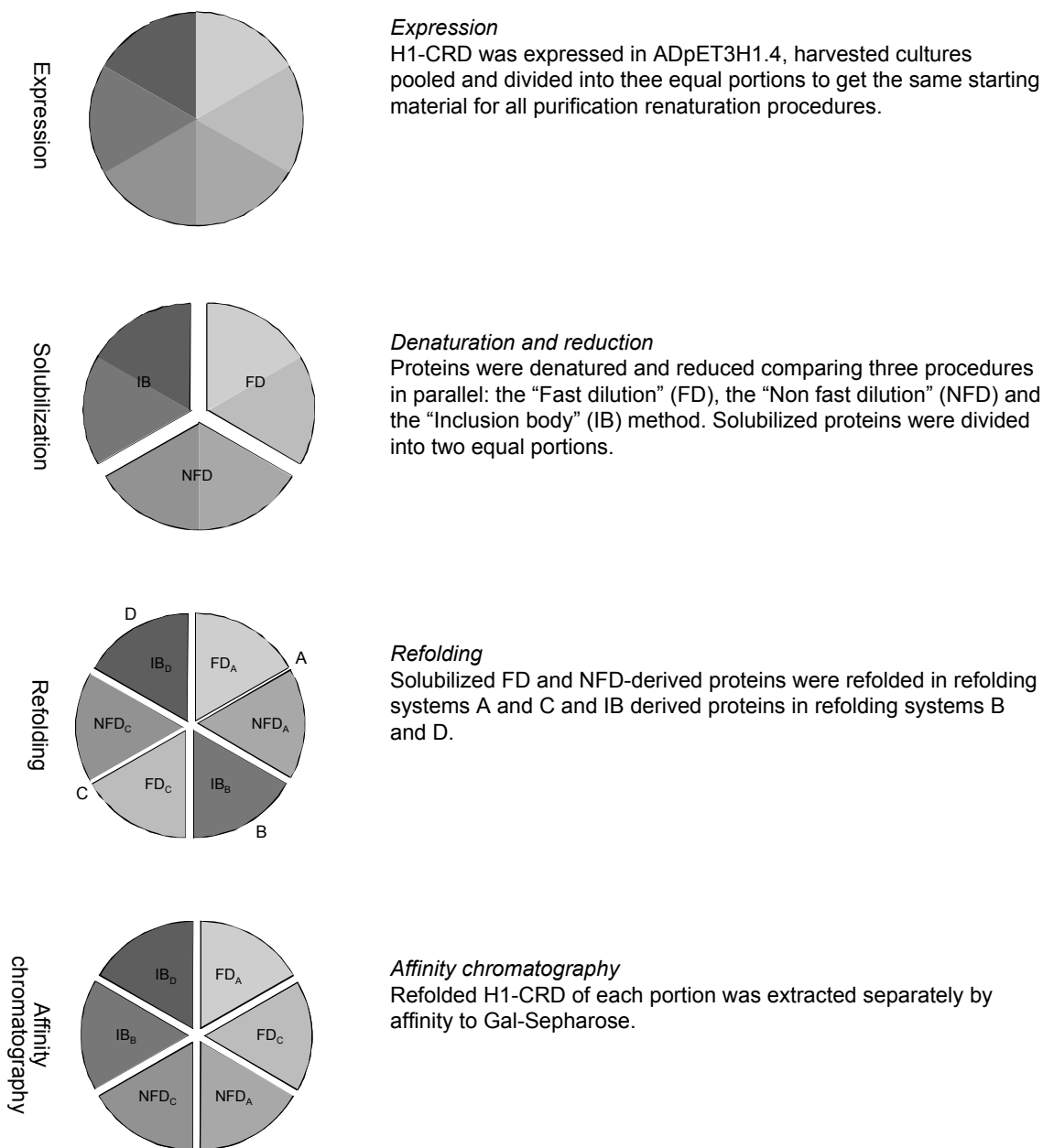


Figure 153: Optimization of the H1-CRD purification, composed of three main steps: the denaturation, the refolding and the affinity chromatography using Gal-Sepharose.

Reductive solubilization

The FD method was identical to the original solubilization method of Meier *et al.* The NFD method was adapted from the FD method. Both reduced and denatured the inclusion bodies without separation from soluble bacterial proteins and differed mainly in the protein concentration upon solubilization. Whereas in the FD solubilization, the total cell proteins were solubilized in a small volume and were fast diluted prior to the refolding, in the NFD solubilization, the proteins were solubilized in a large volume and

were no more diluted prior to the refolding. Consequently, the protein concentration during solubilization and the protein, the denaturant and the reductant concentration at the refolding start differed.

In contrast to both other methods, the IB method isolated the insoluble inclusion bodies from soluble bacterial proteins prior to the solubilization. Therefore, the total protein concentration, but not the H1-CRD concentration at the refolding start, was much lower compared to the other methods. Another main difference was, that proteins were reduced with β -mercaptoethanol in the FD and NFD, but with DTT in the IB procedure, which may strongly influence the following refolding.

Oxidative refolding

The refolding system A was identical to the original refolding method of Meier M. *et al.* and refolded proteins in a single calcium-containing salt buffer (see Figure 154). The presence of calcium may be essential for the proper refolding of active H1-CRD, as the native H1-CRD contains 3 integral calcium ions. Since during refolding, the 7 Cys have to pair in 3 correct S-S bonds, the effect of thiol-active compounds onto the refolding of the H1-CRD were investigated. DTT was only included in the first two refolding steps of refolding systems B and D to slow the refolding rate and therefore, to minimize the formation of false disulfide bridges.¹³⁷ Reduced and oxidized glutathione were added in the last two refolding steps of refolding systems A, B and C to reshuffle mispaired disulfide bonds of refolding intermediates. Finally, glycerol that assists hydration and structure stabilization of globular proteins⁵⁶ was included in the first four steps of refolding systems B and D.

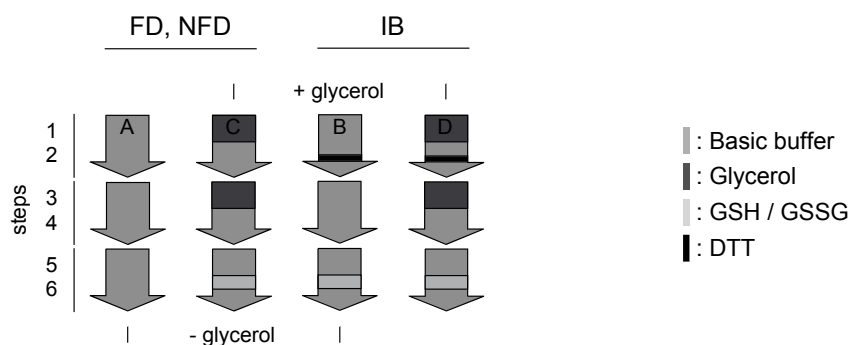


Figure 154: Refolding buffer systems A to D, were composed of the basic refolding buffer, with or without additives, during 6 refolding steps. A only used 1, the basic buffer in all 6 steps. C used 2 buffers, containing additive glycerol in the first 4 and glutathione in the last 2 steps. B consisted of 3 buffers, additionally contained DTT in the first 2, no additives in the following 2 and glutathione in the last 2 steps. Finally, D was composed of 3 buffers, identical to B, but in addition contained glycerol in the first 4 steps.

Whereas glycerol had no effect, the addition of thiol-active compounds significantly influenced the refolding of the H1-CRD. However, also the rate of buffer exchanges was delicate. A slow removal of denaturant and reductant during the first and second refolding step was crucial to prevent aggregation. Since the refolding of the NFD-solubilized proteins was successful, when reducing with β -mercaptoethanol, but failed, when reduction was performed with DTT, there can be speculated, that a critical reductive-capacity concentration exists for the correct refolding (see Figure 155). The presence of a low concentration of thiol-active compounds may facilitate the proper S-S bond formation. When the reductant concentration falls too fast below the critical concentration, correct disulfide bridges may not yet be formed and the H1-CRD aggregate. But when the critical concentration is reached after finishing the proper S-S bond pairing, the H1-CRD may not precipitate and is refolded quantitatively. Therefore, it was suggested, that the precipitation was mainly due to the formation of false disulfide bridges. The β -mercaptoethanol seemed to facilitate the correct disulfide formation compared to DTT.

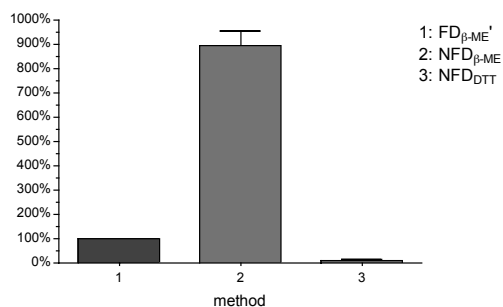


Figure 155: Effect of the reductants β -mercaptoethanol and DTT onto the refolding.

Whereas the loss of H1-CRD during NFD $_{DTT}$ procedure was caused by the formation of an insoluble H1-CRD aggregate, the low yield of FD $_A$ and FD $_C$ procedures was mainly due to the refolding to a soluble, but inactive H1-CRD intermediate, which could not bind to Gal-Sepharose.

Affinity chromatography

The extraction of the refolded active H1-CRD by affinity to galactose was efficient. Surprisingly, dependent on the refolding method, one or two species of monomeric and dimeric H1-CRD were extracted with Gal-Sepharose, seen on a non-reducing SDS-PAGE gel and a native PAGE gel. This could be explained by the formation of the native H1-CRD and a folding intermediate, which is also active, but differs in the disulfide

bridge pattern. Considering the refolding buffer composition, it can be suggested, that glutathione caused the variation. Since glutathione can reshuffle disulfide bonds, the H1-CRD intermediate may be converted into proper folded active H1-CRD with a uniform disulfide pattern.

The highest yields of active H1-CRD were purified by the IB and slightly less by the NFD procedures. Compared to the yield received, following the original purification method FD_A , the yields of IB and NFD methods were more than double (see Figure 156).

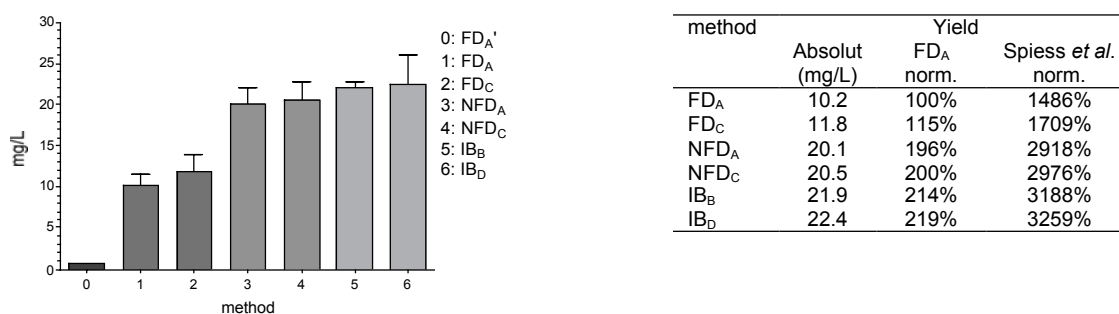


Figure 156: Comparison of the 6 different purification procedures. FD_A yielded 10.2mg/L (SEM 1.2mg/L), FD_C 11.8mg/L (SEM 2.2mg/L), NFD_A 20.1mg/L (SEM 2.0mg/L), NFD_C 20.5mg/L (SEM 2.2mg/L), IB_B 21.9mg/L (SEM 0.8mg/L) and IB_D 22.4mg/L (SEM 3.6mg/L) culture.

Since the NFD method is less time consuming, exhibited better reproducibility and supplied uniform active H1-CRD when refolded in buffer system C, the NFD_C purification procedure, using reductant β -mercaptoethanol is the method of choice for the H1-CRD extraction.

In summary, the uniformity of active H1-CRD seemed independent of the solubilization method, but was significantly influenced by the refolding buffer system. Highly uniform H1-CRD was only obtained after refolding in buffer systems B to D, which all contained the reshuffling agent glutathione. In contrast, the yield of active H1-CRD was strong dependent on the solubilization method, mainly on the used reductant and on the protein concentration, but was only minor affected by the refolding system.

4.2.4 Conclusion – the optimized H1-CRD “protein-factory”

The original expression system, identical to the published by Meier *et al.* yielded only incredibly low amounts of H1-CRD with 128µg/L culture. This was also 82% lower than published with 688µg/L (see Figure 157). To produce the planned amount of 50mg, the H1-CRD would have had to be purified from 400L expression.

It was inevitable to optimize the procedure for the preparative production of the H1-CRD. Three different steps were improved, i.e. the *E.coli* strain used for expression, the expression conditions and the purification procedure for extraction of active H1-CRD.

An outstanding contribution was achieved by expression of the H1-CRD in another *E.coli* expression strain and clone. The switch from JMpET3H1 to ADpET3H1.4 expression cultures increased the yield 820% to 1.2mg/L. The adaptation of the expression conditions to the needs of clone ADpET3H1.4 resulted in an additional 82% higher yield of 2.1mg/L. Finally, the renaturation optimization raised the yield of active H1-CRD another 186% to 6.1mg/L.

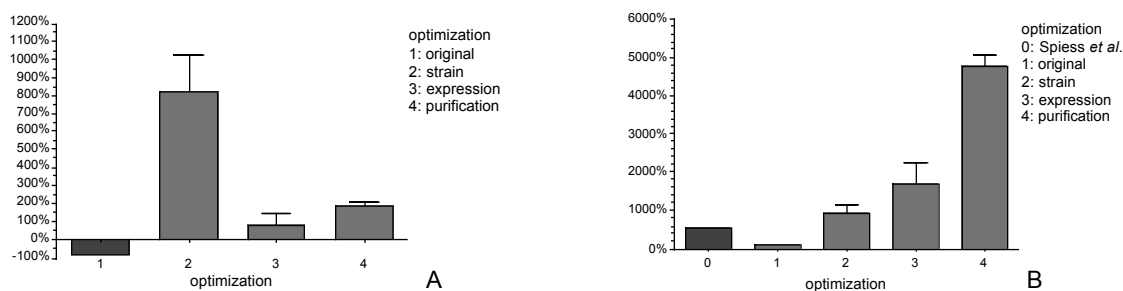


Figure 157: Optimization of the H1-CRD production. The yield obtained with the original expression system (B1, 100%) was 82% lower than published by Meier *et al.* The optimization of the *E.coli* expression strain increased the yield 820% (A2) to 920% (B2), the optimization of expression conditions 82% (A3) to 1670% (B3) and the optimization of the purification procedure another 186% (A4) to 4770% (B4).

The optimized production resulted in an impressive 48-fold higher yield compared to the amount received with the original strategy or a 9-fold higher yield compared to the published yield by Spiess *et al.* (see Figure 157B). This method enabled to produce 50mg H1-CRD in only 8L ADpET3H1 culture.

Since the H1-CRD eluted highly concentrated, the ultrafiltration was no longer necessary. Consequently, the substantial loss of 10-60% H1-CRD in the ultrafiltration step was omitted and the H1-CRD yield further increased to 20mg/L culture.

In future, this will permit to achieve quantities of 50mg in only 2.5L ADpET3H1.4 culture.

4.3 From active H1-CRD to highly pure monomeric and dimeric H1-CRD species – a one step strategy

For the production of polyclonal antibodies, an outstanding purity of the H1-CRD antigen was crucial. Therefore, it was necessary to remove traces of impurities still present after the affinity purification. In addition, the separation of monomeric and dimeric H1-CRD for the characterization of produced anti-H1 antibodies was suggested to be of advantage. To fulfill both needs in one step, SEC was the method of choice.

In buffer containing 20mM calcium, the H1-CRD did not elute, until the buffer was changed to water and the ionic strength decreased approximately to zero. This buffer did not allow the separation of monomeric and dimeric H1-CRD, but foreign proteins were successfully removed. The H1-CRD seemed to bind to the matrix. Ionic interactions with the matrix can appear, if the ionic strength of the buffer is below 0.5M, which was not the case. However, considering that Sephadex is a polymer, consisting of D-galactose and 3,6-anhydro-L-galactose, it may be hypothesized, that the H1-CRD specifically bound to the galactose residues of the Sephadex in the presence of calcium, although 3'-OH of galactose, which interacts with the H1-CRD, was not free but linked to 3,6-anhydro-L-galactose.¹⁴ Another explanation may be, that galactose and anhydrogalactose were not quantitatively linked, exposing enough free 3'-OH groups for H1-CRD binding. To verify the calcium-dependent specific binding, SEC was also run with calcium-free buffers.

In buffer containing only the integral calcium of H1-CRD, several small peaks overlapped and the H1-CRD eluted over a long period of time. The H1-CRD eluted in a mixture of monomeric and dimeric H1-CRD. As active intermediates were obtained in the previous step (see Section 4.2.3), it was supposed, that the fractionation was not driven by the molecular weight but by affinity differences of the various H1-CRD folding intermediates to the matrix. In contrast, in buffer with 1mM EDTA, the monomeric and dimeric H1-CRD eluted according to the molecular weight in an overlapping peak, and therefore were only partially separated. The lower flow rate did not enhance the resolution.

In conclusion, the H1-CRD SEC was only partially successful in buffer, containing EDTA to chelate calcium. In the presence of calcium, a specific interaction between the H1-CRD and the Sephadex matrix was observed. Therefore, FPLC SEC only enabled to remove traces of foreign proteins but was not suitable to separate monomeric and dimeric H1-CRD species.

4.4 Monoclonal and polyclonal anti-H1 antibodies – overview of the production, purification and characterization

Monoclonal and polyclonal antibodies have other features. Depending on the application, the one or the other can be of advantage.

Strategies for the production of polyclonal and monoclonal anti-H1 antibodies differed, but there existed also some similarities. For both, animals were first immunized with the active H1-CRD and finally, purified antibodies were characterized by identical *in vitro*, *on cell* and *on tissue* assays. But in contrast to the supply of polyclonal antibodies, for the raise of monoclonal antibodies, lymphocytes had to be fused with immortal cells to generate incessant antibody-producing hybridomas in culture (see Figure 158).

In the preparation of monoclonal antibodies, hybridomas are screened to identify specific anti-H1 antibody-producing cells, whereas in the production of polyclonal antibodies no selection takes place. As a consequence, the purity of the antigen used for immunization is of different importance. Pure antigen is crucial for high quality polyclonal but not decisive for monoclonal antibodies. Hence, for mice immunization active H1-CRD was taken, whereas for chicken immunization active H1-CRD was supplementary cleared by SEC.

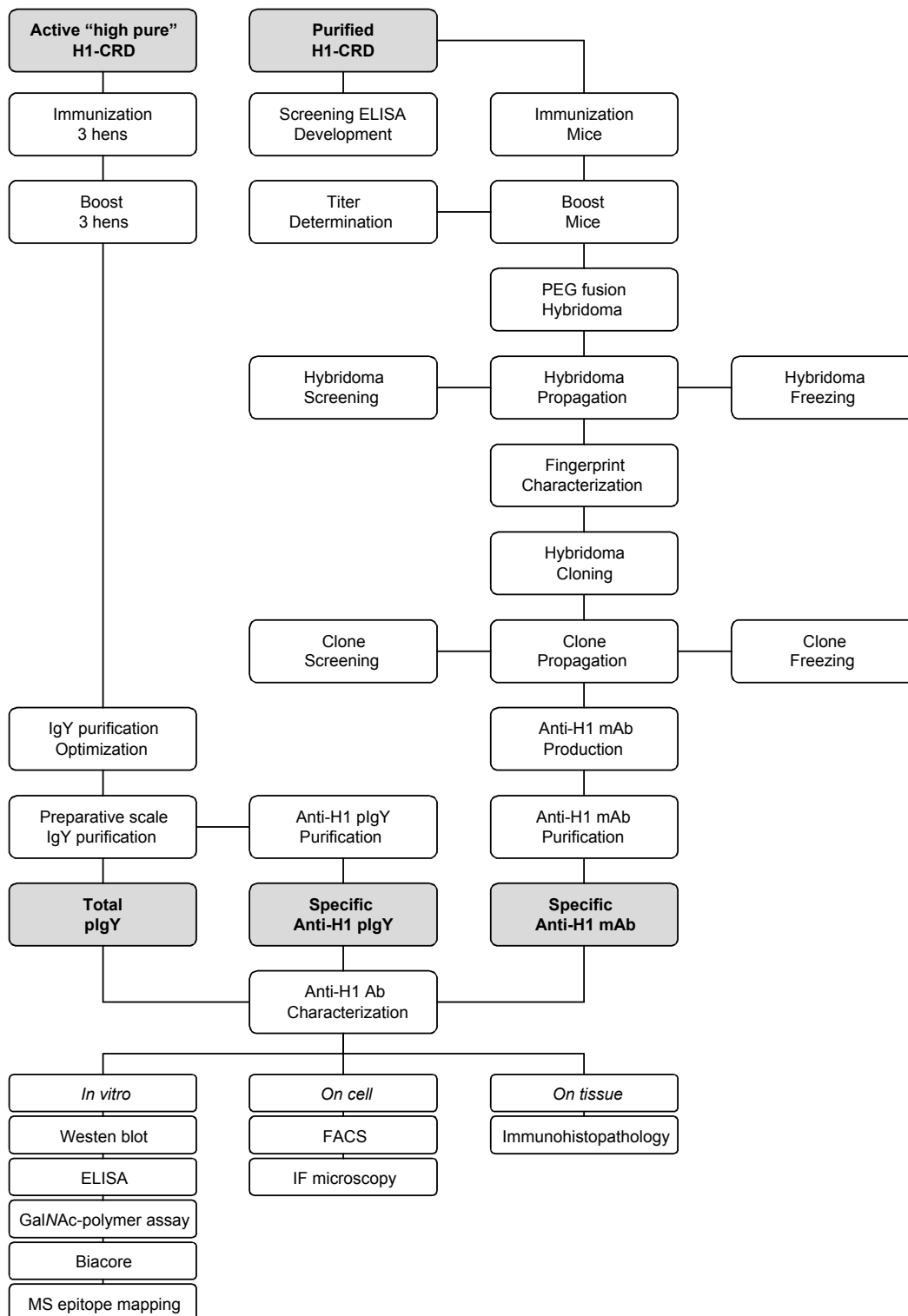


Figure 158: Overview of the monoclonal and polyclonal anti-H1 antibody production and the antibody characterization *in vitro*, *on cell*, and *on tissue* level.

4.5 Polyclonal antibodies – the way from hen to pure anti-H1 IgY

Chicken IgY are closely related to mammalian IgG, and both have many characteristics in common. As a consequence, polyclonal yolk IgY can be applied instead of polyclonal serum IgG in immunochemical methods.

Hens were immunized with highly pure H1-CRD, as a higher purity of the antigen increases the portion of specific antibodies in the polyclonal antibodies.⁶⁵ Specific IgY appear in the egg 20 days and reach the plateau 30 days post immunization,⁸⁵ and hence, eggs were collected starting after day 30. To keep the specific IgY concentration high, hens were boosted once prior and three times during the egg collection (see Figure 159).

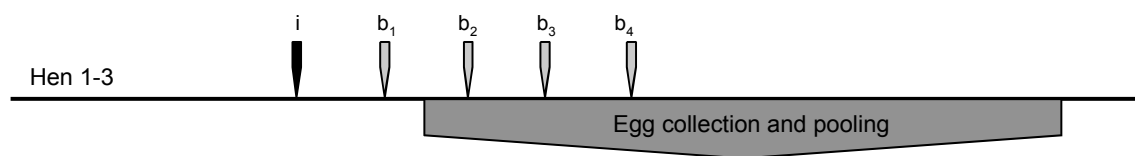


Figure 159: Immunization scheme of hens to produce polyclonal anti-H1 IgY in eggs: immunization (i) and 4 boost injections (b₁ to b₄) every 20-40 days. Eggs were collected after b₂ for a period of about 120 days.

The IgY separation from IgM and IgB is easier than the IgG extraction from total serum Ig due to the compartmentalization in eggs. In the yolk, large amounts of IgY but no IgM and IgB are present, whereas in the egg white only traces or no IgY are found. Unfortunately however, IgY bind neither to Protein A nor to Protein G, a feature that is exploited for simple isolation of IgG from serum. Nevertheless, there exist a big array of other chromatographic or precipitation procedures for IgY extraction.

Since none of these is a standard method and since the various isolation methods are discussed controversially in literature, it was worthwhile to compare the effectiveness of several extraction strategies prior to the purification of IgY in preparative scale.

Most procedures have four purification steps in common, i.e. the separation of yolk and egg white, the precipitation of lipids, the extraction of the total IgY and finally, the isolation of the antigen-specific IgY. The first step is identical for all and the last step depends on the antigen and is given. Only the second and third step can vary. For each of both steps, three methods were chosen and combined, which resulted in a panel of nine distinct methods (see Figure 160). All were ranked according to the obtained yield, purity and activity.

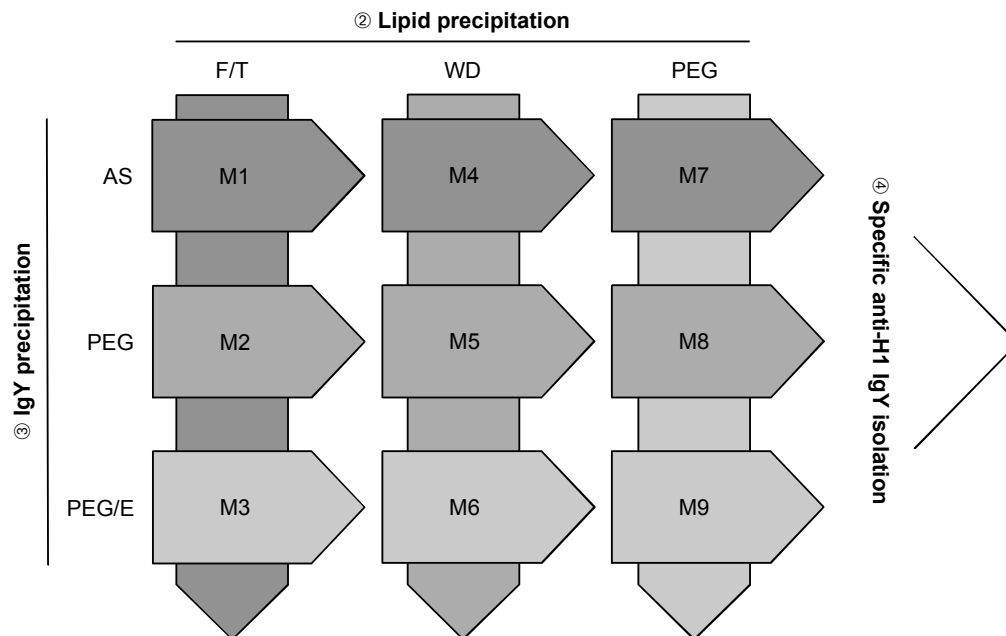


Figure 160: Extraction of specific IgY from egg yolk in four purification steps: separation of egg white and yolk ①, removal of lipids to get the total proteins ②, extraction of the total IgY from total proteins ③ and isolation of the specific IgY from total IgY ④.

Lipid precipitation – separation of water soluble and insoluble yolk portions

The WD and F/T methods were significantly less efficient in the precipitation of lipids than the PEG method, since they only yielded about 40% and 25% of the total yolk proteins/egg. In contrast, the ranking according to the activity/egg clearly favored the WD method over PEG and F/T methods. In respect to the activity but not to the yield, the observation was in agreement with Nakai S *et al.*¹⁶¹. They reported the WD method to be superior to the PEG, regarding yield and activity.

Total IgY precipitation – extraction of IgY from crude yolk proteins

The AS method removed the irrelevant proteins insufficiently. The most prominent contaminant was supposed to be the 41kDa lipovitellin. In addition, some 45kDa ovalbumin and traces of phosphovitellin that dissociated into a variety of different proteins, remained. In contrast the IgY, which were isolated by the PEG and the PEG/EtOH method exhibited a high purity. Consequently, the IgY yields/egg were only about 20% and 10% compared to the AS method. But decisive was the IgY activity/egg that was even slightly higher for PEG methods than for the AS method. As expected, the yield and activity of PEG/EtOH-derived IgY was lowest, since the procedure included an additional precipitation step.

In reference to the yield but not to the activity, Svendsen L. *et al.*¹⁴³ and Schwarzkopf C. *et al.*¹⁶² observed the same. They reported the highest recovery and activity of the total and the specific IgY by the AS, followed by the PEG/EtOH and the PEG method.

Anti-H1 IgY isolation – separate unspecific from specific IgY

The specific anti-H1 IgY were extracted from total IgY by affinity to H1-Sepharose. One drawback of this chromatographic method was, that the matrix-coupled H1-CRD and the H1-CRD used for the hens immunization were identical. As a consequence, also traces of irrelevant proteins may be linked to the support, which allow irrelevant IgY to bind specifically, too.

The portion of specific IgY was four times higher in the PEG-derived total IgY than in the AS-derived total IgY. This was expected, since the purity of the AS-derived total IgY was lower. In mean, the resulting amounts of AS-derived and PEG-derived specific IgY were similar (see Figure 161). However, AS-originated specific IgY still contained contaminants.

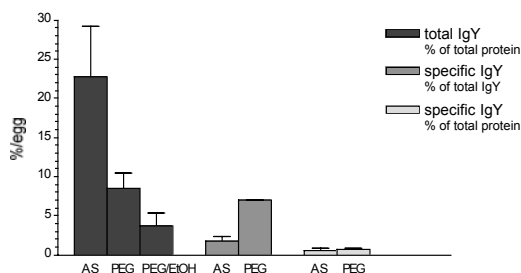


Figure 161: IgY yield/egg arranged by the method used for the total IgY extraction.

The extraction of the specific IgY by H1-Sepharose chromatography was efficient as the activity recovery was high.

Nine procedures - lipid and IgY extraction in combination

The optimal extraction procedure should not only provide a good yield but more importantly should supply pure IgY with the highest activity. For the isolation of the specific anti-H1 IgY, the total yolk proteins may directly be applied to the H1-Sepharose column without prior extraction of the total IgY.

All in all, procedure M8 is optimal for the extraction of the total IgY. Furthermore, a procedure composed of the WD method, showing the highest recovered activity, and the H1-CRD affinity chromatography may be superior to isolate the specific anti-H1 IgY. But since the total IgY are often as suitable as pure specific IgY in immunological assays

and since unspecific IgY can stabilize and protect the specific IgY from degradation,¹⁶² procedure M8 was selected for the preparative scale extraction to obtain the total IgY.

Preparative scale extraction of polyclonal anti-H1 IgY – from hundreds of eggs to grams of pure total IgY

The scale-up of procedure M8 was accompanied by an increased yield of total IgY/egg. Schwarzkopf *et al.*¹⁶² reported this positive scaling-up effect too and recommended the processing of more than 10 eggs in once. Though the obtained yield of 45mg/egg total IgY was still quite low, but the portion of specific IgY was rather good with 7%. Published are yields of 50-100mg/egg total IgY, which contain 2-10% specific IgY.¹⁶³

12g total IgY antibodies were achieved from 3 hens in about 120 days. In other words, each hen provided about 1g/month IgY. This is only half the amount reported by Schade R. *et al.*¹⁶⁴ but still 5-fold the amount of serum IgG/month, obtained from one rabbit.

Polyclonal anti-H1 IgY features – application in vitro and on cell

The purified IgY antibodies were successfully applied in some but not in all immunochemical methods.

In vitro the specific as well as the total IgY were suitable in immunoblotting of non-reduced and reduced, denatured H1-CRD and native H1-CRD. Since they bound to traces of H1-CRD oligomers, which were not visible on a silver-stained PAGE gel, it can be supposed, that their avidity is high. Extra bands on the blot may originate from the specific interaction between an irrelevant IgY and its antigen, which contaminated the H1-CRD, or from binding of specific anti-H1 IgY to another protein that carried a related epitope.⁶⁵ Since on the blot only monomeric H1-CRD in reduced state and no other proteins were detected, it was assumed, that higher molecular weight proteins are H1-CRD oligomers or aggregates.

The total and the specific IgY also worked in AP-ELISA, but they have further to be titrated to determine their EC₅₀ and to proof their concentration-dependent binding.

On cell level, the TR-labeled specific IgY were internalized into HepG2 cells, but also unspecifically into SK-Hep1 cells. Hence, the immunostaining of cells has further to be refined to minimize the cross-reactivity.

4.6 Monoclonal antibodies – the way from mice to anti-H1 Ig

4.6.1 Mice, fusion and hybridomas – from mortal to immortal anti-H1 “antibody factories”

The standard method for the production of monoclonal antibodies is still the hybridoma technique, which was introduced by Köhler and Milstein⁸² 30 years ago.

Only the specific antibody-producing cells are selected and thus, the antigen purity is not of prime importance. The native and active antigen structure however is crucial to maximize the portion of hybridomas, which provide antibodies that recognize a conformational epitope at the protein surface. Unfortunately, it was not known, if the H1-CRD changed the conformation, when emulsified with the adjuvant for immunizations.

Two strategies were followed to get the monoclonal anti-H1 antibody-producing hybridomas. They differed in the immunization (mouse strain, antigen dose, immunization schedule) and in the PEG fusion procedure.

Immunization – H1-CRD goes in vivo

In the first strategy, outbred NMRI mice were immunized and boosted with 20µg H1-CRD in emulsion sc in the neck. Each mouse was three times finally boosted 3, 2 and 1 day prior to fusion with 20µg H1-CRD in solution, also sc in the neck. In contrast, in the second strategy, inbred Balb/c mice were immunized and boosted with a 10-fold higher amount of 200µg H1-CRD in emulsion ip. Each mouse was only once finally boosted 3 days prior to fusion with 200µg H1-CRD in solution but iv (see Figure 162).

Both strategies had in common, that CFA and IFA were used to improve the immune response, and that mice were boosted every about 20 days.

Inbred mice and especially mice of the Balb/c strain are generally taken, whereas outbred mice, e.g. mice of the NMRI strain are rarely used. Outbred strains however are often advantageous when the immune response is low, due to the lack of a suitable MHCII receptor or due to self-tolerance. But for some highly conserved antigens, the immunization may fail in one mouse strain due to tolerance but can induce an immune response in another strain.¹⁰² Therefore, testing both types of strains seemed promising.

The dose of H1-CRD, used for immunization, was in the middle range or very high, with 20µg or 200µg, respectively. Amounts of 5-50µg/injection are normally used.¹⁰² Both routes, ip and sc, are recommended for immunization and boost injections.¹⁰² Only for

the final boosting, iv or ip are favored, because after sc injection, the response is too slow and low. But the H1-CRD antigen led already sc and ip to a good immune stimulation, as the spleens were huge. The immune response to a final iv boost was excessive and killed mice. Taking the high sequence similarity of the ASGPR-1 and the MHL-1 into consideration, the death of mice was probably caused by an autoimmune reaction or an anaphylactic shock.¹⁰²

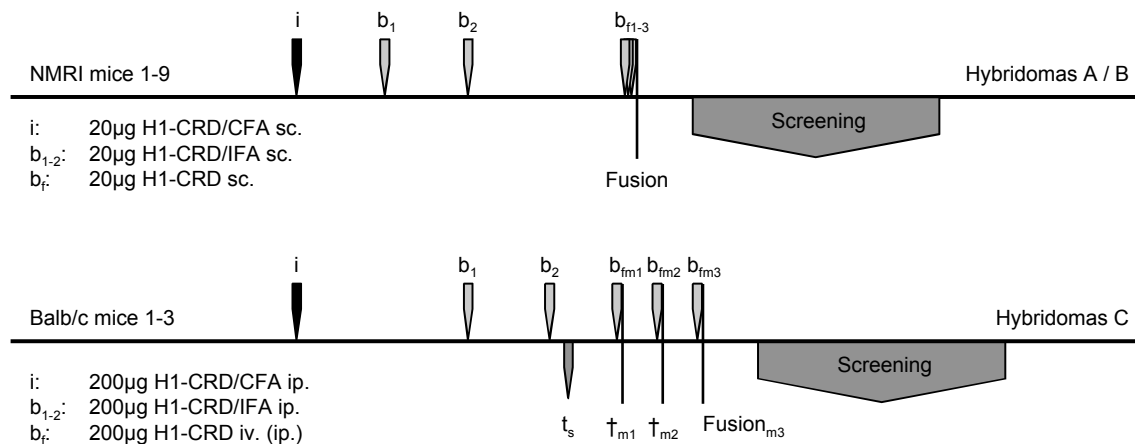


Figure 162: Immunization scheme of mice to produce monoclonal anti-H1 antibodies by the hybridoma technology, showing the immunization (i) with H1-CRD / CFA emulsion, at least two boosts (b₁ to b₂) with H1-CRD / IFA emulsion followed by the serum titer (t_s) determination and three final boosts 1, 2 and 3 days prior to fusion (b_{f1-3}) or one final boost of mice 1-3 (b_{fm1} to b_{fm3}) 1 day prior to fusion, with H1-CRD solution. Two mice died after final boosting (†_{m1} and †_{m2}) iv.

For further immunizations, a lower dose and the use of the NZB mouse strain could be advantageous. NZB mice tolerate the autoantibody production easier than others.¹⁰²

PEG fusion – it is fusion time

In the first strategy, cells were fused using PEG1500, and the hybridomas were plated on macrophages feeder-layer in IMDM-5. In the second strategy, the fusion was initiated with PEG4000 and the hybridomas were cultured in RPMI-15, supplemented with β-mercaptoethanol and human IL-6.

Both strategies had in common, that splenocytes and Balb/c P3X63-Ag8.563 myeloma cells were fused, and that hybridomas were selected with HAT. The growth-factor-secreting macrophages or IL-6 were essential for hybridomas growth at this stage. The use of IL-6 was preferred since no additional mice were needed to prepare macrophages. Both strategies provided a high number of hybridomas.

4.6.2 Hybridomas screening, expansion and fingerprint characterization – sift the chaff from the wheat

During expansion, 88% (fusion A) and 0% (fusion B) of NMRI-derived hybridomas and 60% (fusion C) of Balb/c-derived hybridomas were lost (see Figure 163). They either stopped the antibody production or the cell division. During propagation or mainly during single-cell cloning 8% (fusion A) and 17% (fusion C) of the hybridomas were instable.

The screening ELISA was selective for hybridomas, which recognized an accessible epitope at the surface of the active H1-CRD.

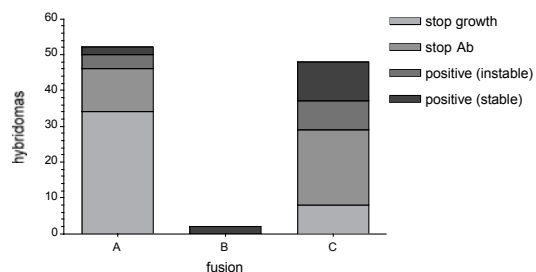


Figure 163: Total number of hybridomas from fusions A, B and C, subdivided into stable and instable positive, specific anti-H1 antibody-secreting hybridomas. Latter were subdivided according to the reason for loss: hybridomas, which stopped to grow, which gave up the secretion of anti-H1 antibodies or which were instable during propagation or single-cell cloning.

The anti-H1 antibodies of the different hybridomas were compared in various *in vitro* and *on cell* assays to identify the most promising ones for further characterization. The selected hybridomas should include one IgM and at least one IgG of each subclass. To have the entire set of (sub)classes is advantageous for simultaneous indirect multi-detection. The IgG are preferred due to their lower molecular weight and valency.

The hybridomas were favored those antibodies preferentially bound to native and not denatured H1-CRD in immunoblotting. They may recognize a predominantly conformational epitope also present at the ASGPR surface *on cells*, and probably even may bind the binding site epitope. Also in respect of the desired blocking antibody, calcium-sensitive binding in ELISA was guessed to be superior. Furthermore, a higher affinity to the H1-CRD compared to the H2-CRD was preferred.

However, decisive was, that the antibodies recognized the ASGPR on HepG2 cells. Only the corresponding hybridomas were selected, because the epitope accessibility in the entire ASGPR is a prerequisite for potential therapeutic or diagnostic application.

Ten candidates passed the selection, i.e. the hybridomas A41, A47, B01, C09, C11, C14, C17, C18, C23 and C48. A41 was excluded, because it was very instable.

The antibodies of all selected hybridomas worked fine in immunoblotting. C11, B01, C18 and C23 were the most promising as they favored the binding to native compared to reduced H1-CRD. Interestingly, all antibodies of the IgG1 isotype recognized the native similar or better than the reduced H1-CRD, whereas all non-IgG1 showed a comparable or stronger interaction with reduce than with native H1-CRD. All antibodies were applicable in ELISA. Most interesting features were maintained for C11 and C48, in the H1/H2 selectivity as well as in the calcium sensitivity ELISA. Their affinity to the H1-CRD was higher than to the H2-CRD and was further increased in the presence of calcium. A47, B01, C17 and C23 bound calcium-dependent stronger, too.

Seow *et al.*¹¹ reported, that beside HepG2 also Jurkat cells express the ASGPR, but HL-60 cells do not, and that human macrophages are known to express the ASGPR-homologous macrophage lectin. Hence, the antibodies of selected hybridomas were tested for the binding to HepG2, HL-60 and THP-1 cells and B01 additionally for the interaction with Jurkat cells. Only C14 cross-reacted with HL-60 and THP-1 cells. In contrast to Seow *et al.*, B01 was not able to recognize Jurkat cells. This was probably caused by receptor loss on Jurkat cells during cell passages, since carcinogenic cell are instable in their characteristics.

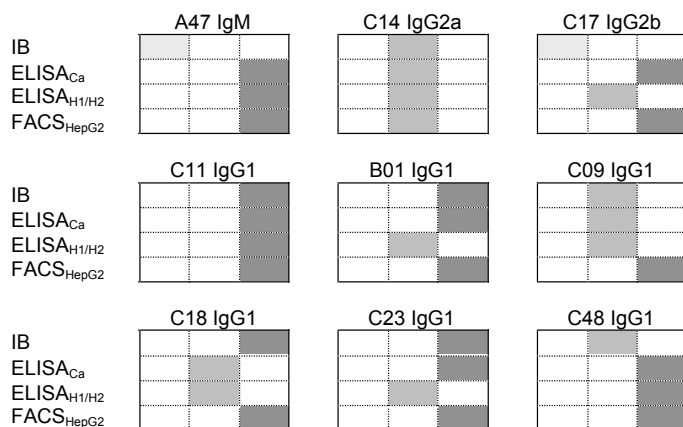


Figure 164: Selected hybridomas and their features (bad , balanced and good) in the fingerprint characterization. IB was regarded to be superior, when binding to the native H1-CRD was favored compared to the reduced H1-CRD; ELISA was best, when the binding to H1-CRD was preferred to H2-CRD and when the affinity to H1-CRD was stronger in the presence of calcium; FACS was valued to be good, when HepG2 were specifically stained and balanced when in addition other cells were recognized.

In the fingerprint ranking, most promising hybridomas were C11 and C48, decreasing to B01, C23 and C18, then to C17, C09 and C14 and lastly to A47 (see Figure 164).

Prior to further investigations of the selected hybridomas, they were single-cell cloned, to ensure their antibodies to be monoclonal.

4.7 Monoclonal anti-H1 Ig – features *in vitro*, on cell and on tissue

In the result part, each monoclonal antibody is described individually, whereas a cross-comparison will follow in this chapter. This may permit to assess, which one is most suitable for the application in different assays. Only one monoclonal antibody, the B01.4 will be discussed in detail in the following section. But, this will explain most features of the other seven monoclonal antibodies too.

The H1-CRD used for the characterization was a mixture of mainly monomeric species with a low fraction of two different dimeric species, if not clearer defined.

4.7.1 Antibody B01.4 – take a look at the monoclonal anti-H1 IgG1

Clone B01.4 was derived from hybridoma B01. The following section will give a closer look to the features of the monoclonal B01.4 antibody.

The B01.4 antibody is a member of the IgG κ class and IgG1 κ subclass, which is the main antibody class of the second immune response in blood.

4.7.1.1 Purification

The yield of murine B01.4 IgG1, extracted by affinity to Protein G and Protein A was identical. Due to the low affinity of IgG1, only a small fraction was extracted in once and thus, multiple extractions of the supernatant were necessary. The low elution pH did not harm the B01.4 IgG1. The antibody was still active in the HRP-ELISA. Because Protein G chromatography is simpler (no increase of the ionic strength is necessary) and supplies the same yield and activity, this method was favored.

4.7.1.2 Epitope mapping by immunoaffinity / MS

The characterization of the B01.4 epitope has had some pitfalls. These were not surprising in reference to the SEC and immunoblotting (see Sections 3.7.1.3 and 4.3).

To test the binding specificity of the H1-CRD to B01.4, immobilized on Sepharose, native and alkylated H1-CRD was also applied to blank Sepharose. The H1-CRD tended to adhere to Sepharose, similar to the observation in SEC. Furthermore, the binding of reduced-alkylated H1-CRD in the excision and slightly in the extraction turned out to be tricky. In agreement with the immunoblotting results, the affinity of reduced-alkylated H1-CRD was low. The observation, that the extraction of alkylated H1-CRD was less

affected than the excision, is probably due to the separation of the sterically interfering alkylation and the epitope residues onto different fragments (probably F2 and F3).

Fragments T¹⁵¹-R¹⁶² and S¹⁶³-R¹⁶⁹ were found in the extraction of the trypsin-digested H1-CRD. Additionally, the corresponding double fragment T¹⁵¹-R¹⁶⁹ was present in the excision. This demonstrated nicely the shielding effect, which protected the paratope-bound epitope against proteolysis. The independent binding of both fragments T¹⁵¹-R¹⁶² and S¹⁶³-R¹⁶⁹ also indicated, that the minimal epitope was either discontinuous, including continuous sequences on each fragment, or continuous, overlapping both fragments.

To diminish the antigenic site, the B01.4-bound H1-CRD was also excised with proteinase K. Many not identifiable fragments appeared in the wash and the elution. They were supposed to origin from B01.4. Probably, the antibody was less resistant to the proteinase K than to the trypsin digest. However, the two fragments V¹⁵⁸-S¹⁶³ and C¹⁶⁴-S¹⁶⁸ were identified, which represented a partial sequence of the epitope fragments obtained in the trypsin digest. To sum up, it can be suggested, that some residues of the continuous minimal epitope V¹⁵⁸EHERSCYWFS¹⁶⁸ form the functional epitope and mainly contribute to the binding affinity.

The minimal epitope is located on strands β 1 and β 2 of the H1-CRD and close to the N and C-terminus. Therefore the epitope is situated opposite to the Gal binding site in the molecule (see Figure 165). The calcium 3 is in close proximity to the epitope, but none of the epitope residues is involved in the calcium coordination (V¹⁹⁰, E¹⁹⁶, E²⁷⁷).²⁶

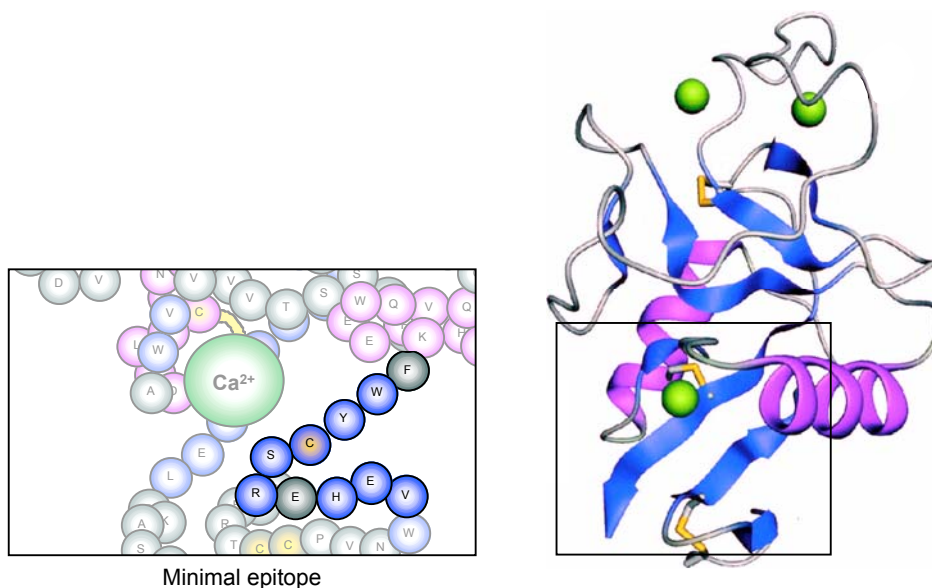


Figure 165: Minimal epitope of the monoclonal B01.4 IgG1.

Welling *et al.*⁸⁰ suggested, that His, Lys, Ala, Leu, Asp and Arg are the most frequent amino acids in epitopes. In the B01.4 epitope, only H and R are represented once.

The comparison with the antigenicity plots showed, that the partial B01.4 epitope VEHER indeed lies in a high antigenic, accessible and hydrophilic region of the H1-CRD, but that the partial epitope CYWFS is low antigenic and accessible due to the reduced polarity and the high content of aromatic amino acids.

In human, epitopes that differ only in two amino acid residues from the B01.4 epitope are present in the ASGPR-2, the macrophage lectin 2 and the CLEC10A protein of the pancreas and spleen. Unwanted cross-reactivity with these receptors seems probable. In addition, the ASGPR and the macrophage lectins of other mammals exhibit high homologous epitopes and consequently, B01.4 might also be applicable for investigations of the ASGPR in these species. Surprisingly, a variant-specific antigen of *Plasmodium falciparum*, as well as a protein of *Trypanosoma brucei* is quite similar.

4.7.1.3 Immunoblotting

The B01.4 antibody was applicable in immunoblotting, and it stained specifically. B01.4 recognized a denaturation-resistant epitope since the blot of the native as well as of the denatured H1-CRD showed a clear signal.

The dimeric H1-CRD was stronger detected than the monomeric H1-CRD. This let assume, that both Fv of the B01.4 antibody can bind simultaneously to the two identical epitopes of the dimeric H1-CRD species.

In the context of the epitope mapping results (see previous section), which indicated, that the epitope fragment F2+3 included the Cys¹⁵², Cys¹⁵³ and Cys¹⁶⁴, the native and the reduced H1-CRD were alkylated (see Figure 166).

The alkylation of the free or β -mercaptoethanol-paired Cys residue of the monomeric H1-CRD (see Section 4.2.1) did not alter the binding of B01.4. This was not surprising, since the dimerization of the H1-CRD via this Cys did not hinder the binding too. Also dimeric H1-CRD was recognized by B01.4, and the H1-CRD is really a much bulkier "group" than the acetamide group. However, the alkylation of at least one Cys, which is natively paired in a disulfide bridge, prevented the binding of B01.4. The four Cys, which are involved in the disulfide bridges C¹⁸¹-C²⁷⁶ and C²³⁶-C²⁶⁸, lie outside of the epitope region and are supposed not to contribute to this effect. The remaining two Cys form part

of the epitope. Two hypotheses seemed possible, depending on the position of the third S-S bond (see Figure 166, A and B) that is not yet defined in X-ray.

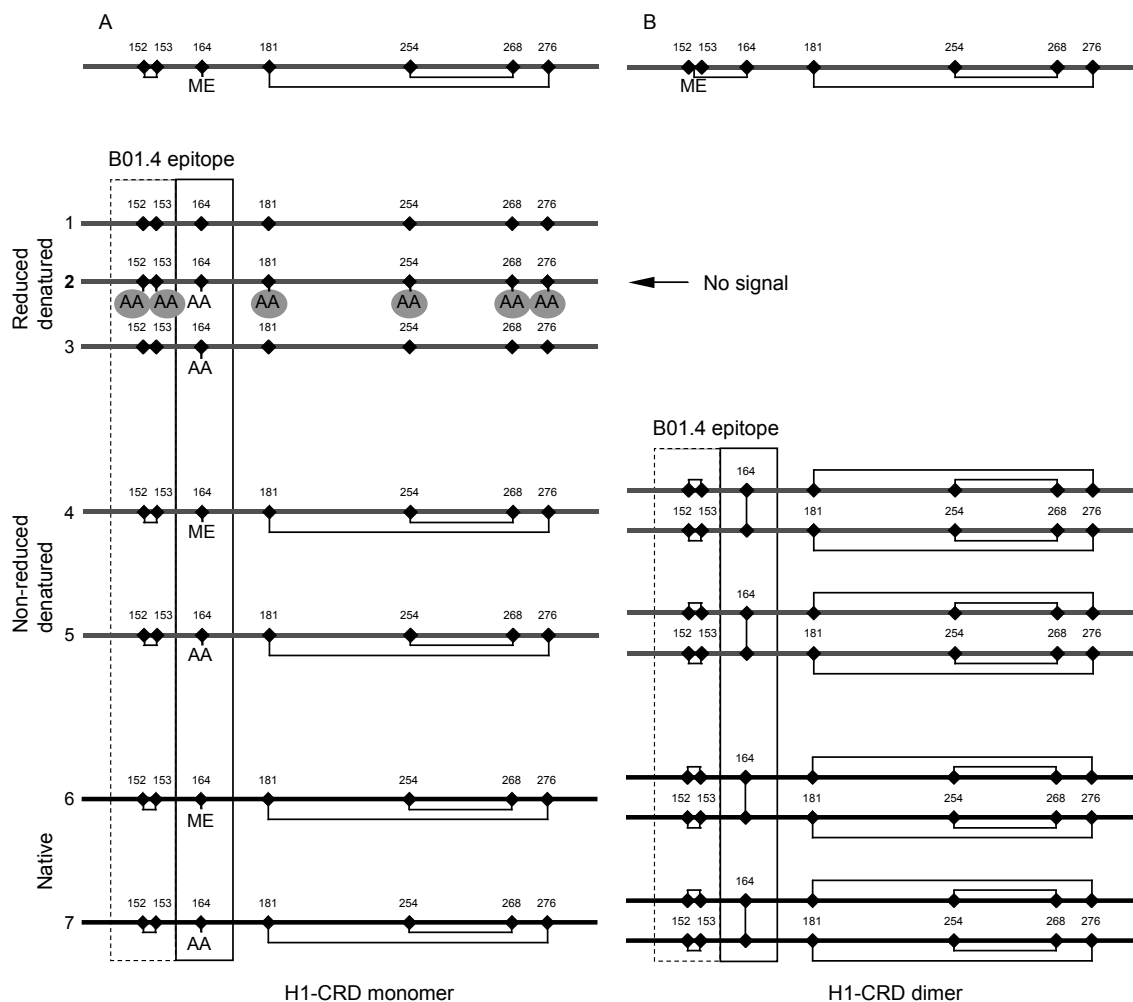


Figure 166: Immunoblotting with B01.4. A: Proposed disulfide linkage according to MS (see Section 3.2.2.4). B: Suggested disulfide linkage by Meier *et al.*²⁶ Blotting of reduced denatured H1-CRD without alkylation (1), reduced-alkylated (2) or native-alkylated (3) with acetamide (AA); Blotting of non-reduced denatured H1-CRD without alkylation (4) or native-alkylated (5); Blotting of native H1-CRD without alkylation (6) or native-alkylated (7). Numbers designate the Cys position in the H1-CRD amino acid sequence; β -mercaptoethanol (ME).

The hypothesis A bases on the MS result (see Section 4.2.1) that determined a disulfide bridge between the vicinal Cys¹⁵² and Cys¹⁵³ (although reshuffling of disulfide bridges under experimental conditions was not excluded). In this case, the alkylation of Cys^{152/153} adjacent to the minimal epitope might sterically hinder the binding of B01.4. However, this would also mean, that the C¹⁶⁴ in the determined minimal epitope is the free Cys, which did not alter the binding, when alkylated. This seems astonishing, as at least steric hindrance of the antibody-antigen interaction would be expected.

The hypothesis B is based on the assumption of Meier *et al.*²⁶ that one of the vicinal Cys^{152/153} is paired with Cys¹⁶⁴. In that case, the C¹⁶⁴ alkylation may cause the failure of the binding, whereas the alkylation of the two adjacent Cys has no effect or hinders sterically. Hence, it could be speculated, that the Cys¹⁶⁴ is part of the functional epitope.

In summary, B01.4 recognized a denaturation-resistant, probably discontinuous epitope. The binding of B01.4 to the structural epitope is independent of the Cys, which is involved in the H1-CRD dimerization but might be dependent on the accessibility of the two other Cys, in or adjacent to the minimal epitope.

4.7.1.4 Immunoassay

The monoclonal B01.4 was first titrated in an antibody-capturing ELISA to estimate the EC₅₀. As the H1-CRD contains integral calcium ions, which are important for the ligand recognition and the structural maintenance, the calcium sensitivity of the B01.4 binding was investigated. Finally in a competitive assay, the influence of B01.4 onto the binding of a polymer, exposing GalNAc residues, was tested to identify blocking ability.

Estimation of B01.4 avidity, EC₅₀

The monoclonal B01.4 IgG was titrated in an antibody-capturing HRP-ELISA in the presence of 20mM calcium to enforce the calcium-dependent native conformation of the H1-CRD. With an EC₅₀ of about 3·10⁻¹⁰M, the avidity was subnanomolar and in the middle range of the expected affinities for IgG antibodies of 10⁻⁷ to 10⁻¹²M.⁶⁵

The titration allowed a rough estimation of the avidity. The exact affinity is most accurately determined by Biacore assay (see Section 4.7.1.5).

Calcium sensitivity of B01.4 binding

The binding of B01.4 in the presence of a high and a low calcium concentration was compared to the binding in the absence of calcium. To minimize avidity effects due to a high local concentration of the H1-CRD, the plate was coated at a lower concentration. Hence the assay reached the detection limit and therefore, small absorbance variations resulted in high proportional binding differences.

The interaction between B01.4 and the H1-CRD was slightly calcium-sensitive. Calcium enforced the binding but independent of its level. Probably, a calcium-induced conformational change of the H1-CRD might cause a distinct exposure of the B01.4 epitope and lead to a decreased maximal binding. However, the calcium might directly

be involved into the binding of the antibody too, or differences in the ionic strength during capturing might influence the affinity.

In contrast, when the local concentration of the H1-CRD increased, it seemed, that independent of calcium, the same maximal binding occur, but that the affinity might be slightly lower without calcium. It may be speculated, that in the absence of calcium, the affinity of B01.4 to its epitope is lower, but that due to avidity effects, i.e. concerted reaction, the B01.4 avidity increase. This effect may overlap with and conceal the calcium dependence.

Competition of GalNAc and B01.4 IgG1 for binding to H1-CRD

The B01.4 IgG1 clearly interfered concentration-dependent with the GalNAc binding to the H1-CRD. An irrelevant IgG1 exhibited an approximately five times higher IC_{50} . Unfortunately, the blocking effect cannot only be caused by real competition for binding to the Gal binding site. B01.4 may induce and stabilize an H1-CRD conformation, which abolishes the binding of GalNAc. This seemed probable, since the putative epitope lies opposite to the Gal binding site. Nevertheless, steric hindrance of the GalNAc interaction may occur too, since the molecular weight of the H1-CRD is approximately a tenth of the weight of B01.4 and much below the weight of the GalNAc-polymer.

In summary, B01.4 worked excellent in immunoassays, with an EC_{50} in the subnanomolar range. At a low H1-CRD or antibody concentration, the binding of B01.4 seemed to be slightly calcium-dependent. It hindered the binding of the GalNAc-polymer, most probably not by competition but by steric or conformational interference.

4.7.1.5 Affinity and kinetics of the B01.4 IgG1 by Biacore

The first screen to investigate the calcium sensitivity, intensity and stability of the binding and the differences in the binding to monomeric and dimeric H1-CRD was performed at a constant B01.4 concentration. The following fine-resolution screen for the determination of binding kinetics used various B01.4 concentrations.¹⁴⁰

The B01.4 binding to the monomeric, but especially to the dimeric H1-CRD surface was slightly calcium-sensitive. In the presence of calcium particularly the stability was increased. Calcium and EDTA however did not affect the binding strength. Only the B01.4 interaction with dimeric H1-CRD was increased in the presence of EDTA. The loss of structure-maintaining calcium ions probably facilitated conformational changes, necessary for the concerted binding of one B01.4 molecule to both epitopes on the H1-

CRD dimer. In respect to the epitope mapping (see Section 4.7.1.2) it can be speculated, that B01.4 is sensitive for the calcium in site 3.

The B01.4 affinity to the monomeric and dimeric H1-CRD was similar and in the subnanomolar range. A closer look however revealed huge differences in their kinetics. The on and off-rates of the dimer are approximately half the values of the monomer and hence, the dimer binding is much slower but tighter. The reduced epitope accessibility may cause a lower association rate, while a higher local epitope concentration may enhance rebinding and concerted binding, and therefore reduce the dissociation rate.

In contrast to the GalNAc-polymer assay, B01.4 IgG1 did not hinder the galactose binding to the Gal binding site of the monomeric and dimeric H1-CRD (see Sections 4.7.1.4, 4.7.2.4. and 4.7.2.5 too). The discrepancy is supposed to originate from the different approaches of both assays. The Biacore assay determines real competition of galactose and B01.4 for the interaction with the Gal binding site. In contrast, the GalNAc-polymer assay mainly detects steric hindrance of the GalNAc-polymer binding.

In summary, B01.4 binds slightly calcium-sensitive to the H1-CRD with an affinity K_D of approximately 0.3nM. The rate constants of the interaction between B01.4 and the H1-CRD monomer are about double compared to the binding to the H1-CRD dimer, but this compensate in the calculated K_D . Finally, B01.4 did not interfere with the galactose binding.

4.7.1.6 Immunostaining of cells and tissue

The monoclonal B01.4 was tested in the immunostaining of various hepatic and extrahepatic cells and of non-pathological liver tissue.

Interaction of B01.4 with the ASGPR on cells

The B01.4 antibody bound to HepG2 hepatoma cells, which express the ASGPR. In contrast, SK-Hep1 hepatoma cells, which do not carry the ASGPR were not recognized. Hence, the B01.4 IgG1 epitope is also accessible in the entire ASGPR. Since human macrophages and immature dendritic cells expose the homologous macrophage and dendritic cell ASGPR respectively, these primary cells and the continuous THP-1 cell were investigated by flow cytometry. B01.4 however did not cross-react with any epitopes on these cells, and thus specifically recognizes the hepatic ASGPR.

The examination by immunofluorescence microscopy showed bright fluorescent cellular vesicles. This demonstrates, that B01.4 not only bound to the receptor but also initiated

internalization into living HepG2. Because SK-Hep1 did not invaginate B01.4, the endocytosis is regarded to be ASGPR-specific.

Interaction of B01.4 with the ASGPR in tissue

B01.4 was further applied in the immunostaining of paraffin-embedded non-pathological liver tissue sections. Although they successfully stained paraformaldehyde-fixed cells, they failed in tissue staining. Hence, the B01.4 epitope is either altered or not yet accessible after antigen retrieval, although various methods were tested.

Nevertheless, B01.4 might probably work in the staining of cryopreserved liver tissue sections or of pathological liver tissue. Autoimmune hepatitis tissue might differ in the expression of the ASGPR, because in some types of autoimmune hepatitis anti-ASGPR antibodies are detected in blood.

In conclusion, B01.4 bound not only to the purified H1-CRD but also and specifically to the entire hepatic ASGPR on fixed and not fixed HepG2 cells. The binding to living HepG2 cells initiated endocytosis. The antibody worked excellent in the fluorophor-staining of HepG2 cells but failed in the chromophor-staining of non-pathological liver tissue.

4.7.2 Comparison of the monoclonal anti-H1 Ig – which one is “the best”

4.7.2.1 Extraction of different isotypes of antibodies from culture supernatant

Analogous to polyclonal antibodies, monoclonal antibodies are purified by precipitation or extraction methods, mainly by Protein A or Protein G affinity chromatography. In general, chromatography yields higher amounts of purer antibodies in a shorter time. Since Protein A and G binds strong to murine IgG2a, but only fair to IgG1 and not to IgM, also the chromatographic extraction using Protein L and H1-CRD were tested. The interaction with Protein L is independent of the heavy chain isotype and though, IgM can be purified; but the light chain must be κ . The advantage of the extraction by affinity to Protein L and H1-CRD versus Protein A and G is, that they exhibit lower affinity to bovine Ig. Hence, the hybridoma clone propagation in medium, containing a suboptimal low concentration of expensive FCS (low IgG) can be circumvented. This was crucial for clones C23.8 and C48.9, which grew and secreted antibodies only in dense cell cultures and in the presence of growth-stimulating IL-6 or of a high FCS concentration.

The murine IgG1 better bind to Protein G than to Protein A, especially at a low ionic strength. But as a consequence, IgG1 bound to Protein G often elute at a lower pH than IgG bound to Protein A. The acidic condition may cause antibody aggregation or inactivation.¹⁰² The comparison of both methods showed however, that the extraction by Protein G was less troublesome and restored the activity of all anti-H1 IgG1 antibodies.

The antibody yields varied significantly in the range of 1 - 24mg/L culture (see Figure 167). This can be explained by variation of the cell numbers and periods until harvesting. Both depends on the sensitivity of the clones towards suboptimal grow conditions (low FCS concentration, low pH of the medium).

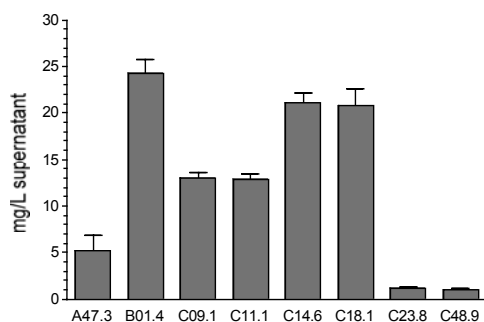


Figure 167: Monoclonal antibody yields of the eight clones from 1L cultures.

The obtained yields of anti-H1 Ig were rather low, since batch cultures generally provide 20-50mg/L antibodies.¹⁰²

4.7.2.2 Epitope mapping by immunoaffinity / MS

Epitope mapping by excision and extraction in combination with MS is a promising technique. In contrast to most other methods, excision enables not only the identification of continuous but also of discontinuous epitopes.

The immunoaffinity / MS technique however, turned out troublesome for the characterization of the antibodies C11.1 and C18.1. One possible reason is, that in the epitope excision the shielding effect was weak and therefore, the epitopes were cut to several fragments, which separately exhibited a too low affinity. A second reason may be, that the Cys alkylation prevented the binding (see also immunoblotting, following section). Additionally, it cannot be excluded, that the paratopes were degraded in the excision, although antibodies are generally resistant to proteolysis. The epitope extractions probably failed, because their epitope are conformational or were proteolytically cleaved in the trypsin digest.

Nevertheless, in the extraction of trypsin-digested alkylated H1-CRD with C11.1, three fragments could be identified. The fragment T¹⁵¹CCPVNWVEHER¹⁶² is located on strand β 1 and β 2, fragment F¹⁹⁹VQHHIGPVNTWMGLHDQNGPWK²²¹ on helix α 2, strand β 3 and on loop1. The fragment N²³⁴WRPEQPDDWYGHGLGGGEDCAHFTDDGR²⁶² includes the binding site. The extraction of the trypsin-digested alkylated H1-CRD, followed by excision of the bound fragments with pronase K allowed to diminish the epitope fragment N²³⁴-R²⁶² to a minimal epitope of W²³⁵RPEQPD²⁴¹. Since R²³⁶PEQPD²⁴¹ is part of the binding site, Q²³⁹ and D²⁴¹ coordinate the essential calcium in site 2 and interact also with GalNAc, the C11.1 is a highly promising candidate an antibody, blocking the Gal binding site (see Figure 168).

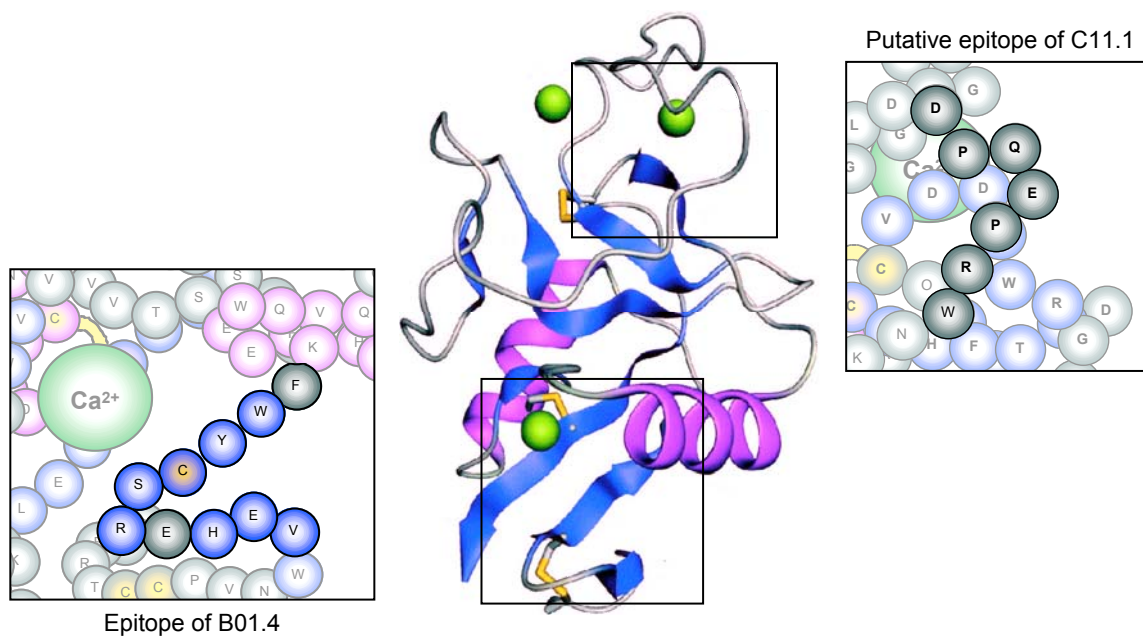


Figure 168: Distinct immunogenic epitopes on the surface of the H1-CRD, recognized by B01.4 and by C11.1 antibodies.

To sum up, it can be suggested, that W²³⁵-D²⁴¹ mainly forms the C11.1 epitope, but that residues T¹⁵¹-R¹⁶² and F¹⁹⁹-W²²¹ contribute to the binding too. This indicates, that the epitope is predominantly discontinuous and conformational, which is in agreement with the result of the immunoblotting (see Section 4.7.2.3). The putative epitope of C11.1 and the blocking ability however have to be demonstrated in further experiments.

First characterizations of the C18.1 epitope indicated the epitope to be located C-terminal in the area of R²⁷³-L²⁹⁰. In addition, first data of the C14.6 mapping showed, that

its epitope is probably located in the areas of T¹⁵¹-R¹⁶² and F¹⁹⁹-K²²¹ (results not shown). However, both have further to be investigated.

In conclusion, only the B01.4 epitope has been proven yet. The epitopes of C11.1, C14.6 and C18.1 were also investigated, but for these the epitope can only be assumed. It seems likely, that more than one epitope at the surface of the H1-CRD is immunogenic, and that these antibodies might be directed against distinct epitopes. Particularly C11.1 is promising, since its epitope may overlap with the Gal binding site.

4.7.2.3 Immunoblotting

On the one hand, immunoblotting permits to characterize a monoclonal antibody, but on the other hand also to explore the features of the antigen.

Applicability and sensitivity of anti-H1 Ig

The parallel investigation of the distinct monoclonal anti-H1 Ig makes it not only possible to see if they are applicable in immunoblotting and if they bind to a denaturation-resistant or denaturation-sensitive epitope but also to compare their sensitivities.

All monoclonal antibodies were very sensitive except A47.3, which needed a 10-fold higher antibody concentration (m/w). This may be the consequence of the distinct isotype, i.e. class IgM versus IgG, the isotype of all others. The sensitivity and therefore the avidity on the immunoblot was highest for C09.1, C18.1 and C14.6 followed by B01.4, C23.8 and C48.9 and lowest for C11.1 antibodies.

Characterization of anti-H1 Ig epitopes

Most of them, C09.1, C18.1, C23.8 and C48.9 recognized the denatured as well as the native H1-CRD, while C11.1 preferentially bound to the native H1-CRD. C14.6 and A47.3 almost uniquely interacted with the denatured H1-CRD. This let suggest, that the epitope of C11.1 is predominantly discontinuous and the epitope of C14.6 mainly continuous, but partially buried in the undenatured conformation. All other investigated antibodies may recognize more continuous epitopes, which are situated at the surface of the H1-CRD too.

Based on the findings for B01.4, all monoclonal antibodies were tested simultaneously for binding to H1-CRD modifications, which differed in the Cys alkylation pattern (see Figure 169). This could indicate if the monoclonal antibodies recognize B01.4-related epitopes. The antibodies C09.1, C18.1, C23.8 and C48.9 exhibited the same

immunostaining pattern as B01.4. Hence, they probably interact with an identical or overlapping structural epitope (see Section 4.7.1.3). The C11.1 binding pattern seemed similar to B01.4 too, but bands of reduced H1-CRD were hardly detected. In contrast to all other monoclonal anti-H1 IgG, the binding of C14.6 to alkylated and not alkylated H1-CRD was completely indifferent. Hence, it can be assumed, that its epitope contains no Cys.

In conclusion, antibodies B01.4, C09.1, C18.1, C23.8 and C48.9 worked excellent in immunoblotting, and they may recognize the same or overlapping structural epitopes. This epitope either includes one Cys or is adjacent to a Cys, which sterically hinder the binding, when alkylated. The C14.6 antibody however, tends to cross-reaction with irrelevant proteins, and it recognizes a distinct structural epitope, containing no Cys that must be accessible. The immunoblotting with A47.3 antibodies is less sensitive and therefore, is not recommendable.

4.7.2.4 Immunoassay

Two distinct antibody-capturing HRP-immunoassays were performed, a non-competitive and a competitive assay. In the non-competitive ELISA, the anti-H1 antibodies were titrated to estimate their EC_{50} . Since the H1-CRD includes three integral calcium ions, which are essential for structure and more importantly for Gal binding, the calcium sensitivity of the antibody binding was investigated. In the competitive GalNAc-polymer assay, the interference of the GalNAc and the antibodies for binding to the H1-CRD was tested.

Applicability of monoclonal anti-H1 antibodies in ELISA

The titration of the monoclonal anti-H1 antibodies in the antibody-capturing HRP-ELISA was performed in the presence of 20mM calcium to stabilize the H1-CRD in its native calcium-dependent conformation. Nevertheless, it cannot be excluded, that due to the immobilization on the plastic surface, the H1-CRD changed conformation.¹⁶⁵

The titration permitted to rank the distinct anti-H1 Ig according to their affinities, but was not accurate to determine K_D values. Antibody affinities with lower k_{off} rates would be overestimated, as the outcome of an immunoassays mainly depends on the stability of the antibody-antigen complex, to survive long incubation times and stringent washing. So, K_D and binding kinetics were best determined by Biacore assays (see Section 4.7.2.5).

All IgG1 antibodies, C11.1, B01.4, C23.8, C18.1 and C09.1 have similar and C48.9 only a slightly higher, still subnanomolar EC_{50} . In contrast, the EC_{50} of C14.6 IgG2a and A47.3 IgM are approximately ten times higher (see Figure 170). The lower avidity of C14.6 and A47.3 compared to the others agreed with the findings in immunoblotting. These two preferred the binding to the denatured H1-CRD compared to the native H1-CRD (see Section 4.7.2.5). In addition, IgM are often of lower affinity, as they are the main antibodies of the first immune response, which lack the affinity maturation.

Calcium sensitivity of anti-H1 Ig binding

As already mentioned, calcium-dependent binding of the anti-H1 Ig may be initiated by mimicking the binding mode of Gal and GalNAc, but more probably by calcium-induced changes of the epitope conformation or by direct coordination with calcium.

On the basis of their calcium-dependence, the anti-H1 Ig could be grouped in three sensitivity types (see Figure 169). The first type included only C14.6 that bound calcium-independent. The second type is formed by B01.4, C09.1, C23.8 and C48.9. Their binding was dependent on the presence of calcium, but was not sensitive to the calcium level. Particularly the C23.8 and C48.9 interaction was nearly abolished in the absence of calcium. Finally, C11.1 referred to the third type. Its binding was sensitive to the calcium level. These observations let assume once more, that the C14.6 epitope is linear, whereas the others more probably recognize a mainly conformational epitope.

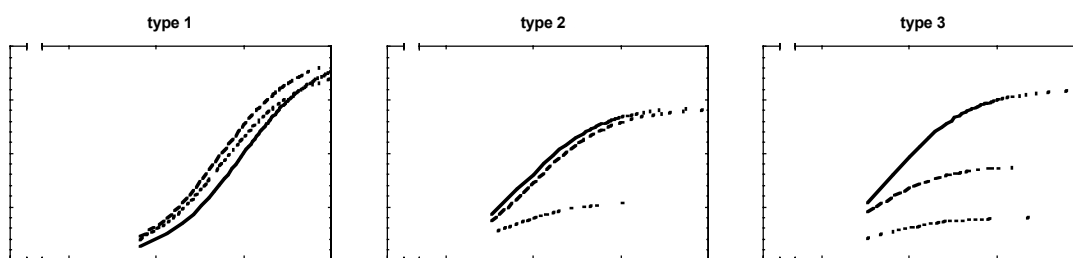


Figure 169: Types of calcium sensitivity

For all antibodies, the calcium effect was only detected at a low local H1-CRD concentration, as discussed for B01.4 (see Section 4.7.1. 4).

In conclusion, all anti-H1 IgG1 worked excellent in ELISA and had a subnanomolar EC_{50} . Only the binding of C14.6 IgG2a and A47.3 IgM antibodies was fair.

Epitope characterization by GalNAc-polymer and anti-H1 Ig competition

As discussed for B01.4 (see Section 4.7.1.4), anti-H1 Ig may not only interfere with the GalNAc binding by real blocking, due to the recognition of the binding site epitope, but also by other mechanisms. First, anti-H1 Ig can interact with a binding site-overlapping or an adjacent epitope and sterically hinder the GalNAc binding. This is very likely, since the molecular weight of the GalNAc-complex and the antibody is more than ten times the weight of the H1-CRD monomer. Second, the anti-H1 Ig binding may induce another H1-CRD conformation, which prevents the GalNAc interaction. Hence, the GalNAc-polymer assay allows only the antibody ranking either according to the inhibition concentrations (IC_{50}) or to the inhibition factors (IC_{50}/EC_{50}). Whereas the IC_{50} also depends on the antibody affinity, the inhibition factor only reflects the interference and therefore, may tell about the epitope localization relative to the Gal binding site.

All anti-H1 IgG but not A47.3 IgM hindered the GalNAc-polymer binding in a concentration-dependent manner. The anti-H1 IgG, except C11.1 have similar IC_{50} and inhibition factors (see Figure 170). Since the IC_{50} and particularly the inhibition factor of C11.1 are higher, the interference mechanism and probably the location of the C11.1 epitope may be distinct from the other antibodies.

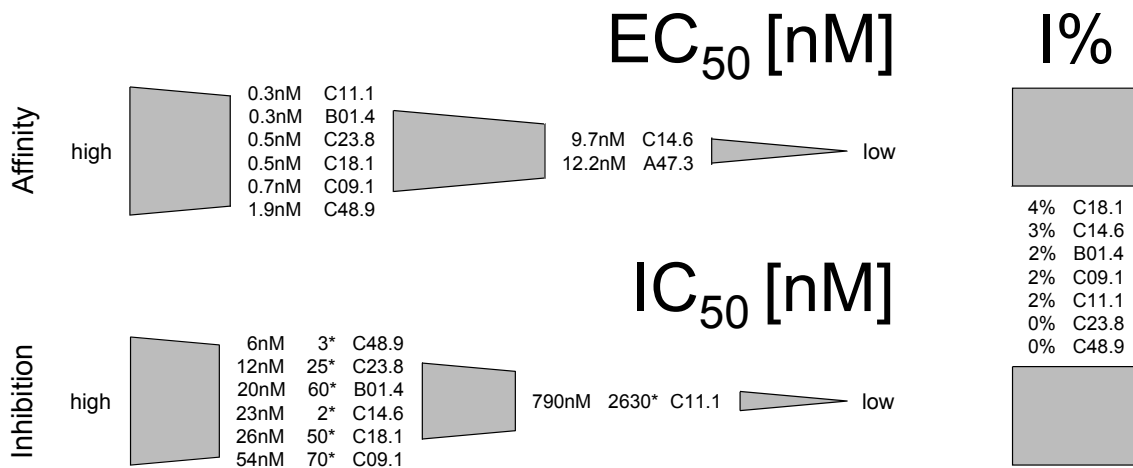


Figure 170: Ranking of the anti-H1 Ig according to the EC_{50} in the non-competitive assay, the IC_{50} in the competitive GalNAc-polymer assay with the corresponding inhibition factor and the relative inhibition I% in Biacore assay. The inhibition factor compares EC_{50} and IC_{50} , determined on plates with the same H1-CRD coating concentration and in TBS or HAB buffer with 1mM calcium. The relative inhibition I% describes difference of the second Gal injection signal in % of the first Gal injection signal.

Taking the immunoblot findings and the putative epitope of C11.1 and B01.4 into account, a hypothesis can be suggested.

The anti-H1 antibodies B01.4, C09.1, C18.1, C23.8, C48.9 showed a similar binding pattern in immunoblotting and a similar interference with the GalNAc binding. Hence, they may bind to epitopes in the area of the B01.4 epitope, opposite to the Gal binding site. Nevertheless, the GalNAc interaction may sterically be hindered or simultaneously, the antibody binding may stabilize an inactive H1-CRD conformation.

C11.1 may recognize another epitope, hopefully the proposed epitope, which overlaps with the Gal binding site and the calcium site 2. The steric hindrance was probably diminished by stabilization of the active binding site conformation, which enforced the GalNAc binding. However, since the epitope is not proven yet, C11.1 may also bind to another epitope, which simply did not interfere with the GalNAc binding.

The hypothesis is supported by Irimura *et al.*¹⁶⁶ They reported, that the homologous mouse macrophage C-type lectin changes calcium-dependently the conformation, and that a monoclonal antibody directed against this lectin, binds calcium-dependently to its epitope. The epitope was separated from the carbohydrate binding site, but the antibody binding stabilized the carbohydrate binding activity by a conformational lock of the CRD.

Unlike to the GalNAc-polymer assay, the anti-H1 Ig binding did not interfere with the galactose binding in the Biacore assay. This discrepancy may be caused by the use of distinct interfering sugars in type (Gal *versus* GalNAc) and in size (monosaccharide *versus* polymer). Hence, kinetics and steric hindrance of the sugar binding can vary. Though, since the putative physiological ASGPR ligands are glycoproteins and glycolipids of larger molecular weight, the antibodies may prevent the binding *on cell* too.

In summary, all anti-H1 IgG block the binding of GalNAc in a concentration-dependent manner. All except C11.1 exhibit similar IC_{50} . The interference is probable not due to real competition for binding to the Gal binding site. To enhance the assay reliability, the anti-H1 Ig and an irrelevant antibody of the same isotype should be examined in parallel on the same plate. This comparison would allow to distinguish accurately between specific and unspecific interference and to rank the distinct anti-H1 Ig properly.

4.7.2.5 Affinity and kinetics of anti-H1 IgG1 by Biacore

Biacore permits to determine the affinities K_D and also the binding kinetics, i.e. the association constants k_{on} and the dissociation constants k_{off} . All monoclonal anti-H1 IgG1 antibodies were screened for binding to the monomeric and dimeric H1-CRD, comparing both, and were ranked according to their binding intensity, binding stability, blocking properties and calcium sensitivity of the binding.

Ranking screen of monoclonal anti-H1 IgG1

In contrast to the competitive GalNAc-polymer assay (see Section 4.7.2.4), all antibodies evinced a non-blocking behavior, slightly varied in their binding to the monomeric and dimeric H1-CRD species and bound very stable. The high binding stability was expected as the screening to select anti-H1 Ig-producing hybridomas is based on ELISA that favors antibodies, which bind stable.

The binding kinetics of the monomeric H1-CRD fluctuated stronger than the kinetics of the dimeric H1-CRD in the presence of EDTA. This might be explained by the lack of the two calcium ions in site 1 and 3, which are involved in the structural maintenance. Thus, conformational changes are more likely. These influence the accessibility of the epitopes in the monomeric and dimeric H1-CRD and the antibody binding behavior.

Compared to the monomeric H1-CRD, the dimeric H1-CRD exhibited identical or higher binding stabilities and intensities to the anti-H1 Ig, independent of calcium and EDTA. The sole exception was C11.1 that bound with decreased intensity to dimeric H1-CRD in the presence of calcium. The higher stability is supposed to be the consequence of avidity effects. The bivalent IgG may bind to both identical epitopes of dimeric H1-CRD. The variation of the binding intensities may result from differences in the epitope accessibilities. In the presence of EDTA, the H1-CRD conformation is probably less stringent controlled and that may facilitate the binding of one IgG antibody to both epitopes of the dimer by induced fit. The restricted interaction of C11.1 with the dimeric H1-CRD is possibly due to the partial epitope concealment in the dimer (see Figure 171).

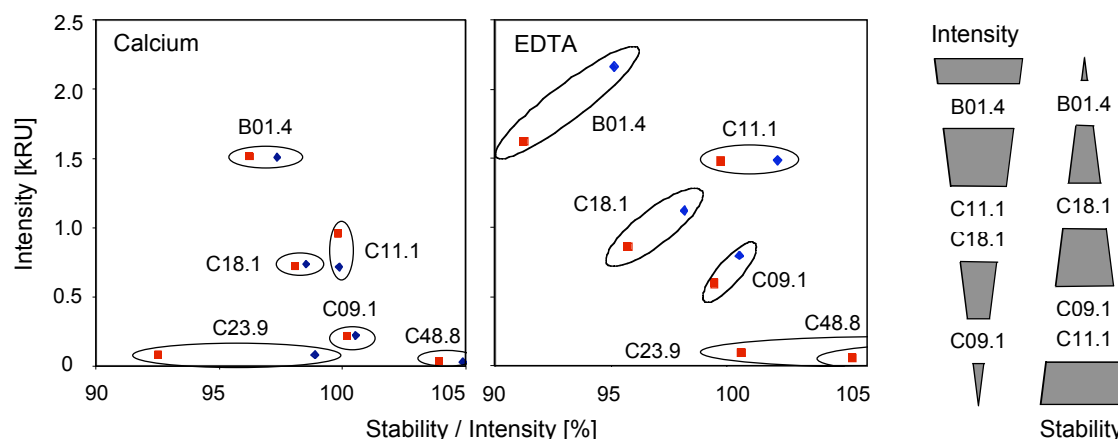


Figure 171: Plot of the monoclonal anti-H1 IgG1 ranking in Biacore assay, in the presence of 50mM calcium or 3mM EDTA. The binding of antibodies to the monomeric (red) and dimeric (blue) H1-CRD was compared.

Calcium and EDTA particularly influenced the binding intensity. Nevertheless, the ranking of the anti-H1 IgG1 remained the same. The strongest binding was observed with B01.4, followed by C11.1 and C18.1 and finally by C09.1, C48.9 and C23.8. The highest stability however was detected for C11.1 and C09.1, lowered to C18.1 and down to B01.4. In contrast to these three antibodies, the stability of the H1-CRD interaction with C23.8 and C48.9 varied calcium-dependently, in agreement with the findings in ELISA (see Section 4.7.2.4).

High-resolution screen of selected anti-H1 IgG1

Since for most applications IgG antibodies with a fast and tight binding profile are preferred, the three antibodies B01.4, C11.1 and 18.1 were selected for further screening of their binding kinetics to the monomeric and dimeric H1-CRD surfaces.

All bound in a concentration-dependent manner and exhibited a very slow dissociation. While the K_D differences of the monomeric and dimeric H1-CRD were rather low in the case of B01.4, the affinity of C18.1 to the dimer was almost double. All showed the tendency of a slower but tighter binding to the dimeric (lower k_{on} and k_{off}) than to the monomeric H1-CRD (see Figure 172).

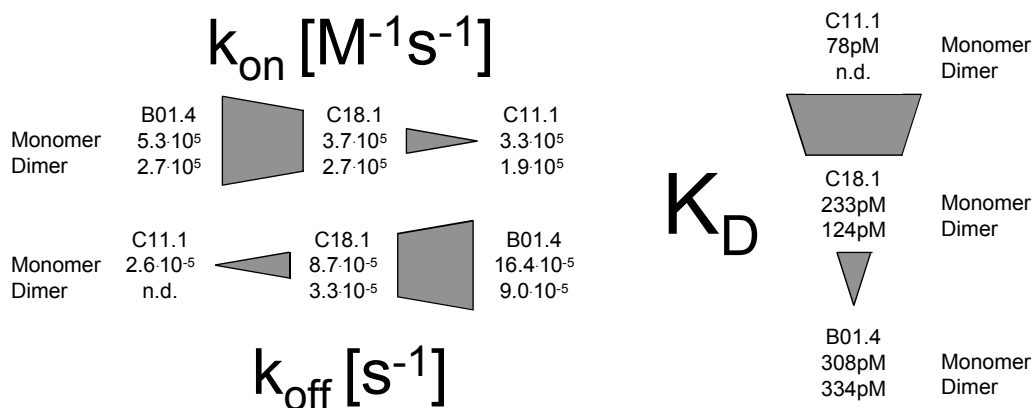


Figure 172: Binding kinetics of the anti-H1 IgG1 B01.4, C11.1 and C18.1.

In conclusion, none of the anti-H1 IgG1 clearly hindered the interaction between galactose and the Gal binding site. Most exhibited a slight calcium-dependent binding. The binding to dimeric H1-CRD was tighter and more stable in the presence of EDTA. The high resolution screening of the tightest binders B01.4, C11.1 and C18.1 showed, that mainly an extreme slow dissociation caused high affinities. This high stability is an

important advantage for the application in most immunomethods, since after antibody capturing bleeding effects may be minimal. The highest affinity was obtained for C11.1.

4.7.2.6 Immunofluorescence staining of cells and tissue

The monoclonal anti-H1 Ig antibodies were further investigated *on cell* level by indirect and direct immunofluorescence flow cytometry and microscopy of fixed and not fixed cells. In addition, the anti-H1 IgG binding to non-pathological paraffin-embedded liver tissue sections was examined.

Anti-H1 Ig binding to the entire ASGPR and cross-reaction with homologous receptors

Several human hepatoma cell lines like the HepG2, HUH-7 and PRF/5 cells are known to express the ASGPR whereas the receptor is not present on SK-Hep1 and Chang hepatoma cells. HepG2 and SK-Hep1 (see Appendix 5, page 282) cells were extracellularly stained with anti-H1 Ig to confirm, that their epitope is also accessible in the entire ASGPR, and that the recognition is ASGPR-specific. Since macrophages and immature dendritic cells express the ASGPR-homologous macrophage lectin and the dendritic cell ASGPR respectively, continuous THP-1 cells, primary macrophages and dendritic cells were examined to assess specific cross-reactions. Monocytes were isolated from human blood and their differentiation to dendritic cells was induced with IL-2.

All anti-H1 IgG bound to the ASGPR on not fixed HepG2 except A47.3 IgM. The brightest staining was obtained with C09.1, C18.1 and B01.4, followed by C11.1, C48.9 and C14.6 and finally by C23.8, ranked on the basis of the median. Since C23.8 showed to initiate endocytosis very efficiently (see below), internalization may cause the weak staining. In contrast to the anti-H1 Ig the commercial monoclonal anti-ASGPR antibody (Calbiochem) failed in the staining of HepG2 cells.

The other cells, SK-Hep1, THP-1, monocytes and dendritic cells did not cross-react with the anti-H1 Ig, except C14.6. The C14.6 antibodies recognized also an epitope on dendritic cells. In contrast to the originating hybridoma C14 however, they did not interact with THP-1 cells.

Binding and internalization of anti-H1 Ig via the ASGPR

The ability of the different anti-H1 Ig to initiate internalization into living HepG2 cells upon ASGPR binding was examined by fluorescence microscopy. SK-Hep1 cells were stained

in parallel to distinguish unspecific invagination and specific endocytosis of antibody-ASGPR complexes into endosomes.

The anti-H1 C23.8 and C11.1 were extensively and B01.4 and C18.1 highly internalized into HepG2 cells. All showed the same pattern of big bright spots. Compared to these, C09.1 and C14.6 were only poorly endocytosed and exhibited another staining pattern with more but smaller dots. It might be speculated, that they differed in the patch formation at the cell surface, the internalization rate or even in the endocytosis pathway. Hence, the antibodies C09.1 and C14.6 probably only bound to the ASGPR but did not induce endocytosis and therefore may only be constitutively internalized with the ASGPR. A47.3 IgM and the commercial anti-ASGPR antibody bound but were not internalized into HepG2. Since none of the anti-H1 antibodies interacted with or were taken up into SK-Hep1, the endocytosis into HepG2 seemed to occur via the ASGPR. However, only the immunostaining of ASGPR-transfected (e.g. SK-Hep1) cells would proof the specificity.

In summary, the different anti-H1 IgG worked fine in the immunostaining of cells. Only A47.3 IgM failed. All anti-H1 IgG are able to recognize their epitope in the entire ASGPR and specifically on HepG2. They do not cross-react with SK-Hep1, THP-1, monocytes or dendritic cells, except C14.6. Finally, all are internalized into HepG2 but to different extent.

Staining of non-pathological liver tissue

Non-pathological paraffin-embedded liver tissue was stained with the anti-H1 antibodies to test their applicability in immunohistochemistry.

All anti-H1 Ig failed except C14.6. The fixation and embedding procedure seemed to mask or alter their epitopes. This is not surprising, since C14.6 was found to recognize a denaturation-resistant more continuous epitope, whereas all other anti-H1 Ig are supposed to bind a more conformational epitope. However, they would probably work on cryo-conserved, not paraffin-embedded tissue. Furthermore they might stain pathological tissue. As in autoimmune hepatitis patients, anti-ASGPR antibodies can be found in blood, the ASGPR expression on hepatocytes may differ in pathological tissue.

C14.6 specifically stained the sinusoidal, basolateral surface of hepatocytes, which express the ASGPR.

4.8 Conclusion

Although the similarity of the ASGPR-1 and MHL-1 CRD is high, hybridoma clones were obtained and monoclonal anti-H1 antibodies were produced successfully in mice.

The characterization enables to rank the antibodies, on the one hand according to their applicability in different immunochemical methods (see Figure 173) and on the other hand according to their potential value in diagnostic or therapeutic applications.

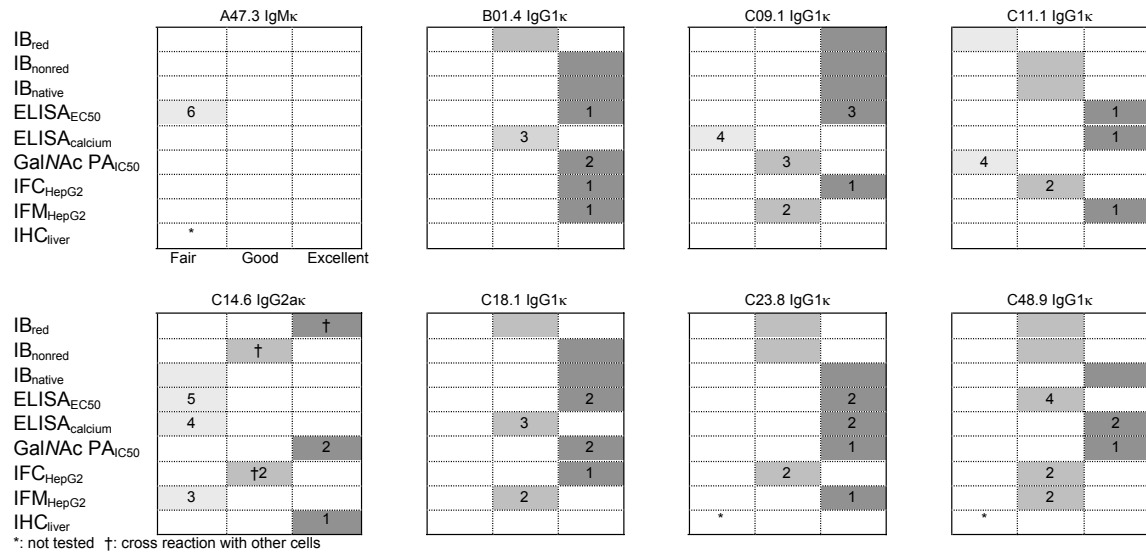


Figure 173: Applicability and ranking of the monoclonal anti-H1 antibodies. Binding to the H1-CRD in the reducing, non-reducing and native immunoblotting (IB_{red}, IB_{nonred} and IB_{native}), in the ELISA according to the calcium-dependence (ELISA_{calcium}) and the EC₅₀ in the presence of calcium (ELISA_{EC50}) and in the GalNAc-polymer assay (GalNAc PA_{IC50}). Binding to the ASGPR on HepG2 cells in the immunofluorescence flow cytometry (IFC_{HepG2}) and in the immunofluorescence microscopy (IFM_{HepG2}) and on non-pathological liver tissue in the immunohistochemistry (IHC_{liver}). Numbers indicate the ranking of the monoclonal antibodies.

All selected monoclonal IgG antibodies B01.4, C09.1, C11.1, C14.6, C18.1, C23.8 and C48.9 worked fine in the tested immunochemical methods, but not the A47.3 IgM. This IgM may be inactivated during purification, when eluted at a low pH.

B01.4

B01.4 is a stable and robust clone that also grows fine at a low FCS concentration and provides the highest yield/L culture. The B01.4 IgG1 antibodies work excellent in all immunochemical applications, except in the staining of paraffin-preserved non-pathological liver tissue. Although the B01.4 epitope is opposite to the Gal binding site, B01.4 interfere with the binding of high molecular weight ligands and may block the binding of natural ligands to the ASGPR, maybe also *in vivo*. The epitope lies in the H1-

CRD dimerization area and the putative binding area for induction of conformational changes or fit, needed for ligand binding. Consequently, B01.4 may be a precious tool for the ASGPR structure examination and for the investigation of the ligand-induced up regulation of the endocytosis or the signal transduction mechanism. The B01.4 IgG1 may be rewarding for commercial use due to its unproblematic handling, stability and broad applicability.

C09.1 and C18.1

C09.1 and C18.1 clones are stable and neither delicate in growth nor in the antibody production. C09.1 and C18.1 IgG1 are similar to B01.4 IgG1, stain slightly less intensive in immunofluorescence microscopy but are more sensitive in immunoblotting. Hence, they are suitable for the use in all immunochemical methods too, except in the immunostaining of paraffin-embedded liver tissue. Assuming that these three antibodies do not bind to the same epitope region, their combination to pooled anti-H1 IgG1 could be advantageous for some applications.

C23.8 and C48.9

C23.8 and C48.9 clones are troublesome. Especially C48.9 is instable, but both need high FCS or IL-6 supplemented medium for proper growth and the antibody production. Hence, to obtain acceptable yields, they must be cultured in enriched medium, and their antibodies then be purified by H1-Sepharose affinity chromatography to get rid of the bovine Ig.

C23.8 and C48.9 IgG1 are good or excellent applicable in all tested immunochemical methods in the presence of calcium. They only failed in immunohistochemistry. C23.8 are particularly valuable for studies of the endocytosis by immunofluorescence microscopy. C48.9 IgG1 may be interesting when a maximal specificity is essential, since in affinity they seem to distinguish even between H1 and H2-CRD.

The two antibodies C23.8 and C48.9 cannot be recommended for routine applications due to their difficult supply, but they may be the first choice for special investigations. If recurrent antibody supply is needed they are best subcloned to get more stable clones.

C14.6

C14.6 is a stable clone, which endures the suboptimal growth conditions during antibody production without any problems.

The C14.6 IgG2a are sensitive in all immunochemical methods even in immunohistochemistry. The specificity however is low. They cross-react with irrelevant proteins in immunoblotting and with dendritic cells in immunofluorescence flow cytometry. This may be of advantage for the discovery of ASGPR-homologous receptors. The main advantage is, that its epitope is denaturation-resistant, but as a consequence, the affinity in ELISA is poor. C14.6 seem to bind to but not to increase the internalization rate via the ASGPR. It might be interesting to test, if they block the binding and the signal transduction of high molecular weight ligands and to investigate the ligand-induced endocytosis rate of unlabeled synthetic low molecular weight ligands by co-internalization of labeled C14.6.

C14.6 IgG2a may be interesting for commercial use, particularly because they bind to a denaturation-resistant epitope and work excellent in immunohistochemistry. It may also be advantageous for simple double staining e.g. in combination with B01.4, detecting with a subclass specific secondary antibody.

C11.1

The C11.1 clone is stable and can be propagated for the antibody production without significant problems.

The C11.1 IgG1 seem to be “the best” ones. The putative conformational and denaturation-sensitive epitope overlaps with the Gal binding site and the calcium site 2, which coordinates the calcium essential for binding. The C11.1 affinity is calcium-sensitive and high, particularly due to the extraordinary stable binding. Furthermore, C11.1 antibodies induce extensive internalization via the ASGPR on HepG2 cells and do not cross-react with the ASGPR-homologous receptors on monocytes and dendritic cells. However, C11.1 IgG1 are not only ASGPR-specific, but even seem to prefer significantly the binding to the H1-CRD compared to the H2-CRD, considering the fingerprint characterization of C11. All together, C11.1 IgG1 may be the desired antibodies, which interfere with the binding site. It would be tremendous to further characterize the epitope, blocking ability, action in tissue and *in vivo* i.e. in a mouse model.

The collection of distinct monoclonal anti-H1 antibodies and of polyclonal anti-H1 antibodies enables to find a suitable one for all immunochemical applications and probably also for diagnostic and therapeutic applications. Especially C14.6 and C11.1 are promising candidates. C14.6 may be of diagnostic value, particularly *in vitro*. C11.1 may be precious for diagnostic but also for therapeutic purpose to target genes or drugs into hepatocytes.

These antibodies may allow further structure and function studies of the H1-CRD and of the ASGPR *in vivo*, under physiological and pathological conditions. It would be interesting to see if they may be valuable for diagnosis and detection of liver diseases, which are accompanied by a change in the ASGPR expression level, e.g. a decreased expression as found in cirrhotic or cancer liver tissue. Additionally, autoantibodies against the ASGPR, mainly against the H1 subunit are found in 80% of all patients with chronic active autoimmune hepatitis, in more than 70% with hepatitis B and in about 20% of the patients with primary biliary cirrhosis.¹⁶⁷ The antibody-based detection of distinct ASGPR expression pattern may permit to localize damaged tissue, similarly to the Tc⁹⁹-galactosyl-human serum albumine-diethylenetriamine-pentaacetic acid scintigraphy, introduced by Kokudo *et al.*¹⁶⁸ that is a routine test for liver function in Japan. Furthermore, it would be exciting to see if these antibodies or fragments of them could be applied as carrier for therapy of liver diseases and gene defects. Until nowadays, only natural ligand-based (ASF, ASOR, asialotransferrin), galactosylated polymer-based (Gal-polylysine, Gal-histones, Gal-lipopolyamine) and Sendai virus F protein-based delivery systems were tested.¹ In contrast to these delivery systems, which are founded on carbohydrate-protein interactions, targeting with antibodies rely on protein-protein recognitions that exhibit in general higher affinity and stability. In addition, fewer cross-reactions with other cell types may occur. E.g. the antibody-based targeting systems may enhance the specificity of the liver tumor treatment by the targeted rescue method, reported by Fukuma *et al.*¹ or of the targeted therapy with antiviral or anti-malaria drugs.

The monoclonal anti-H1 antibodies may open a new window in research, diagnosis and therapy and further investigations of their applicability are promising and crucial.

5 References

- 1 Fukuma T, Wu G, Wu C.H. (2000) Liver-selective nucleic acid targeting using the asialoglycoprotein receptor, *Gene Therapy and Regulation*, **1(1)**: 79 – 93.
- 2 Hashida M, Nishikawa M, Yamashita F, Takakura Y. (2001) Cell-specific delivery of genes with glycosylated carriers, *Adv. Drug Delivery Rev*, **52**: 187 – 196.
- 3 Bischoff J, Lodish H.F. (1987) Two asialoglycoprotein receptor polypeptides in human hepatoma cells, *J. Biol. Chem*, **262(24)**: 11825 – 11832.
- 4 Bider M.D, Spiess M. (1998) Ligand-induced endocytosis of the asialoglycoprotein receptor: evidence for heterogeneity in subunit oligomerization, *FEBS Letters*, **434**: 37 – 41.
- 5 Park JH, Cho EW, Shin S.Y, Lee YJ, Kim K.L. (1998) Detection of the asialoglycoprotein receptor on cell lines of extrahepatic origin, *Biochem. Biophys. Res. Comm*, **244**: 304 – 311.
- 6 Schwartz A.L, Rup D. (1983) Biosynthesis of the human asialoglycoprotein receptor, *J. Biol. Chem*, **258(18)**: 11249 – 11255.
- 7 Kohgo Y, Kato J, Nakaya R, Mogi Y, Yago H, Sakai Y, Matsushita H, Niitsu Y. (1993) Production and characterization of specific asialoglycoprotein receptor antibodies, *Hybridoma*, **12(5)**: 591 – 598.
- 8 Morell A.G, Irvine R.A, Sternlieb I, Scheinberg H, Ashwell G. (1968) Metabolic studies on sialic acid-free ceruloplasmin *in vivo*, *J. Biol. Chem*, **243(1)**: 155 – 159.
- 9 Valladeau J, Duvert-Frances V, Pin J.J, Kleijmeier M.J, Ait S, Ravel O, Vincent C, Vega F, Helms A, Gorman D, Zurawski S.M, Zurawski G, Ford J, Saelman S. (2001) Immature human dendritic cells express asialoglycoprotein receptor isoforms for efficient receptor-mediated endocytosis, *J. Immunol*, **167**: 5767 – 5774.
- 10 Higashi N, Fujioka K, Denda K, Hashimoto S, Nagai S, Sato T, Fujita Y, Morikawa A, Tsujii M, Miyata M, Sano Y, Suzuki N, Yamamoto K, Matsushima K, Irimura T. (2002) The macrophage C-type lectin specific for Gal / GalNAc is an endocytic receptor expressed on monocyte derived immature dendritic cells, *J. Biol. Chem*, **277(23)**: 20686 – 20693.
- 11 Seow Y.Y.T, Tan M.G.K, Woo K.T. (2002) Expression of a functional asialoglycoprotein receptor in human renal proximal tubular epithelial cells, *Nephron*, **91**: 431 – 438.
- 12 Harvey H.A, Porat N, Campbell C.A, Jennings M, Gibson B.W, Phillips NJ, Apicella M.A, Blake M.S. (2000) Gonococcal lipooligosaccharide is a ligand for the asialoglycoprotein receptor on human sperm, *Mol. Microbiol*, **36(5)**: 1059 – 1070.
- 13 Marino M, McCluskey R.T. (2000) Role of thyroglobulin endocytic pathways in the control of thyroid hormone release, *Am. J. Physiol. Cell Physiol*, **279**: C1295 – 1306.
- 14 Fadden A.J, Holt O.J, Drickamer K. (2003) Molecular characterization of the rat kupffer cell glycoprotein receptor, *Glycobiol*, **13(7)**: 529 – 537.
- 15 Schwartz A.L, Fridovich S.E, Knowles B.B, Lodish H.F. (1981) Characterization of the asialoglycoprotein receptor in a continuous hepatoma line, *J. Biol. Chem*, **256(17)**: 8878 – 8881.
- 16 Treichel U, Meyer zum Büschenfelde KH, Stockert RJ, Poralla T, Gerken G. (1994) *J. Gen. Virol*, **75**: 3021-3029.
- 17 Mu J.Z, Gordon M, Shao J.S, Alpers D.H. (1997) Apical expression of functional asialoglycoprotein receptor in the human intestinal cell line HT-29, *Gastroenterol*, **113(5)**: 1501 – 1509.
- 18 Mu J.Z, Fallon R.J, Swanson P.E, Carrol S.B, Danaher M, Alpers D.H. (1994) Expression of an endogenous asialoglycoprotein receptor in a human intestinal epithelial cell line Caco-2, *Biochim. Biophys. Acta*, **1222(3)**: 483 – 491.

- 19 Tanabe T, Pricer W.E, Ashwell J, Ashwell G. (1978) Subcellular membrane topology and turnover of a rat hepatic binding protein specific for asialoglycoproteins, *J. Biol. Chem*, **254(4)**: 1038 – 1043.
- 20 Bischoff J, Libressco S, Shia M.A, Lodish H.F. (1988) The H1 and H2 polypeptides associate to form the asialoglycoprotein receptor in human hepatoma cells, *J. Cell Biol*, **106**: 1067 – 1074.
- 21 Hardy M.R, Townsend R.R, Parkhurst S.M, Lee Y.C. (1985) Different modes of ligand binding to the hepatic Gal/GalNAc lectin on the surface of rabbit hepatocytes, *Biochemistry*, **24**: 22 – 28.
- 22 Bider MD, Wahlberg JM, Kammerer RA, Spiess M. (1996) The oligomerization domain of the asialoglycoprotein receptor preferentially forms 2:2 heterotetramers in vitro, *J. Biol. Chem*, **271**: 31996 – 32001.
- 23 Henis Y.I, Katzir Z, Shia M.A, Lodish H.F. (1990) Oligomeric structure of the human asialoglycoprotein receptor: nature and stoichiometry of mutual complexes containing H1 and H2 polypeptides assessed by fluorescence photobleaching recovery, *J. Cell Biol*, **111**: 1409 – 1418.
- 24 Spiess M, Lodish F. (1985) Sequence of a second human asialoglycoprotein receptor: conservation of two receptor genes during evolution, *Proc. Natl. Acad. Sci. USA*, **82(19)**: 6465 – 6469.
- 25 Spiess M, Schwartz A.L, Lodish H.F. (1985) Sequence of human asialoglycoprotein receptor cDNA, *J. Biol. Chem*, **260(4)**: 1979 – 1982.
- 26 Meier M, Bider M.D, Malashkevich V.N, Spiess M, Burkhard P. (2000) Crystal structure of the carbohydrate recognition domain of the H1 subunit of the asialoglycoprotein receptor, *J. Mol. Biol*, **300**: 857 – 865.
- 27 Kolatkar A.R, Leung A.K, Isecke R, Brossmer R, Drickamer K, Weis W.I. (1998) Mechanism of *N*-acetylgalactosamine binding to a C-type animal lectin carbohydrate-recognition domain, *J. Biol. Chem*, **273(31)**: 19502 – 19508.
- 28 Baenziger J.U, Maynard Y. (1980) Human hepatic lectin, *J. Biol. Chem*, **255(10)**: 4607 – 4613.
- 29 Park E.I, Baenziger J.U. (2003) Closely related mammals have distinct asialoglycoprotein receptor carbohydrate specificities, *J. Biol. Chem*, **279(39)**: 40954 – 40959.
- 30 Lee Y.C, Townsend R.R, Hardy M.R, Lonngren J, Anarp J, Haraldsson M, Lonn H. (1983) Binding of synthetic oligosaccharides to the hepatic Gal/GalNAc lectin, *J. Biol. Chem*, **258**: 199 – 202.
- 31 Biessen E.A, Beuting D.M, Roelen H.C, Van de Marel G.A, Van Boom J.H, Van Berkel T.J. (1995) Synthesis of cluster galactosides with high affinity for the hepatic asialoglycoprotein receptor, *J. Med. Chem*, **38(9)**: 1538 – 1546.
- 32 Bider M.D, Cescato R, Jenoe P, Spiess M. (1995) High-affinity ligand binding to subunit H1 of the asialoglycoprotein receptor in the absence of subunit H2, *Eur. J. Biochem*, **230**: 207 – 212.
- 33 Inhibashi S, Hammer R.E, Herz J. (1994) Asialoglycoprotein receptor deficiency in mice lacking the minor receptor subunit, *J. Biol. Chem*, **269(45)**: 27803 – 27806.
- 34 Tozawa R, Inhibashi S, Osuga J, Yamamoto K, Yagyu H, Ohashi K, Tamura Y, Yahagi N, Iizuka Y, Okazaki H, Harada K, Gotoda T, Shimano H, Kimura S, Nagai R, Yamada N. (2001) Asialoglycoprotein receptor deficiency in mice lacking the major receptor subunit, *J. Biol. Chem*, **276(16)**: 12624 – 12628.
- 35 Steer C.J, Weiss P, Huber B.E, Wirth P.J, Thorgeirsson S.S, Ashwell G. (1987) Ligand-induced modulation of the hepatic receptor for asialoglycoprotein in the human hepatoblastoma cell line HepG2, *J. Biol. Chem*, **262(36)**: 17524 – 17529.
- 36 Weigel P.H, Yik J.H.N. (2002) Glycans as endocytosis signals: the cases of the asialoglycoprotein and hyaluronan / chondroitin sulfate receptors, *Biochim. Biophys. Acta*, **1572**: 341 – 363.
- 37 Tolchinsky S, Yuk M.H, Ayalon M, Lodish H.F, Lederkremer G.Z. (1996) Membrane-bound versus secreted forms of human asialoglycoprotein receptor subunits, *J. Biol. Chem*, **271(24)**: 14496 – 14503.

- 38 Yik J.H.N, Saxena A, Weigel P.H. (2002) The minor subunit splice variants, H2b and H2c of the human asialoglycoprotein receptor are present with the major subunit H1 in different heterooligomeric receptor complexes, *J. Biol. Chem*, **277(25)**: 23076 – 23083.
- 39 Schwartz A.L, Fridovich S.E, Lodish H.F. (1982) Kinetics of internalization and recycling of the asialoglycoprotein receptor in a hepatoma cell line, *J. Biol. Chem*, **257(8)**: 4230 – 4237.
- 40 Tycko B, Keith C, Maxfield F. (1983) Rapid acidification of endocytic vesicles containing asialoglycoprotein in cells of a human hepatoma line, *JCB*, **97**: 1762 – 1776.
- 41 Weiss P, Ashwell G, Morell A.G, Stockert R. (1994) Modulation of the asialoglycoprotein receptor in human hepatoma cells: effect of glucose, *Hepatology*, **19**: 432 – 439.
- 42 Kato J, Mogi Y, Kohgo Y, Takimoto R, Kobune M, Hisai H, Nakamura T, Takada K, Niitsu Y. (1998) Suppressive effect of ethanol on the expression of hepatic asialoglycoprotein receptors augmented by interleukin-1 β , interleukin-6 and tumor necrosis factor- α , *J. Gastroenterol*, **33**: 855 – 859.
- 43 Bujanover Y, Legenthal E, Petell JK. (1991) Reduced levels of galactose-terminated glycoproteins in rat serum during perinatal development, *Biol. Neonate*, **60(1)**: 45-51.
- 44 Windler E, Greeve J, Levkau B, Kolb-Bachopen V, Daerr W, Greten H. (1991) The human asialoglycoprotein receptor is a possible binding-site for low-density lipoproteins and chylomicron remnants, *J. Biochem*, **276(1)**: 79-87.
- 45 Vierling JM, Steer CJ, Hickman JW, Ashwell G. (1978) Cell-mediated cytotoxicity of desialylated human lymphocytes induced by a mitogenic mammalian liver protein, *Gastroenterology*, **75**: 456-461.
- 46 Hajoui O, Martin S, Alvarez F. (1998) Study of antigenic sites on the asialoglycoprotein receptor recognized by autoantibodies, *Clin. Exp. Immunol*, **113**: 339 – 345.
- 47 Roccatello D, Picciotto G, Torchio M, Ropolo R, Ferro M, Francescini R, Quattrocchio G, Cacace G, Coppo R, Sena LM (1993) Removal systems of immunoglobulin A and immunoglobulin A containing complexes in IgA nephropathy and cirrhosis patients. The role of asialoglycoprotein receptors, *Lab. Invest*, **69(6)**: 714 – 723.
- 48 Becker S, Spiess M, Klenk H.D. (1995) The asialoglycoprotein receptor is a potential liver-specific receptor for Marburg virus, *J. Gen. Virol*, **76**: 393 – 399.
- 49 De Meyer S, Gong Z.J, Suwandhi W, Van Pelt J, Soumillion A, Yap S.H. (1997) Organ and species specificity of hepatitis B virus (HBV) infection: a review of literature with a special reference to preferential attachment of HBV to human hepatocytes, *J. Viral Hepatitis*, **4**: 145 – 153.
- 50 Makrides S.C. (1996) Strategies for achieving high-level expression of genes in *Escherichia coli*, *Microbiol. Rev*, **60(3)**: 512 – 538.
- 51 Studier F.W, Moffatt B.A. (1986) Use of bacteriophage T7 RNA polymerase to direct selective high-level expression of cloned genes, *J. Mol. Biol*, **189**: 113-130.
- 52 Bass S, Yang M. (2002) Protein function: a practical approach, expressing cloned genes in *Escherichia coli*, *PAS Oxford University Press*, 2nd edition.
- 53 Fabianek R.A, Hennecke H, Thöny L. (2000) Periplasmic protein thiol:disulfide oxidoreductases of *Escherichia coli*, *FEMS Microbiol. Rev*, **24**: 303-316.
- 54 Lilie H, Schwarz E, Rudolph R. (1998) Advances in refolding of proteins produced in *E.coli*, *Curr. Opin. Biotechnol*, **9**: 497 – 501.
- 55 Deutscher M.P. (1990) Methods in enzymology: guide to protein purification, *Academic press*, **182**.
- 56 Rudolph R, Böhm G, Lilie H, Jaenicke R. (2002) Protein function: a practical approach, folding proteins, *PAS Oxford University Press*, 2nd edition, **3**: 57 – 99.
- 57 Wetlaufer D.B. (1984) Nonenzymatic formation and isomerization of protein disulfides, *Methods Enzymol*, **107**, 301 – 304.

- 58 Creighton T.E. (1984) Disulfide bond formation in proteins, *Methods Enzymol*, **107**, 305 – 329.
- 59 Leibiger H, Wüstner D, Stigler R.D, Marx U. (1999) Variable domain-linked oligosaccharides of a human monoclonal IgG: structure and influence on antigen binding, *Biochem. J*, **338**: 529 – 538.
- 60 Endo T, Wright A, Morrison S.L, Kobata A. (1995) Glycosylation of the variable region of immunoglobulin G – site specific maturation of the sugar chains, *Mol. Immunol*, **32(13)**: 931 – 940.
- 61 Suzuki N, Lee C.Y. (2004) Site-specific N-glycosylation of chicken serum IgG, *Glycoobiology*, **14(3)**: 275 - 292.
- 62 Larsson A, Wejaker P.E, Forsberg P.O, Lindahl T. (1992) Chicken antibodies – a tool to avoid interference by complement activation in ELISA, *J. Immunol. Methods*, **156(1)**: 79-83.
- 63 Schmidt P, Erhard M.H, Schams D, Hafner A, Folger S, Los C.U. (1993) Chicken egg antibodies for immunohistochemical labeling of growth-hormone and prolactin in bovine pituitary gland, *J. Histochem. Cytochem*, **41**: 1441-1446.
- 64 Warr W, Mayor K.E, Higgins D.A. (1995) IgY: clues to the origin of modern antibodies, *Immunol. Today*, **16**: 392 – 398.
- 65 Harlow E, Lane D.P. (1999) Using antibodies: a laboratory manual, *Cold Spring Harbor Laboratory*, New York.
- 66 Landon J, Chard T. (1995) Therapeutic antibodies, *Springer Verlag*, Berlin, Heidelberg, New York.
- 67 Leslie G.A, Clem L.W. (1969) Phylogeny of immunoglobulin structure and function: Immunoglobulins of the chicken, *J. Exp. Med*, **130(6)**: 1337 – 1352.
- 68 Akita E.M, Nakai S. (1993) Production and purification of Fab' fragments from chicken egg yolk immunoglobulin Y (IgY), *J. Immunol. Methods*, **162**: 155 - 164.
- 69 Tonegawa S. (1983) Somatic generation of antibody diversity, *Nature*, **302**: 575 – 581.
- 70 Bezzubova O.Y, Buerstedde J.M. (1994) Gene conversion in chicken immunoglobulin locus: A paradigm of homologous recombination in higher eukaryotes, *Experientia*, **50**: 270 – 276.
- 71 Ambrosius *et al.* (1972)
- 72 Van Regenmortel M.H.V. (1996) Mapping epitope structure and activity: from one-dimensional prediction to four-dimensional description of antigenic specificity, *Methods Enzymol*, **9**: 465 – 472.
- 73 Al-Lazikani B, Lesk A.M, Chothia C. (1997) Standard conformations for the canonical structures of immunoglobulins, *J. Mol. Biol*, **273**: 927 – 948.
- 74 Alt F.W, Blackwell T.K, Yancopoulos G.D. (1987) Development of the primary antibody repertoire, *Science*, **238**: 1079 – 1087.
- 75 Bradford C.B, Poljak R.J. (1995) Structural features of the reactions between antibodies and protein antigens, *FASEB J*, **9**: 9 – 16.
- 76 Berzofsky J.A. (1985) Intrinsic and extrinsic factors in protein antigenic structure, *Science*, **229**: 932 – 940.
- 77 Hopp T.P, Woods K.R. (1983) A computer program for predicting protein antigenic determinants, *Mol. Immunol*, **20(4)**: 483 – 489.
- 78 Parker J.M.R, Guo D, Hodges R.S. (1986) New hydrophilicity scale derived from high-performance liquid chromatography retention data: correlation of predicted surface residues with antigenicity and X-ray derived accessible sites, *Biochemistry*, **25**: 5425.
- 79 Fraga S. (1982) Theoretical prediction of protein antigenic determinants from amino acid sequences, *Can. J. Chem*, **60**: 2606-2610.

- 80 Welling G.W, Wiejer W.J, Van der Zee R, Welling S. (1985) Prediction of sequential antigenic regions in proteins, *FEBS Letters*, **188**: 215 – 218.
- 81 Saha S, Raghava G.P.S (2004) PcePred: prediction of continuous B-cell epitopes in antigenic sequences using physico-chemical properties, *ICARIS*, LNCS 3239, Springer.
- 82 Köhler G, Milstein C. (1975) Continuous cultures of fused cells secreting antibody of predefined specificity, *Nature*, **256**: 495-497.
- 83 Yoo E.M, Chintalacharuvu K.R, Penichet M.L, Morrison S.L. (2002) Myeloma expression systems, *JIM*, **261**: 1 - 20.
- 84 Polson A, Von Wechmar M.B, Van Regenmortel M.H.V. (1980) Isolation of viral IgY antibodies from yolk of immunized hens, *Immunol. Commun*, **9(5)**: 475 – 493.
- 85 Gassmann M, Thömmes P, Weiser T, Hübscher U. (1990) Efficient production of chicken egg yolk antibodies against a conserved mammalian protein, *FASEB J*, **4**: 2528-2532.
- 86 Larsson A, Karlsson A, Sjöquist J. (1991) Use of chicken antibodies in enzyme immunoassays to avoid interference by rheumatoid factors, *Clin. Chem*, **37(3)**: 411 – 414.
- 87 Kronvall G, Seal U.S, Finstad J, Williams R.C. (1970) Phylogenetic insight into evolution of mammalian Fc fragment of gamma G globulin using staphylococcal protein A, *J. Immunol*, **104(1)**: 140 – 147.
- 88 Larsson A, Lindahl T. (1993) Chicken anti-protein G for the detection of small amounts of protein G, *Hybridoma*, **12(1)**: 143 – 147.
- 89 Camenisch G, Tini M, Chilov D, Kvietikova I, Srinivas V, Caro J, Spielmann P, Wenger RH, Gassmann M. (1999) General applicability of chicken egg yolk antibodies: the performance of IgY immunoglobulins raised against the hypoxia-inducible factor 1alpha, *FASEB J*, **13(1)**: 81 - 88.
- 90 Rosol T.J, Steinmeyer C.L, Mc Cauley L.K, Merryman J.I, Werkmeister J.R, Gröne A, Weckmann M.T, Swayne D.E, Capen C.C. (1993) Studies on chicken polyclonal anti-peptide antibodies specific for parathyroid hormone-related protein (1-36), *Vet. Immunol. Immunopathol*, **35(3-4)**: 321 – 337.
- 91 Lemamy G.J, Roger P, Mani J.C, Robert M, Rochefort H, Brouillet J.P. (1999) High-affinity antibodies from hens egg yolks against human mannose-6-phosphate/insulin-like growth-factor-II receptor: characterization and potential use in clinical cancer studies, *Int. J. Cancer*, **80(6)**: 896 - 902.
- 92 Schade R, Behn I, Erhard M, Hlinak A, Staak C. (2001) Chicken egg yolk antibodies, production and application: IgY-technology, *Springer Verlag*, Berlin, Heidelberg, New York.
- 93 Glick B, Chang T.S, Japp R.G (1956) The bursa of fabricius and antibody production in the domestic fowl, *Poultry Sci*, **35**: 224 – 226.
- 94 Akerström B, Brodin T, Reis K, Börg L. (1985) Protein G: a powerful tool for binding and detection of monoclonal and polyclonal antibodies, *J. Immunol*, **135**: 2589-2592.
- 95 Schwarzkopf C. (1994) Gewinnung und immunologische Charakterisierung speciespezifischer IgY, sowie deren Einsatz zur Bestimmung der Wirtstierart aus dem Abdominalblut hämatophager Insekten, *Dr. Thesis*, F.U. Berlin.
- 96 Jensenius J.C, Andersen I, Hau J, Crone M, Koch C. (1981) Eggs: conveniently packaged antibodies. Methods for purification of yolk IgG, *J. Immunol. Methods*, **46**: 63 – 68.
- 97 Polson A. (1990) Isolation of IgY from the yolks of eggs by a chloroform polyethylene glycol procedure, *Immun. Invest*, **19**: 253 – 258.
- 98 Akita E.M, Nakai S. (1993) Comparison of four purification methods for the production of immunoglobulins from eggs laid by hens immunized with enterotoxigenic E.coli strain, *J. Immunol. Methods*, **160**: 207 – 214..

- 99 Devi C.M, Bai M.V, Lal A.V, Umashankar P.R, Krishnan L.K. (2002) An improved method for isolation of anti-viper venom antibodies from chicken egg yolk, *J. Biochem. Biophys. Methods*, **51**: 129 – 138.
- 100 Polson A, Coetzer T, Kruger J, Von Maltzahn E, Van der Merwe K.J. (1985) Improvements in the isolation of IgY from the yolks of eggs laid by immunized hens, *Immin. Invest*, **14(4)**: 323 – 327
- 101 Hansen P, Scoble J.A, Hanson B, Hoogenraad N.J. (1998) Isolation and purification of immunoglobulins from chicken eggs using thiophilic interaction chromatography, *JIM*, **215**: 1-7.
- 102 Harlow E, Lane D.P. (1988) Antibodies: a laboratory manual, *Cold Spring Harbor Laboratory*, New York.
- 103 Stokmaier D. (2004) Receptor-mediated endocytosis in human hepatocytes, *Diploma Thesis*, University of Basel.
- 104 Sherpherd P, Dean C. (2002) monoclonal antibodies: a practical approach, *Oxford University Press*.
- 105 Suckau D, Köhl J, Karwath G, Schneider K, Casaretto M, Bitter D, Przybylski M. (1990) Molecular epitope identification by limited proteolysis of an immobilized antigen-antibody complex and mass spectrometric peptide mapping, *Proc. Natl. Acad. Sci. USA*, **87**: 9848 – 9852.
- 106 Macht M, Fiedler W, Kürzinger K, Przybylski M. (1996) Mass spectrometric mapping of protein epitope structures of myocardial infarct markers myoglobin and troponin T, *Biochem*, **35(49)**: 15633 – 15639.
- 107 Jemmerson R, Paterson Y. (1986) Mapping epitopes on a protein antigen by the proteolysis of antigen-antibody complexes, *Science*, **232(4753)**: 1001 – 1004.
- 108 Shimada M, Mizuno M, Uesu T, Nasu J, Okada H, Shimomura H, Yamamoto K, Tsuji T, Shiratori Y. (2003) A monoclonal antibody to rat asialoglycoprotein receptor that recognizes an epitope specific to its major subunit, *Hepatology Res*, **26**: 55 – 60.
- 109 Altschul SF, Gish W, Miller W, Myers EW, Lipman DJ. (1990) Basic local alignment search tool, *J. Mol. Biol*, **215(3)**: 403-410.
- 110 Tatusova T.A, Madden T.L. (1999) Blast 2 sequences – a new tool for comparing protein and nucleotide sequences, *FEMS Microbiol. Lett*, **174**: 247-250.
- 111 T-Coffee: A novel method for multiple sequence alignments, *J. Mol. Biol*, **302**: 205-217.
- 112 Hopp TP, Woods KR. (1981) Prediction of protein antigenic determinants from amino acid sequences, *PNAS USA*, **78**: 3824-3828.
- 113 Kyte J, Doolittle RF. (1982) A simple method for displaying the hydrophatic character of a protein, *J. Mol. Boil*, **157**: 105-132.
- 114 Sweet RM, Eisenberg D. (1983) Correlation of sequence hydrophobicities measures similarities in three-dimensional protein structure, *J. Mol. Biol*, **171**: 479-488.
- 115 Janin J. (1979) Surface and inside volumes in globular proteins, *Nature*, **277**: 491-492.
- 116 Fauchere JL, Pliska V. (1983) Hydrophobic parameters π of amino-acid side chains from the partitioning of N-acetyl-amino-acid amides, *Eur. J. Med. Chem*, **18**: 369-375.
- 117 Manavalan P, Ponnuswamy P.K. (1978) Hydrophobic character of amino acid residues in globular proteins, *Nature*, **275**: 673-674.
- 118 Sambrook J, Fritsch E.F, Maniatis T. (1989) Molecular cloning: a laboratory manual, 2nd edition, *Cold Spring Harbor Laboratory Press*, USA.
- 119 Novagen (2000) pET system manual, *Novagen Technical Bulletin*, TB055, 9th edition.
- 120 Morrison D.A. (1977) Transformation in Escherichia coli: cryogenic preservation of competent cells, *J. Bacteriol*, **132(1)**: 349-351.

- 121 Wetmur J.G. (1991) DNA probes: applications of the principles of nucleic acid hybridization, *Crit. Rev. Biochem. Mol. Biol.*, **26**: 227-259.
- 122 Suggs S.V, Hirose T, Miyake E.H, Kawashima M.J, Johnson K.I, Wallace R.B. (1981) Using purified genes, ICN-UCLA Symposia on developmental biology, *Academic Press*, New York, **23**: 683-693.
- 123 QIAGEN (1997) *Taq PCR handbook. QIAGEN Technical Bulletin.*
- 124 Saiki R.K, Scharf S, Faloona F, Mullis K.B, Horn G.T, Ehrlich H.A, Arnheim N. (1985) Primer-directed enzymatic amplification of DNA with a thermostable DNA polymerase, *Science*, **230**: 1350-1354.
- 125 New England Biolab (2001) T4 DNA ligase *Technical Bulletin*, M0202.
- 126 Novagen (2001) Competent cell manual, *Novagen Technical Bulletin* TB009.
- 127 Bollag D.M, Rozycki M.D, Edelstein S.J. (1996) *Protein Methods*, 2nd edition, *Wiley-Liss publication.*
- 128 Ornstein L. (1963) Discontinuous electrophoresis – I. Background and theory, *Ann. N. Y. Acad. Sci.*, **121**: 321-349.
- 129 Davis B.J. (1964) Discontinuous electrophoresis – D. Method and application to human serum proteins, *Ann. N. Y. Acad. Sci.*, **121**: 404-427.
- 130 Laemmli E.K. (1970) Cleavage of structural proteins during the assembly of the head of bacteriophage T4, *Nature*, **227**: 680-685.
- 131 Heukeshoven J, Dernick R. (1988) Improved silver-staining procedure for fast staining in PhastSystem Development Unit: I. Staining of sodiumdodecylsulfate gels, *Electrophoresis*, **9(1)**: 28-31.
- 132 Kyhse-Andersen J. (1984) Electroblotting of multiple gels: A simple apparatus without buffer tank for rapid transfer of proteins from polyacrylamide to nitrocellulose, *J. Biochem. Biophys. Methods*, **10**: 203-209.
- 133 Towbin H, Staehelin T, Gordon J. (1979) Electrophoretic transfer of proteins from polyacrylamide-gels to nitrocellulose sheets: Procedure and some applications, *Proc. Natl. Acad. Sci.*, **76**: 4350-4354.
- 134 Layne E. (1957) Spectrophotometric and turbidimetric methods for measuring proteins, *Methods Enzymol*, **3**: 447-454.
- 135 Peterson G.L. (1983) Determination of total protein, *Methods Enzymol*, **91**: 95-119.
- 136 Bradford M.M. (1976) A rapid and sensitive method for the quantitation of microgram quantities of protein utilizing the principle of protein-dye binding, *Analyt. Biochem*, **72**: 248-254.
- 137 Walker J.M. (2002) *The protein protocol handbook*, 2nd edition, *Humana Press.*
- 138 Reisner A.H, Nemes P, Bucholtz C. (1975) The use of Coomassie Brilliant Blue G250 perchloric acid solution for staining in electrophoresis and isoelectric focusing on polyacrylamide-gels, *Analyt. Biochem*, **64**: 509-516.
- 139 Fornstedt N, and Porath J. (1975) Characterization studies on a new lectin found in seeds of *Vicia ervilia*, *FEBS Lett.* **57**: 187-191.
- 140 Ricklin D. (2005) Surface plasmon resonance applications in drug discovery: with an emphasis on small molecules and low affinity systems, *Ph.D. thesis*, University of Basel.
- 141 Amersham (2000) *Gel filtration: principles and methods*, *Amersham Pharmacia Biotech*, 8th edition, Sweden.
- 142 Bootz F, *Institute for laboratory animals*, ETHZ.
- 143 Swendsen L, Crowley A, Ostergaard L.H, Stodulski G, Hau J. (1995) Development and comparison of purification strategies for chicken antibodies from egg yolk, *Lab. Animal Science*, **45(1)**: 89-93.

- 144 AmminoLink Plus Immobilization kit manual.
- 145 De Libero G, De Libero L.M, Gober H.J, Kistowska M, Mariotti S, *ZLF University hospital*, Basel, personal communication.
- 146 Fischer Rene, *Institute of Biochemistry ETHZ*, Zurich, personal communication.
- 147 Galfre G, Howe S.C, Milstein C, Butcher G.W, Howard J.C. (1977) Antibodies to major histocompatibility antigens produced by hybrid cell lines, *Nature*, **266**: 550-552.
- 148 Ey P.L, Prowse S.J, Jenkin C.R. (1978) Isolation of pure IgG₁, IgG_{2a} and IgG_{2b} immunoglobulins from mouse serum using protein A-Sepharose, *Biochemistry*, **15**: 429-436.
- 149 Westwood O.M.R, Hay F.C. (2001) Epitope mapping: practical approach, *Oxford University Press*, **7**: 170.
- 150 Weitz-Schmidt G, Stokmaier D, Scheel G, Nifant'ev N.E, Tuzikov A.B, Bovin N.V. (1996) An E-selectin binding assay based on a polyacrylamide-type glycoconjugate, *Anal. Biochem*, **238(2)**: 184-190.
- 151 Przybylski M, Stefanescu R, *Institute of Biochemistry*, Konstanz, personal communication.
- 152 Salmons Lab (<http://www.bio.unc.edu/faculty/salmon/lab/salmonprotocols.html>)
- 153 Novikoff P, *et al.* (1996) Three-dimensional organization of rat hepatocyte cytoskeleton: relation to the asialoglycoprotein endocytosis pathway, *J. Cell Science*, **109(1)**: 21-32.
- 154 Terracciano L, *Institute of Pathology, University hospital*, Basel.
- 155 Smith G.P. (1985) Filamentous fusion phage: novel expression vectors that display cloned antigens on the virion surface, *Science*, **228**: 1315-1317.
- 156 Hanes J, Plückthun A. (1997) In vitro selection and evolution of functional proteins by using ribosome display, *Proc. Natl. Acad. Sci. USA*, **91**: 9022-9026.
- 157 He M, Taussig M.J. (1997) ARM complexes as efficient selection particles for *in vitro* display and evolution of antibody combining sites, *Nucleic Acids Res*, **25**: 5132-5134.
- 158 Spiess M, Department of Biochemistry, *Biocenter*, University of Basel.
- 159 Dragic Zorica (2005) E-selectin as an anti-inflammatory drug target: Expression, purification and characterization for structural studies. Assay development for antagonists evaluation, *Ph.D. thesis*, University of Basel.
- 160 Hirel P.H, Schmitter M.J, Dessen P, Fayat G, Blanquet S. (1989) Extent of N-terminal methionine excision from *Escherichia coli* proteins is governed by the side-chain length of the penultimate amino acid, *Proc. Natl. Acad. Sci. USA*, **86(21)**: 8247-8251.
- 161 Nakai S, Akita E.M. (1993) Comparison of four purification methods for the production of immunoglobulins from eggs laid by hens immunized with an enterotoxigenic *E.coli* strain, *J. Immunol. Methods*, **160**: 207-214.
- 162 Schwarzkopf C, Thiele B. (1996) IgY technology: effectivity of different methods for the extraction and purification of IgY, *ALTEX supplement*, **13**: 35-39.
- 163 Schecklies E. (1996) Eine Einführung in die Theorie und Praxis der Antikörperherstellung, *VCH*, Weinheim, New York, Basel, Cambridge, Tokyo.
- 164 Schade R, Pfister C, Halatsch R, Henklein P. (1991) Polyclonal IgY antibodies from chicken egg yolk – an alternative to the production of mammalian IgG type antibodies in rabbits, *ATLA*, **19**: 403-419.
- 165 Hollander Z, Katchalski E. (1986) Use of monoclonal antibodies to detect conformational alterations in lactate dehydrogenase isoenzyme 5 on heat denaturation and on adsorption to polystyrene plates, *Mol. Immunol*, **23(9)**: 927 – 933.

- 166 Hosoi T, Imai Y, Irimura T. (1998) Coordinated binding of sugar calcium and antibody to macrophage C-type lectin, *Glycobiology*, **8(8)**: 791 – 798.
- 167 Schreiter T, Liu C, Gerken G, Treichel U. (2005) Detection of circulating autoantibodies directed against the asialoglycoprotein receptor using recombinant receptor subunit H1, *J. Immunol. Methods*, **301(1-2)**: 1 – 10.
- 168 Kokudo N, Vera D.R, Makuuchi M. (2003) Clinical application of TcGSA, *Nuclear Med. Biol*, **30**: 846 – 849.

Appendix 1: Substances

Substance	Designation	Source
β -GalNAc BP	β -N-acetyl-D-galactosamine BP	Synthesome
β -GalNAc FP	β -N-acetyl-D-galactosamine FP	Synthesome
ABTS (HRP substrate)	ABTS Peroxidase substrate kit (2,2'-azino-di-[3-ethylbenzthiazoline-6-sulfonic acid])	Biorad
Acetic acid	Acetic acid glacial 99%	Hänseler
Acetone	Acetone	Fluka
Acetonitrile	Acetonitrile	Fluka
Acrylamide 30%	Acrylamide 30% (acrylamide:bisacrylamide, 37.5:1)	AppliChem
AD494(DE3)	<i>Escherichia coli</i> AD494(DE3) expression host Resistance: kan	Novagen
Agar	Bacto™ Agar, for microbiological culture	Becton Dickinson BD
Agarose	Agarose, molecular biology grade	Eurogent
Aminocaproic acid	6-Aminocaproic acid, $\geq 99\%$	Fluka
Ammoniumsulfate	Ammoniumsulfate, grade I, $\geq 99.0\%$	Sigma
Amphotericine B	Amphotericine B (250 μ g/ml, 100x)	Sigma
Ampicilline Na	Ampicilline sodium	Sigma
Anti- β -tubulin antibody	Monoclonal mouse anti- β -tubulin antibody	Boeringer Mannheim
Anti-ASGPR antibody	Anti-human(mouse) asialoglycoprotein receptor antibody (1:100)	Calbiochem
APS	Ammonium persulfate, $>98\%$, for electrophoresis	Sigma
Asialofetuin	Asialofetuin (type I) from fetal calf serum	Sigma
<i>BamH</i> I	<i>BamH</i> I restriction enzyme from <i>Bacillus amyloliquefaciens</i> H (10'000U/ml)	New England BioLabs
5'-g \downarrow gatcc-3'	<i>BamH</i> I buffer (10x), 37°C, 50-fold overdigest	
3'-cctag \uparrow g-5'		
Biotin-polymer-GalNAc	Biotin-polyacrylamide β -GalNAc glycoconjugate (5mol% biotin, 20mol% GalNAc)	Lectinity holding
BL-21(DE3)	<i>Escherichia coli</i> BL-21(DE3) expression host Resistance: kan	Novagen
Brefeldin A	Brefeldin A, from <i>penicillium brefeldianum</i>	(ZLF)
Bromphenol blue	Bromphenol blue, for electrophoresis	Biorad
BSA	Bovine Serum Albumine, Fraktion V, $>98\%$	Sigma
BSA	Bovine Serum Albumin (400 μ g/ml) Protein Standard	Sigma
CaCl ₂ ·2H ₂ O	Calciumchloride dihydrate, pa $\geq 99.0\%$	Fluka
Carbenicilline Na ₂	Carbenicilline disodium	Sigma
Chloroform-phenol		
Chymotrypsine	α -Chymotrypsine, TLCK treated, from bovine pankreas	Sigma
CIAP	Calf intestine alkaline phosphatase (1U/ μ l) CIAP buffer (10x)	MBI Fermentas
Ciprofloxacin	Ciproxine infusion 2mg/ml (100x)	Bayer (ZLF)
Collagen S	Collagen S (type I, 3mg/ml, pH3.0)	Roche

Substance	Designation	Source
Coomassie Blue G250	Coomassie Brilliant Blue G250	Biorad
DAM-IgG(H+L)-Cy3	Donkey anti-mouse IgG(H+L), Cy3 labeled	Jackson Immuno Research
Dendritic cell	Dendritic cells differentiated from monocytes (human blood)	De Libero G.
Diethanolamine	Diethanolamine, ≥98%	Sigma
Divinylsulfone	Divinylsulfone, purum	Fluka
DMEM high glucose	Dulbecco's Modified Eagle's Medium high glucose	Gibco™
DMEM high glucose (HEPES)	Dulbecco's Modified Eagle's Medium high glucose (without phenolred, with 25mM HEPES)	Gibco™
DMSO	Hybrimax® dimethyl sulfoxide, sterile	Sigma
DMSO	Dimethyl sulfoxide, >99.9%	Sigma
DNA molecular ladder	DNA molecular weigh marker X (12216-75bp)	Roche
dNTP	2'-Desoxynucleoside-5'-triphosphate	MBI Fermentas
DPBS	Dulbecco's Phosphate Buffered Saline (without Ca, without Mg)	BioWhittaker™ (ZLF)
DPBS	Dulbecco's Phosphate Buffered Saline (without Ca, without Mg)	Gibco™
DTT	Dithiothreitol, >99%, molecular biology	Sigma
EDTA-2H ₂ O Na ₂	Disodium ethylenediaminetetraacetate dihydrate	Sigma
Ethanolamine	Ethanolamine, ps.	Sigma
Ethanol 99%	Ethanol 99%	Fluka
Ethidium bromide	Ethidium bromide solution (10mg/ml)	Boeringer Mannheim GmbH
EZNA gel extraction kit	ENZA® Gel Extraction Kit	PEQLAB
FACSRinse	FACSRinse solution (hypoton)	Becton Dickinson (ZLF)
FACSSafe	FACSSafe solution (isoton)	Becton Dickinson (ZLF)
FCS	Fetal Calf Serum (US)	BioWhittaker™ (ZLF)
FCS	Fetal Calf Serum (Australia)	Gibco™
Freund's complete (CFA)	Complete Freund's Adjuvans	Sigma
Freund's incomplete (IFA)	Incomplete Freund's Adjuvans	Sigma
Galactosamine	D-galactosamine	Pfanstiehl Laboratories
Galactose	D-galactose	Senn chemicals
Galactose	D-galactose	Merck
GAB-IgG-HRP	Goat anti-biotin IgG, horseradish peroxidase labeled	Sigma
GAM-Ig(H+L)-FITC	Goat anti-mouse IgG(H+L), fluorescein isothiocyanate labeled	Southern Biotechnology SBA
GAM-Ig(H+L)-HRP	Goat anti-mouse IgG(H+L), R phycoerythrine labeled	Southern Biotechnology SBA
GAM-Ig(polyvalent)-AP	Goat anti-mouse Ig (polyvalent) alkaline phosphatase conjugate (1:3'000)	Sigma
GAM-IgG(Fc)-AP	Goat anti-mouse IgG (Fc specific) alkaline phosphatase conjugate (1:40'000)	Sigma
GAM-IgG(H+L)-AF488	Goat anti-mouse IgG (H+L) Alexa Fluor 488 conjugate	Molecular Probes
GAM-IgG(whole)-AP	Goat anti-mouse IgG (whole molecule) alkaline phosphatase conjugate (1:30'000)	Sigma
GAM-IgM/G/A(H+L)-FITC	Goat anti-mouse IgM+IgG+IgA (H+L) fluorescein isothiocyanate conjugate (1µg/10 ⁶ cells)	Southern Biotechnology SBA

Substance	Designation	Source
GAM-IgM/G/A(H+L)-HRP	Goat anti-mouse IgM+IgG+IgA (H+L) horseradish peroxidase conjugate (1:8'000)	Southern Biotechnology SBA (ZLF)
GAM-IgM/G/A(H+L)-RPE	Goat anti-mouse IgM+IgG+IgA (H+L) R phycoerythrine conjugate (0.1µg/10 ⁶ cells)	Southern Biotechnology SBA
Gel filtration standard	Gel filtration standard (5 proteins)	Biorad
Gel loading solution	Gel loading solution (6x), for molecular biology	Sigma
Gentamicine	Gentamicine sulfate solution 50mg/ml (1000x)	Sigma
GKN		(ZLF)
Glucose	D-glucose	Merck
GlutaMAX	GlutaMAX [®] I 200mM (100x)	Gibco [™] (ZLF)
Glutathione oxidized	Glutathione oxidized, free acid	Calbiochem
Glutathione reduced	Glutathione reduced, free acid	Calbiochem
Glycerol	Glycerol 98%	Fluka
Glycerol anhydrous	Glycerol anhydrous, for molecular biology	Fluka
Glycine	Glycine, ≥99.0%	Fluka
GMCSF	Human granulocyte-macrophage colony-stimulating factor	De Libero G.
H ₂ SO ₄	Sulphuric acid	Fluka
H ₃ PO ₄ 85%	Ortho-phosphoric acid 85%	Fluka
HAT media supplement	Hybrimax [®] HAT media supplement (50x) (500mM hypoxanthine, 2mM aminopterin, 80mM thymidine)	Sigma
HAT media supplement	HAT media supplement (50x) (500mM hypoxanthine, 2mM aminopterin, 80mM thymidine)	Gibco [™] (ZLF)
HCl	Hydrochloric acid 37%	Fluka
HEPES	4-(2-hydroxyethyl)piperazine-1-ethanesulfonic acid	Fluka
HEPES	HEPES Buffer (1M, 0.85% NaCl)	BioWhittaker [™]
HEPES	HEPES Buffer (1M, pH7.2-7.5, pK _a 7.3 at 37°C)	Gibco [™]
HepG2	Human cell line HepG2 (ATCC: HB-8065) Hepatocellular carcinoma (liver) Morphology: epithelial (adherent)	DSMZ GmbH
HL-60	Human cell line HL-60 (ATCC: CCL-240) Acute promyelocytic leukaemia (peripheral blood) Morphology: myeloblastic (suspension)	De Libero G.
HSA	Human Serum Albumine 3%	University hospital Basel
HT media supplement	Hybrimax [®] HT media supplement (50x) (500mM hypoxanthine, 80mM thymidine)	Sigma
HT media supplement	HT media supplement (50x) (500mM hypoxanthine, 80mM thymidine)	Gibco [™] (ZLF)
Human IL-2	Human interleukin-2 containing supernatant	De Libero G.
Human IL-6	Human interleukin-6 containing supernatant	De Libero G.
Human serum	Human serum	De Libero G.
IMDM	Iscove's Modified Dulbecco's Medium (with GlutaMAX I, 25mM HEPES)	Gibco [™]
Iodoacetamide (IAA)	Iodoacetamide, Sigmapure	Sigma
IPTG	Isopropyl-β-D-thiogalactopyranoside	Promega
IPTG	Isopropyl-β-D-thiogalactopyranoside	Roche

Substance	Designation	Source
Isopropanol	Isopropanol, puriss.	Fluka
Isotyping ELISA	Clonotyping™ System/HRP ELISA (GAM-Ig-HRP(1:500), ABTS)	Southern Biotechnology SBA
Isotyping strip	IsoStrip mouse monoclonal antibody isotyping kit	Roche
JM109	<i>Escherichia coli</i> JM109 transformation host Resistance: none	Promega
JM109(DE3)	<i>Escherichia coli</i> JM109(DE3) expression host Resistance: none	Promega
Jurkat	Human cell line Jurkat (ATCC: TIB-152) Acute T-cell leukaemia (T-lymphocyte) Morphology: lymphoblast (suspension)	De Libero G.
K-562	Human cell line K-562 (ATCC: CCL-243) Chronic myeloid leukaemia (bone marrow) Morphology: lymphoblast (suspension)	De Libero G.
Kanamycine	Kanamycine sulfate solution (10mg/ml, 100x)	Gibco™ (ZLF)
Kanamycine SO ₄	Kanamycine monosulfate (component A, B, C)	Fluka
KCl	Potassium chloride, pa.	Fluka
KH ₂ PO ₄	Potassium dihydrogenphosphate, pheur	Fluka
KOAc	Potassium acetate	Fluka
Lactose	D-lactose	Merck
Lambda λ DNA	Standard λ DNA (250µg/ml)	MBI Fermentas
L-glutamine	L-glutamine (200mM, 100x)	Gibco™
LPS	Lipopolysaccharid from <i>E.coli</i> serotype 055:B5 (5mg/ml)	Fluka
Lysozyme	Lysozyme (111'000U/mg), from hen egg white	Boeringer Mannheim
MEM	Minimal Essential Medium (without L-glutamine, with Earl's salt)	BioWhittaker™ (ZLF)
Mercaptoethanol	β-mercaptoethanol	Fluka
Methanol	Methanol	Fluka
Metofane	Methoxyflurane	Schering-Plough animal health
MgCl ₂ ·6H ₂ O	Magnesium chloride hexahydrate, molecular biology	Fluka
MgSO ₄ ·7H ₂ O	Magnesium sulfate heptahydrate	Fluka
Milk powder not fat dried	Not fat dried milk powder	Coop
Monocyte	Monocytes isolated from human blood	De Libero G.
Mouse Balb/c	Balb/c mouse Inbred, albino	
Mouse NMRI	National Medical Research Institute mouse Outbred, albino	Biological Research Laboratories
Mowiol	Mowiol Hoechst 4-88	Calbiochem
MW marker protein (high range)	SigmaMarker™, protein high range (MW 36'000-205'000)	Sigma
MW marker protein (low range)	SigmaMarker™, protein low range (MW 6'500-66'000)	Sigma
Myeloma cell	Balb/c mouse myeloma cells P3X63-Ag8.563 (ATCC CRL-1580) Morphology: lymphoblast (suspension)	De Libero G., Fischer R.

Substance	Designation	Source
Na ₂ HPO ₄	Disodium hydrogenphosphate, anhydrous	Fluka
NaBH ₄	Sodium borohydride	Fluka
NaBorate·10H ₂ O	Sodium borate decahydrate, SigmaUltra	Sigma
N-Acetylgalactosamine	N-Acetyl-D-galactosamine	Acros Organics
N-Acetylgalactosamine	N-Acetyl-D-galactosamine	Pfanstiehl laboratories
NaCl	Sodium chloride, puriss pa ≥99.5%	Fluka
NaHCO ₃	Sodium hydrogencarbonate, pa.	Fluka
NaN ₃	Sodium azide	Fluka
NaOAc·3H ₂ O	Sodium acetate trihydrate	Fluka
NaOH	Sodium hydroxide	Merck
NaPyruvate 100x	Sodium pyruvate 100mM (100x)	BioWhittaker™ (ZLF)
NBT-BCIP solution	NBT-BCIP solution (1.1g/ml) (nitro-blue tetrazoliumchloride, 5-bromo-4-chloro-3-indolylphosphate toluidine, 67% DMSO)	Fluka
<i>Nde</i> I	<i>Nde</i> I restriction enzyme from <i>Neisseria denitrificans</i> (20'000U/ml)	New England BioLabs
5'-ca↓tatg-3'	NEBuffer (10x) 4, 37°C, 20-fold overdigest	
3'-gtat↑ac-5'		
NEAA 100x	MEM Non Essential Amino Acids (100x)	BioWhittaker™ (ZLF)
NP-40	Nonidet P40 (Tergitol)	Fluka
NPP (AP substrate)	Sigma 104® NPP tablet (p-nitrophenylphosphate, 5mg)	Sigma
OPD (HRP substrate)	Sigma fast™ OPD tablet (o-phenylenediamine dihydrochloride, 400µg/ml)	Sigma
Oxalic acid	Oxalic acid, pa.	Fluka
Paraformaldehyde	Paraformaldehyde	Fluka
PEG 1500	Polyethylene glycol, MW 1'500	Boehringer Mannheim (ZH)
PEG 4000	Polyethylene glycol, MW 4'000 (9727)	Merck
PEG 8000	Polyethylene glycol, MW 8'000	Sigma
PenStrep	Penicilline (10 ⁴ U/ml), streptomycine (10mg/ml, 100x)	Gibco™
<i>Pfu</i> DNA polymerase	<i>Pfu</i> DNA polymerase from <i>Pyrococcus furiosus</i> (2.5U/µl) <i>Pfu</i> DNA polymerase buffer (10x)	Promega
<i>Pfu</i> DNA polymerase	<i>Pfu</i> DNA polymerase from <i>Pyrococcus furiosus</i> (2.5U/µl) <i>Pfu</i> DNA polymerase buffer (10x)	Stratagene
Plasmid extraction kit	Plasmid DNA Extraction Kit	Quiagen
Plasmid extraction kit	GFX™ Micro Plasmid Prep Kit	Amersham Pharmacia
Plasmid pET21c	Bacterial plasmid vector Resistance: amp, T7 promotor, T7-tag(N), His-tag(C)	Novagen
Plasmid pET3b	Bacterial plasmid vector Resistance: amp, T7 promotor, T7-tag(N)	Novagen
Plasmid pET3H1	Plasmid pET3b with H1-CRD insert	Martin Spiess (BZ)
Plasmid pEZZ18	Bacterial plasmid vector Resistance: amp, protein A-tag (ZZpeptide)	Amersham Pharmacia
PMSF	Phenylmethane sulfonylfluoride, >99%	Fluka

Substance	Designation	Source
Ponceau S	Ponceau S solution 0.1% (5% acetic acid)	Sigma
Primer H1-bw	H1-backward primer, 21bp (ggatccttattaaaggagagg)	Microsynth
Primer H1-fw	H1-foreward primer, 21bp (catatgggctcagaaaggacc)	Microsynth
Primer M13 standard	M13 standard primer	Microsynth
Primer T7	T7 primer for forward sequencing	Microsynth
Primer T7term	T7term primer for backward sequencing	Microsynth
Probidiumiodide	Probidiumiodide	(ZLF)
Protease	Protease from <i>Streptomyces griseus</i>	Sigma
Protein G agarose	Protein G agarose, lyophilized	Sigma
Proteinase K	Proteinase K from <i>Tritirachium album</i>	Sigma
RACH-IgG(whole)-AP	Rabbit anti-chicken IgG (whole molecule) alkaline phosphatase conjugate (1:35'000)	Sigma
RACH-IgG(whole)-FITC	Rabbit anti-chicken IgG (whole molecule) fluoresceine isothiocyanate conjugate (1:640)	Sigma
RNAse A	RNAse A (10mg/ml) from bovine pancreas	Roche
Rosetta-gami TM (DE3)	E.coli Rosetta-gami TM (DE3) expression host Resistance: kan, tet, cam	Novagen
RPMI1640	RPMI1640 (without L-glutamine)	BioWhittaker TM (ZLF)
Saponine	Saponine from quillaja bark	(ZLF)
SDS	Sodiumdodecylsulfate, for electrophoresis	Biorad
Sepharose 4B	Sepharose® 4B, CH-activated, lyophilized (bead diameter 40-165µm)	Sigma
Sepharose 6B	Sepharose® 6B, for chromatography (bead diameter 45-165µm)	Fluka
Silver staining kit	Plus one TM silver staining kit protein	Amersham biosciences
SK-Hep1	Human cell line SK-Hep1 Adencarcinoma (liver) Morphology: epithelial (adherent)	DSMZ GmbH
<i>Sma</i> I	<i>Sma</i> I restriction enzyme From <i>Serratia marcescens</i> S (10U/µl) Y+/Tango TM buffer, 30°C, 50-fold overdigest	MBI Fermentas
Streptavidin-peroxidase	Streptavidin-peroxidase (POD) conjugate	Roche
Sucrose	Sucrose (Saccharose)	Sigma
T4 DNA ligase	T4 DNA ligase (400U/µl) From T4 infected E.coli T4 DNA ligase buffer (10x)	New England BioLabs
<i>Taq</i> DNA polymerase	<i>Taq</i> DNA polymerase (5U/µl) From <i>Thermus aquaticus</i> recombinant in <i>E.coli</i> <i>Taq</i> PCR buffer with MgCl ₂ (10x)	Sigma
TCA	Trichloroacetic acid	Fluka
TEMED	N,N,N,N'-Tetra-methylene-diamine	Serva
Texas Red labeling kit	FluoReporter® Texas Red® X protein labeling kit Active Texas Red-X dye (A), DMSO anhydrous (B)	Molecular Probes
TFA	Trifluoroacetic acid	Fluka

Substance	Designation	Source
THP-1	Human cell line THP-1 (ATCC TIB-202) Acute monocytic leukaemia (peripheral blood) Morphology: monocyte (suspension)	De Libero G.
Top10	<i>Escherichia coli</i> Top 10 cloning host Resistance: none	Invitrogen
Tris	Tris(hydroxymethyl)aminomethane, ≥99.0%	Fluka
Triton-X100	Triton-X100 (PEG ter-octylphenylether)	Fluka
Trypsine	Trypsine modified, sequencing grade 20µg/vial	Promega
Trypsine-EDTA	Trypsine-EDTA in HBSS (1x) (0.25% trypsin, 1mM Na ₂ EDTA)	Gibco™
Trypan blue	Trypan blue 0.4%	Gibco™
Tryptone	Bacto™ Trypto Peptone (for microbiological culture)	Becton Dickinson BD
Tween20	Tween20 (polyoxyethylenesorbitan monolaurate)	Sigma
Urea	Urea, purum pa	Fluka
Water MilliQ	Double distilled filtrated water	(ZLF)
Water Nanopure	Double distilled filtrated water	
Yeast extract	Bacto™ Yeast Extract (for microbiological culture)	Becton Dickinson BD

Appendix 2: Equipments

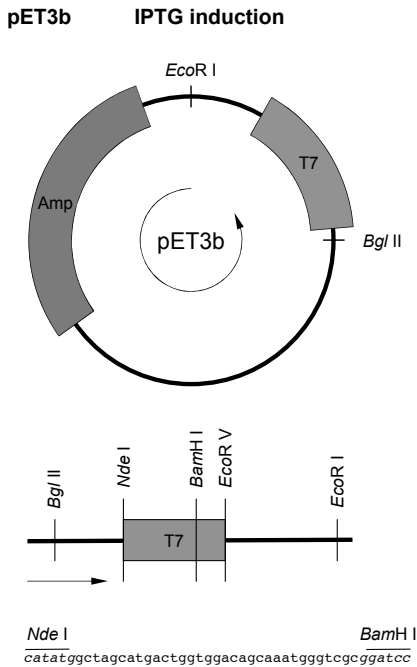
Equipment	Designation	Source
Blotting cell, semi-dry	Trans-Blot® SD, demi-dry electrophoretic transfer cell	Biorad
Cell sieve	Cell sieve	(ZLF)
Cell counting chamber	Improved Neubauer counting chamber	Brand
Centrifuge	Heraeus Megafuge 1.0	Heraeus Instruments (ZH)
Centrifuge	Heraeus 400R (Functionline)	Heraeus Instruments (ZLF)
Centrifuge, bench	Centrifuge 5415D	Vaudaux-Eppendorf
Centrifuge, labor	Centrifuge 5804R	Vaudaux-Eppendorf
Chromatography apparatus	BioLocig HR work station	Biorad
	Auto injection valve AV7-3, low pressure	
Column AminoLink plus	AminoLink Plus Immobilization Trial Kit	Pierce
Column FPLC 10ml	Bio-Scale MT10 column	Biorad
Column FPLC 20ml	Bio-Scale MT20 column	Biorad
Column HPLC 2ml	Bio-Scale MT2 column	Biorad
Column Mobicol 1ml	Mobicol 1ml	MoBiTec
Column Protein A 1ml	Affi-gel protein A agarose cartridge	Biorad
Column Protein G 1ml	HiTrap protein G HP	Amersham Biosciences
Column Protein L spin	Nab™ Protein L spin purification kit	Pierce
Column SEC 15ml	Bio-Prep SE-10/17 column	Biorad
Coverslip	Coverslip round (18mm)	Menzel-Gläser
Cryotube, 1.2ml	Cryotubes, 1.2ml, free standing	Techno Plastic Products TPP
Cryotube, 1.8ml	Cryotube™ 1.8ml (PP), conical, free standing	Nunc Brand (ZLF)
Cuvette quartz semi-micro	Cuvette quartz semi-micro	
Cuvette semi-micro	Cuvette semi-micro (10-10-45mm)	Greiner
Dialysis mini unit	Slide-A-Lyzer® mini dialysis unit (MWCO 10'000)	Pierce
Dialysis tube	ZelluTrans/Roth 6.0, 25mm (MWCO 10'000)	Roth GmbH
Electrophoresis chamber	Agarose gelelectrophoresis, flat	
Electrophoresis, cell	Mini-PROTEAN 2 system, vertical	Biorad
FACS reader	FACScan	Becton Dickinson BD (ZLF)
Filter syringe	MILLEX GP (0.22µm)	Millipore
Filter centrifugal unit 0.5ml	Biomax ultrafree®-0.5 centrifugal filter unit (MWCO 10'000)	Millipore
Filter centrifugal unit 0.5ml	Microcon® YM-10 centrifugal filter unit (MWCO 10'000)	Millipore
Filter centrifugal unit 2.0ml	Centricon® YM-10 centrifugal filter unit (MWCO 10'000)	Millipore
Filter disc membrane	Supor® (0.45µm), low protein binding	Pall Gelman Laboratory
Filter Mobicol column	Mobicol large filter (35µm pore size) Mobicol small filter (35µm pore size)	MoBiTec
Filter paper (blot)	Chromatography paper 3MM	Whatman
Filter round paper	Filter MN615	Macherey-Nagel
Filter syringe (0.2µm)	IC-Millex-LG (0.2µm), low protein binding	Millipore (ZLF)

Equipment	Designation	Source
Filter syringe (0.22µm)	Millex-GV (0.22µm), low protein binding	Millipore (ZLF)
Filter vacuum Stericup™	Stericup™ (0.22µm) vacuum-driven filter unit, sterile	Millipore
Flask T ¹⁵⁰	Tissue culture flask (690ml/150cm ²), vent	Techno Plastic Products TPP
Flask T ¹⁷⁵	Tissue culture flask (175cm ²), filter	Falcon™ Becton Dickinson (ZLF)
Flask T ²⁵	Tissue culture flask (60ml/25cm ²), vent	Techno Plastic Products TPP
Flask T ⁷⁵	Tissue culture flask (270ml/75cm ²), vent	Techno Plastic Products TPP
Gel documentation	GelDoc™ 2000	Biorad
Glass fritte	glass fritte (borosilicate 3.3, pore 4)	
Incubator CO ₂	Hera cell	Heraeus Instruments
Incubator CO ₂	Revca ultima, model 05000T-7-VBB	Kendro Laboratory product (ZLF)
Incubator shaker	Innova 4000	New Brunswick Scientific
Laminar flow	Heraeus HSP18 class II	Heraeus Instruments (ZLF)
Laminar flow (vertical)	Skanair MSF 120 (model 1.2)	Skan AG
Laminar flow (vertical)	Skanair MSF 90 (model 0.9)	Skan AG
Mass spectrometer		
Microscope	Inverse microscope Nikon TMS	Nikon (ZLF)
Microscope	Inverse microscope Zeiss IM binocular Kpl-W10x/18 objective F2.5/0.08 objective Ph1F10/0.25 objective F-LD20/0.025	Zeiss
Microscope	Apofluorescence microscope binocular 10x/20 objective 100x/1.3oil Ph3plan-neofluor filter red BP546/FT580/LP590 filter green 450-490/FT510/515-565	Zeiss
Microscope slide	Microscope slide (extra white)	Huber
Needle (middle)	Microlance™ 3 (18G-40mm)	Becton Dickinson BD
Needle (thick)	Microlance™ 3 (25G-25mm)	Becton Dickinson BD
Needle (thin)	Microlance™ 3 (27G-13mm)	Becton Dickinson BD
Nitrocellulose membrane	Trans-Blot® Transfer Medium (0.45µm)	Biorad
Paper towel Kimwipe	Kimwipe, precision paper towel	Kimberly Clark
Petri dish Ø 60mm	Petri dish with vent (60-15mm)	Greiner
Petri dish Ø 94mm	Petri dish with vent (94-16mm)	Greiner
Pipet 10µl	Eppendorf research 10	Vaudaux-Eppendorf
Pipet 1000µl	Gilson® Pipetman 200-1000µl	Gilson
Pipet 10ml	Serologic pipet 10ml (1/10ml), sterile	Falcon™ Becton Dickinson (ZLF)
Pipet 10ml	Serologic pipet 10ml (1/10ml), sterile	Techno Plastic Products TPP
Pipet 1ml	Serologic pipet 1ml (1/100ml), sterile	Techno Plastic Products TPP
Pipet 20µl	Gilson® Pipetman 5-20µl	Gilson
Pipet 200µl	Gilson® Pipetman 20-200µl	Gilson
Pipet 25ml	Serologic pipet 25ml (2/10ml), sterile	Falcon™ Becton Dickinson (ZLF)
Pipet 25ml	Serologic pipet 25ml (2/10ml), sterile	Techno Plastic Products TPP
Pipet 2ml	Serologic pipet 2ml (1/100ml), sterile	Falcon™ Becton Dickinson (ZLF)
Pipet 2ml	Serologic pipet 2ml (1/100ml), sterile	Techno Plastic Products TPP

Equipment	Designation	Source
Pipet 5'000µl	Eppendorf research 5000	Vaudaux-Eppendorf
Pipet 5ml	Serologic pipet 5ml (1/10ml), sterile	Falcon™ Becton Dickinson (ZLF)
Pipet 5ml	Serologic pipet 5ml (1/10ml), sterile	Techno Plastic Products TPP
Pipet multichannel 1200µl (multidispense)	Eppendorf research multichannel pro 1200	Vaudaux-Eppendorf
Pipet multichannel 300µl	Eppendorf research multichannel 300	Vaudaux-Eppendorf
Pipet pipetboy	Easypet	Vaudaux-Eppendorf
Pipet Terasaki	Terasaki-plate multipipet (Hamilton syringes)	
Plate ELISA (96 wells)	Nunc-Immuno™ 96 well plate MaxiSorp™ (400µl/2.7cm ²)	Nunc Brand
Plate FACS (96 wells)	Microtest™ 96 well TC plate, U bottom (0.32ml/0.36cm ²)	Falcon™ Becton Dickinson (ZLF)
Plate TC (12 wells)	Test culture plate 12 wells plate, flat (6.30ml/3.66cm ²)	Techno Plastic Products TPP
Plate TC (24 wells)	Microtest™ 24 well TC plate, flat bottom (3.5ml/2.0cm ²)	Falcon™ Becton Dickinson (ZLF)
Plate TC (24 wells)	Test culture plate 24 wells plate, flat bottom (3.29ml/1.91cm ²)	Techno Plastic Products TPP
Plate TC (6 wells)	Microtest™ 6 well TC plate, flat bottom (15.5ml/9.6cm ²)	Falcon™ Becton Dickinson (ZLF)
Plate TC (6 wells)	Test culture plate 6 wells plate, flat (15.53ml/9.03cm ²)	Techno Plastic Products TPP
Plate TC (96 wells)	Microtest™ 96 well TC plate, flat bottom (0.37ml/0.32cm ²)	Falcon™ Becton Dickinson (ZLF)
Plate TC (96 wells)	Test culture plate 96 wells plate, flat bottom (0.34ml/0.31cm ²)	Techno Plastic Products TPP
Plate Terasaki (60 wells)	Nunclon™ Δ surface (mini tray, 6x10)	Nunc (ZLF)
Plate washer (96 wells)	EL X50 auto strip washer	Bio-Tek Instruments (ZLF)
Power supply	POWER Pac 300	Biorad
Software (FACSscan)	CellQuest Pro	Becton Dickinson BD
Software (FPLC analysis)	EZLogic	Biorad
Software (GelDoc™ 2000)	Quantity one® version 4.1	Biorad
Software (graphs)	Prism4 software	
Software (platereader)	SOFTmax PRO version 4.0	Molecular devices
Sonication apparatus	VibraCell	Sonics & Materials
Spectrophotometer (UV/Vis, cuvette)	SmartSpec™ 3000 cuvette reader (200-800nm)	Biorad
Spectrophotometer (UV/Vis, plate reader)	Spectramax 190 plate reader (190-850nm)	Molecular devices
Syringe 10ml	Syringe Discardit™ II 10ml (0.5) Luer, sterile	Becton Dickinson BD
Syringe 10ml	Syringe 10ml (0.5) Luer, sterile	Once (ZLF)
Syringe 1ml	Syringe Plastipak™ 1ml (0.01) Luer, sterile	Becton Dickinson BD
Syringe 20ml	Syringe 20ml (1.0) Luer, sterile	Once (ZLF)
Syringe 2ml	Syringe Discardit™ II 2ml (0.1) Luer, sterile	Becton Dickinson BD
Syringe 50ml	Syringe Plastipak™ 50ml (0.2) Luer, sterile	Becton Dickinson BD
Syringe 5ml	Syringe Discardit™ II 5ml(0.2) Luer, sterile	Becton Dickinson BD
Syringe 5ml	Syringe 5ml (0.2) Luer, sterile	Once (ZLF)

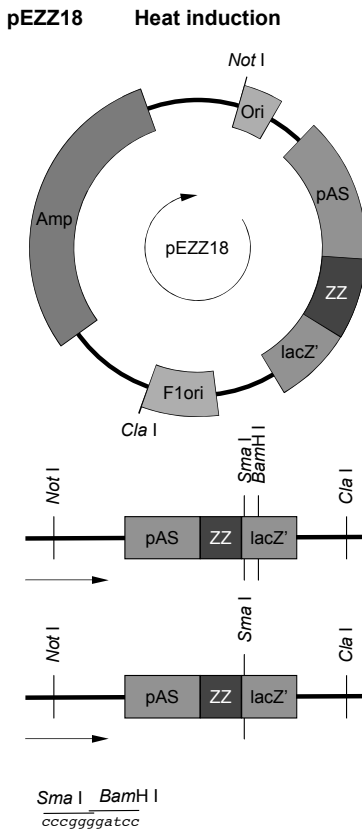
Equipment	Designation	Source
Thermal cycler	Icycler thermal cycler, gradient	Biorad
Tip 1000µl	Micropipet ect blue 1/1000µl	Treff
Tip 20µl	Micropipet tip micro cristall 0.5/20µl	Treff
Tip 200µl	Sarstedt tip yellow stock pack 1/200µl	Sarstedt (ZLF)
Tip 200µl	Micropipet tip yellow 1/200µl	Treff
Tip multichannel 1250µl	EpTIPS standard 50-1250µl	Vaudaux-Eppendorf
Tip multichannel 200µl	EpTIPS standard 2-200µl	Vaudaux-Eppendorf
Tip multichannel 300µl	EpTIPS standard 20-300µl	Vaudaux-Eppendorf
Tip pipet	EpTIPS standard 100-5'000µl	Vaudaux-Eppendorf
Tissue potter	Glass potter, conical	Fisher scientific (ZH)
Tube 0.5ml	Microtube 0.5ml, click cap, conical	Treff
Tube 1.5ml	Microtube 1.5ml, click cap, conical	Treff
Tube centrifugal 15ml	Centrifuge tube 15ml (PS), screw cap, conical	Falcon™ Becton Dickinson
Tube centrifugal 15ml	Blue max™ tube 15ml (PS), conical	Falcon™ Becton Dickinson (ZLF)
Tube centrifugal 15ml	Centrifuge tube 15ml (PP), screw cap, conical	Techno Plastic Products TPP
Tube centrifugal 50ml	Centrifuge tube 50ml (PP), screw cap, conical	Falcon™ Becton Dickinson
Tube centrifugal 50ml	Blue max™ tube 50ml (PP), conical	Falcon™ Becton Dickinson (ZLF)
Tube centrifugal 50ml	Centrifuge tube 50ml (PP), screw cap, conical	Techno Plastic Products TPP
Tube culture 14ml	Culture tube 14ml (PP), dual snap cap, round	Falcon™ Becton Dickinson
Tube FACS	FACS tubes, TPS-05	Milan Geneve (ZLF)
Tube test 5ml	Test tube 5ml (PS), dual snap cap, round	Falcon™ Becton Dickinson
Ultracentrifuge	Beckman L7 ultracentrifuge	Beckman coulter
	Rotor type 50.2Ti (50'000rpm)	
ZipTip	ZipTip C-18, 0.6µl	Millipore

Appendix 3: Expression vectors



Characteristics

Promotor T7, coding for Amp^R, no tag (or a N terminal T7-tag).
 Length 4639bp (pBR322 plasmid derivative).
 Multiple cloning site N-terminal *Nde* I (549) to C-terminal *Bam*H I (510) with the T7-tag between. Restriction sites *Hin* III (29), *Bam*H I (510), *Nde* I (549), *Sal* I (927), *Pst* I (3889) and *Eco*R I (4637).
 T7 promotor 614-630
 T7 transcription start 613
 T7-tag 518-550
 T7 terminator 404-450
 pBR322 origin 2813
bla coding region (Amp^R) 3574-4431



Characteristics

Promoters lacUV5 and Protein A (*staphylococcus aureus*), coding for Amp^R, N-terminal fusion protein, ZZ peptid of 14kD (secretion sequence / IgG binding domain, cleavable by factorXa)
 α -complementation (blue/white screening).
 Length 4591bp (pEMBL8+ plasmid derivative).
 Multiple cloning site N-terminal to C-terminal *Eco* RI (2914), *Sac* I (2920), *Kpn* I (2926), *Sma* I (2930), *Bam*H I (2935), *Xba* I (2941), *Sal* I (2947), *Pst* I (2953), *Sph* I (2959) and *Hind* III (2965).
 Protein A promotor (*pspa*) 2390-2400 and 2366-2377
 lacUV5 promotor (*plac*) 2144-2149 and 2180-2200
 Protein A signal sequence 2432-2539
 Partial E domain 2540-2557
 Synthetic ZZ domain 2558-2731 and 2732-2905
 Multiple cloning site 2914-2970
 lacZ' coding region 2973-3130
 f1 origin region 3136-4352
bla coding region (Amp^R) 154-1059
 Origin 1820

Appendix 4: *E. coli* cloning and expression strains

<i>E. coli</i> strain	Genotype	Characteristics
JM109	<i>endA1 recA1 gyrA96 thi hsdR17 (r_K⁻ m_K⁺) relA1 supE44 Δ(lac-proAB) F' [traD36 proAB lac^fZΔM15]</i>	JM109 is a cloning host for general cloning, which allows blue/white screening.
JM109(DE3)	<i>endA1 recA1 gyrA96 thi hsdR17 (r_K⁻ m_K⁺) relA1 supE44 Δ(lac-proAB) F' [traD36 proAB lac^fZΔM15] (DE3)</i>	JM109(DE3) is the same as JM109 but is an expression host and allows induction of protein expression by adding IPTG. The only difference is, that the λ prophage gene, coding for the T7 RNA polymerase, is inserted, which allows the induction of protein expression by adding IPTG, if it contains a plasmid with a T7 or T7lac promotor.
AD494(DE3) (K-12 derivative)	<i>Δara-leu 7697 ΔlacX74 ΔphoAPvull phoR ΔmalF3 F'[lac^f(lac^o)pro] trxB::kan(DE3)</i>	AD494(DE3) is a trxB mutant expression host, which therefore allows a better disulfide bond formation in the cytoplasm and is used to maximize the amount of soluble properly folded protein. The strain is kanamycine resistant.
Rosetta-gami(DE3) (K-12 derivative)	<i>Δara-leu 7697 ΔlacX74 ΔphoAPvull phoR araD139 galE galK rpsL F' [lac^f(lac^f)pro] gor522::Tn10(Tc^R)trxB::kan (DE3) pRARE (argU, argW, ileX, glyT, leuW, proL) (Cm^R)</i>	Rosetta-gami(DE3) is a trxB/gor mutant expression host, which therefore allows a better disulfide bond formation in the cytoplasm. Furthermore it contains a pRARE plasmid, which codes for all amino acids tRNAs, known to be rare in <i>E. coli</i> strains as arg / gly / pro / leu / ile. The strain is kanamycine, tetracycline and chloramphenicol resistant. Compatible vectors must carry a ColE1-based origin of replication (as pBR, pUC). Rosetta-gami is compatible with <i>E. coli</i> promotor based vectors as tac, trc, T5, λ. Rosetta-gami(DE3) as λDE3 lysogen strain is compatible with T7 and T7lac based pET vectors.
Top10	<i>F, mcrA Δ(mrr hsdRMS⁻ mcrBC) Φ80lacZΔM15 ΔlacX74 hsdR(r_K⁻ m_K⁺) rpsL(str^R) thi-1 mcrB P3 [kan^R amp^R(amber) tet^R(amber)]</i>	Top10 is used for cloning, expression and for library construction.

Appendix 5: Cell lines

Cell line	Characteristics
P3X63Ag8.653	Organism: <i>Mus musculus</i> Strain: Balb/c Cell type: B-lymphoblast, myeloma Life span: Infinite Properties: Suspension, 8-azaguanine resistant, HAT sensitive, no immunoglobuline secretion
HepG2	Organism: <i>Homo sapiens</i> Strain: Caucasian Cell type: Liver, carcinoma, hepatocellular Morphology: Epithelial-like Life span: Infinite Properties: Adherent
SK-Hep1	Organism: <i>Homo sapiens</i> Strain: Caucasian Cell type: Liver, adenocarcinoma Morphology: Epithelial-like Life span: Infinite Properties: Adherent
K-562	Organism: <i>Homo sapiens</i> Strain: Caucasian Cell type: Pleural effusion, leucaemic, chronic myeloid Morphology: Lymphoblast-like Life span: Infinite Properties: Suspension , undifferentiated
HL-60	Organism: <i>Homo sapiens</i> Strain: Caucasian Cell type: Peripheral blood, leucaemia, promyelocytic Morphology: Lymphoblast-like Life span: Infinite Properties: Suspension, differentiated , phagocytosis
THP-1	Organism: <i>Homo sapiens</i> Strain: Caucasian Cell type: Peripheral blood, monocytic leukaemia Morphology: Monocyte Life span: Infinite Properties: Suspension

Cell line	Characteristics
Jurkat	Organism: <i>Homo sapiens</i> Strain: Caucasian Cell type: T-lymphocyte, acute T-cell leukaemia Morphology: Lymphoblast-like Life span: Infinite Properties: Suspension
Monocytes	Organism: <i>Homo sapiens</i> Properties: Suspension, primary cells
Dendritic cells	Organism: <i>Homo sapiens</i> Properties: Suspension, primary cells, differentiated from monocytes with IL-2

Rita BORN Curriculum Vitae

Address: Johanniterstrasse 13, CH-4056 Basel, Switzerland

Phone: +41 (0)61 382 89 54

Email: rita.born@unibas.ch



Particulars

Date of Birth: 17.07.1975

Place of Birth: Niederbipp, CH

Profession: Pharmacist

Education

- | | |
|-------------|---|
| 1982 – 1991 | Primary & Secondary School, Worb. |
| 1991 – 1995 | College of Economy, Berne.
Graduate Meier Award for Outstanding Results in the Subjects of Biology; Chemistry; Geography and Physics. |
| 1995 – 1997 | Study of Pharmacy, University of Berne. |
| 1997 – 1998 | Training of Pharmacist, Pharmacy Neuenschwander, Gümliigen.
National Diploma: Assistant Pharmacist. |
| 1998 – 2000 | Study of Pharmacy, University of Basel.
Graduate Thesis at the Institute of Molecular Pharmacy, University of Basel.
Thesis: Polyketide Synthase Gen Cluster in <i>Saccharopolyspora erythraea</i> : Identification, Cloning and Sequencing of Gen Fragments.
National Diploma: Pharmacist. |
| 2001 – 2005 | Ph.D. Thesis in Pharmaceutical Sciences, Institute of Molecular Pharmacy, University of Basel.
Ph.D. Thesis in the Group of Prof. B. Ernst, in Collaboration with Prof. Dr. Med. Phil. Nat. G. De Libero (University Hospital, Basel) and with Prof. Dr. Rer. Nat. M. Przybylski (Department of Chemistry, Konstanz, D).
Thesis: Benefit and Application of Antibodies Against the H1 Carbohydrate Recognition Domain of the Human Hepatic Asialoglycoprotein Receptor
Financial Support by the Roche Research Foundation. |
-

Professional Experiences

1999 – 2000	Assistant Pharmacist, Pharmacy Neuenschwander, Gümüliĝen. Representative Pharmacist, 10% part time.
2000 – 2001	Pharmacist, Pharmacy Adler, Basel. Representative Pharmacist, 75% part time.
2001 – 2005	Pharmacist, Pharmacy Adler, Basel. Representative Pharmacist, 10% part time.

Skills

Teaching	Supervisor of Graduate Students Diploma Theses. Thesis in 2002: Production of the H1-CRD of the Human Asialoglycoprotein Receptor. Thesis in 2003: Polyclonal IgY Antibodies against the H1-CRD of the Human Asialoglycoprotein Receptor: Optimization of the IgY Extraction from Egg Yolk. Thesis in 2004: Binding of Sugar Ligands, Mimetics and Monoclonal Antibodies to the H1-CRD of the Human Asialoglycoprotein Receptor: Development of a Competitive Assay and Investigation of Receptor-mediated Endocytosis into Human Hepatoma Cells HepG2 by Fluorescence Microscopy. Assistant of Students Practical Training in "Modern Drug Design".
Computer	Experience with Office Applications, Databases, Internet
Language	German: fluent (mother tongue) English: good French: fair
Management	Member of the Organization Team of the Pharmacy Students Seminar Week, 2000, Grindelwald. Responsible for Sponsoring; Seminar Topics and Lecture Program with External Speakers from Pharmaceutical Companies. Coordinator of Project Meetings in Molecular Pharmacy, 2002 – 2004, University of Basel.

Courses, Lectures and Programs

Courses	Cultivation of Animal and Human Cells, 2001, Wädenswil. From <i>in vivo</i> Immunogen to Monoclonal Antibody, 2001, Wädenswil.
Lectures	Key Issues in Drug Discovery & Development, 2004, ETH Zurich and University of Basel. Postgraduate Lectures and Seminars, University of Basel.
Mentoring program	WIN04 Mentoring Program, 2004, Novartis and University of Basel. Woman to Industry Mentoring Program, for Selection and Promotion of High Potential Graduate Students for Future Collaboration.

Publications

Papers	Born R, Ricklin D, Johansson K, Ernst B. (2005) Optimized High Yield Expression and Purification of the H1 Carbohydrate Recognition Domain of the Human Asialoglycoprotein Receptor, in preparation. Born R, Stefanescu R, Przybylski M, Ernst B. (2005) Mapping the Epitope of the Monoclonal B01.4 IgG1, directed against the H1 Carbohydrate Recognition Domain of the Human Asialoglycoprotein receptor, in preparation. Born R, Gober HJ, Fischer R, De Libero G, Ernst B. (2005) Monoclonal IgG Antibodies against the H1 Carbohydrate Recognition Domain of the Human Hepatic Asialoglycoprotein Receptor: Characterization and Diagnostic Prospects, in preparation.
Posters	Johansson K, Born R, Ernst B. (2005) Characterization of Mutant Forms of the Asialoglycoprotein Receptor H1-CRD, PharmaDay 2005, University of Basel. Riva C, Stokmaier D, Born R, Lill M, Ernst B. (2005) Targeting the Liver via the ASGPR: Synthesis of High Affinity Ligands for the H1-CRD, PharmaDay 2005, University of Basel.
Oral Presentation	Born R, Fischer R, Przybylski M, De Libero G, Ernst B. Asialoglycoprotein Receptor, a Therapeutic Target: Monoclonal Antibodies and their Characterization, Fall Meeting of Swiss Chemical Society 2004, Zurich.

Personal interests

Running

Endurance Running Competition, Switzerland.

Positions in Long Distance Running e.g. Halfmarathon of Basel 2002 (1st position), Jungfrau Marathon 2004 (9th position) and Swiss Marathon Championship Winterthur 2005 (1st position)
